USARTL-TR-78-11

ENGINE/AIRFRAME/DRIVE TRAIN DYNAMIC INTERFACE DOCUMENTATION

D. A. Richardson
J. R. Alwang

Boeing Vertol Company
P.O. Box 16858
Philadelphia, Pa. 19142

April 1978

Final Report

Prepared for

APPLIED TECHNOLOGY LABORATORY
U. S. ARMY RESEARCH AND TECHNOLOGY LABORATORIES (AVRADCOM)
Fort Eustis, Va. 23604

APPLIED TECHNOLOGY LABORATORY POSITION STATEMENT

This report provides the details of a program that is part of a larger effort designed to provide a complete report of past and present engine/airframe/drive train dynamic interface problems. The problems of vibration related interface compatibility in engine/drive system installations are usually complicated by the inherent coupling of the three major multi-degree-of-freedom systems, i.e., engine, airframe and drive train. The result of this effort is a report documenting dynamic interface problems associated with the CH-46, CH-47, Heavy Lift Helicopter (HLH), and the YUH-61A. The ultimate benefit will be the accumulation of data that will eventually lead to a solution of generic problems of this type. This report is one of five reports resulting from engine/airframe/drive train dynamic interface documentation efforts funded by the Applied Technology Laboratory. The related reports and their final report numbers are: Boeing Vertol, USARTL-TR-78-11; Hughes Helicopters, USARTL-TR-78-12; Sikorsky Aircraft, USARTL-TR-78-13; Kaman Aerospace, USARTL-TR-78-14; and Bell Helicopter, USARTL-TR-78-15.

Mr. Allen C. Royal, Propulsion Technical Area, Technology Applications Division, served as the Project Engineer for this effort.

UNCLASSIFIED

SECURITY CLASSIFICATION OF THIS PAGE (When Data Entered)

REPORT DOCUMENTATION PAGE

READ INSTRUCTIONS BEFORE COMPLETING FORM

1. REPORT NUMBER: USARTL-TR-78-11	2. GOVT ACCESSION NO.
3. RECIPIENT'S CATALOG NUMBER	
4. TITLE (and Subtitle): ENGINE/AIRFRAME/DRIVE TRAIN DYNAMIC INTERFACE DOCUMENTATION	5. TYPE OF REPORT & PERIOD COVERED: FINAL REPORT
6. PERFORMING ORG. REPORT NUMBER: D210-11328-1	
7. AUTHOR(s): D. A./Richardson, J. R./Alwang	8. CONTRACT OR GRANT NUMBER(s): DAAJ02-77-C-0040
9. PERFORMING ORGANIZATION NAME AND ADDRESS: BOEING VERTOL COMPANY, P.O. Box 16858, Philadelphia, Pa., 19142	10. PROGRAM ELEMENT, PROJECT, TASK AREA & WORK UNIT NUMBERS: ~~62209A~~ 1L262209AH76 00 203 EK
11. CONTROLLING OFFICE NAME AND ADDRESS: APPLIED TECHNOLOGY LABORATORY, U.S. Army Research and Technology Laboratories (AVRADCOM), Ft.Eustis,Va.23604	12. REPORT DATE: April 1978
	13. NUMBER OF PAGES: 208
14. MONITORING AGENCY NAME & ADDRESS (if different from Controlling Office)	15. SECURITY CLASS. (of this report): Unclassified
	15a. DECLASSIFICATION/DOWNGRADING SCHEDULE

16. DISTRIBUTION STATEMENT (of this Report)

Approved for public release; distribution unlimited.

17. DISTRIBUTION STATEMENT (of the abstract entered in Block 20, if different from Report)

18. SUPPLEMENTARY NOTES

19 KEY WORDS (Continue on reverse side if necessary and identify by block number)

Helicopter	Vibration	Fuel Control
Engine	Oscillation	
Drive Train	Stability	
Airframe	Torque	
Dynamics	Stall	

20. ABSTRACT (Continue on reverse side if necessary and identify by block number)

Engine/airframe/drive train dynamic interface problems of Boeing helicopters are described. The investigation leading to the problem solution, the solution, and its limitations are discussed. Forecasts of potential future problems, recommendation for investigations, and specifications are included.

DD FORM 1 JAN 73 1473 EDITION OF 1 NOV 65 IS OBSOLETE

403 682

UNCLASSIFIED

SECURITY CLASSIFICATION OF THIS PAGE (When Data Entered)

TABLE OF CONTENTS

	Page
LIST OF ILLUSTRATIONS	4
LIST OF TABLES	8
INTRODUCTION	9
DESCRIPTION OF THE PROBLEMS, INVESTIGATIONS AND SOLUTIONS	
CH-46	
Engine Vibration	11
Excessive Torque during Rotor Startup	41
CH-47	
Torque Oscillation	49
Cracking of Engine Inlet Housing	63
HLH	
Demonstration of the Engine Control Rotor Drive System Dynamic Stability	77
HLH/DSTR Torque Oscillation	116
YUH-61A	
Engine Mounting	138
Nonsynchronous Whirl	159
Engine Stall	168
Slow Return from Overspeed	185
Rotor Speed Excursion in Maneuvers not Requiring Collective Pitch Changes	186
Lack of Precise Hover Height Control	188
Fuel Control Dynamics	191
A FORECAST OF POTENTIAL FUTURE DYNAMIC INTERFACING PROBLEMS AND RECOMMENDATIONS FOR INVESTIGATION/ANALYTICAL TESTING EFFORT TO ACHIEVE AN IMPROVED UNDERSTANDING OF THE PROBLEMS AND POTENTIAL SOLUTIONS	196
RECOMMENDATIONS FOR ENGINE/AIRFRAME/DRIVE TRAIN SPECIFICATIONS GOVERNING DYNAMIC INTERACTION	203
SUMMARY OF PROBLEMS LISTED CHRONOLOGICALLY	204
BIBLIOGRAPHY	205
SYMBOLS AND ABBREVIATIONS	206

LIST OF ILLUSTRATIONS

Figure		Page
1	Engine Drive Shaft Assembly.	12
2	Aft Pylon Test Rig	14
3	Drive System Schematic	14
4	Engine Mount Bearing Locations	15
5	0% Torque Location 1-Amplitude and Phase of Shaft Response	18
6	0% Torque Location 2-Amplitude and Phase of Shaft Response	19
7	0% Torque Location 3-Amplitude and Phase of Shaft Response	20
8	0% Torque Location 4-Amplitude and Phase of Shaft Response	21
9	0% Torque Location 5-Amplitude and Phase of Shaft Response	22
10	High Speed Shaft Mode Shape.	23
11	Impedance Change with Frequency.	24
12	Frequency Shift of Points of Maximum Response with Increased Torque	25
13	Frequency Shift with Increased Torque.	26
14	Impedance Change with Frequency.	27
15	Engine Lateral Acceleration.	29
16	Torque Tube Lateral Acceleration	30
17	Engine Crotch Lateral at 325 Hz.	31
18	Aft Torque Tube Lateral - 325 Hz	32
19	Engine Crotch Lateral - 325 Hz.	33
20	Aft Torque Tube Lateral - 325 Hz	34
21	Coupling Bolt Torque Effect.	35
22	Coupling Bolt Torque Effect.	36
23	Curvic Coupling Tip vs Vibration	37
24	Spacer Evaluation.	39
25	Curvic Spacer Evaluation	40
26	Rotor Startup.	42

LIST OF ILLUSTRATIONS

Figure		Page
27	Rotor Startup, 30°F.	45
28	Peak Engine Torque	47
29	Drive System/Fuel Control/Engine Schematic	54
30	Lag Damper Characteristics	54
31	Fuel Control Frequency Response.	56
32	Engine Droop Schedule.	57
33	Lag Damper Schematic	61
34	Engine Mount Schematic	64
35	Baseline Engine Vibration.	66
36	Yaw Mode.	66
37	Pitch Yaw Mode.	67
38	T55-11 Compared to T55-11A	69
39	Effect of Drag Link Bolt Torque.	69
40	Effect of Drag Link Stiffness	70
41	Configuration Effect on Yaw Frequency.	71
42	Baseline 3/Rev Stress Vs RPM.	73
43	Inlet Housing Stress.	74
44	Lateral 3/Rev Engine Vibration.	75
45	Engine to Simulation Comparison	78
46	Response to 10% Rotor Load Change	80
47	Response to Collective Pitch Input.	81
48	Response to Beeper Input.	83
49	Temperature Limiting.	84
50	Power Management Control Effect	85
51	System Response to Collective	87
52	Effect of Control Lag.	88
53	Power Variation Effect	90
54	Linear Simulation Block Diagram.	91
55	Lag Damper System.	92
56	Lag Damper Equations and Constants	93
57	Lag Damper Response - 100 Ft-Lb Torque Input	94

LIST OF ILLUSTRATIONS

Figure		Page
58	Lag Damper Response - 300 Ft-Lb Torque Input. .	95
59	Lag Damper Valve Characteristics.	97
60	Standard Day Lag Damper Effect - Response to Load Change	98
61	Cold Day Lag Damper Effect - Response to Load Effect.	99
62	Simulation Transient, Effect of Isochronous Governing.	101
63	Master Beeper Transient Baseline Isochronous Governing.	102
64	Master Beeper Transient - Isochronous Governing Off.	104
65	Master Beeper Transient, Baseline (T_3=.5 sec) .	106
66	Master Beeper Transient, Reduced Lag (T_3=.15 sec) Compensation.	107
67	Isochronous Governing Switch Off Transient, Reduced Lag (T_3=.15 sec) Compensation. . . .	108
68	Effect of Compensation on Open Loop Frequency Response.	109
69	Notch Filter Compensation Frequency Response .	111
70	Master Beeper Transient, 3.0 Hz Notch Filter Compensation.	112
71	Master Beeper Transient, 2.2 Hz Notch Filter Compensation.	113
72	Master Beeper Transient, 4.0 Hz Notch Filter Compensation.	114
73	DSTR Engine Fuel System	117
74	DSTR Torsional Model	119
75	Residual Torque vs Frequency.	121
76	DSTR Torsional Analysis - Mode Shapes	122
77	Natural Frequency vs Turbine Spring Rate. . . .	123
78	DSTR Engine Engagement and Torque Spike	124
79	DSTR Clutch Disengagement and Overspeed	125
80	DSTR Torque Oscillation with One and Two Engines	126
81	DSTR Torque Oscillation without Accumulator . .	128

LIST OF ILLUSTRATIONS

Figure		Page
82	DSTR Torque Oscillation Investigation with 15-Cubic-Inch Accumulator.	129
83	15-Hz Oscillation DSTR Control with DST" Pump. .	132
84	DSTR Control with Flight Engine Pump and Plumbing.	133
85	Flight Engine Control with Flight Engine Pump and Plumbing	134
86	Flight Engine Control with Flight Engine Pump and Plumbing.	135
87	Alternating Input at High Power - Flight Engine Control, Pump and Plumbing.	136
88	Alternating Input at Idle Flight Engine Control, Pump and Plumbing.	137
89	YUH-61A/T700-GE-700 Engine Mount Configuration .	143
90	Engine Mount Analysis.	144
91	Engine Shake Test Mode Shapes.	147
92	Engine Mount Stiffness	150
93	GTV Engine Shake Test Baseline vs Final.	151
94	Spectral Analysis.	152
95	Effect of Mount Change on 4/Rev Vibration. . . .	153
96	Effect of Vibration Treatment on Engine Vibration (4/rev).	155
97	Effect of Vibration Treatment on Engine Vibration (4/rev).	156
98	Engine Vibration Survey (1/rev).	157
99	Engine Vibration Survey (8/rev).	158
100	Effect of Exhaust Duct Configuration/Weight on 240 Hz Response.	165
101	Quill Shaft Location.	166
102	No. 1 Engine Maximum Inlet Temperature Rise Encountered During IGE Decelerations	172
103	No. 2 Engine Maximum Inlet Temperature Rise Encountered During IGE Decelerations	173
104	Summary of Inlet Temperature Rises Encountered in No. 1/No. 2 Engines.	174

LIST OF ILLUSTRATIONS

Figure		Page
105	Engine Torque and Inlet Temperature Time History During Stall Event.	175
106	Compressor Stall Line and Paths	177
107	Test Cell Engine Stall Results.	178
108	Effects of Fuselage Angle and Rotor Height on Ingestion.	180
109	Effect of Engine Exhaust Velocity on Ingestion.	181
110	Effect of Airspeed on Ingestion	182
111	Gain and Lag vs Frequency.	184
112	Effect of Control Gain.	187
113	Fuel Control Schematic.	189

LIST OF TABLES

Table		Page
1	Measured System Tolerances.	16
2	Summary of Drive System Torsional Natural Frequencies.	118
3	GTV Engine Shake Test Configurations Evaluated.	149
4	Mounting Springs	149
5	Comparison of GTV and Test Cell Data.	162
6	Comparison of Vibration Characteristics of Eight Duct Configurations.	163
7	Electronic Control Unit Comparison.	194

INTRODUCTION

This document describes engine/airframe/drive train dynamic interface problems experienced by the Boeing Vertol Company in the past decade. The problems are grouped in sections by helicopter model.

The CH-46 and CH-47 are tandem rotor twin-engine helicopters. The former uses General Electric T58 engines and the latter T55 Lycoming engines. The YUH-61A is a single main rotor helicopter powered by two General Electric T700 engines.

The HLH (Heavy Lift Helicopter) program was a technology development of components of a large tandem rotor helicopter. Some of these components were combined to make a dynamic system test rig (DSTR) which consisted of three Detroit Diesel Allison Division of General Motors Corporation (DDA) 501-M62B free turbine engines, driving a 92-foot-diameter aft rotor through a combining transmission and aft transmission with interconnecting shafting. These components were mounted on a boiler plate framework not simulating flight airframe dynamics. A power absorber was provided to permit simulation of the power absorption of the forward rotor. The integration of these components provided the means to evaluate the engine drive train/rotor interfaces.

The engine control system for the DSTR is composed of three main units: a single power management control serving the three engines and an engine electronic control, and a hydromechanical fuel control for each engine. The power management control incorporates isochronous or constant rotor speed governing and automatic load sharing between the engines and processes torquemeter signals for output display. The engine electronic control provides proportional power turbine speed governing, power turbine inlet temperature and overspeed limiting, automatic start sequencing, and gas generator speed signal conditioning. The hydromechanical fuel control schedules gas generator speed, compressor variable geometry, and acceleration and deceleration transients. This unit also limits fuel flow and gas generator speed and includes both mechanical and electrical fuel shutoff.

The electronic portions of the control system were designed specifically for the DSTR engines and are functionally similar to HLH prototype hardware.

While all the problems described were resolved, their solution involved significant expenditures by the Government, the Boeing Vertol Company, and the three engine manufacturers. In an effort to use this past experience to prevent or reduce cost of resolution of future problems, a section is included forecasting future dynamic interfacing problems and suggesting efforts that may lead to a better understanding of the dynamic interfaces.

CH-46

PROBLEM - ENGINE VIBRATION

Engine vibration at power turbine/drive shaft frequency (19,500 rpm or 325 Hz) exceeded allowable limits with newly installed shafts on numerous occasions. An investigation was undertaken in 1967.

Description of the Problem

The drive system of the CH-46 helicopters includes two high-speed engine drive shafts shown in Figure 1. One of these shafts is connected between each engine and the combining transmission or mixbox. The General Electric T58 engine has the output shaft connected to the engine coupling adapter. A set of Thomas coupling plates, whose function is to correct for misalignment, joins the engine coupling adapter to the splined adapter. The main shaft body has a male spline at one end which is inserted in the female counterpart of the splined adapter and terminates with a curvic coupling. The use of the spline provides for the freedom of longitudinal motion. A curvic coupling adapter joins the shaft through another set of Thomas coupling plates to the mixbox input pinion adapter. The curvic coupling is provided to facilitate engine or transmission changes. The "balanced shaft assembly" consists of the engine coupling adapter through and including the Thomas coupling plates at the mixbox end of the shaft.

The engine has the following high frequency vibration limits: maximum total vibratory displacement mils double amplitude, at frequencies above 50 cps - 3 mils up to 20,000 rpm (333 cps) decreasing linearly to 1.5 mils at 26,800 rpm (447 cps). The measurement locations specified by General Electric are at engine stations 200.00, 232.00, and 239.75. These correspond generally to the engine forward mounting pad, power turbine flange, and the torque tube to engine attachment flange. The torque tube to engine attachment flange is usually referred to as the engine crotch and is the normal vibration monitor location. The 3-mil double amplitude is equivalent to $\pm$ 16 g at standard shaft operating speed of 325 cps. In order to minimize the possibility of high vibration, certain tolerances have been established which would ensure that vibration levels are acceptable. Prior to installation in an aircraft, the shaft assembly is balanced on a Gisholt Masterline balancing machine. The balance tolerance is given as 0.01 in-oz at 9000 rpm. This results in 6.7 lb of unbalance at the operating speed of 19,476 rpm.

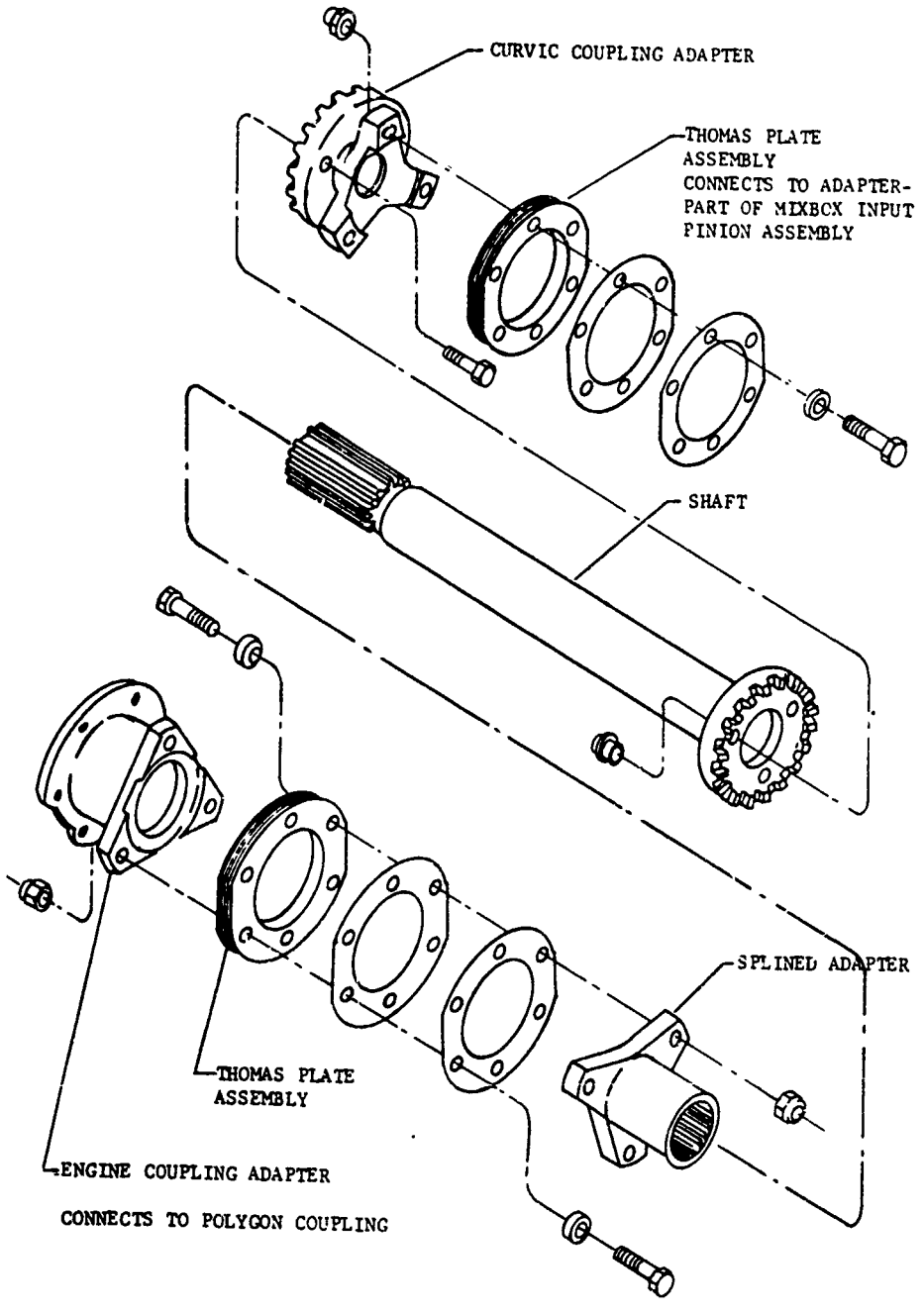

Figure 1. Engine Drive Shaft Assembly.

Despite the care taken in balancing the shaft components and assembly, when the shafts were installed in the aircraft there were numerous instances when the 16g limit was exceeded; there was no straightforward procedure for correcting the condition.

Investigation Leading to a Solution

A laboratory test was undertaken to determine the cause(s) of the problem and to establish corrective measures.

The aft section of the fuselage of a CH-46A was mounted on an I-beam support structure as shown in Figures 2 and 3. A 75-hp electric motor with a variable speed capability and a 40-hp hydraulic motor mounted in series were used to drive the transmission through the synchronizing shaft which normally drives the forward rotor (Figure 2).

The synchronizing shaft drove through the mixbox to motor the engine drive shaft and engine power turbine. In order to drive through the overrunning clutch, the system was rotated opposite to the aircraft rotational direction. General Electric balanced the power turbine rotor prior to the test series. The compressor rotor and gas generator rotor were fixed and nonrotating throughout the testing. In order to restrict airflow through the engine and, thus, reduce the drive power requirements, the intake of the engine was covered. Since there was no rotor load on the aft transmission, the system torque amounted to only about 1% of the normal operating value.

Prior to the start of testing, tolerance measurements were made on engine mount bearing wear, mixbox input pinion total indicator reading (TIR) and perpendicularity, and polygon coupling TIR and perpendicularity. An optional check on the engine to mixbox alignment was also performed. The results of these measurements, along with the allowable tolerances, are shown in Table 1. Figure 4 shows the location of all the engine mount bearings with the same numbering system employed in Table 1.

The nonrotating shake test was performed to determine the first natural lateral bending frequency and the mode shape of the high-speed shaft assembly as installed in the test article. The test was accomplished by attaching a shaker with an output of $\pm$50 lb at the midpoint of the shaft. The attachment of the shaker to the shaft increased the shaft weight by 0.5 lb.

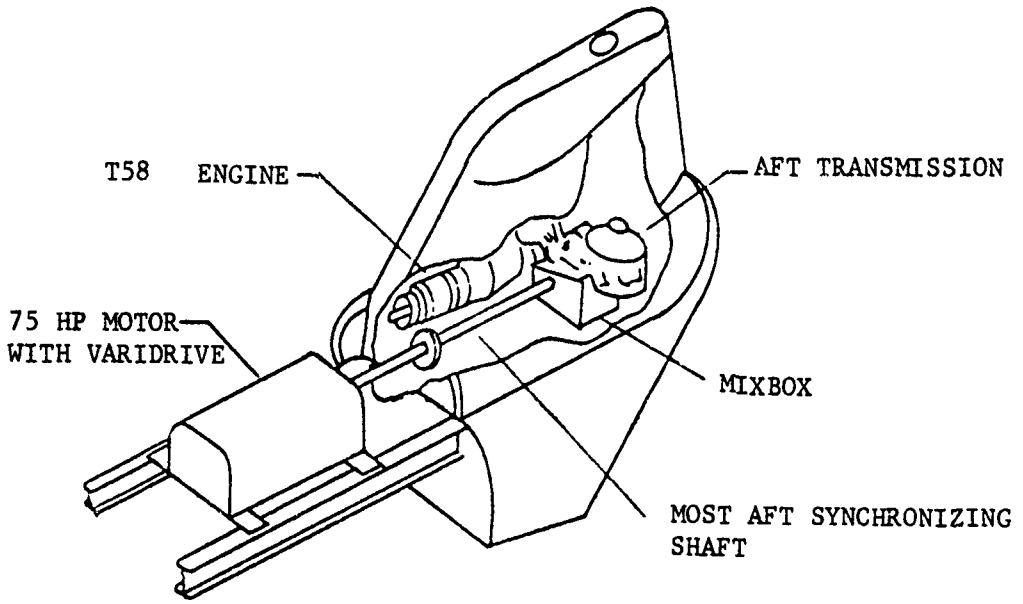

Figure 2. Aft Pylon Test Rig.

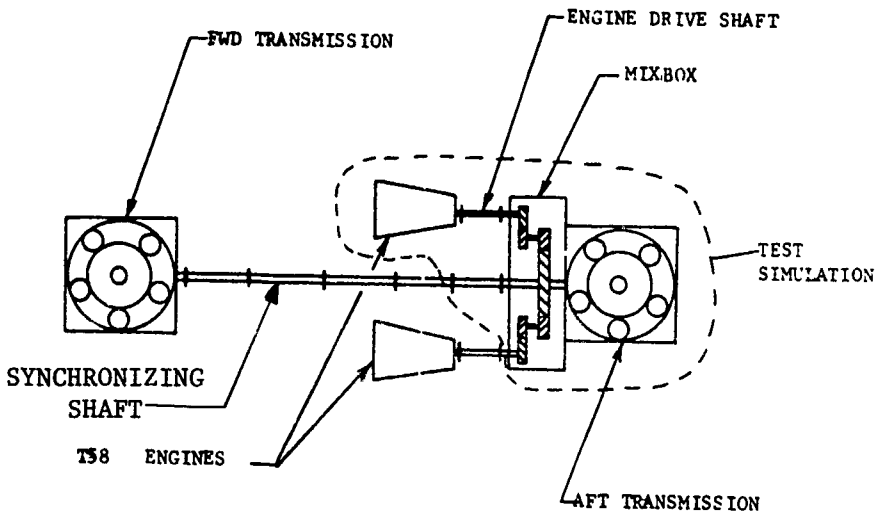

Figure 3. Drive System Schematic.

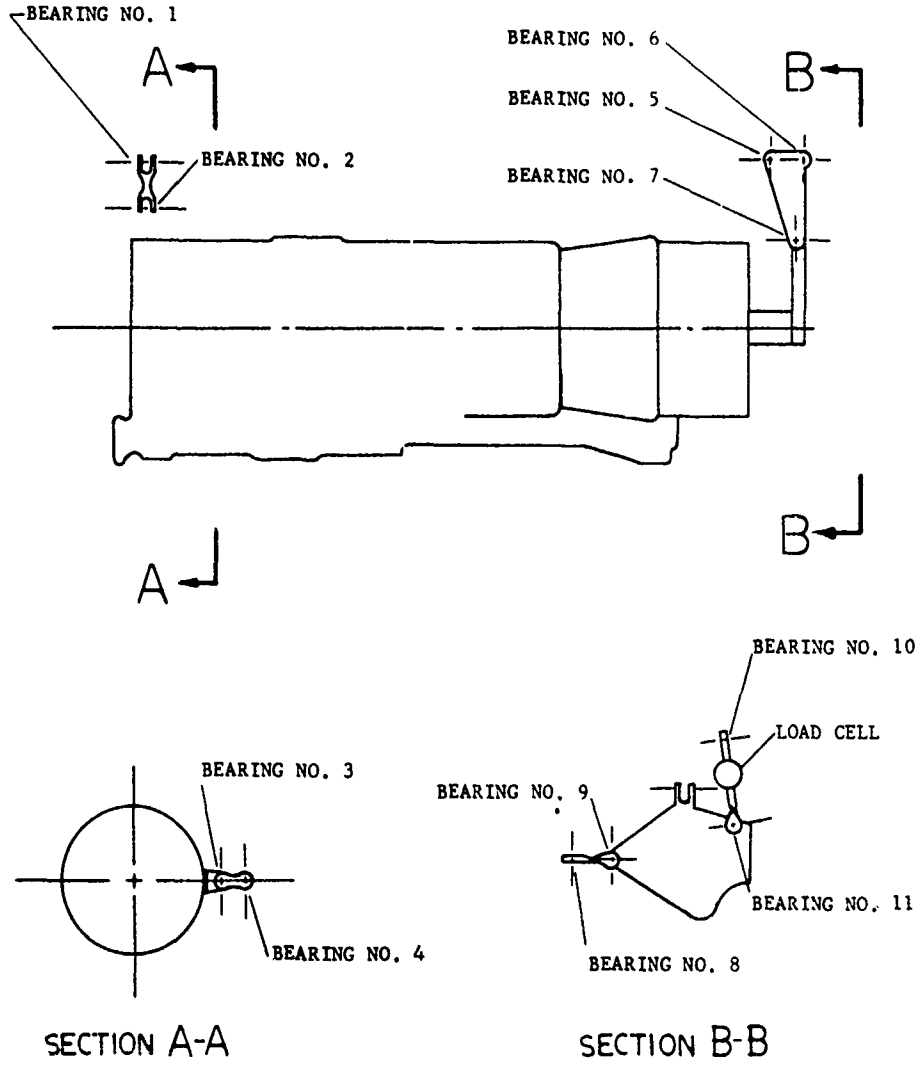

Figure 4. Engine Mount Bearing Locations.

TABLE I
MEASURED SYSTEM TOLERANCES

ENGINE MOUNT BEARINGS (SEE FIG. 4 FOR BEARING LOCATIONS)

BRG NO.	ALLOW-IN	ACTUAL	BRG NO.	ALLOW-IN	ACTUAL
1	.005	.000	7	.005	.000
2	.005	.000	8	.005	.001
3	.005	.000	9	.005	.000
4	.005	.000	10	.005	.001
5	005	.001	11	.005	.001
6	005	.000			

MIXBOX INPUT PINION

T.I.R. IN.		PERPENDICULARITY	
ALLOW	ACTUAL	ALLOW	ACTUAL
.003	.0011	None	.0000

ENGINE COUPLING ADAPTER

T.I.R. IN.		PERPENDICULARITY	
ALLOW	ACTUAL	ALLOW	ACTUAL
.0043	.C016	None	.0010

ENGINE TO MIXBOX ALIGNMENT

ALIGNMENT	
ALLOW	ACTUAL
0°-24'	0°-14'

A strain-gaged force link connected the shaker to the shaft. With the force held constant, a logarithmic frequency sweep was made from 35 cps to 750 cps. The shaft response was measured by accelerometers on the force link and on the shaft. The accelerometer outputs went directly and also through a phase meter to a plotter so that amplitude and phase were recorded. Figures 5 through 9 show the results. Figure 10 shows the locations used for the accelerometer and the mode shapes at amplitude data. In addition, a velocity mechanical impedance plot was generated where the impedance is simply the input force divided by the velocity of response (if the input force is constant this is equal to a constant divided by the velocity). This confirmed the selection of 190, 290, and 425 as the significant frequencies (Figure 11).

The power turbine was restrained and a static torque was applied to the shaft. An accelerometer was attached to the shaft near the midpoint. The static torque was applied in increments of about 5% with a frequency sweep from 35 to 350 cps made at each torque setting. Figure 12 shows the accelerations measured. Figure 13 is a plot of the peak accelerations identified on Figure 12 as "A", "B", or "C".

This shows significant "stiffening" effect of torque. Limitations of the test equipment prevented going to torques greater than 30%. Since it was not possible to mount a pickup on the shaft during the rotating portion of the test, a static position must be selected to monitor shaft response with the response of the static position closely matching that of the shaft itself. A velocity transducer was mounted at the engine crotch in the lateral direction, the normal GE monitor position. With a static torque of 5%, a frequency sweep was made and the velocity response at the engine crotch was recorded. From this, a velocity impedance plot was generated (Figure 14) and compared with the shaft response. The engine crotch response compares favorably with the shaft response; therefore, during the rotating portion of the test, the engine crotch pickup was the primary reference of shaft behavior. The torque on the shaft during all tests with rotation was less than 10% of normal operating torque.

The imbalance in the shaft assembly as installed in the test rig was minimized. This was done by measuring the effect of a known weight and location on the azimuth and magnitude of the shaft motion, making a vector plot, and determining the correct weight and location for balance. This balancing was done at the normal rpm (19,500) at each end of the shaft.

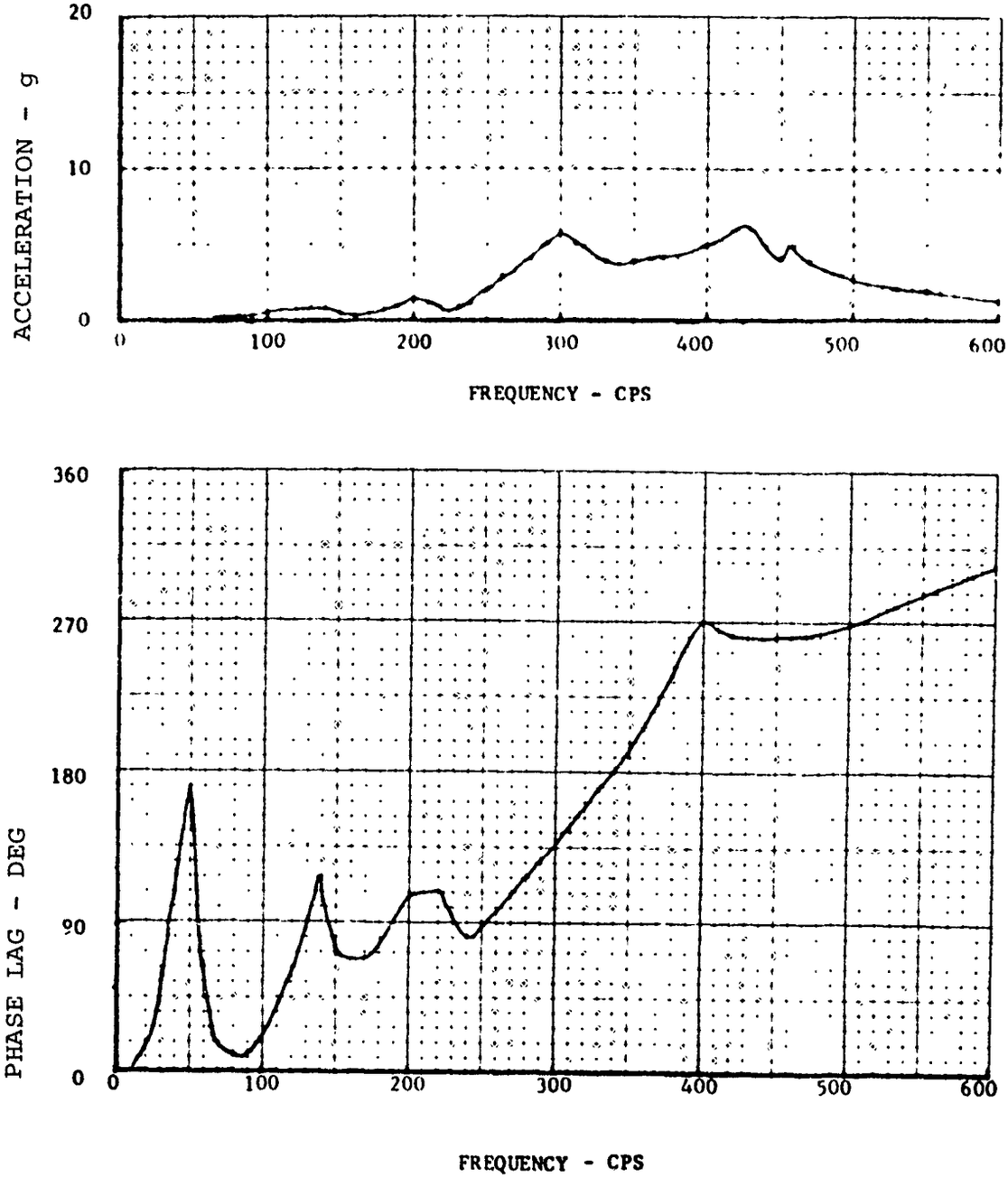

Figure 5. 0% Torque Location 1 - Amplitude and Phase of Shaft Response.

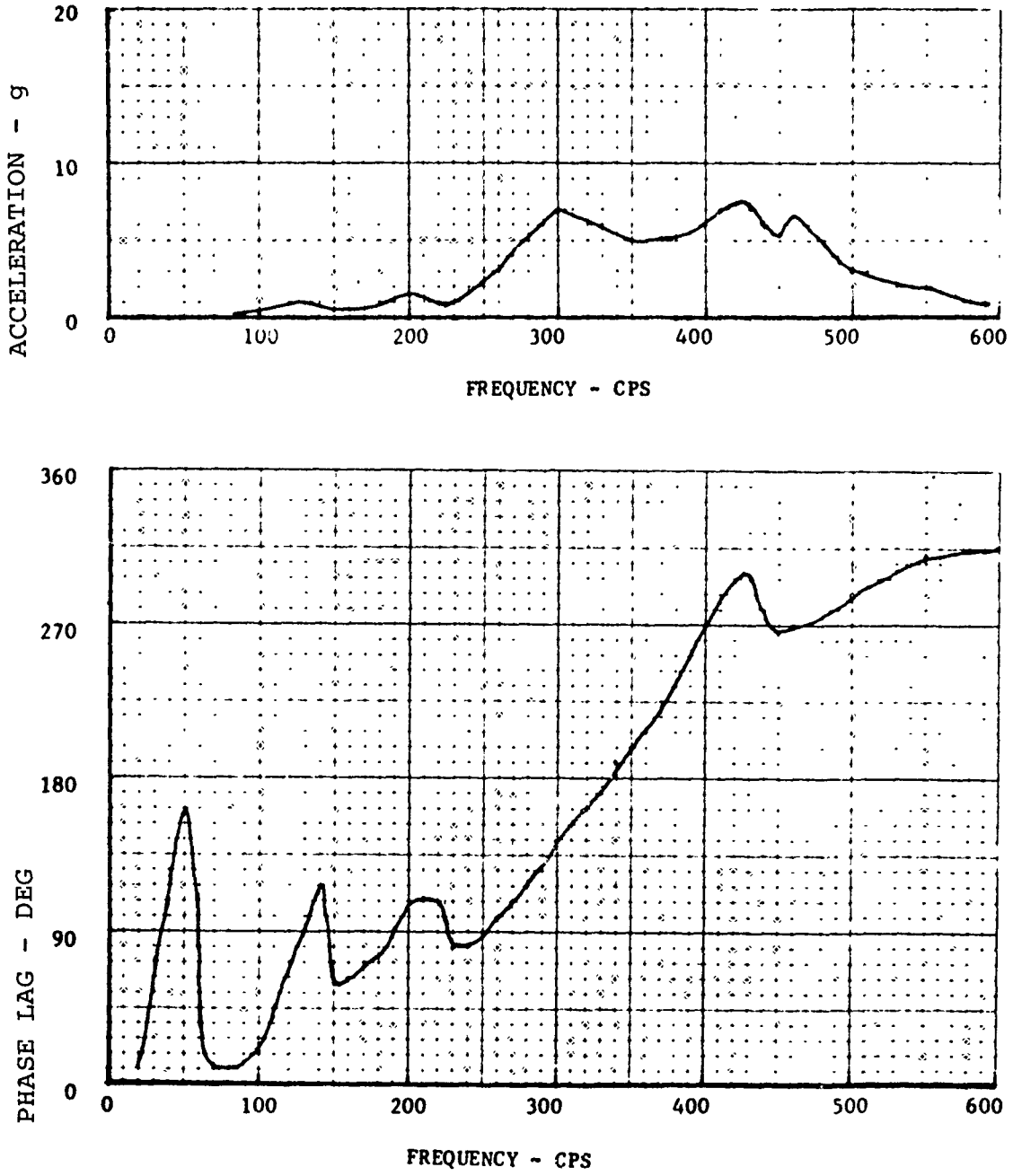

Figure 6. 0% Torque Location 2 - Amplitude and Phase of Shaft Response.

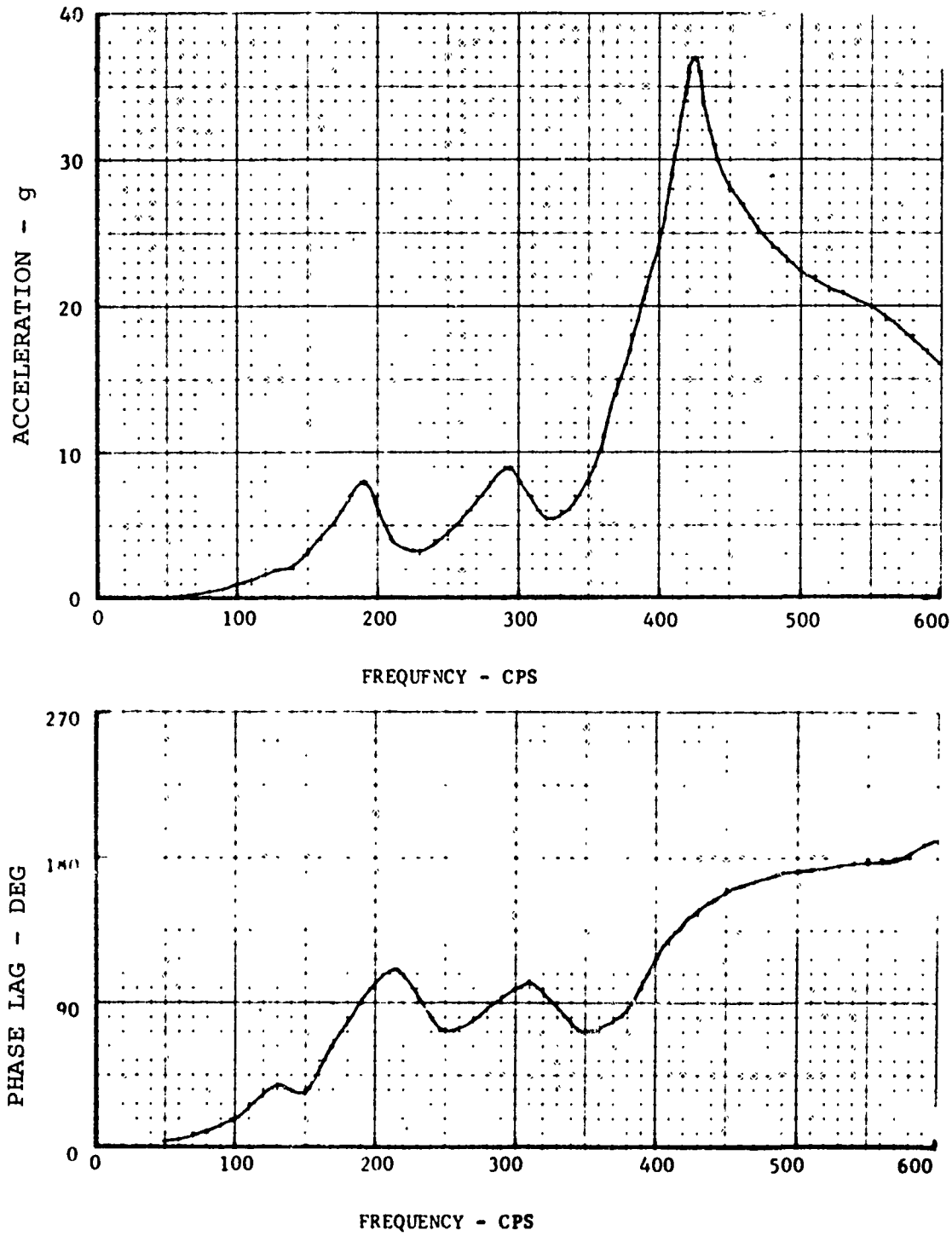

Figure 7. 0% Torque Location 3- Amplitude and Phase of Shaft Response.

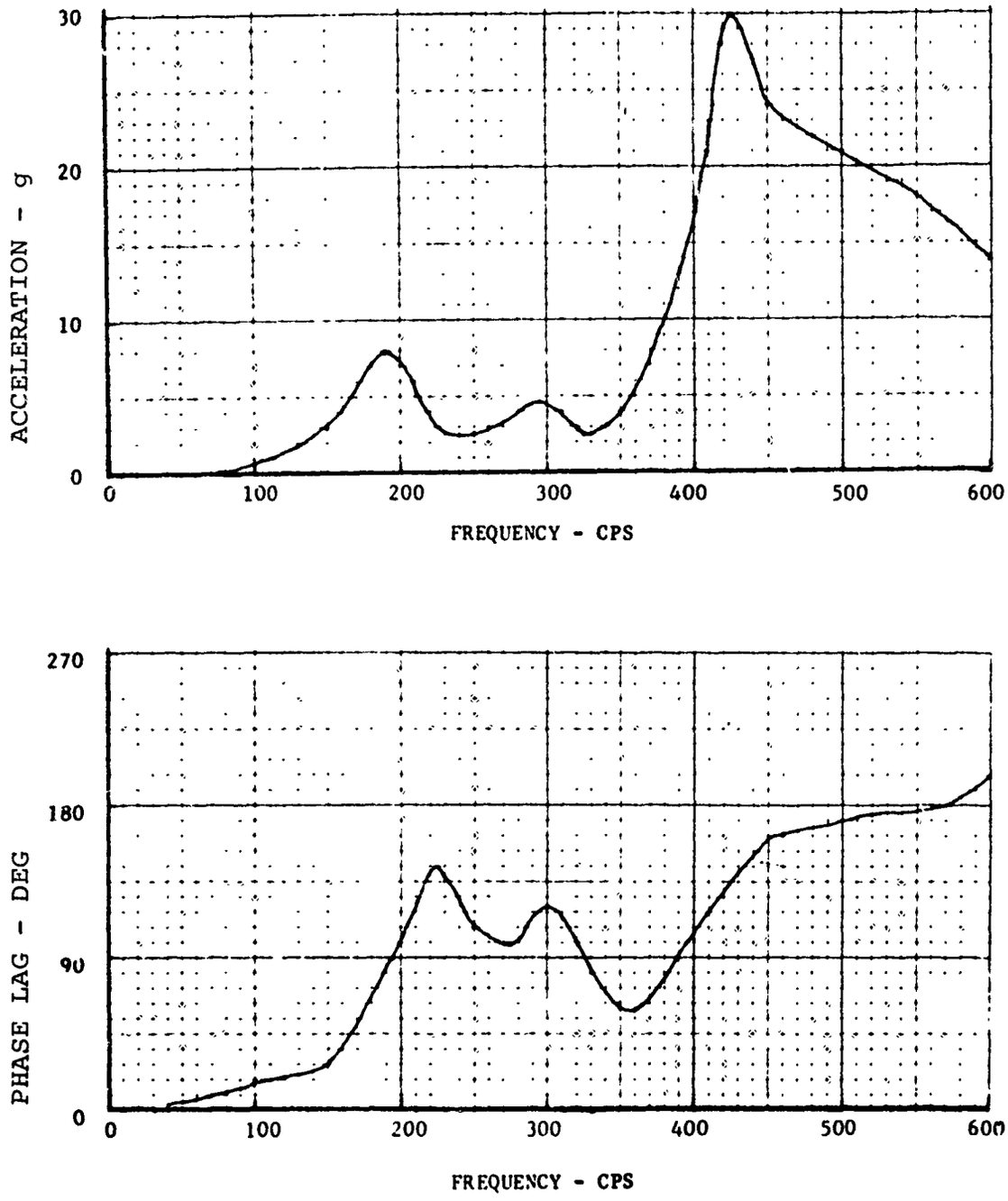

Figure 8. 0% Torque Location 4 - Amplitude and Phase of Shaft Response.

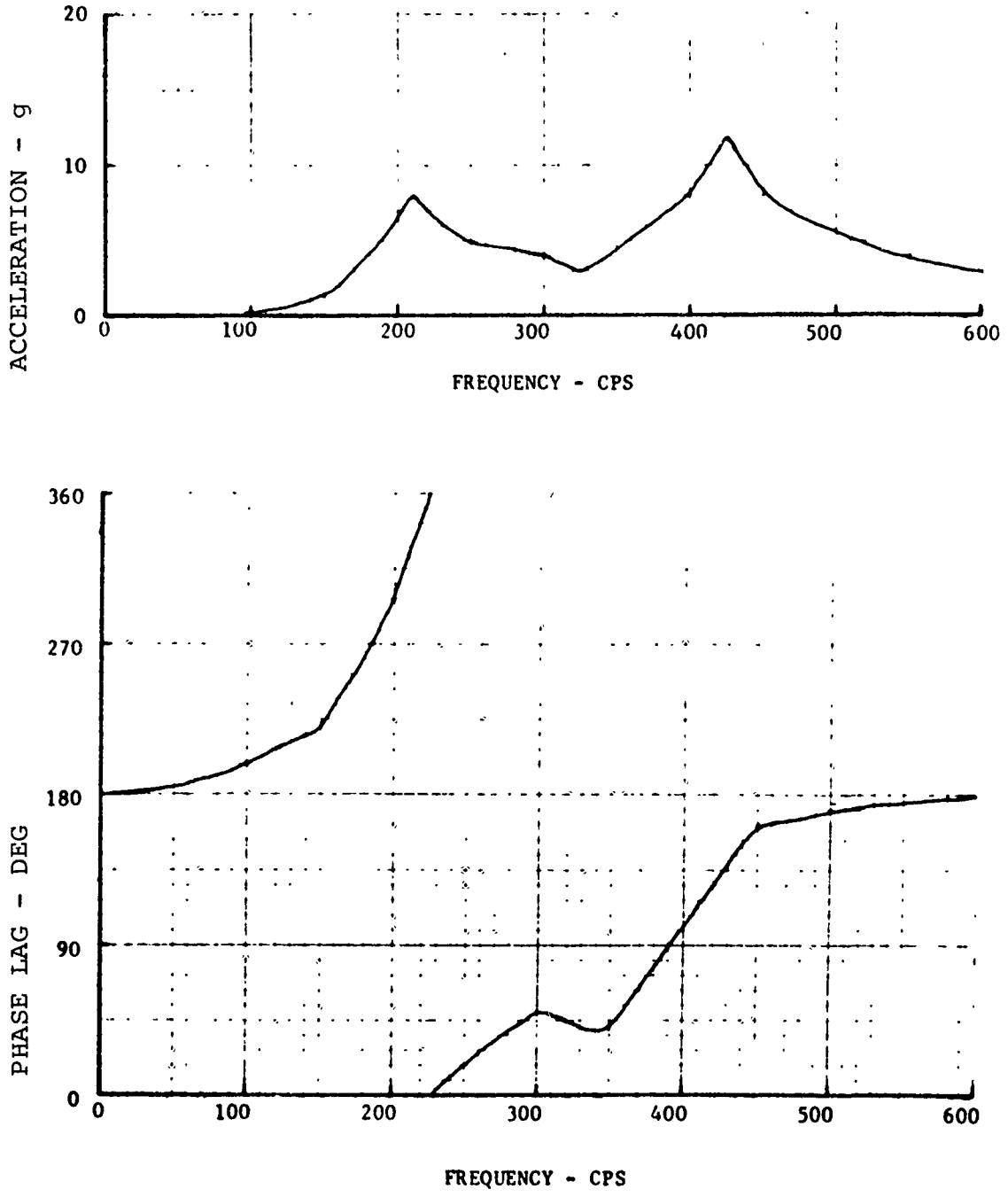

Figure 9. 0% Torque Location 5 - Amplitude and Phase of Shaft Response.

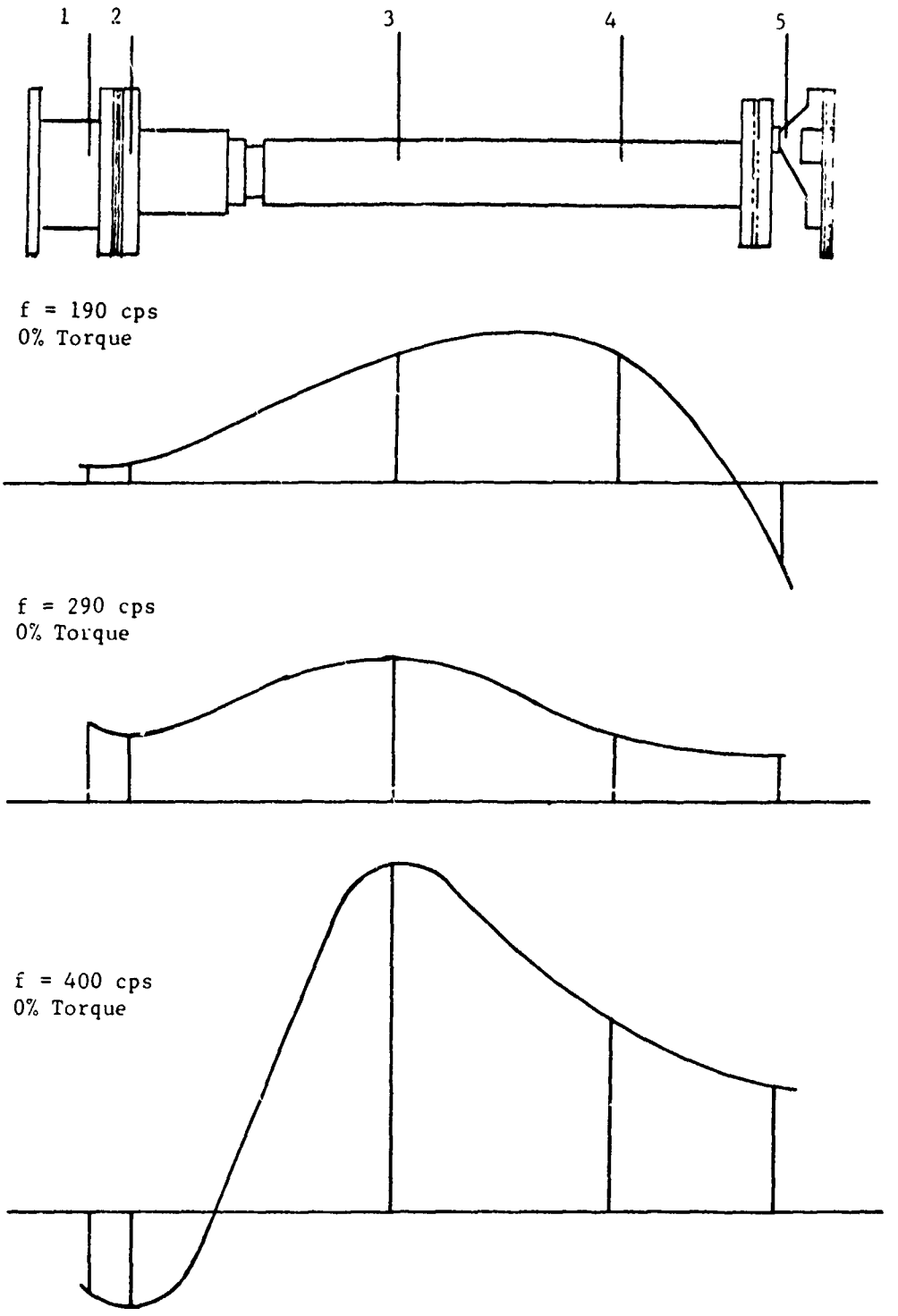

Figure 10. High Speed Shaft Mode Shape.

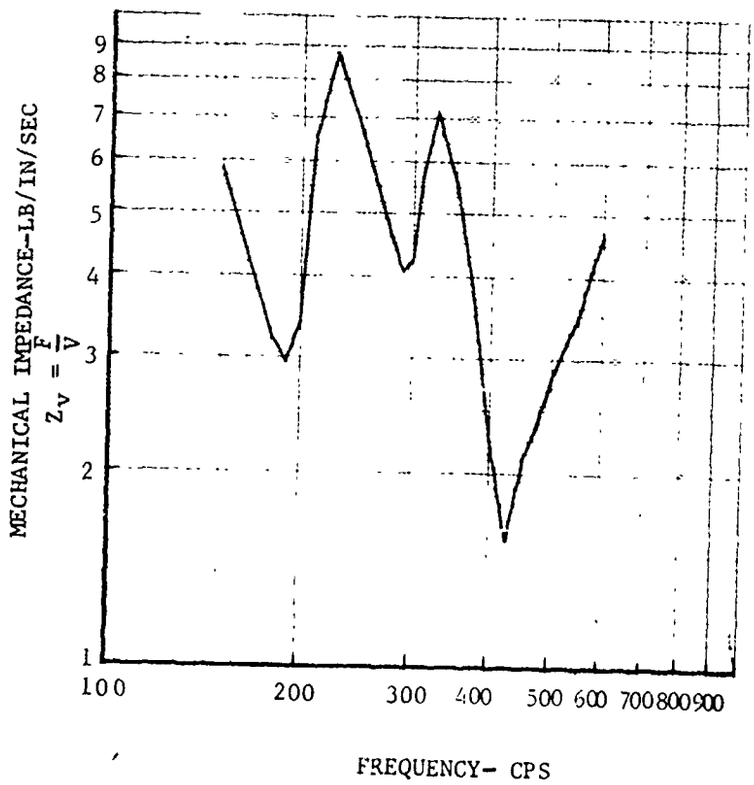

VARIATION IN MECHANICAL IMPEDANCE, Z_v, WITH CHANGES IN FREQUENCY

0% TORQUE LOCATION 3

Figure 11. Impedance Change with Frequency.

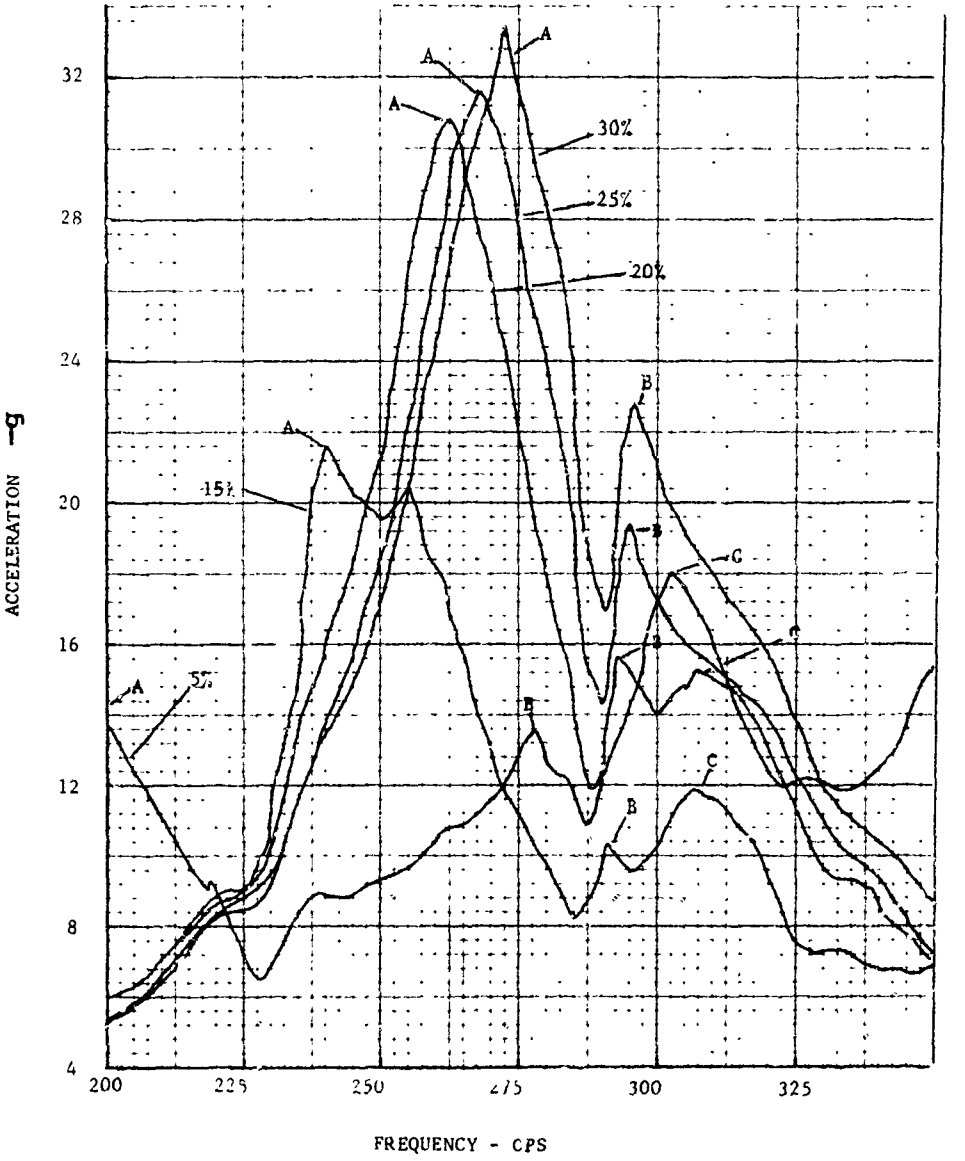

Figure 12. Frequency Shift of Points of Maximum Response with Increased Torque.

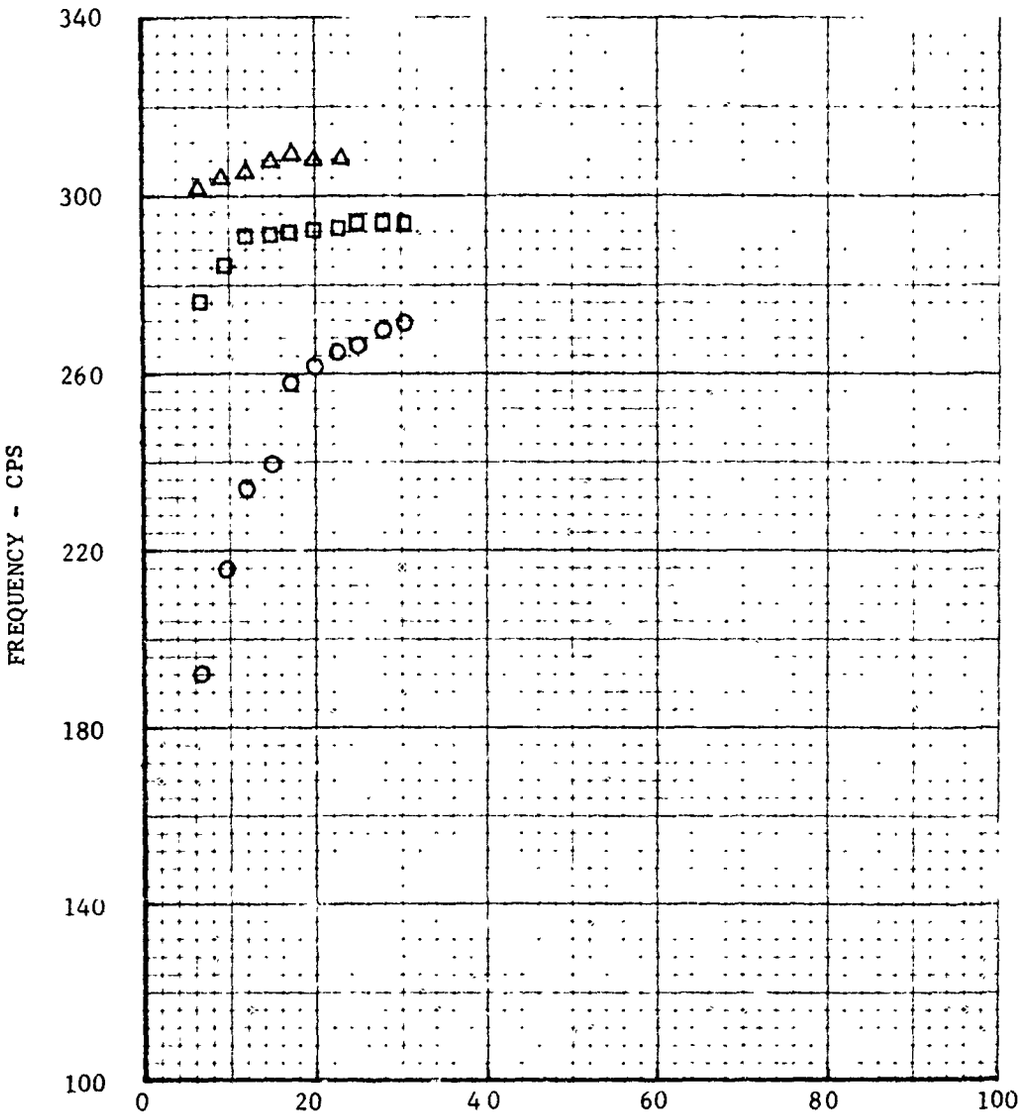

100% Torque = Max. single-engine torque T58GE-10

Frequency of points of maximum response

○ Peak A

□ Peak B

△ Peak C

Figure 13. Frequency Shift with Increased Torque,

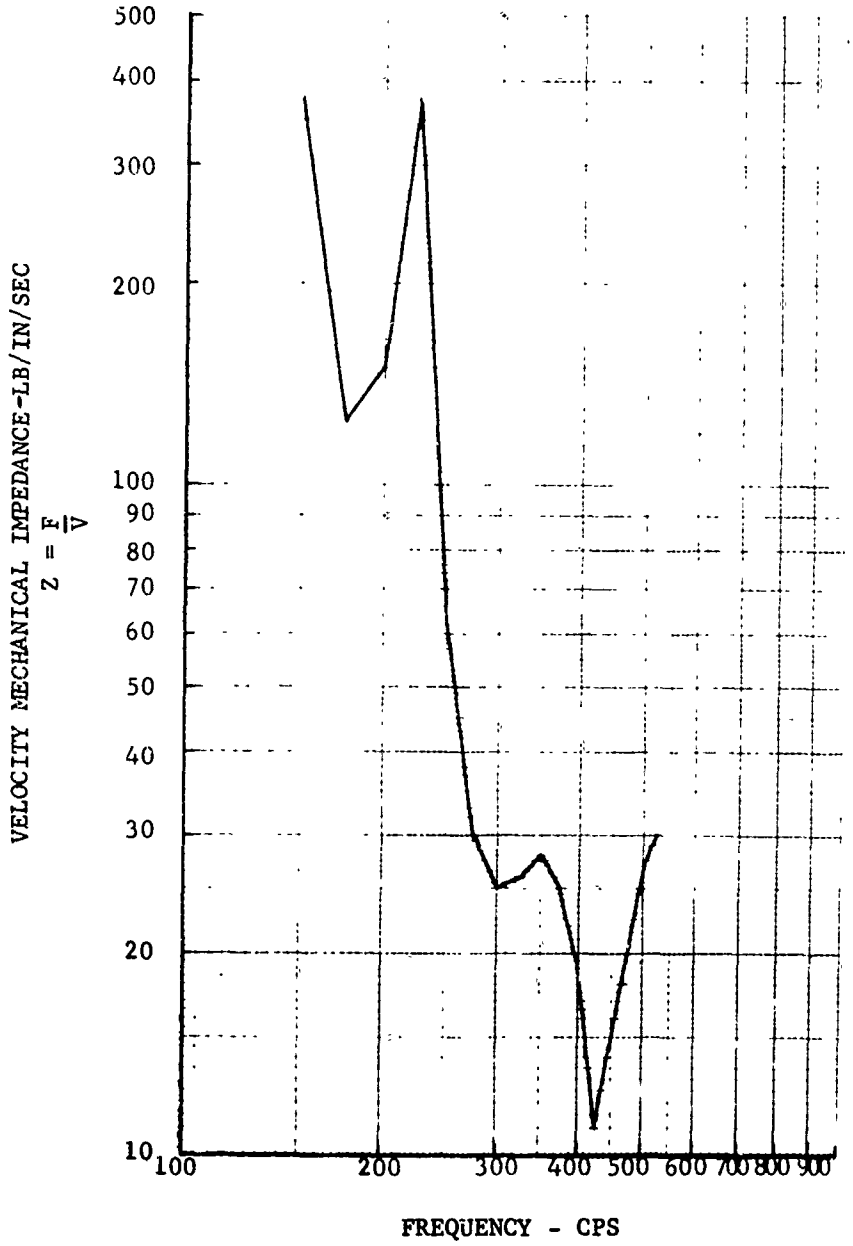

IMPEDANCE VARIATION WITH FREQUENCY CHANGE
AT 5% TORQUE AS MEASURED AT THE ENGINE CROTCH

Figure 14. Impedance Change with Frequency.

The effect of mass imbalance was then measured. Weights were added to the input pinion adapter curvic coupling and engine coupling bolts. Each location was evaluated separately with increasing weight added in the same azimuthal location on successive runs.

With the balanced shaft, the lateral responses at the engine and at the transmission were $\pm$ 1g and $\pm$ .5g. Vertical response at both locations was $\pm$ .25g. The effects at the engine and at the transmission of unbalancing the shaft at the transmission are shown in Figures 15 and 16. Similar data on unbalance at the engine end of the shaft and at the curvic coupling are shown in Figures 17, 18, 19 and 20. Unbalance at the curvic coupling produced higher "g" levels than unbalance at the other locations.

There are five sets of bolts which are part of the rotating shaft assembly: engine coupling adapter to Thomas coupling, Thomas coupling to splined adapter, curvic coupling, curvic coupling adapter to Thomas coupling, and Thomas coupling to input pinion adapter (Figure 1). The investitation of the effect of improper torque applied to some of these bolts constituted the succeeding portion of the test program. Having either one or two of the input pinion adapter bolts undertorqued by 50% had no effect on shaft vibration level as mreasured at the engine crotch and aft torque tube.

A similar test with undertorqued bolts at the engine adapter also had no effect on shaft vibration.

Unlike the previous couplings, the curvic coupling proved to be very sensitive to changes in bolt torque and torquing sequence. Numerous combinations of torque were evaluated in an attempt to correlate bolt torque with crotch acceleration. Figures 21 and 22 show the results. This one variable can be responsible for the total allowable "g" level.

It was presumed that the torque variations were causing the curvic coupling to cock. If this were true, the TIR as measured at the curvic coupling should be related to the vibration level. Since the TIR at each condition had been recorded, the data was reviewed from this aspect.

A plot of the TIR of the curvic coupling compared with crotch acceleration measured at operating speed is shown in Figure 23. It can be seen that there is a linear relationship, allowing for some degree of scatter, between the vibration and TIR. A TIR of .005 or .006 in. would be sufficient to cause the GE limit to be exceeded. The tolerance at the time of the balancing operation is .004 in.

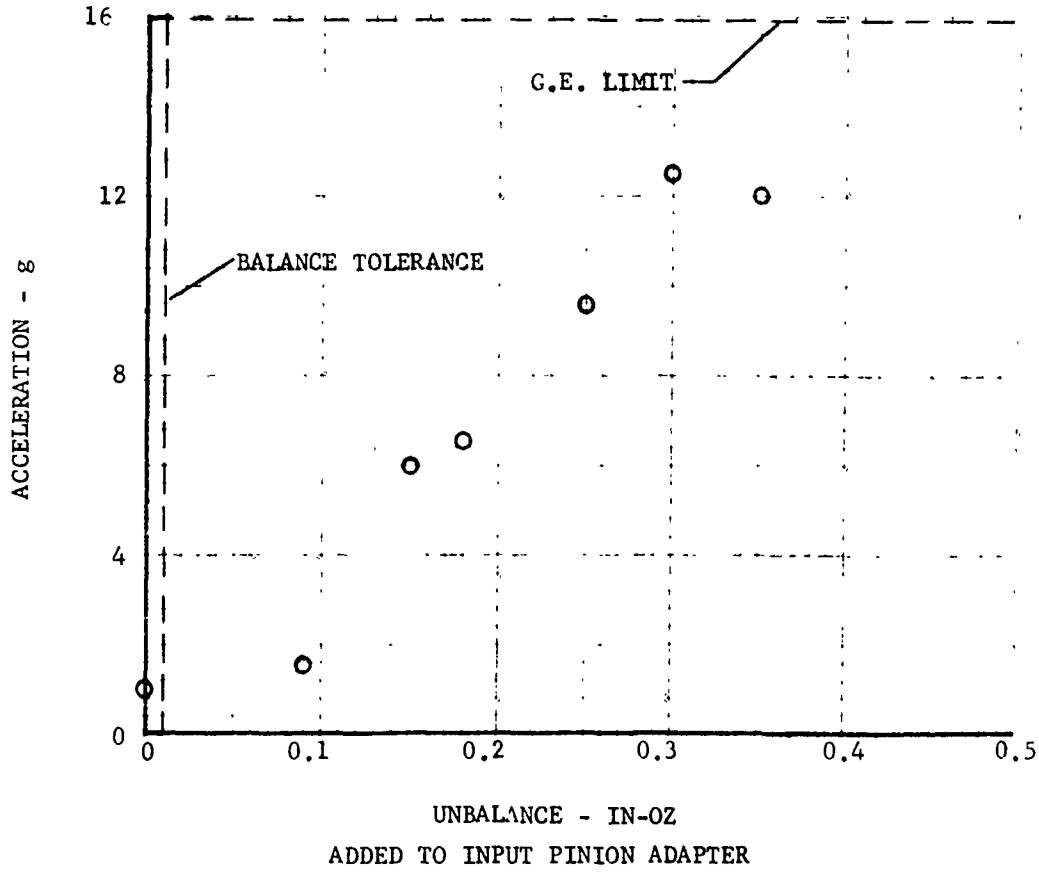

ENGINE CROTCH LATERAL ACCELERATION WITH
INCREASED UNBALANCE AT INPUT PINION ADAPTER
325 CPS

Figure 15. Engine Lateral Acceleration.

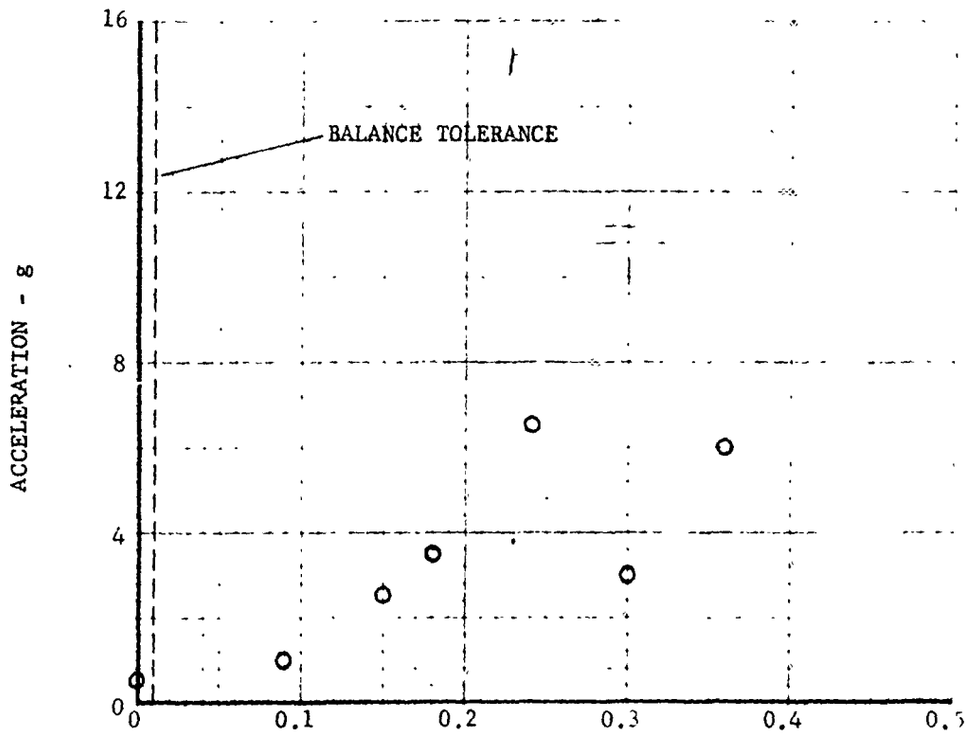

Figure 16. Torque Tube Lateral Acceleration.

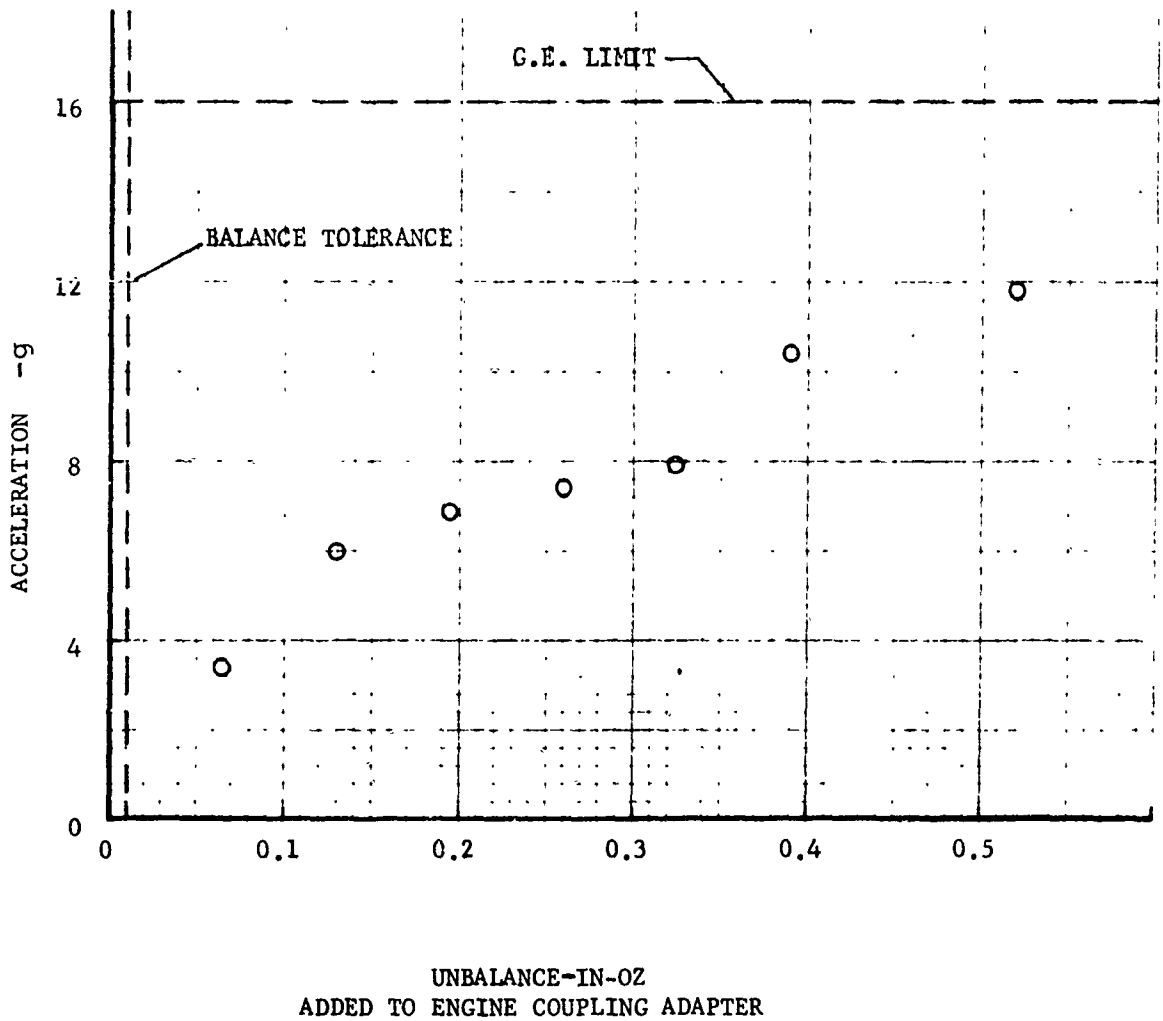

Figure 17. Engine Crotch Lateral at 325 Hz.

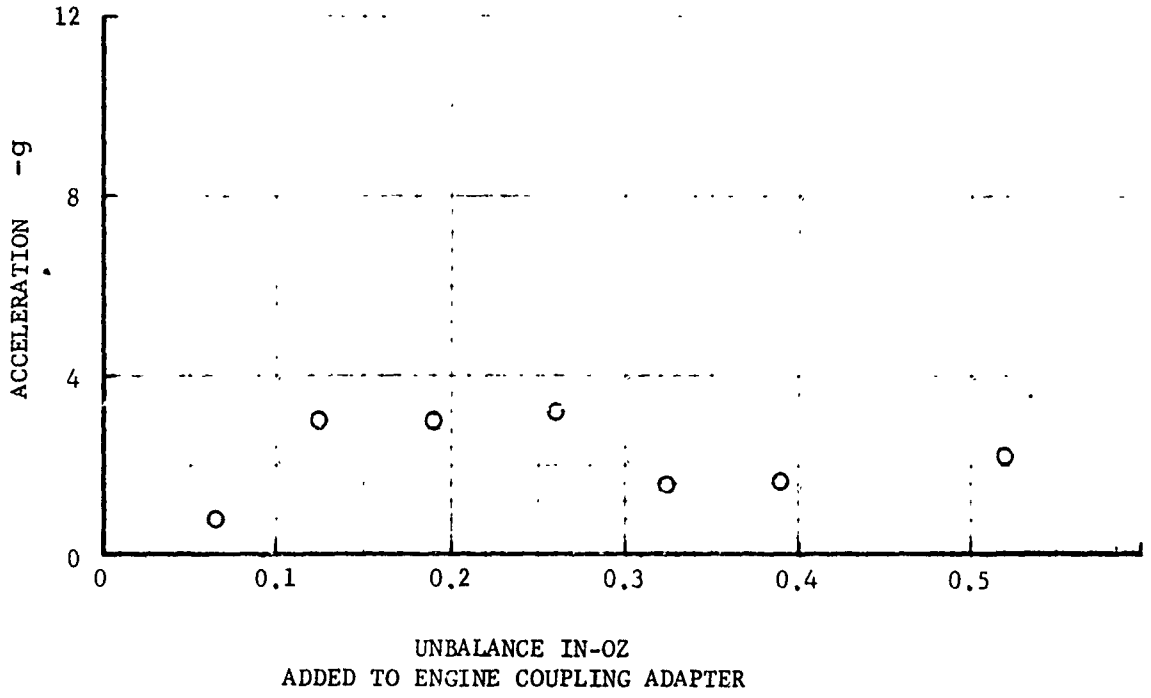

Figure 18. Aft Torque Tube Lateral - 325 Hz.

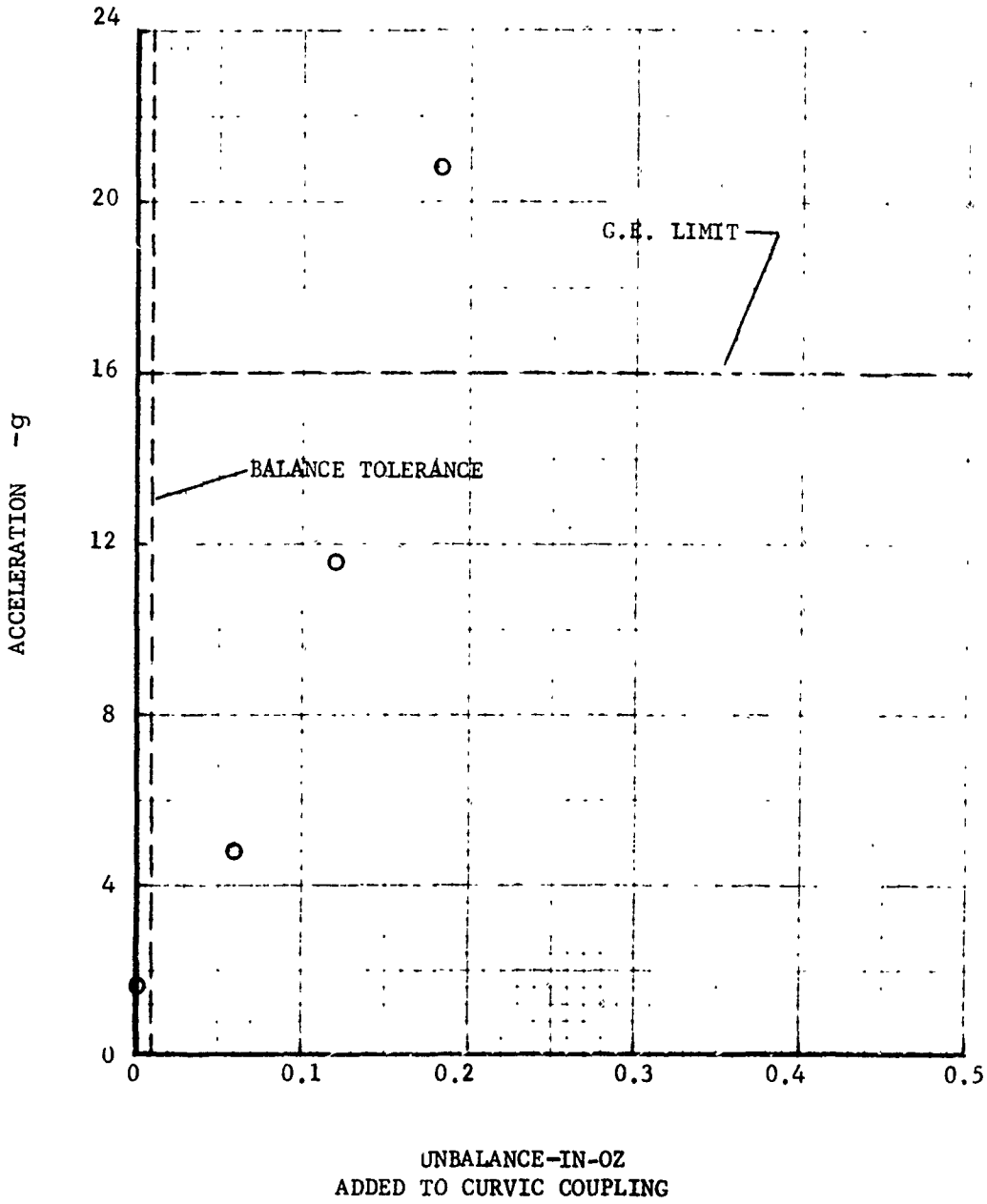

Figure 19. Engine Crotch Lateral - 325 Hz.

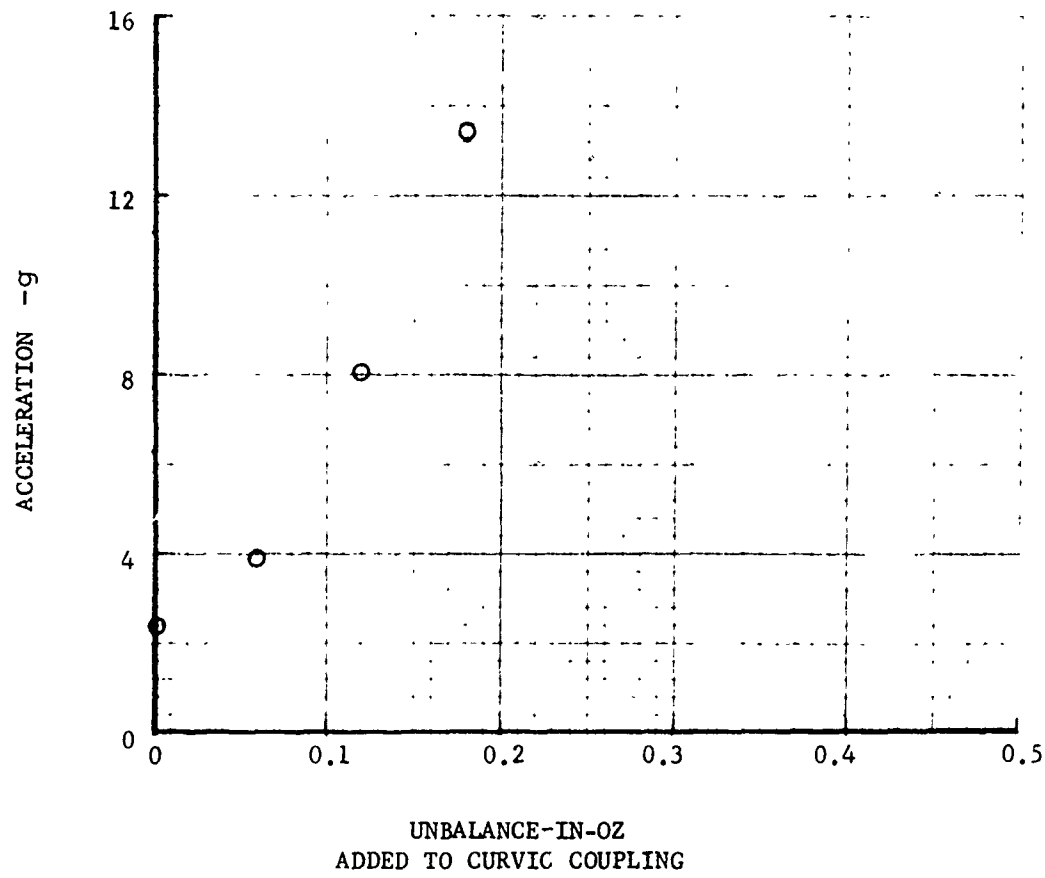

Figure 20. Aft Torque Tube Lateral - 325 Hz.

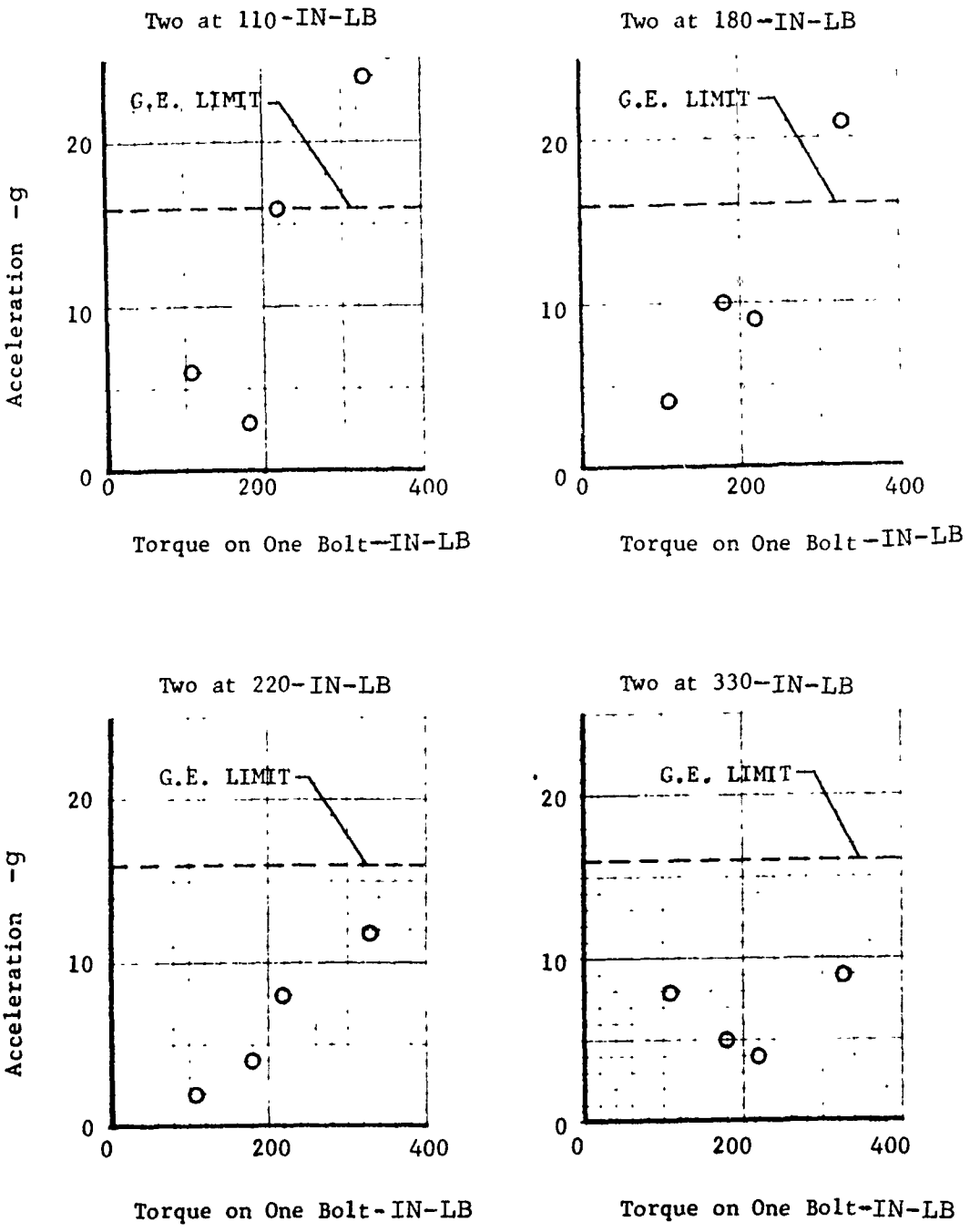

Figure 21. Coupling Bolt Torque Effect,

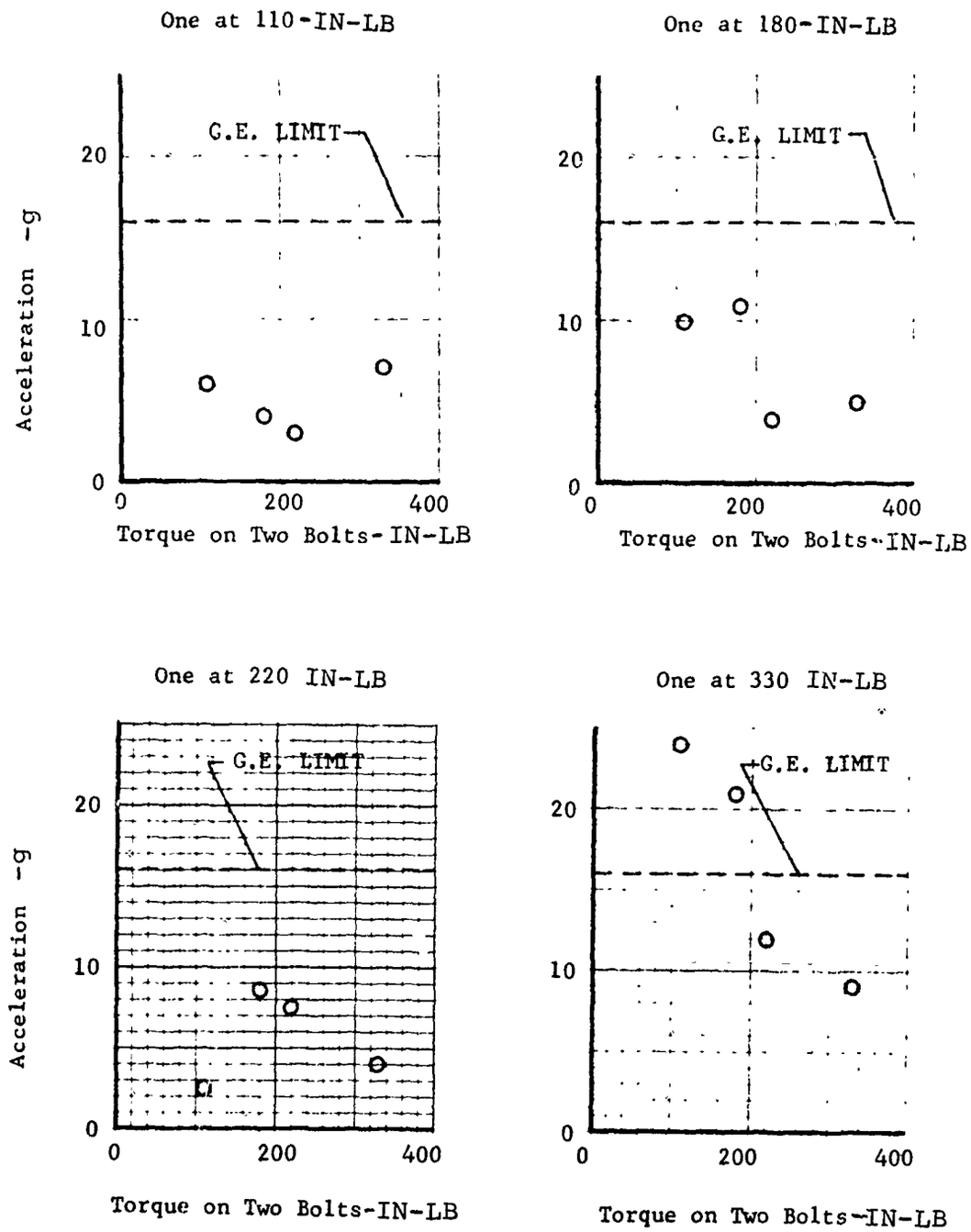

CURVIC COUPLING BOLT TORQUE EFFECT ON ENGINE CROTCH VIBRATION

ONE BOLT HELD CONSTANT

Figure 22. Coupling Bolt Torque Effect.

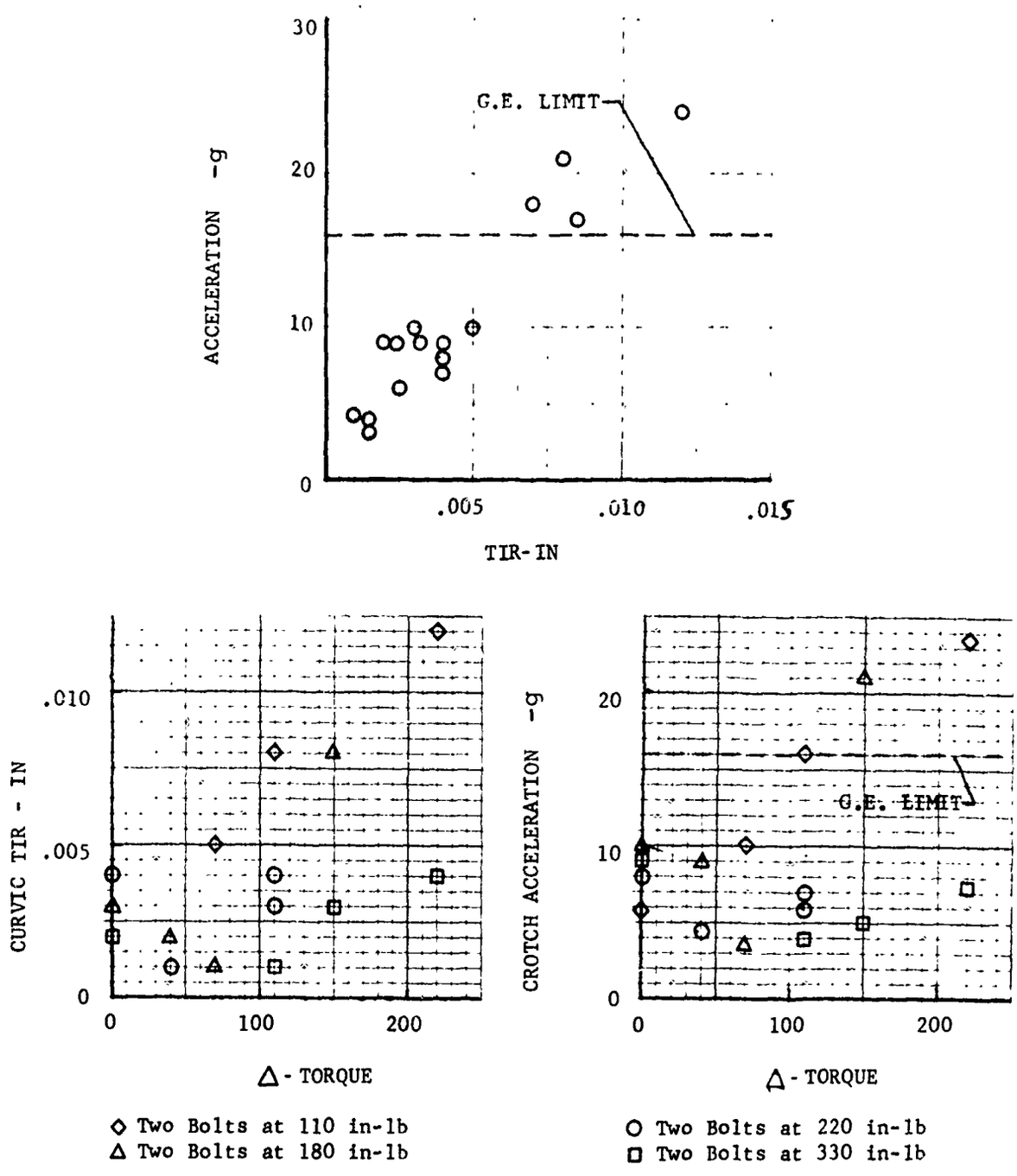

CURVIC COUPLING TIR RELATED TO
ENGINE CROTCH VIBRATION

Figure 23. Curvic Coupling TIR vs Vibration.

Description of the Solution

To eliminate the cocking of the curvic coupling, a washer with adjustable thickness was placed inside the curvic coupling. The outside diameter of this washer just fitted inside the three bolts which clamp the curvic coupling halves together. This was adjusted so that the halves of the coupling bottomed on the washer when the curvic teeth were fully engaged and was intended to keep the curvic coupling halves parallel

This arrangement was evaluated on the GISHOLT balance machine and found to be less sensitive to bolt torque, as shown in Figure 24. This was confirmed by tests in the test rig and by ground tests in a flight aircraft (Figure 25).

To further investigate the problem, the effect of worn bearings in the engine mount was evaluated. There was no change in vibration level due to worn bearings.

Limitations Associated with the Solution

After the washer was installed in service aircraft, field reports showed that 90% of the shaft order vibration problems were eliminated. Since a supercritical shaft is relatively sensitive, small asymmetric desultory variations which ha e not been defined could still be present which unbalance the shaft.

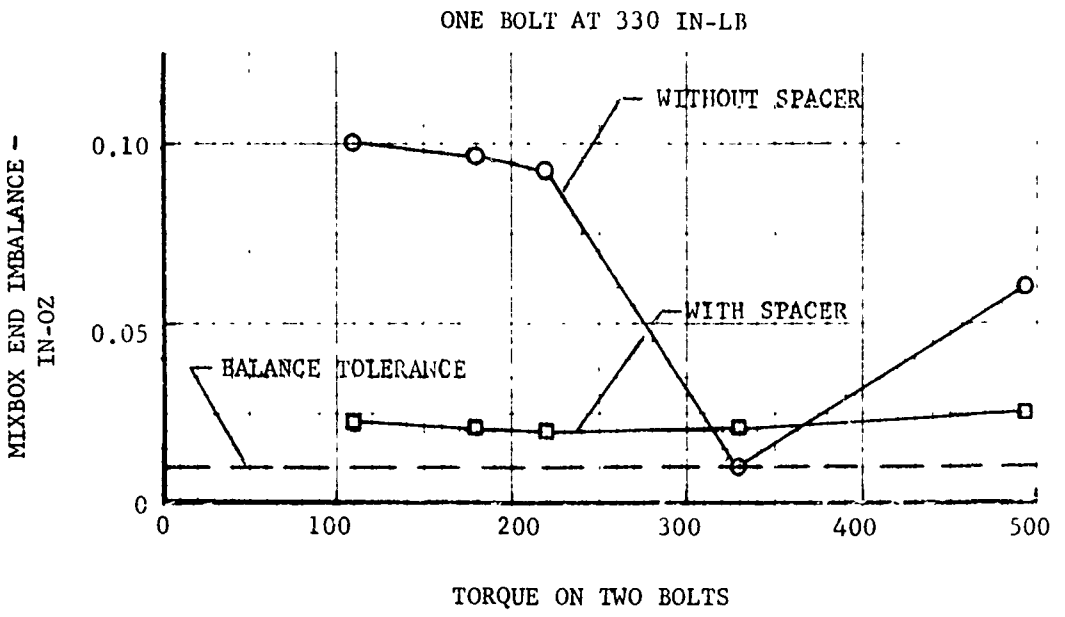

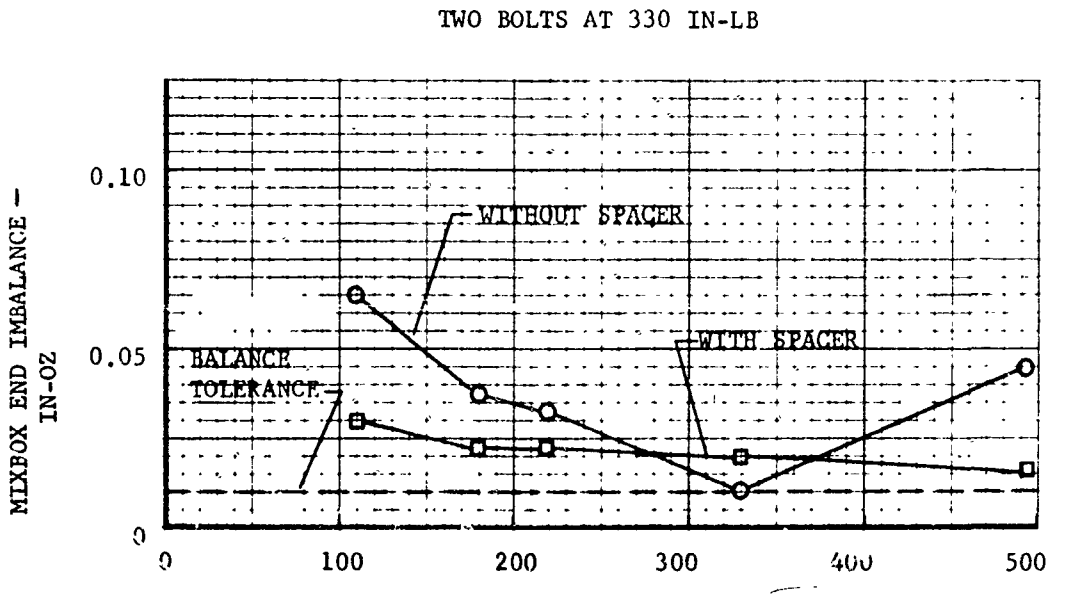

CURVIC COUPLING SPACER EVALUATION
BALANCE MACHINE INVESTIGATION
WITH AND WITHOUT SPACER

Figure 24. Spacer Evaluation.

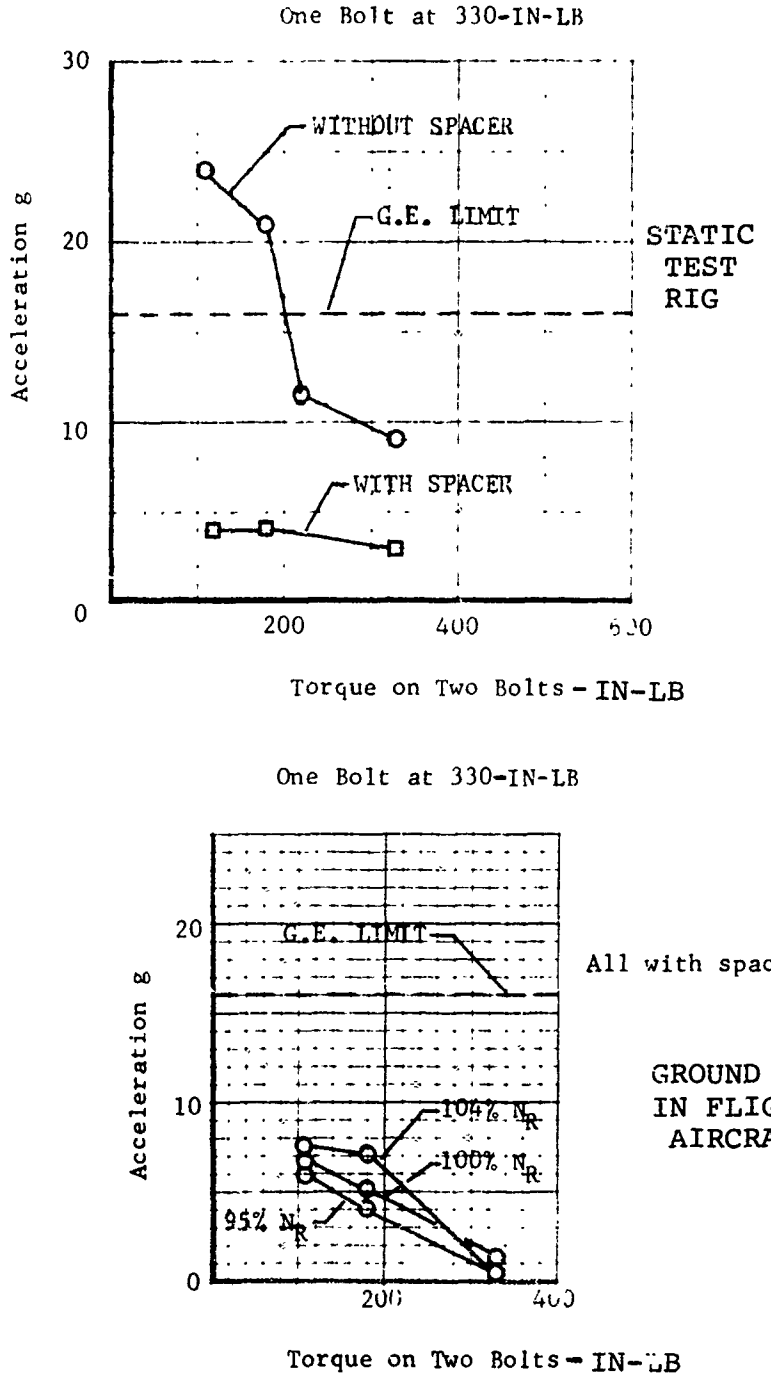

Figure 25. Curvic Spacer Evaluation.

PROBLEM - EXCESSIVE TORQUE DURING ROTOR STARTUP

Description of the Problem

During a twin-engine rotor start, three lag dampers were damaged due to overstressing. This occurred in 1975 after installing higher power engines.

Investigation Leading to a Solution

The allowable torque which the articulated rotor can withstand is a function of rotor speed, since centrifugal forces on the blade provide a relieving moment about the lag hinge and thereby decrease the amount of torque which must be absorbed by the lag damper acting as a stop during rapid low rotor speed accelerations.

The engine fuel control has a control shaft (designated AM). The position of this shaft has essentially a linear relationship to torque from ground idle to maximum power during steady state operation. During transient, engine dynamic effects, various limiting functions within the control, and the required switchover from gas generator power control to power turbine speed governing tend to affect the apparent system linearity. As the requested power turbine speed is reached, engine output torque is reduced by the governing system, and will be increased only if the speed decreases because of power demand or if the requested speed (beep) is increased.

Each AM is positioned by a quadrant (condition lever) in the cockpit which is connected electrically to an electromechanical actuator mechanically attached to the AM lever.

A startup transient during which the condition lever is advanced from ground idle (GI) to FLY in about 15 seconds is described on Figure 26. The AM position was stepped from 16° to 34° because of a nonlinearity within the quadrant, rendering low power modulation ineffective. The engine acceleration characteristic provides very little torque for about 4 seconds following a condition lever advance, as shown in the same figure. This typical lack of response off GI indicates there is no need for modulation between GI and minimum speed governing power, since during the 4-second deadzone the condition levers would have most likely been advanced through the 16° to 34° range.

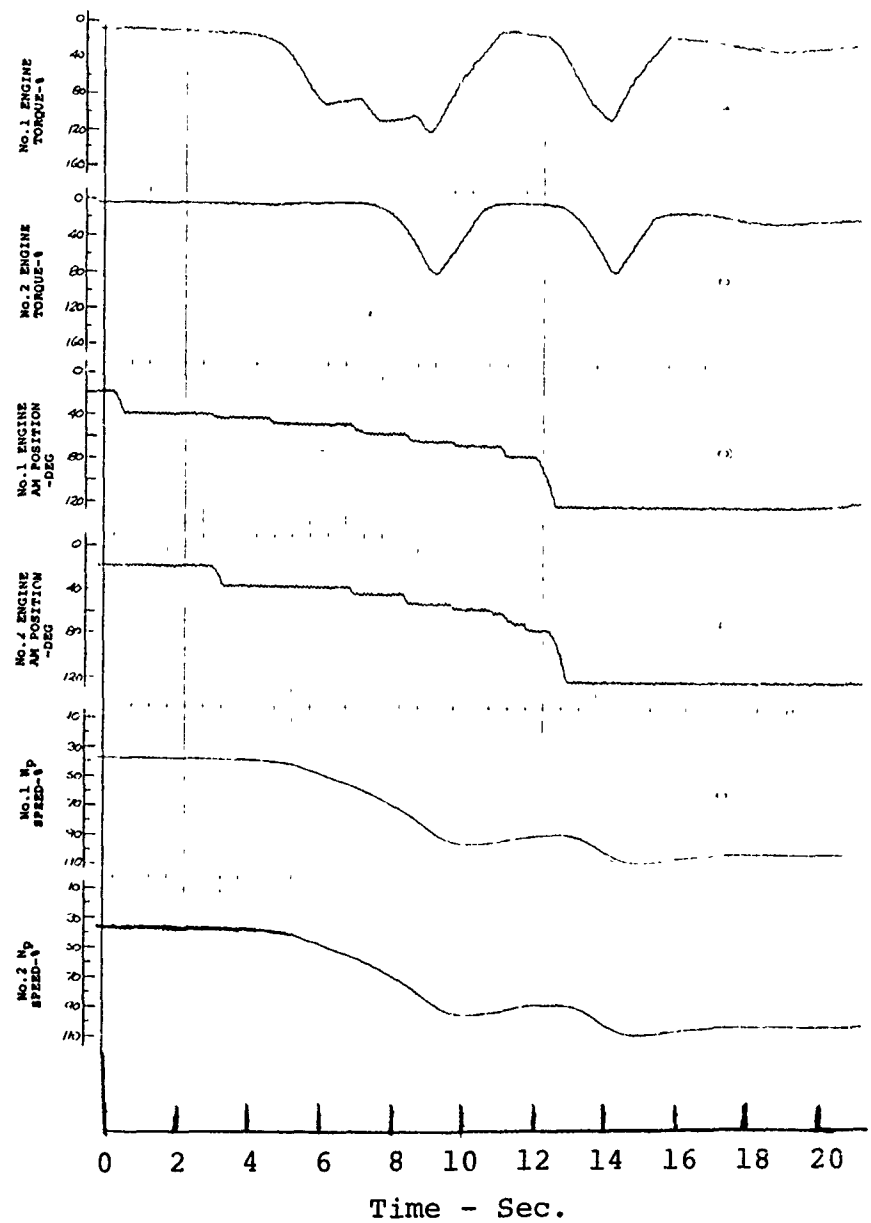

67°F 15 Sec Ramp

Figure 26. Rotor Startup.

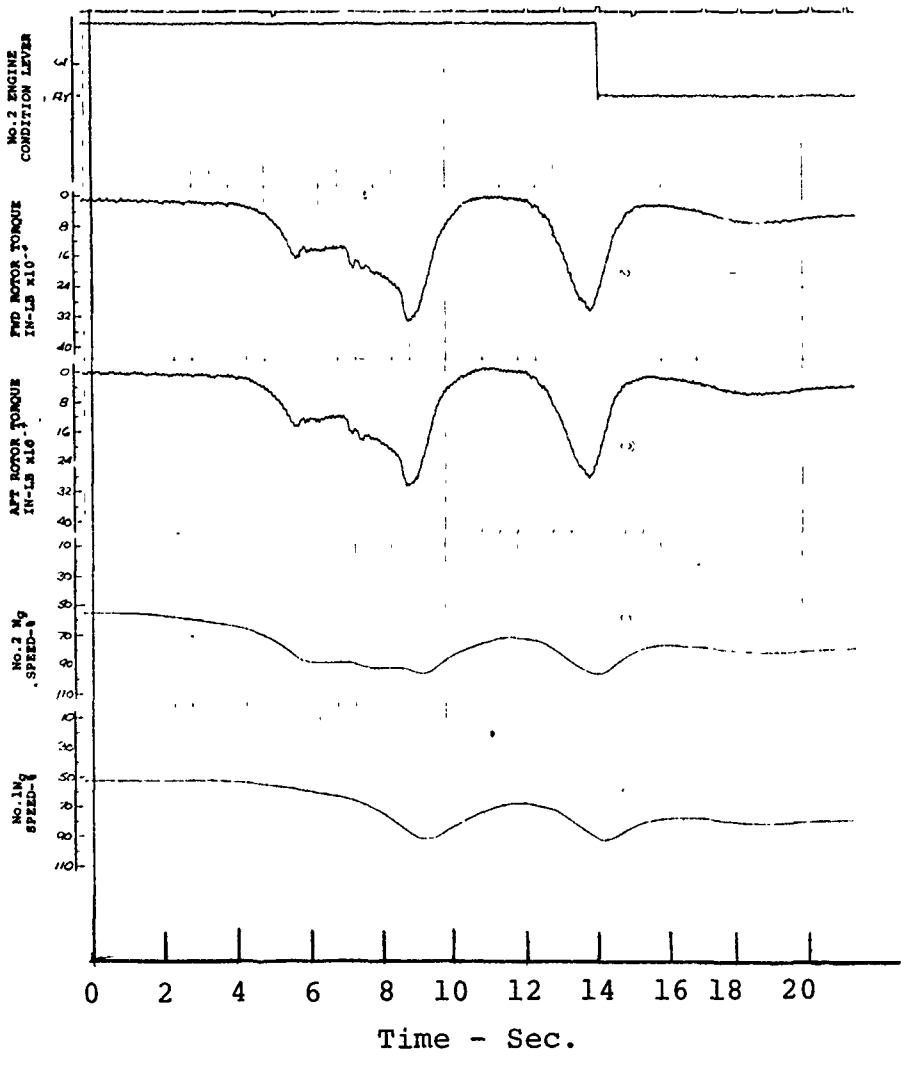

67° 15 Sec Ramp

Figure 26. Continued - Rotor Startup.

When the minimum power turbine governing speed (about 85%) is reached, the engines cut back in power. This creates an undesirable second deadband with no engine response to condition lever inputs prior to the increase in speed request from 72° to 120° AM position.

An AM lever of 34° is adequate to accelerate the rotors at flat pitch to minimum governing speed on a standard day with two engines. Any additional AM input increases the engine output and decreases the time to operating speed. The project pilot indicated that this sensitivity was unacceptable, in that he had very little control of the torque peak, with a high probability of exceeding 120%. This situation is aggravated by the 4-second deadzone in initial engine output.

Figure 27 shows a rapid rotor startup transient during which three lag dampers were damaged.

The very fast condition lever increase (up to the FLY detent in less than 5 seconds) coupled with the low ambient temperature (30°F) and the low initial rotor speed (10%) contributed to the failure.

Solution to the Problem

It was decided to provide a detent, or gate, between the GI and FLY positions to enable the pilot to accurately dwell at a safe engine power setting, and thereby reduce the possibility of an overtorque. From the data presentation (Figure 28), a detent set at 40° AM position will maintain torque below the continuous twin-engine transmission torque limit of 100% down to 0°F ambient.

In addition, it was required that the rotors be at a speed of 80 rpm (30%) prior to advancing the condition levers from the GI detent. This ensures that the blades develop sufficient CF to eliminate the possibility of overstressing the lag dampers when rotor shaft torque is applied.

Limitations Associated with the Solution

Originally both a modification to the fuel control and a new actuator system were planned.

The second deadband which occurs when the minimum governing speed is reached could be significantly reduced by revising the fuel control N_g request cam to increase the quadrant

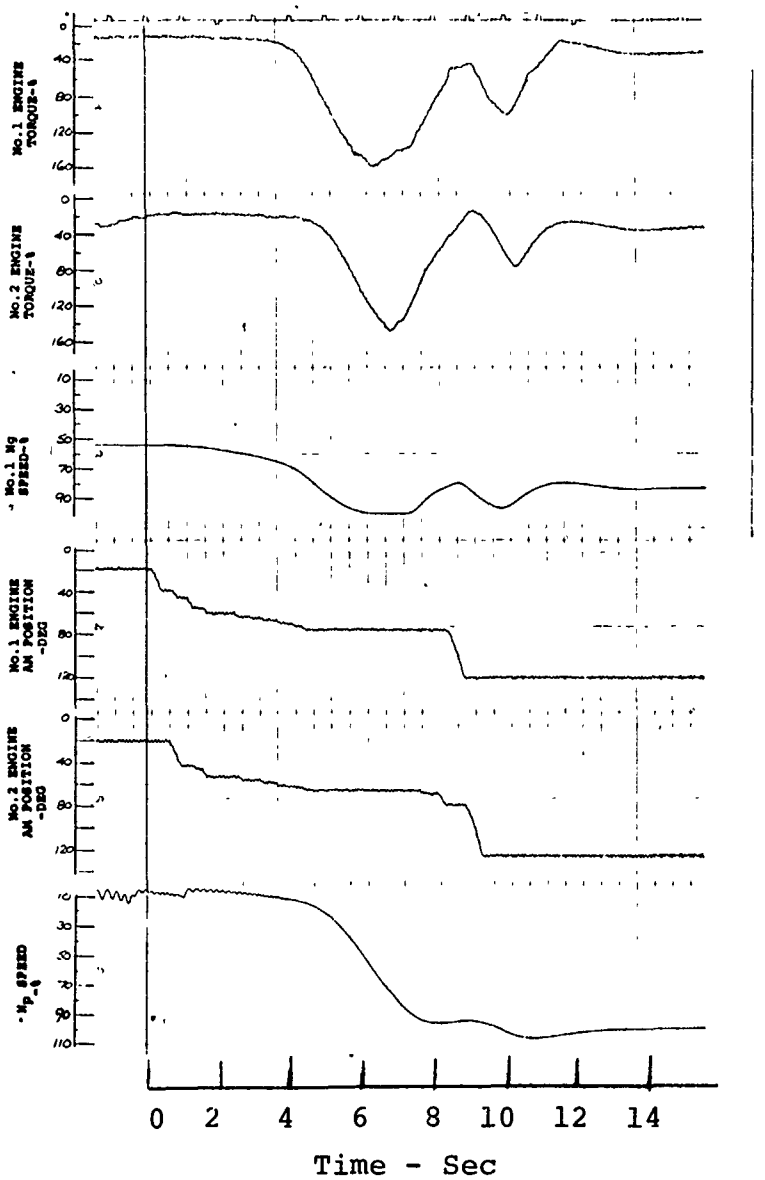

30°F

Figure 27. Rotor Startup, 30°F.

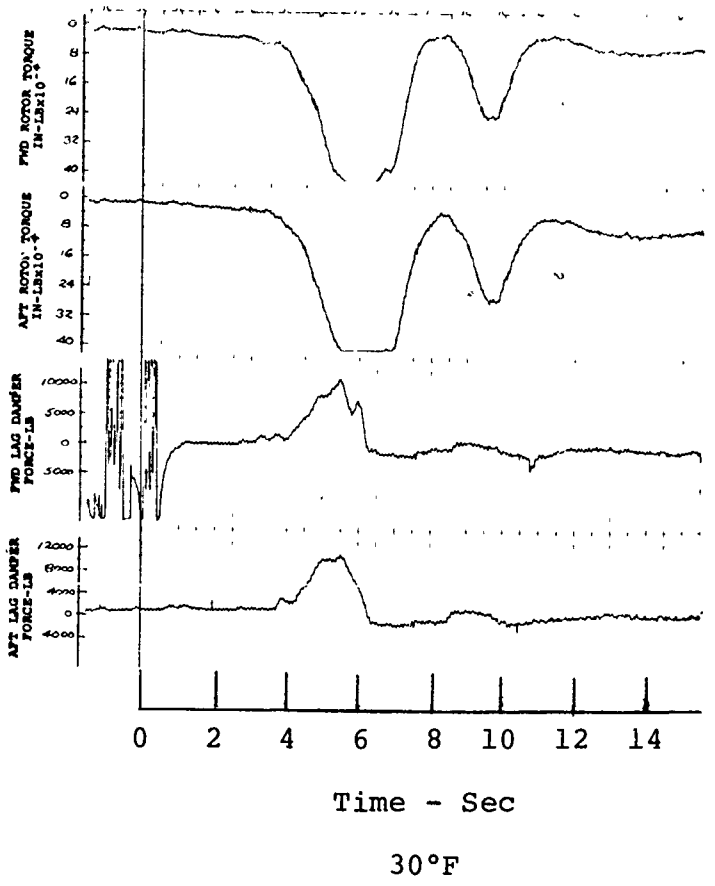

Figure 27. continued - Rotor Startup, 30°F.

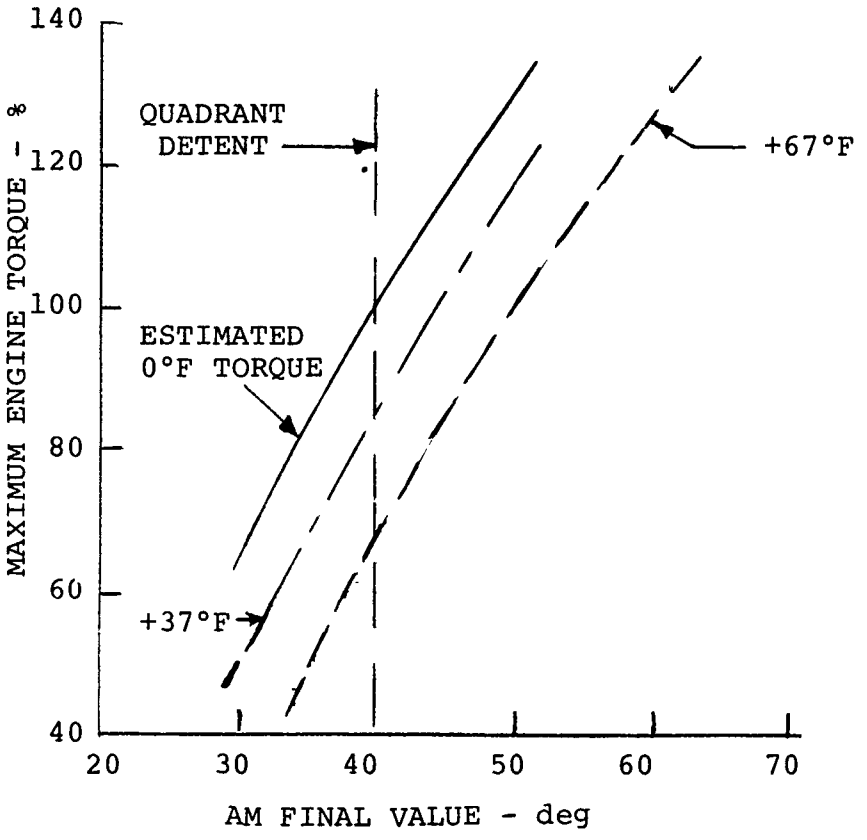

PEAK ENGINE TORQUE RESULTING FROM
RAPID ADVANCE FROM GROUND IDLE

Figure 28. Peak Engine Torque.

travel and controllability of start. This would decrease the gain of the cam from ground idle (16°) to 60°, then increase the gain to FLY.

A revision to the aircraft quadrant schedule could provide results similar to those noted above. Bending the straight line schedule of AM position with condition lever travel to allow greater AM movement prior to attaining governed speed will decrease the second deadband.

These modifications were not incorporated because of cost considerations.

CH-47

PROBLEM - TORQUE OSCILLATION

Description of the Problem

Starting in 1969, when CH-47 C-model helicopters (with T55-L-7C engines) were converted to the full "C" model by incorporating T55-L-11 engines, variations in engine and rotor shaft torque were observed. These torque oscillations, at a frequency of 4.1 cycles per second (dual engine) and 4.7 cps (single engine), were audible and disconcerting to the pilot and crew. The significant differences between the -7C and -11 engines were a 50% increase in inertia and a new fuel control configuration. Figure 29 shows a schematic of the drive/fuel control/engine arrangement.

Investigation Leading to a Solution

This problem was first discovered due to the magnitude of the noise associated with the oscillations. The forward transmission sounded like it was loading and unloading. Oscillations were evident on the ground and in hover, and rotor speed fluctuations of $\pm$ 2 rpm were noted during the oscillations. Recorded data indicated large rotor shaft torque oscillations (forward and aft hubs in phase) at the same frequency as engine fuel flow fluctuations.

The next several flights and ground runs were an investigation to determine the cause of the torque oscillation. Engine inlet screens were removed with no effect on torque oscillation. Circuit breakers were pulled deactivating the N_2 speed setting actuator, but the oscillations continued. Oscillation frequency was 4.05 cps dual engine and 4.7 cps single engine.

The fuel control on No. 1 engine was changed between ground runs. Both of these were unmodified production fuel controls. Testing revealed that there was no audible torque oscillation when operating on No. 1 engine. The oscillation was present with both engines operating or during No. 2 engine operation only. Replacement of the No. 2 fuel control, however, did not eliminate the oscillation when operating on No. 2 engine. These fuel controls were removed from the aircraft, functionally checked by the engine manufacturer, and found to be within specification limits. The only difference between the "C"-model prototypes experiencing oscillation and the "C" model which exhibited no perceptible oscillation was the incorporation of the -11 engines, with significantly higher inertia and a more responsive fuel control than the -7C engine.

Approximately 1 month after the torque oscillation was discovered, a CH-47C was ferried to Eglin Air Force Base for climatic hangar testing. No torque oscillation occurred until the third test in the hangar (at 70°F) when operating on the No. 1 engine alone. During the dual-engine operation that followed the oscillation also occurred.

Elimination of the N_2 (power turbine speed) governing was evaluated. Rotor speed was set at 240 rpm, and rotor thrust was increased causing a drop in rotor rpm at this topping level, which in effect removed the N_2 governor from the power control system. Under these conditions, power oscillations could not be induced; hence, the problem was not in the N_1 (gas producer speed) governing.

An attempt was made to change the engine response characteristics and hence eliminate torque oscillation by installing an accumulator in the fuel pressure manifold. However, torque oscillations were undiminished during testing with the accumulator.

Torque oscillations were also present when the hangar temperature was reduced to -25°F. Oscillations were present on either single- or dual-engine operation. A reduced gain fuel control was shipped from Lycoming and installed on No. 1 engine. At -25°F, torque oscillation could not be induced during No. 1 engine operation; however, No. 2 engine and dual-engine operation were still unstable. A reduced gain fuel control was sent to Eglin by Lycoming for the No. 2 engine. It was installed and tested at -45°F. No. 2 engine experienced no torque oscillations; however, oscillations were now observed during No. 1 engine operation.

During the first and second tests at -65°F, no evidence of any torque oscillation was observed. However, as hangar temperature rose to -35°F, a torque oscillation was again in evidence on No. 1 engine. An investigation into lag damper operation in cold temperatures, begun after climatic hangar tests, led to the conclusion that the damper effectiveness was significantly reduced below 0°F. This was the apparent cause of torque oscillations in the climatic hangar even with the reduced gain fuel controls.

Further testing at Boeing Vertol was done with a CH-47C with production fuel controls with a nominal steady-state droop of approximately 7.0% and time constants of roughly .03 second.

Data was taken during a ground run with these fuel controls and standard lag dampers. The following were the results.

a. Audible torque oscillation observed during No. 1 engine testing above 80% torque, No. 2 engine at all percents torque. Oscillation also observed in dual-engine operation.

b. Oscillation of up to ± 2 rpm in rotor speed noted on cockpit tachometer during occurrence of oscillation.

c. Oscillation frequency during single-engine operation was 4.7 cps; during dual-engine operation, frequency was 4.1 cps.

d. Recorded data revealed oscillations as high as ± 135,600 in-lb on the forward rotor shaft, ± 116,700 in-lb on the aft rotor shaft, ± 12.6% torque on the No. 1 engine, and ± 13.4% torque on the No. 2 engine.

e. There was no substantial rpm effect in single-engine operation from 235 to 250 rpm.

f. Alternating shaft torques were slightly higher at 245 rpm during dual-engine operations; 245 rpm (4.08 cps) is near the dual-engine resonance of approximately 4.1 cps.

g. Removal of N_2 system circuit breakers did not stop oscillation, eliminating N_2 actuator hunting as a cause.

h. Oscillation was only slightly less severe with cyclic trim fully extended.

i. Upon switching from N_2 to N_1 governing, oscillation ceased, indicating problem is not in N_1 governing.

j. Since self-sustained oscillation frequency was 4.7 cps single engine, one per rev forcing vibration was eliminated as a cause of oscillation.

A typical torque oscillation of the forward rotor was ± 116,000 in-lb while the engine torque was ± 7.6% of maximum torque (1300 ft-lb = max torque), and fuel flow fluctuations were ± .455 gallon per minute (or 8.95% of maximum fuel flow). Fuel flow was approximately 180° out of phase with both rotor and engine torque, while engine and rotor torque fluctuations were in phase.

Fluctuations in compressor discharge pressure (P3) were 90° out of phase with fuel flow, while fuel pressure was in phase with fuel flow.

The forward rotor lag damper load reached its peaks at maximum rotor shaft deflection, indicating that the damper was acting as a spring rather than a viscous damper. The maximum peak load at the torque oscillation frequency was ± 2800 lb and some blade motion was evident at 1.6 Hz (the blade lag natural frequency). The torques of both rotor shafts and both turbines were in phase, with fuel flow out of phase. It is important to note that fuel flow (as well as other fuel control parameters) followed along closely with the torque oscillations. For example, No. 2 engine fuel flow fluctuations of ± .39 gal/min were experienced. Since maximum fuel flow is about 5.1 gal/min, this represents a variation in fuel flow of ± 7.7%. No. 2 engine torque fluctuations are ± 6.9%. No. 1 engine fuel flow fluctuations of ± .33 gal/min (6.5%) are experienced, compared with engine torque oscillations of 8.3%. Thus, it appears that the No. 2 fuel control was slightly more responsive than the No. 1 control, since it produced a larger change in fuel flow for the same change in rotor speed (or torque). We know this was true since the No. 2 engine was susceptible to torque oscillation at all torque levels and the No. 1 engine only at the higher torques.

Operating one engine at a time showed that during No. 1 engine operation, fluctuations of ± 77,500 in-lb in forward rotor shaft torque and ± 4.6% in engine torque were experienced, with accompanying fuel flow variations of ± .27 gal/min (5.3%). No. 2 operation shows forward shaft oscillations of ± 106,500 in-lb torque, engine torque variations of ± 4.5%, and fuel flow fluctuations of ± .49 gal/min (9.4%). Clearly, original production fuel controls provide no attenuation of any torque fluctuation at these frequencies.

During the development of the fuel control for the T55-L-11 engine, the engine manufacturer performed simulations of the combined CH-47C/T55-L-11 dynamic system to insure control stability.

An economical approach was taken in which the dual-rotor, dual-engine system was simplified to a single-rotor, single-engine arrangement. This was justifiable since in the mode of interest (3-4 Hz), both rotors and both engines are in phase. The turbine-to-hub system has been simplified to a single inertia (equal to the sum of turbine and transmission inertias) and a single spring (equal to the aft rotor shaft stiffness , which is the "softest" spring in the system when

referred to turbine speed). The rotor system itself is simulated by a single blade inertia (equivalent to three times the inertia of one blade), the rotor hub, the blade centrifugal spring at a given rotor speed, and a nonlinear viscous damper in parallel with the centrifugal spring.

These studies showed a stable system with a .03 time constant and 7.5% droop. Shortly after the oscillation was observed on the aircraft, efforts were made to duplicate the oscillation on the computer simulation. A parametric study was made during which various system parameters, such as rotor shaft spring rate, turbine inertia, hub inertia, centrifugal spring, and engine gain, were varied in an attempt to reproduce the oscillation. It was found that the only parameter change that could induce a significant oscillation was an increase in the preload slope of the lag damper force-velocity curve. The damper was now represented by a spring and damper in series. The hub and turbine inertia and the shaft spring rate were adjusted to yield the 4.0 Hz frequency. This simulation now duplicated the aircraft oscillation.

A ground run was made to investigate the effect of a "softer" lag damper on torque oscillation. Torque instability was reproduced on the computer analysis only by "stiffening" the damper by reducing the preload breakout velocity. Hence, it seemed feasible that a "softer" damper, i.e., one with a higher breakout velocity or a shallower preload slope, might be an effective torque oscillation fix. The standard production dampers reach breakout force at approximately .50 inch per second; the dampers tested in ground run 12 attained breakout force at 1.25 ips (see Figure 30). This was accomplished by means of a small orifice directly across the piston to increase leakage. The pertinent findings from ground running are as follows:

a. No torque oscillation was evident audibly or on recorded data.

b. From recorded data, large blade motion at 1.6 cps (blade lag natural frequency) was evident throughout the run.

c. Flights (at 41,500 lb GW) and ground runs (at 52,000 lb) with these modified dampers showed ground instability neutral padding throughout the range of collective pitch settings, rotor rpm, and engine torque conditions tested.

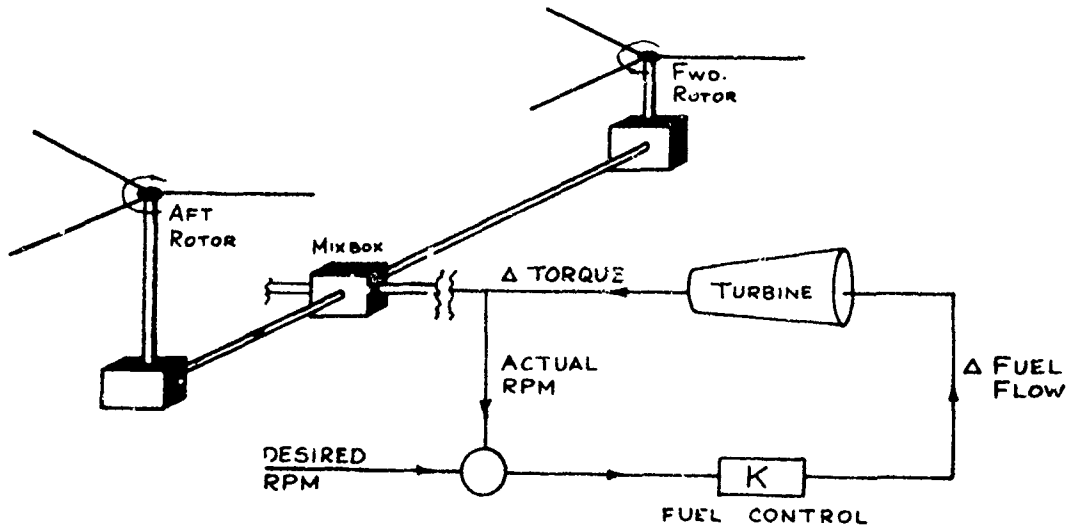

Figure 29. Drive System/Fuel Control/Engine Schematic.

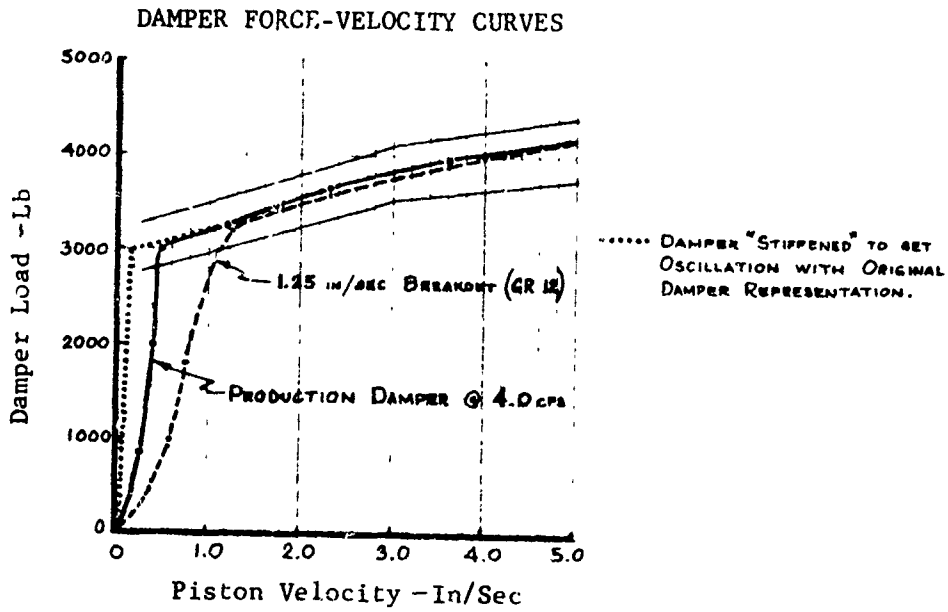

Figure 30. Lag Damper Characteristics.

d. Therefore, the "soft" lag damper fix for torque oscillation is unacceptable due to the degradation of ground stability characteristics.

Since data from tests with original production fuel controls had shown fuel flow fluctuations commensurate with engine shaft torque oscillation, an improvement in fuel control attenuation was considered the most likely torque oscillation fix. Any variation in rotor speed or rotor shaft torque is sensed at the fuel control as an instantaneous change in power turbine speed (N_2). The fuel control compares the actual rpm with the desired rpm, and varies fuel flow (and hence engine torque) to compensate for the speed error.

The actual change in fuel flow per unit change in power turbine speed depends on the frequency of the speed variation, the fuel control steady-state "gain", and the response "break frequency". This is shown on the frequency response plot (Figure 31). For the original production fuel control, it can be seen that at the dual engine resonance (4.1 cps), the fuel flow change per unit change in N_2 is still quite high; hence, we may say there is little fuel control "attenuation" at this frequency.

One way to improve attenuation would be to simply reduce the change in fuel flow per unit change in N_2 at all frequencies. As shown in Figure 31, this amounts to a frequency response curve parallel to the curve of the original fuel control. Assuming a steady-state gain of unity for the original control, a 30% reduced gain control would have a steady-state gain of around .7; hence, for most normal maneuvers, engine response is slightly degraded. Changing fuel control gain has an effect on the engine droop rates, as shown in Figure 32. Engine droop is defined as the reduction in power turbine speed accompanying an increase in engine power. Steady-state droop is defined as the percent reduction in N_2 as power is increased from zero to maximum power. Original production fuel controls yielded a steady-state droop of approximately 7.5%. Reducing the fuel control gain by 30% has the effect of increasing steady-state droop to approximately 10%.

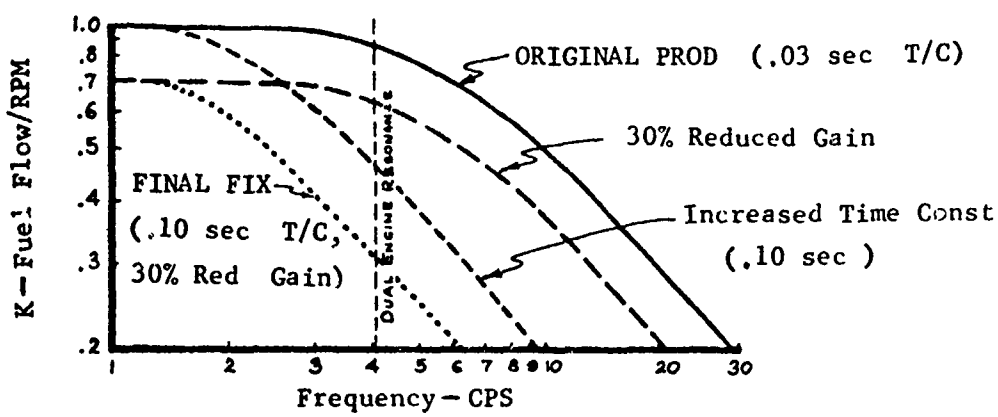

Figure 31. Fuel Control Frequency Response.

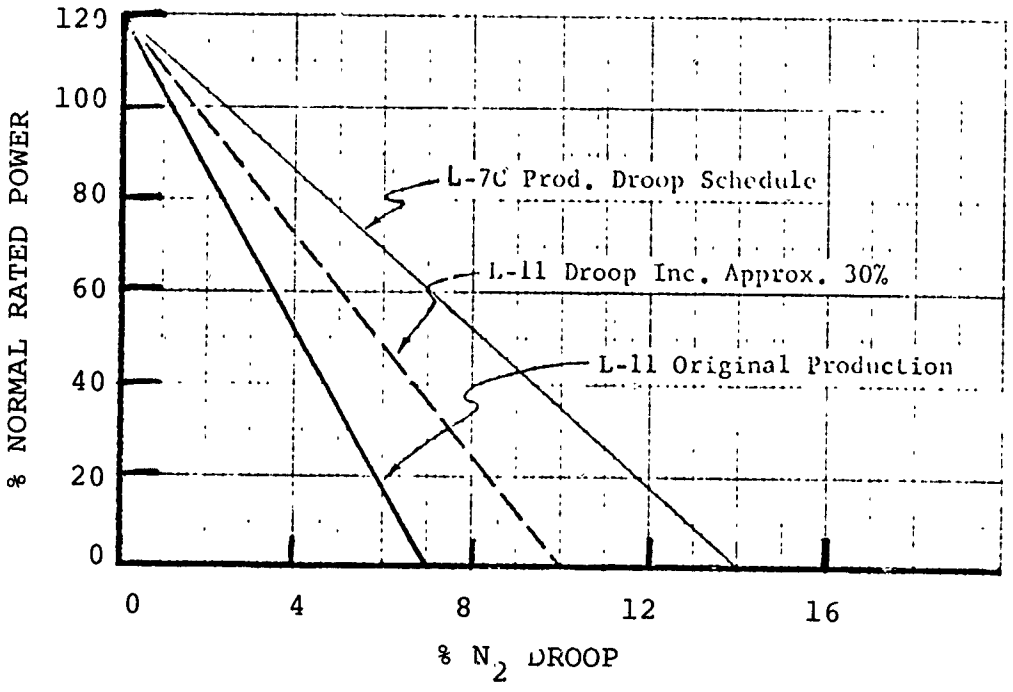

Figure 32. Engine Droop Schedule.

An aircraft with controls set at 70% gain was ground and flight tested with these results:

a. No torque oscillations were observed audibly or on cockpit instrumentation on any of the flights and ground runs.

b. Engine response was satisfactory to Army pilots.

c. Intermittent small amplitude oscillations were observed on recorded data at various conditions during the flights and ground runs. Maximum alternating torques noted were $\pm$ 40,100 in-lb rotor shaft torque and $\pm$ 3.1% engine torque.

d. Pilot comment revealed that engine response characteristics had not noticeably deteriorated due to droop schedule change.

e. As far as engine performance and torque oscillation are concerned, the aircraft with nominal 30% reduced gain fuel controls is acceptable at the ambient temperatures experienced (35-40°F).

Another method of improving attenuation is by lowering the fuel control response break frequency, or, equivalently, by increasing the control time constant. With this method of attenuation, steady-state gain is relatively unaffected, but the frequency at which the control may follow has been reduced significantly, hence reducing the effective gain at 4.1 cps. The time constant is defined as the inverse of two times pi times the response break frequency. Therefore, the original control, with a break frequency in the area of 5.3 cps, has a time constant of .03 second. A response curve is shown (Figure 31) for a control with a .0-second time constant (1.6 cps break frequency). Attenuation at 4.1 cps is even superior to the reduced gain control. Even further attenuation is possible with combinations of reduced gain and increased time constants.

The updated simulation showed that the aircraft with fuel controls with 30% reduced gain and increased time constants would be stable.

The effect of this increased time constant (.10 sec) was evaluated (without any gain change) during a ground run. This showed:

a. No torque oscillation was evident audibly or on cockpit instrumentation.

b. Oscillation could not be induced with collective pitch pulses.

c. Intermittent oscillations in rotor shaft and engine torque were seen occasionally on recorded data. These oscillations were of small amplitude and damped out quickly.

d. No noticeable degradation in engine response was felt by the pilot with the "slowed-down" controls.

Another ground test was run with fuel controls having 70% of the original production gain and a time constant increased from the original .03 to .05. Results were as follows:

a. No torque oscillation was evident audibly.

b. A very low frequency $\pm$ N_R oscillation (later identified as bleed band oscillation) was observed at approximately 33% torque and 87% N_1.

c. Engine response to rapid collective pitch pull-up was judged normal by pilot comment.

d. Intermittent small amplitude oscillations were noted on recorded data. Maximum alternating torque noted was $\pm$ 40,000 in-lb rotor shaft torque and $\pm$ 2.6% engine torque.

In order to evaluate the problem at lower temperatures since Eglin testing had indicated a temperature sensitivity, testing was continued at the Boeing facility at Arnprior, Canada.

The fuel controls had 70% gain and a time constant of .11 sec. The results were:

a. No torque oscillation was evident audibly or on cockpit instrumentation.

b. Maximum alternating torques were ± 41,500 in-lb rotor shaft torque and ± 3.4% engine torque.

c. Rotor speed droop during jump takeoff was 5 rpm.

d. Average temperature during flight was -4°C (25°F).

Since the low temperature test conditions did not materialize, testing was resumed at Philadelphia.

An investigation into the cold temperature operation of the lag damper showed that the decrease in damper force output was apparently due to cavitation caused by flow of hydraulic fluid from the damping chamber into the reservoir, with no replenishing flow of fluid from the reservoir back to the damping cavity. Fluid flow to the reservoir was decreased by plugging one Lee jet and decreasing the diameter of the remaining two, and fluid flow back to the damping chamber was improved by reducing the cracking pressure of the two replenishing check valves from 5 psi to 3 psi. The resulting damper configuration provided satisfactory damping output down to -65°F (see Figure 33).

Description of the Solution

A set of fuel controls with 70% gain and .10 sec time constant were flown with lag dampers which incorporated these low temperature modifications.

a. No torque oscillation was audible to the pilot or crew. Recorded data showed that maximum alternating torques were ± 1.8% on No. 1 engine and ± 2.0% on No. 2 engine.

b. Vigorous collective pitch pulses yielded alternating torques of ± 4% on both engines, which were quickly damped.

c. A rotor speed droop of 4 rpm was experienced during rapid collective inputs.

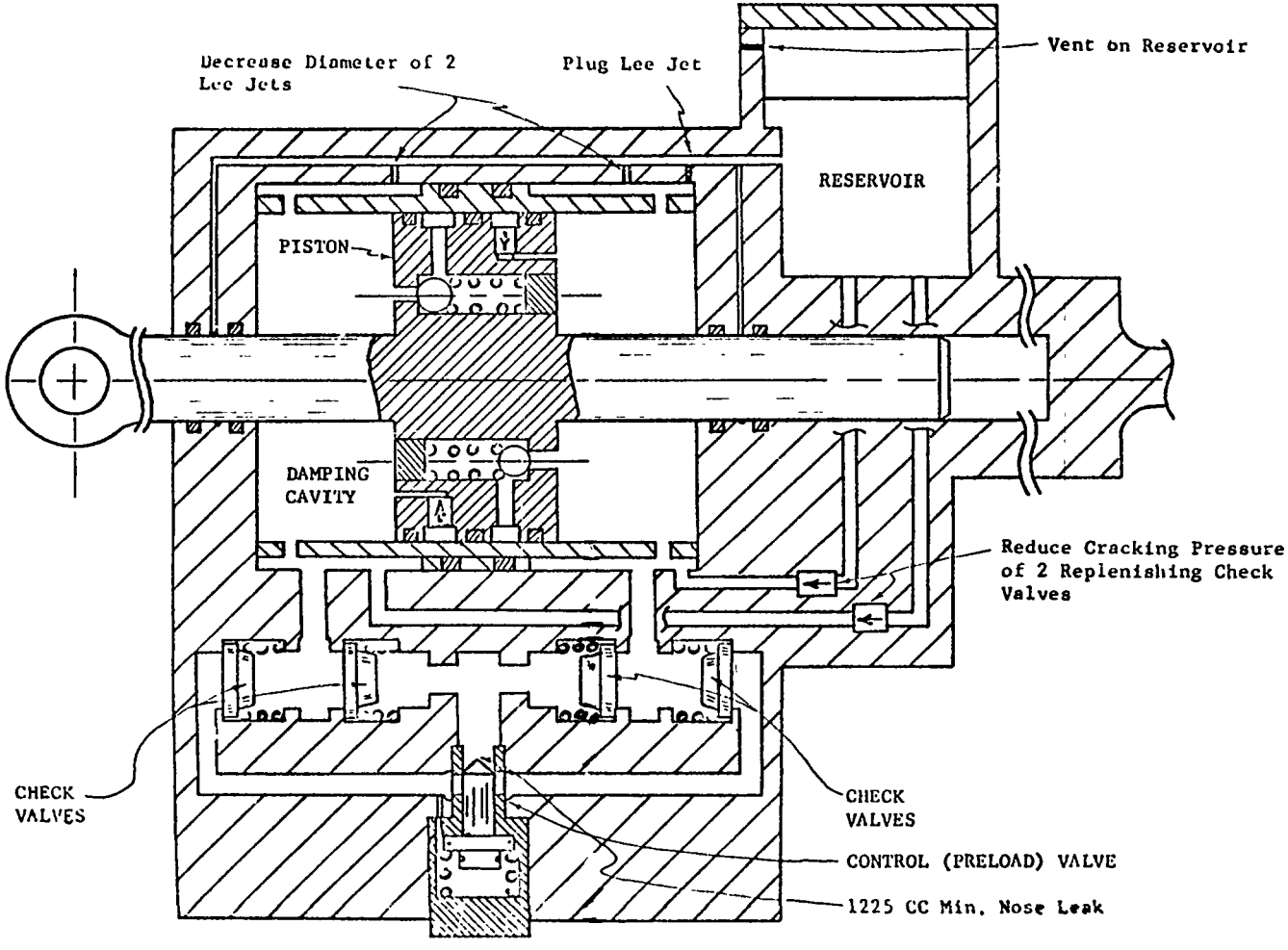

Figure 33. Lag Damper Schematic.

Limitations Associated with the Solution

The reduced gain/increased time constant fuel control fix provided satisfactory torsional stability for the CH-47C production fleet. However, several early production aircraft reported instances of a "pseudo-torque oscillation". This phenomenon is a torque split, followed by a low amplitude torque oscillation of the high torque engine. The problem was traced to high levels of vibration affecting the internal workings of the fuel control. Vibration at cross shaft frequency caused an instantaneous increase in the effective gain of the control, increasing its torque output with respect to the other engine and making it susceptible to torsional instability. The problem was resolved by closely monitoring cross shaft vibration, and with minor fuel control component modifications.

PROBLEM - CRACKING OF ENGINE INLET HOUSING

Description of the Problem

Field service reports had indicated increased engine failures since the introduction of the T55-L-11 and -11A engines in the CH-47C helicopter. Engine inlet housing fatigue cracks had occurred and engine mounting system components wore and failed.

Investigation Leading to a Solution

In August through October 1970, a flight vibration and strain survey of the engine was conducted. A CH-47C engine was instrumented with accelerometers and strain gages. Rpm and speed sweeps were made in the basic configuration and with modifications. The engine mount (Figure 34) consists of two forward engine mounts, both of which react vertical and longitudinal loads (one of which also reacts lateral loads), and a vertical link at the aft end which reacts vertical loads only. To brace the forward outboard engine mount support, a link connects the forward outboard engine mount to the fuselage structure aft of the forward mounts.

From the minimum gross weight flown to 140% of that value, helicopter order (1Ω, 3Ω, 6Ω) data did not show any significant change in stress level or accelerometers for the same airspeeds. (The helicopter airspeed limit was lower for the higher gross weights.) At fixed gross weight, there were usually higher accelerations and stresses at the higher airspeeds.

The rotor rpm sweeps showed no specific trend in accelerations or stresses except that the No. 1 engine drag link 3/rev loads nearly doubled in going from 230 to 250 rpm.

Because of this large change, it was felt that a change in stiffness might be significant. The production drag link is made from aluminum alloy. It was replaced with a steel link. This resulted in nearly halving the No. 1 engine drag link load at high airspeeds (the No. 2 engine link load which was low with the aluminum link did not change).

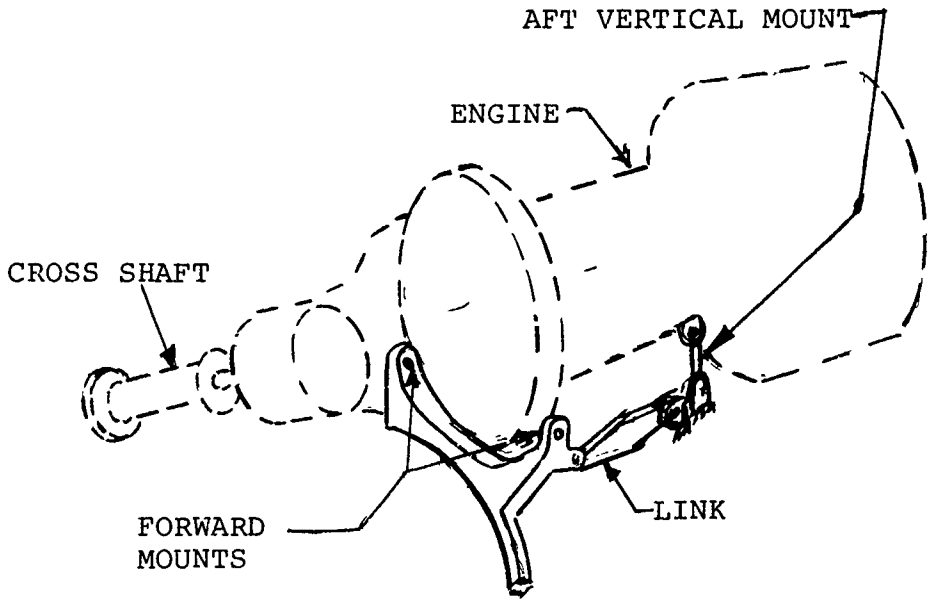

Figure 34. Engine Mount Schematic.

The effect of worn engine mounts was explored. Simulated worn forward mounts were installed on engine No. 1, while a loose aft engine mount was evaluated on engine No. 2. Neither the 3/rev or 6/rev levels of stress or vibration were affected. Frequency (engine order) vibrations were also explored (15,000 rpm), and the cross shaft balance was investigated, as its speed is 81% of the engine power turbine speed.

Cross shaft and power turbine 1/rev were the only predominant high frequency engine excitations. Neither excitation was significantly affected by gross weight, steel drag links, or loose engine mounts. Cross shaft spline wear could increase vibration (measured on the engine) up to 300%. Low engine torque conditions (starts, partial power descents, single engine, and autorotations) also produced an increase in cross shaft 1/rev (of up to 100%). The largest measured engine response to cross shaft vibration was 4.0g (No. 2 diffuser, worn shaft).

Cross shaft unbalance tests show the No. 2 diffuser location to be the most sensitive to cross shaft excitation.

Power turbine 1/rev vibration is most sensitive to rotor rpm (N_2 speed). High rpm (250) produces 10g at the aft end of the engine (fuel manifold), but the corresponding stress levels on power turbine nozzles are less than 1500 psi.

This flight vibration/strain survey revealed that although measured stresses were not clearly sufficient to cause inlet housing cracks, the most significant portion of the stress was at the rotor 3/rev frequency.

The investigation was pursued further by conducting a ground engine shake test in July 1971.

Lateral shaking forces were applied to an engine installed in a CH-47 helicopter. The engine responded as a rigid body at 14.2 Hz causing high inlet housing strains near the engine mounting pads where the service revealed cracks had occurred. Figure 35 shows frequency sweep results in accelerations at the fuel manifold and the strain at the inlet housing.

The engine yaw mode exhibits motions similar to the inflight 3/rev response (Figure 36).

Vertical excitation at the nose box excites a pitch/yaw mode at 25.5 Hz in addition to the 14.22 Hz yaw mode (Figure 37).

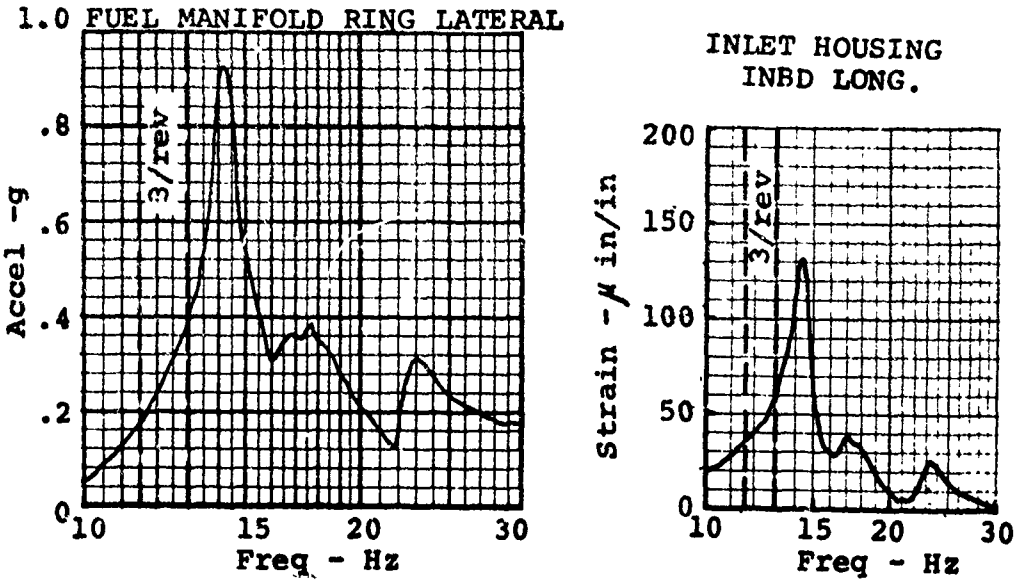

Figure 35. Baseline Engine Vibration.

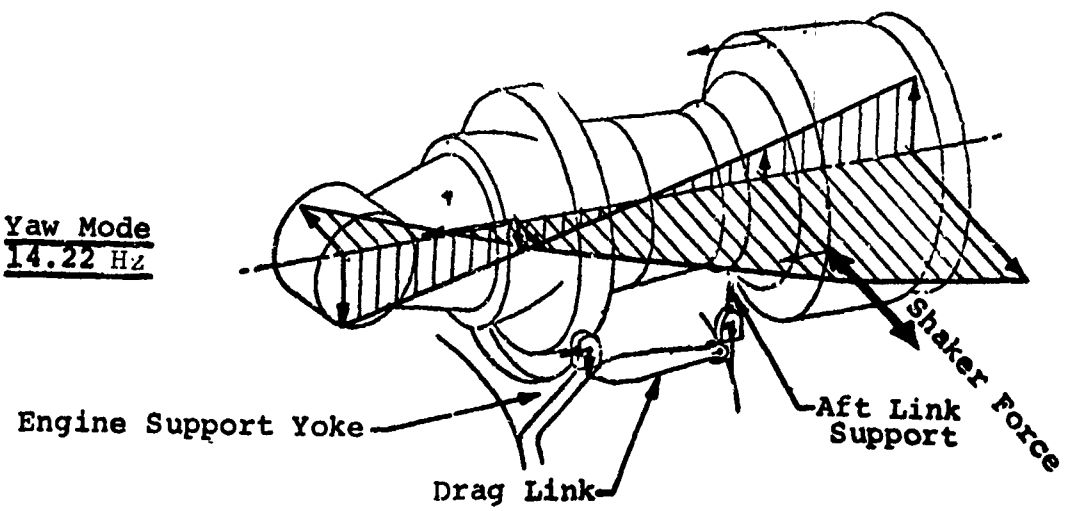

Figure 36. Yaw Mode.

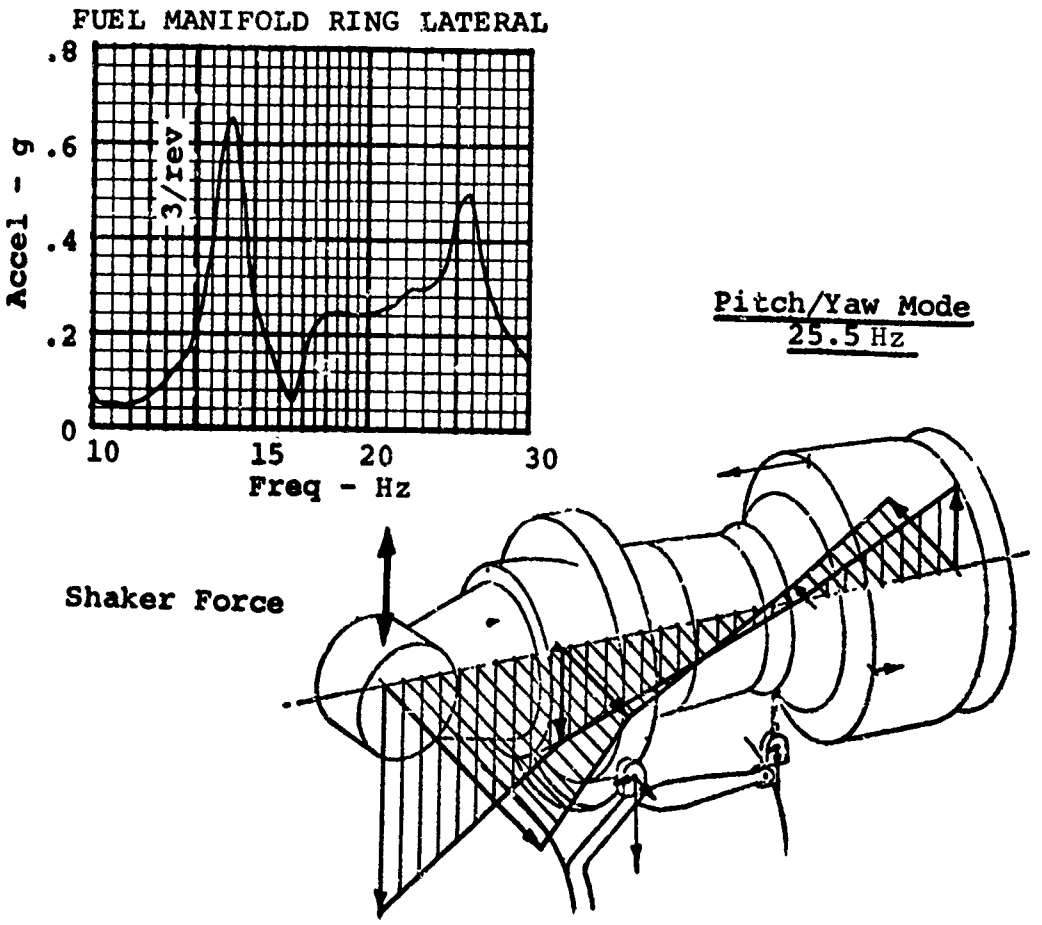

Figure 37. Pitch Yaw Mode.

Growth of the -11 engine to the -11A configuration increases the engine weight 40 pounds. The effect of additional weight and inertia on the yaw mode is to lower the natural frequency 0.39 Hz. Moving the yaw mode closer to the 3/rev frequency results in a significant increase in the inlet housing strains (Figure 38).

Lowering of the drag link bolt torques from specification values to below 100 in/lb causes a significant reduction in the yaw mode frequency (Figure 39).

The combination of -11A engine weight and loosening or wear of drag link bolts could lower the engine yaw mode frequency coincident with the rotor 3/rev frequency. Engine inlet housing cracks could result, since inlet housing stress levels are predominantly 3/rev.

Several engine mounting system changes were designed to reduce the 3/rev inlet housing stresses by shifting the engine yaw mode frequency away from the 3/rev excitation range.

Reducing drag link stiffness can lower the yaw mode frequency well below 3/rev. With no drag link the frequency drops to 7.5 Hz. A large stiffness increase with a steel drag link raises the modal frequency only slightly (Figure 40).

Several fixes to increase mounting system stiffness were evaluated. A vertical strut to the engine mount yoke, frame stiffening and expandable drag link bolts showed only small increases in natural frequency and slight decreases in 3/rev inlet housing stresses. Even the combined effect of all the changes is little different from the individual changes.

Lateral stiffening of the aft link raised the natural frequency a substantial amount and reduced the inlet housing 3/rev stresses to an acceptable level. This change was deemed impractical since it would require redesign of the aft link lower support and the engine connection, with subsequent engine requalification.

Graphic presentation of the engine yaw mode frequencies, inlet housing strains and drag link loads shows the basic levels, the increase in loads with loose parts, the moderate reduction in strains with engine mount stiffening, and the dramatic reduction in levels with the removal of the drag link (Figure 41).

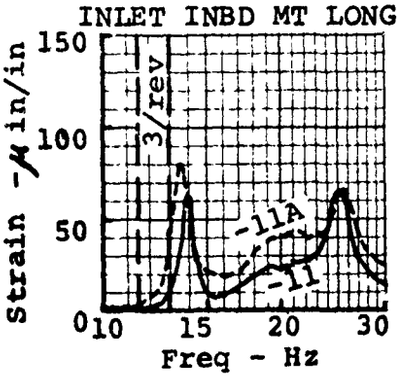

Inlet Housing Mount	-11 @ 3/rev	-11A @ 3/rev
Outbd Long.	30μin/in	65
Outbd 45°	30	70
Outbd Vert.	5	25
Inbd Long.	15	40
Inbd 45°	25	60
Inbd Vert.	10	25

- T55-11A ENGINE WEIGHS 40 POUNDS MORE THAN THE T55-11.

Figure 38. T55-11 Compared to T55-11A.

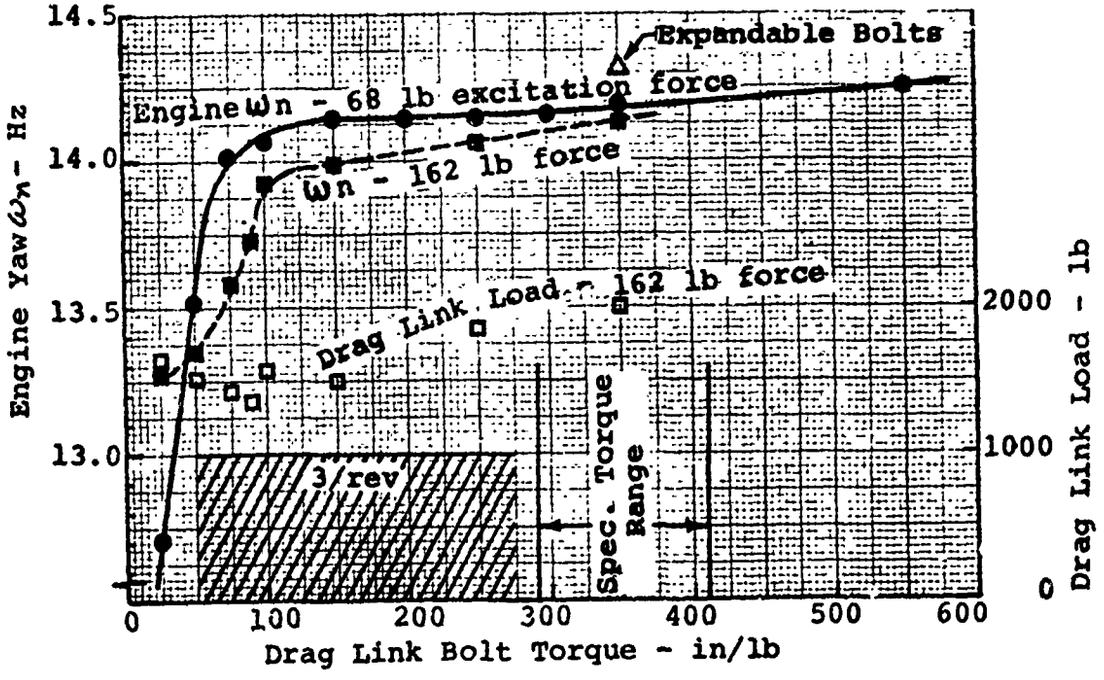

Figure 39.Effect of Drag Link Bolt Torque.

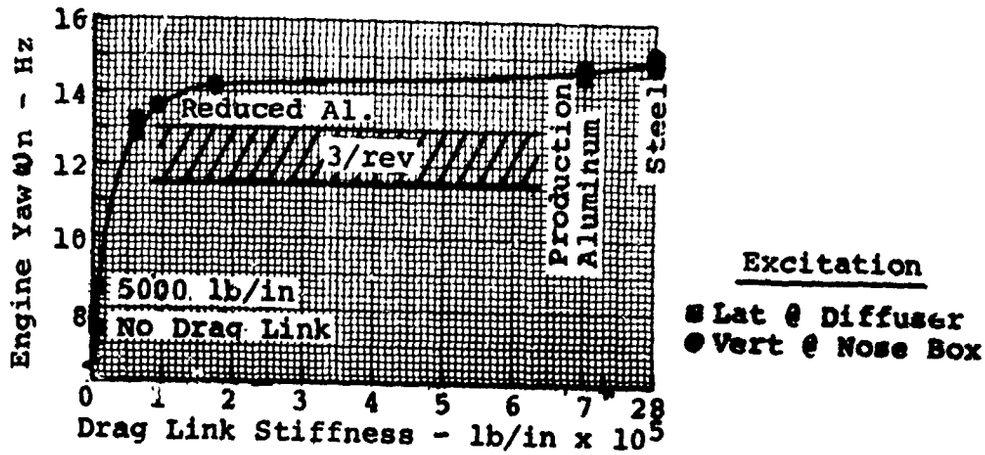

Figure 40. Effect of Drag Link Stiffness.

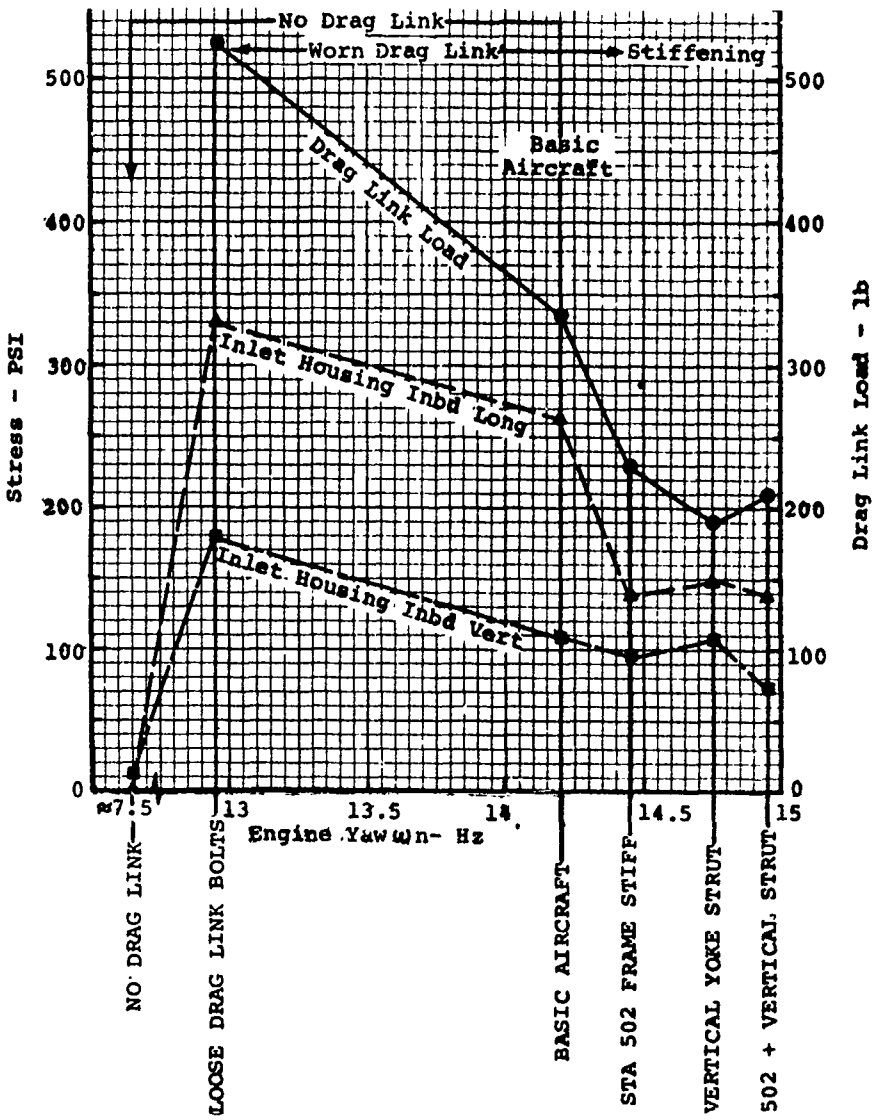

Figure 41. Configuration Effect on Yaw Frequency.

During the flight vibration/stress survey there were significant differences in the vibration/stress levels between the two engines. Figure 42 shows a comparison in the baseline configuration.

Since each engine has a right angle gearbox mounted on its forward end, with the shaft running inward toward the fuselage centerline, the torque reactions of the engines are in opposite directions. This places typically a 500-pound compression load in the aft engine mount link of the No. 1 engine and a 500-pound tension load in the No. 1 engine aft mount link. An engine right angle transmission was locked internally so that a static torque in the cross shaft would be reacted by the engine mounts.

Static torques were applied to the cross shaft to place the aft engine mount link in 500 pounds compression, 500 pounds tension and to unload the link. Frequency sweeps showed no change in engine response between the compression or tension load; but with no load in the aft engine support link, the resonant frequency was decreased from 14.2 Hz to 13.7 Hz as measured by the strain gages on the inlet housing. However, the drag link load did not change in frequency or amplitude.

This work led to the conclusion that the approach which would yield the most favorable results was to "soften" the drag link. The drag strut was needed to assure cross shaft alignment in severe maneuvers; therefore, it could not be eliminated. However, it was found that the alignment conditions could be met if the hole in one end were elongated to a slot which would permit a total motion of .145 inch relative to the mating fitting.

Description of the Solution

A set of these slotted drag struts was evaluated in a flight program. The results are shown in Figures 43 and 44. The No. 1 engine inlet housing 3/rev stress levels, the prime component of the absolute stresses, show as much as a 90% reduction at the higher rotor speeds with the installation of the slotted drag strut. The slotted drag strut does not produce increases in vibration from other prime rotor harmonics (1, 6, 9, 12/rev). The 7.5 Hz yaw mode does not produce any significant 3/rev engine response during start procedure (150 rpm). No rise in stresses occurred when the slot bottomed. (Probably no severe bottoming occurred.) The slotted drag strut eliminates yaw mode effect on 3/rev engine response.

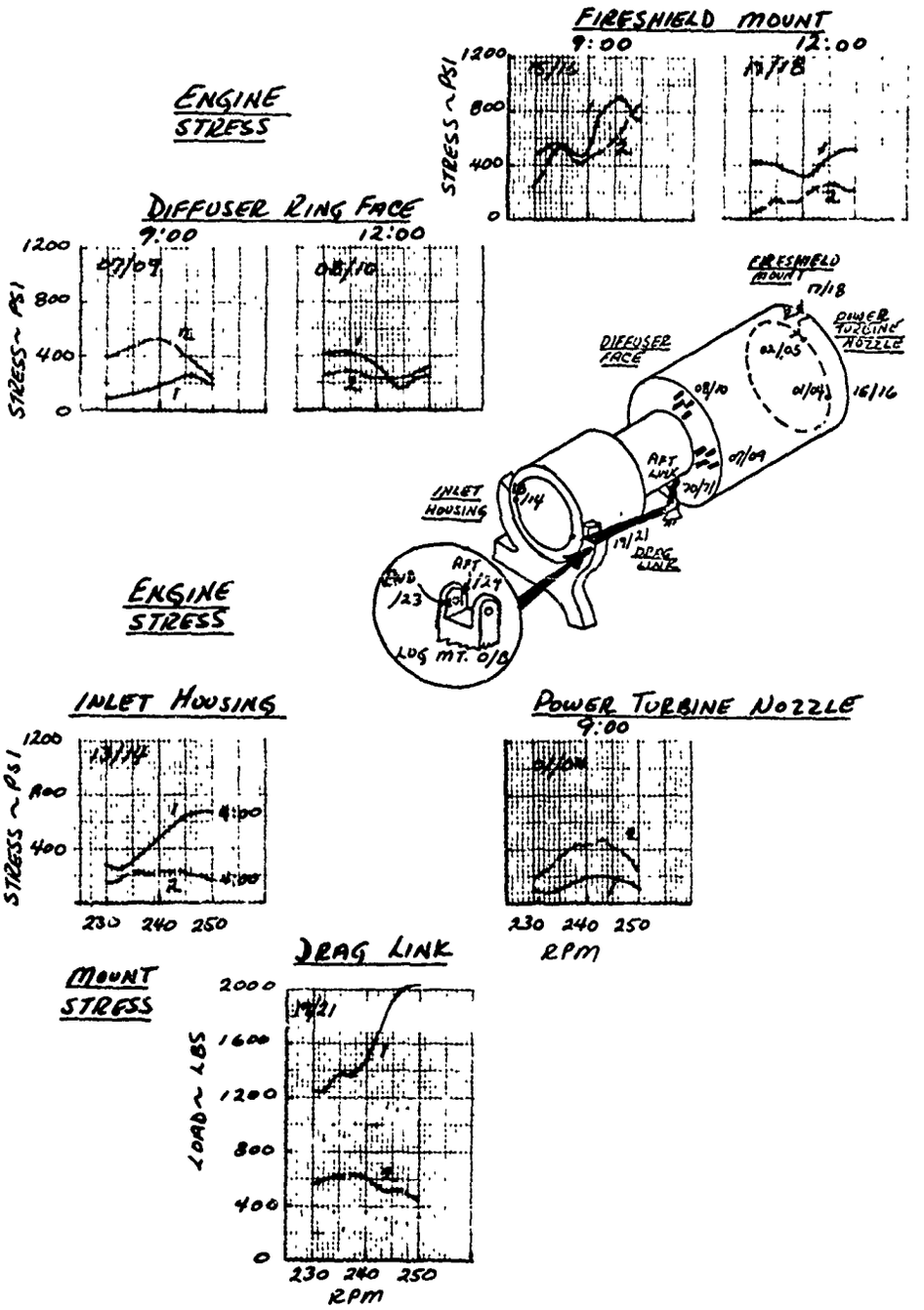

FLIGHT DATA ENGINE NO. 1 COMPARED TO ENGINE NO. 2
GROSS WEIGHT = 35,500 POUNDS, SPEED = 151 KTAS

Figure 42. Baseline 3/Rev Stress vs RPM.

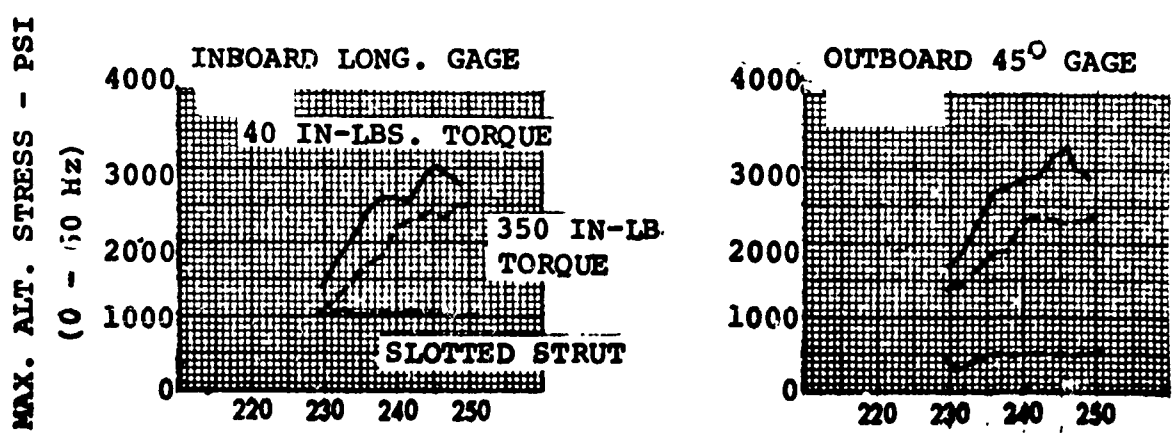

NO. 1 ENGINE INLET HOUSING
140 KNOTS

Figure 43. Inlet Housing Stress.

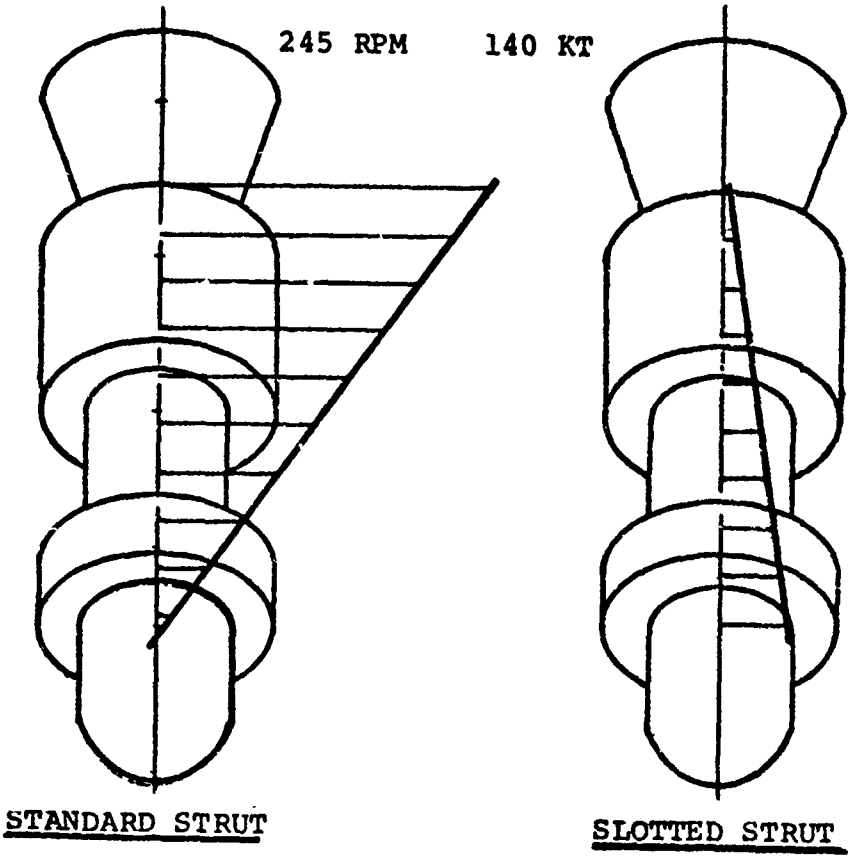

NO. 1 ENGINE MODE SHAPE

Figure 44. Lateral 3/Rev Engine Vibration.

The No. 2 engine inlet housing stresses were generally less than with standard struts.

The life improvement was calculated using a conservative inlet housing stress reduction of 30%. A normalized mean -3σ S/N curve for cast magnesium was used to construct a curve of life factor vs actual stress to endurance limit ratio for a 30% stress reduction. (The S/N curve included a correction for the operating temperature of the magnesium.)

Using this curve and a 30% reduction in stress, a fivefold increase in life is obtained at a stress level over endurance limit of two. This applies to the No. 1 engine. The maximum No. 2 engine inlet housing stress level measured is at the elevated temperature mean -3σ endurance level so that it should not fail. The slotted strut has been installed in production.

Limitations Associated with the Solution

The absolute life will only be established by field experience, since the strain measurement with the slotted drag link was limited to one CH-47C. Currently, no failures have occurred since the slotted strut was incorporated.

HLH

PROBLEM - DEMONSTRATION OF THE HLH ENGINE CONTROL ROTOR DRIVE SYSTEM DYNAMIC STABILITY

Description of the Problem

The problem was to demonstrate a stable system. To do this required that the analytical model be compared to test data. Then modifications or corrections could be made to improve the validity of the model, and finally an analyis could be made to recommend changes to the hardware characteristics to correct any problems that were uncovered.

Investigation Leading to a Solution

A first step was taken in March 1974 when an assessment of the torsional stability of the HLH system, including the engines, engine controls, rotors, and drive train, was completed. The analysis utilized a dynamic digital computer simulation prepared by Detroit Diesel Allison (DDA) capable of describing the transient performance of the HLH system. The simulation included detailed mathematical models of three T701-AD-700 engines, each with an electronic and hydromechanical fuel control, in addition to one power management control and the rotor rive system. DDA employed a simplified rotor dynamic model within the simulation to facilitate program operation. From previous effort, DDA had determined that this simplification results in a model dynamically similar in the frequency range of concern to the Boeing Vertol 12 mass/11 spring representation.

The simplified model was reviewed and found to be adequate for the scope of this program. Because of the relative magnitude of the shaft constants, the overall spring rate is determined primarily by the centrifugal spring with the others more than an order of magnitude greater. This allows the model to be represented by a 3 mass/4 spring system. In addition, the effect of the lag damper was included as a series spring-mass-damper combination with the damper characteristics presented as a function of the damper velocity.

Considerable effort at DDA was required to correlate the engine simulation with actual engine test data. This simulation validation activity was to lead to improvements to match both frequency response and transient characteristics. The limited amount of engine transient data available, as well as the fixed nature of the engine section of the computer program, restricted correlation efforts at Boeing Vertol. A deceleration transient of the 501-M62B engine was compared to the simulation; the results are shown on Figure 45. The good

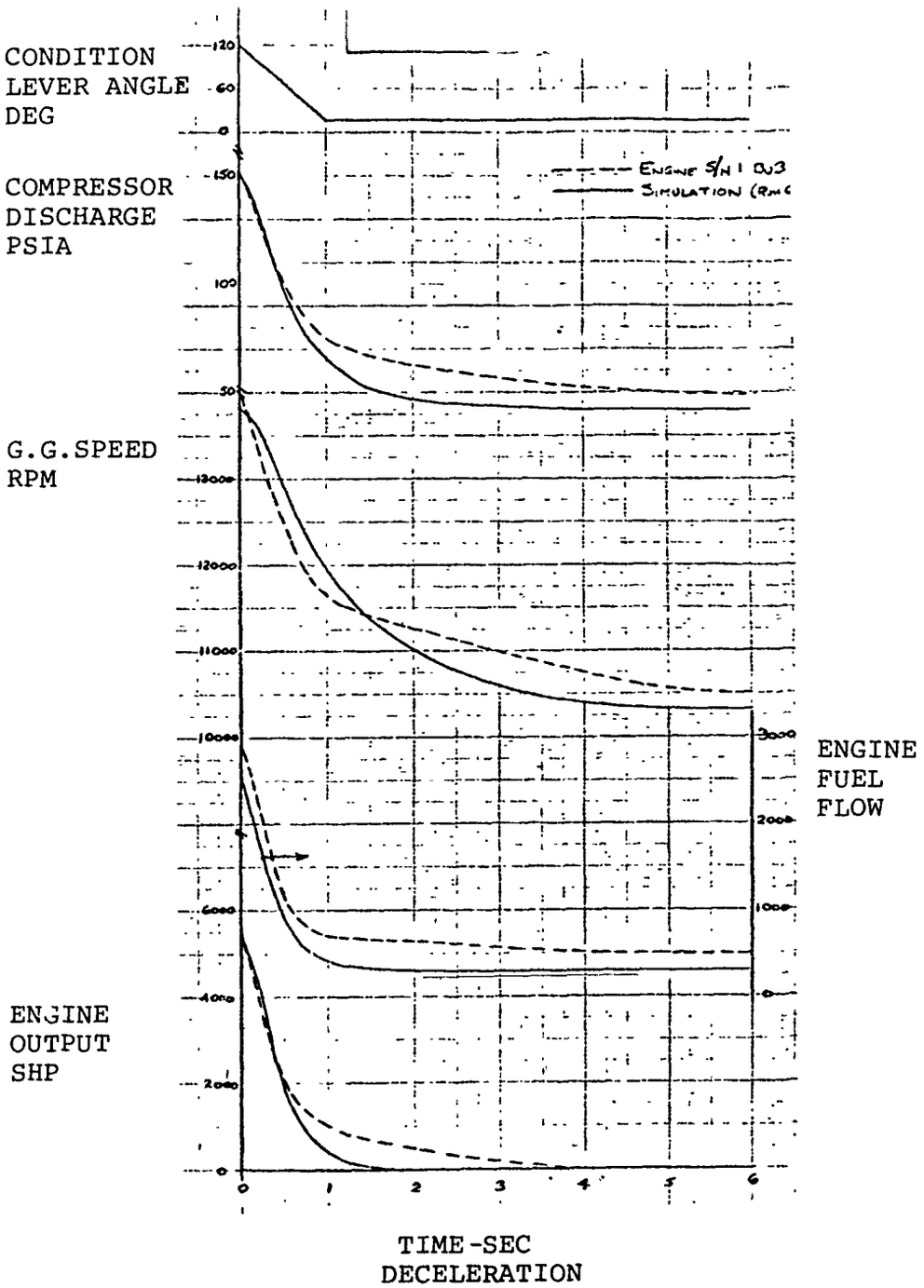

Figure 45. Engine to Simulation Comparison.

correspondence between the two decelerations is evident, especially with respect to the rate of change of each significant engine parameter. However, the tendency of the simulation to continue to zero power while the actual engine hangs up after 0.5 sec required investigation.

Stability was evaluated through observation of transients resulting from small inputs in rotor load, collective pitch, and rotor speed selected. Various flight conditions and operational modes were also reviewed.

The operation of the propulsion/rotor system was analyzed considering small, rapid changes in power required by the rotor at both high and low power levels. Figure 46 describes the time transient resulting from this disturbance and shows the well-damped, stable characteristic of the speed governing system with no collective anticipation. A sudden 10% rotor power change causes a peak power turbine speed deviation of less than 0.25%. The system has essentially returned to the selected speed within 5.0 sec with no tendency to overshoot or oscillate.

Although Figure 46 describes response for sea level, standard day conditions, analysis has shown that these basic stable characteristics are experienced throughout the flight envelope, from -65°F to + 125°F and up to 10,000 feet. In addition, stable performance with one engine inoperative was demonstrated, with the power turbine speed variation being about twice that with all engines operating.

The degree of stability was determined by evaluating transients with higher proportional power turbine speed governor gains. This analysis showed that the control gain could be increased by a factor of 8.0 with no significant increase in the tendency of the system to sustain oscillations. A satisfactory gain margin of at least 18 dB was exhibited. Since it was not considered necessary at the time to decrease the transient rotor droop, no change was recommended.

The stability of the system following collective pitch inputs was evaluated, and typical results are given on Figure 47. The initial power turbine speed increase immediately after a collective pull was the result of the anticipation or compensation directly affecting fuel flow and engine power. This speed change was seen only at the power turbine; no impulse was noted at the rotor because of shaft flexibility. The effectiveness of this anticipation toward improving transient

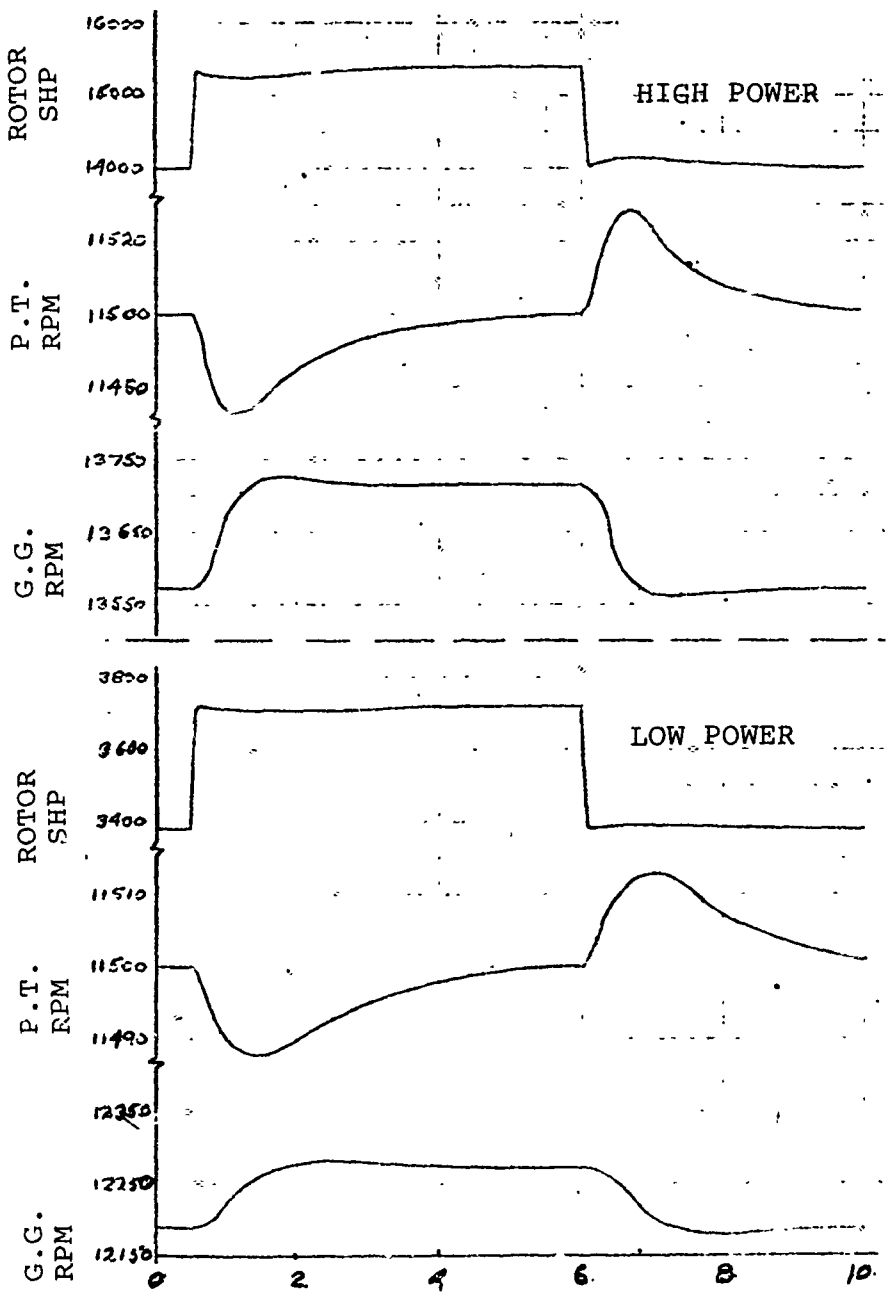

3 ENGINES SLS 59°F

Figure 46. Response to 10% Rotor Load Change.

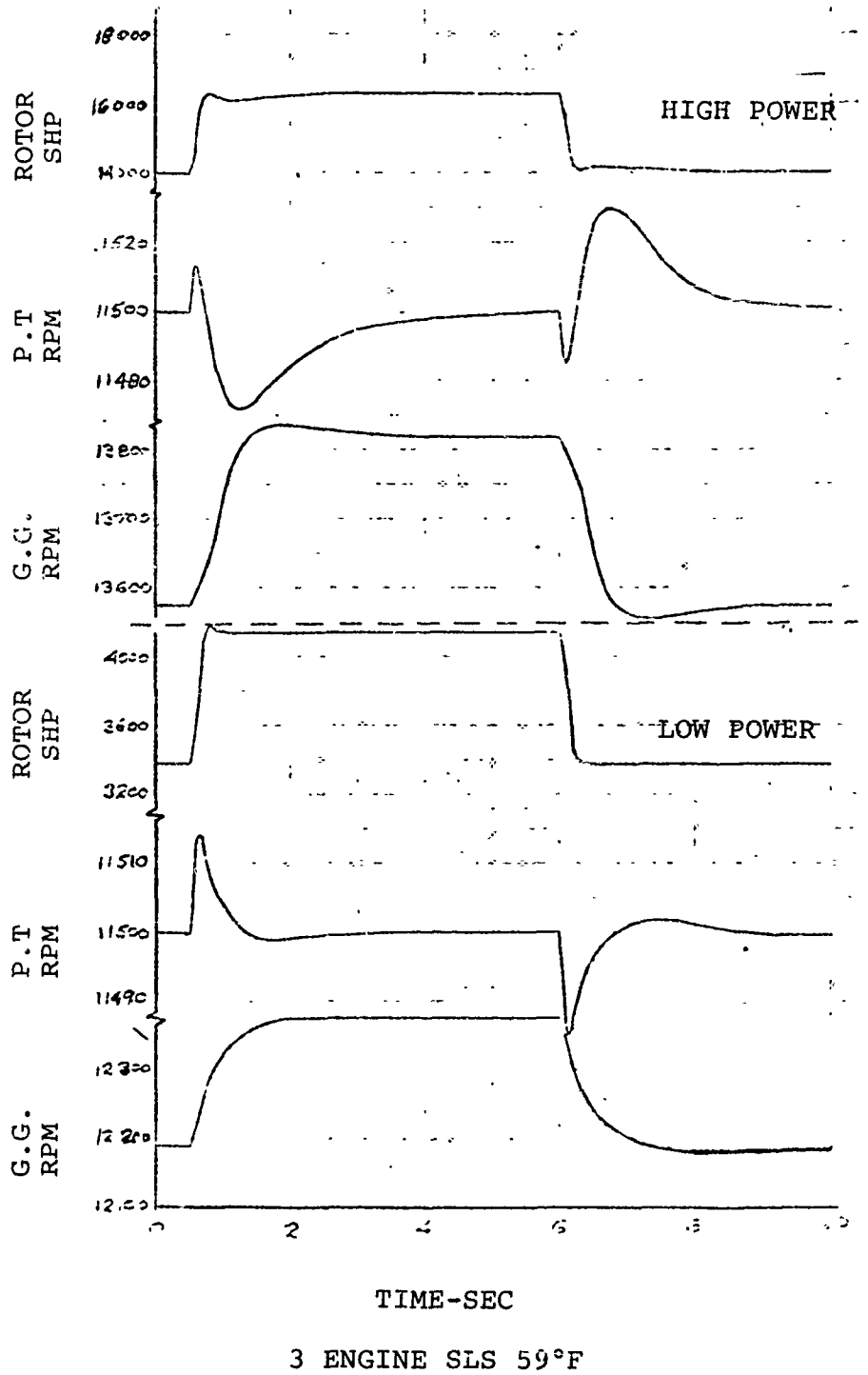

Figure 47. Response to Collective Pitch Input.

response was demonstrated by comparison of the estimated speed droop with and without anticipation (Figures 47 and 46 respectively); a load change of 16% yields the same transient droop as a 10% load change with no anticipation. Good stability characteristics were exhibited with relatively small power turbine speed deviations and rapid recovery to the selected speed.

Evaluation of the system operating with one and two engines also showed acceptable rotor speed variations.

Response to a power turbine speed select or master beep input is depicted on Figure 48, which illustrates the reaction to depressing the increase and decrease speed beeper switches for 1.0 sec. Excellent transient behavior to the 2% speed request change is exhibited. Power turbine speed closely follows the input range with a minimal overshoot of less than 0.1% at both high and low power.

The temperature limiting function of the engine electronic control was investigated to determine system characteristics while operating on the power turbine inlet temperature (MGT) limiter. Figure 49 gives an example of a collective pitch power transient with two engines which would exceed the limit of 2100°R (893°C). The transient results in a momentary overshoot of 19°R above the set point but essentially settles out to the limited value within 1.0 sec. The system was considered to be satisfactory, demonstrating stable and well-damped operation.

The transient operation of the power management system is described on Figure 50 by a comparison of response to an engine disturbance with power management selected "ON" and "OFF". A condition lever cutback was input to one engine, reducing the power requested from that engine by about 35%. With the power management inoperative, a large engine output power split of greater than 50% and a power turbine speed decrease of about 50 rpm resulted from the lever input while operating on the individual proportional governors only. With the power management activated, the load sharing and isochronous governing functions were demonstrated. A rapid reaction to the large input disturbance is exhibited; the engine torques are matched to within 5% in 1.0 sec. Additionally, the isochronous governor maintained power turbine speed within 8 rpm and gradually returned it to the selected value after about two oscillations.

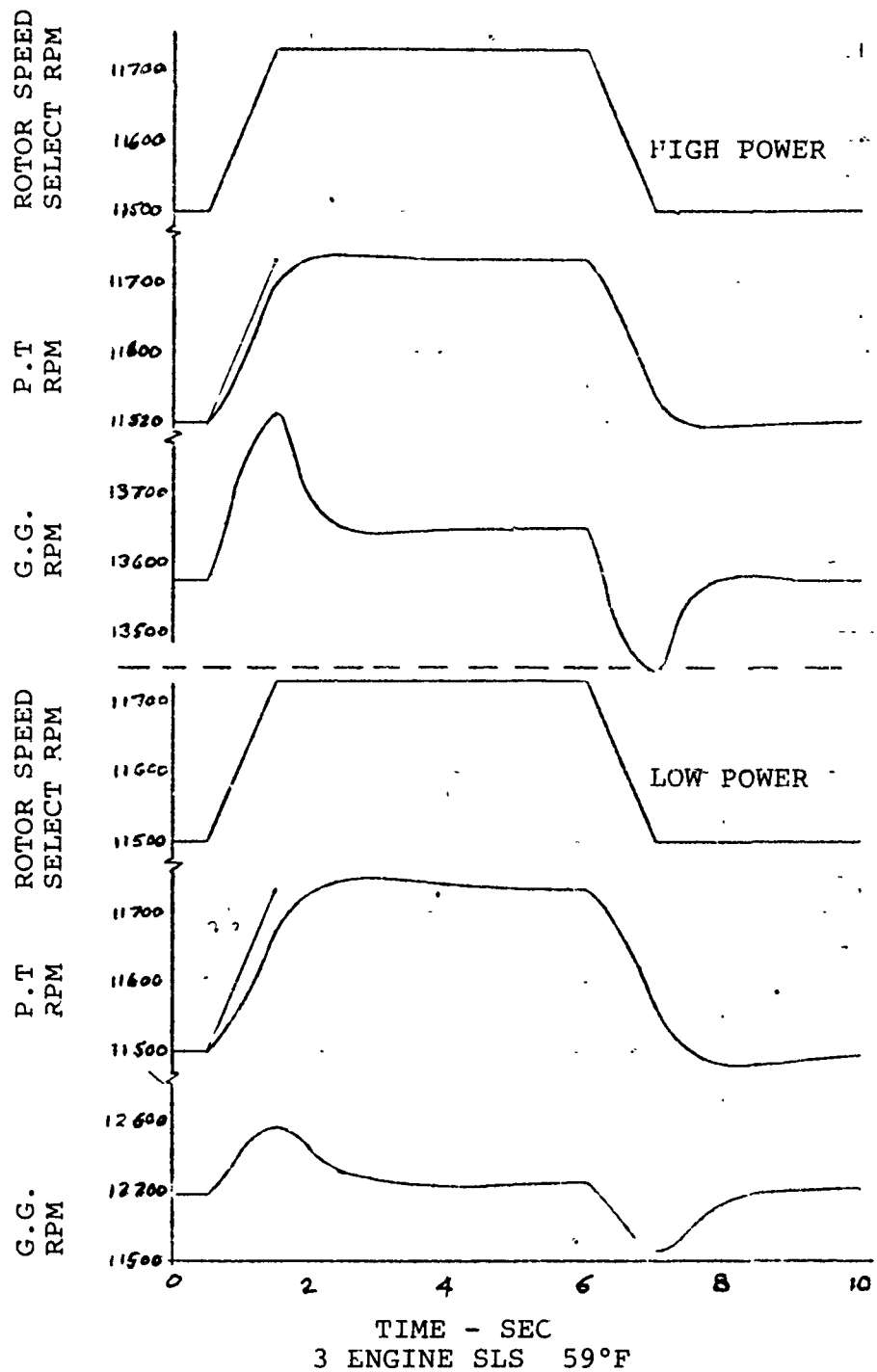

Figure 48. Response to Beeper Input.

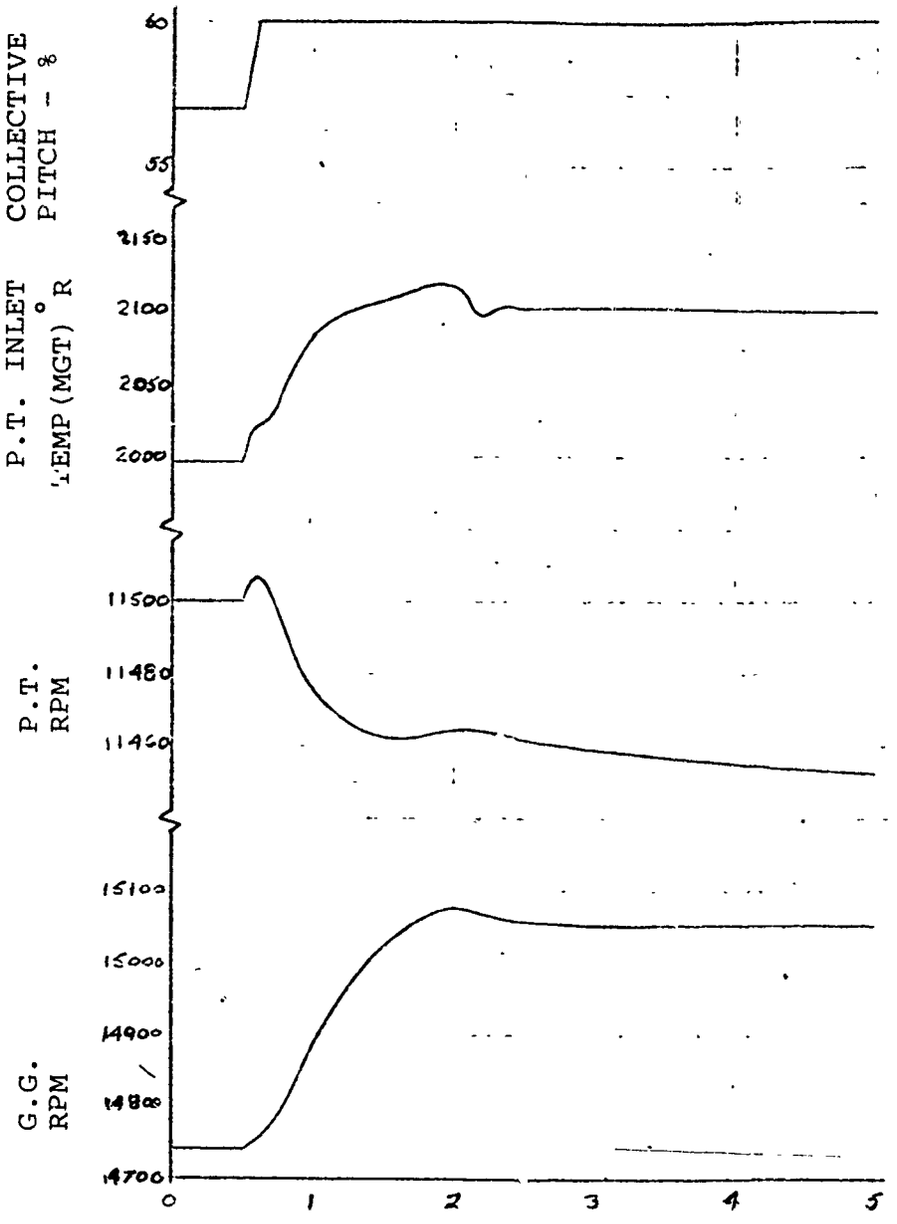

Figure 49. Temperature Limiting.

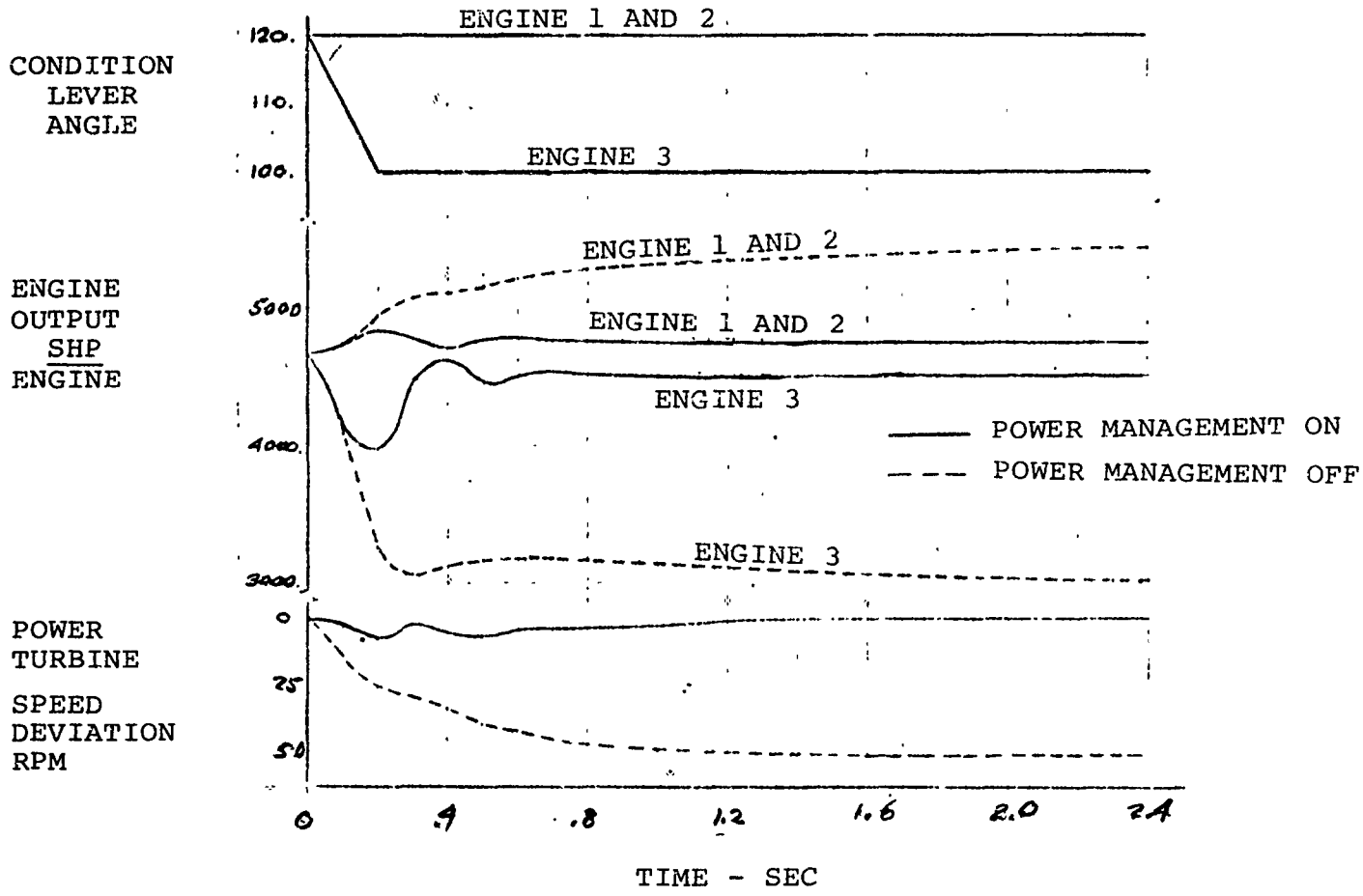

Figure 50. Power Management Control Effect.

These transients demonstrated that the system was very responsive and well damped in both modes of operation.

The effect of the lag damper on system torsional stability was studied primarily to evaluate the validity of the damper simulation. The curves on Figure 51 illustrate the system dynamic response to a collective pitch input with and without a lag damper. The response of the system with no damping was unstable and demonstrates a continuous limit cycle oscillation. Because the validity of the simple lag damper representation was uncertain and the damper was shown to be a critical element of system stability, it was concluded that a more detailed model of the lag damper was required.

By April 1974, the need for a reevaluation of the transient deck became apparent from several observations made during the computer analysis. The results of a stability and transient study showed the response to be unusually good with a very large prototype system gain margin of +18 dB. This led to additional investigations using a simplified linear model which exhibited a much greater tendency to oscillate. Further comparison between the linear and nonlinear simulation uncovered a programming error in the rotor routine significantly affecting stability. By including this revision in the nonlinear digital simulation program, very good dynamic correlation between both models was achieved.

Using the revised simulation and modifying it for DSTR operation, the requirement to improve system stability was demonstrated as illustrated in Figure 52. A power turbine speed request step change was input into the system at a total rotor power of about 7000 hp and standard day conditions. Considering the current system characteristics, Figure 52a shows a sustained oscillation at about 3.0 Hz. The addition of a lag in the speed governing loop was studied as a possible solution to the problems, and its effect is described on Figure 52. Increasing the lag to 0.5 sec provides a system which is adequately damped at this power condition. Although some resonance at the rotor-drive natural frequency remains and a low frequency (0.6 Hz) damped oscillation, caused by the increased phase shift at low frequency, is introduced, the overall characteristic is satisfactory.

Additional analyses were made to evaluate stability while considering the range of DSTR operation and variations in lag damper characteristics to account for temperature and manufacturing tolerance effects. The influence of power level on

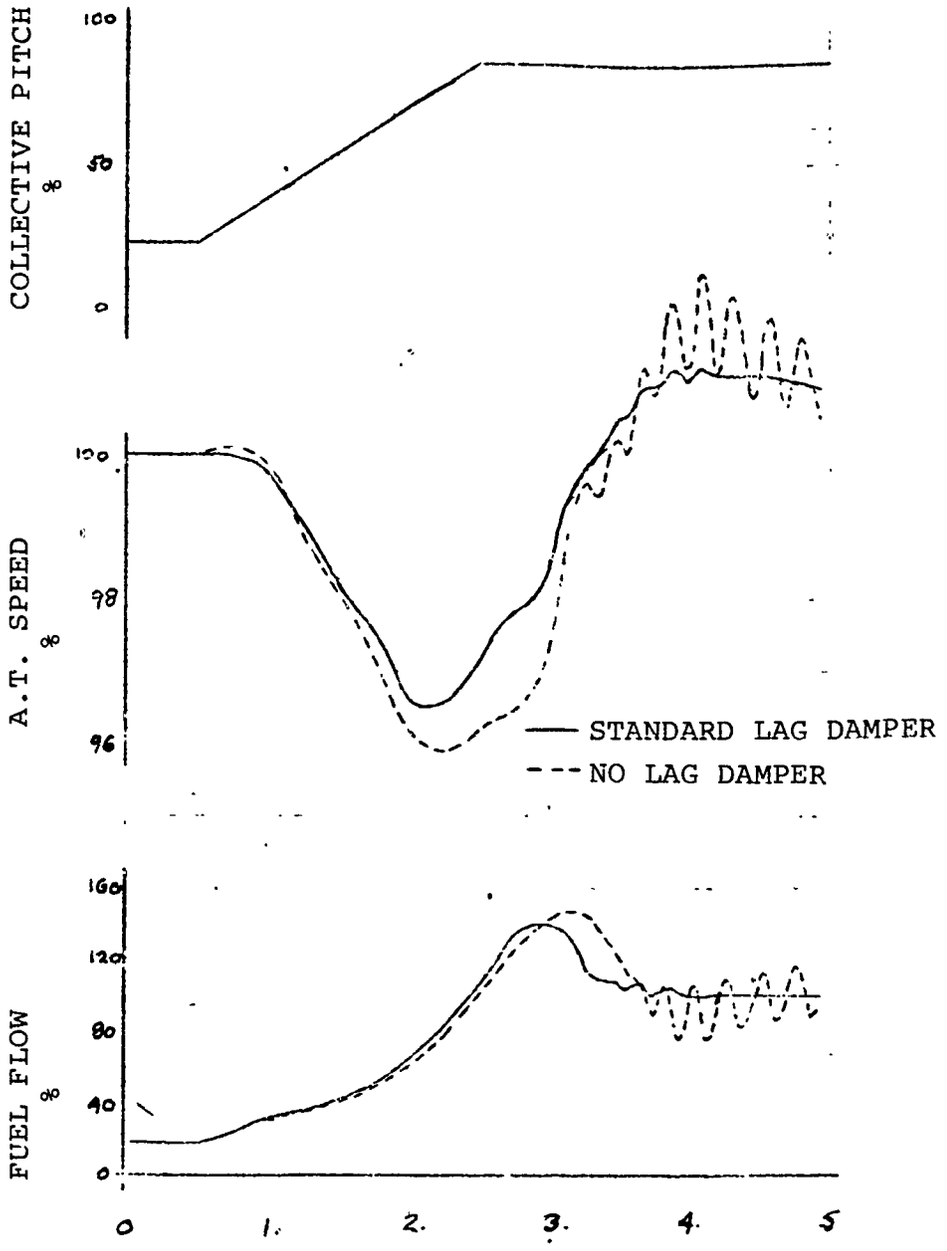

EFFECT OF LAG DAMPER

Figure 51. System Response to Collective.

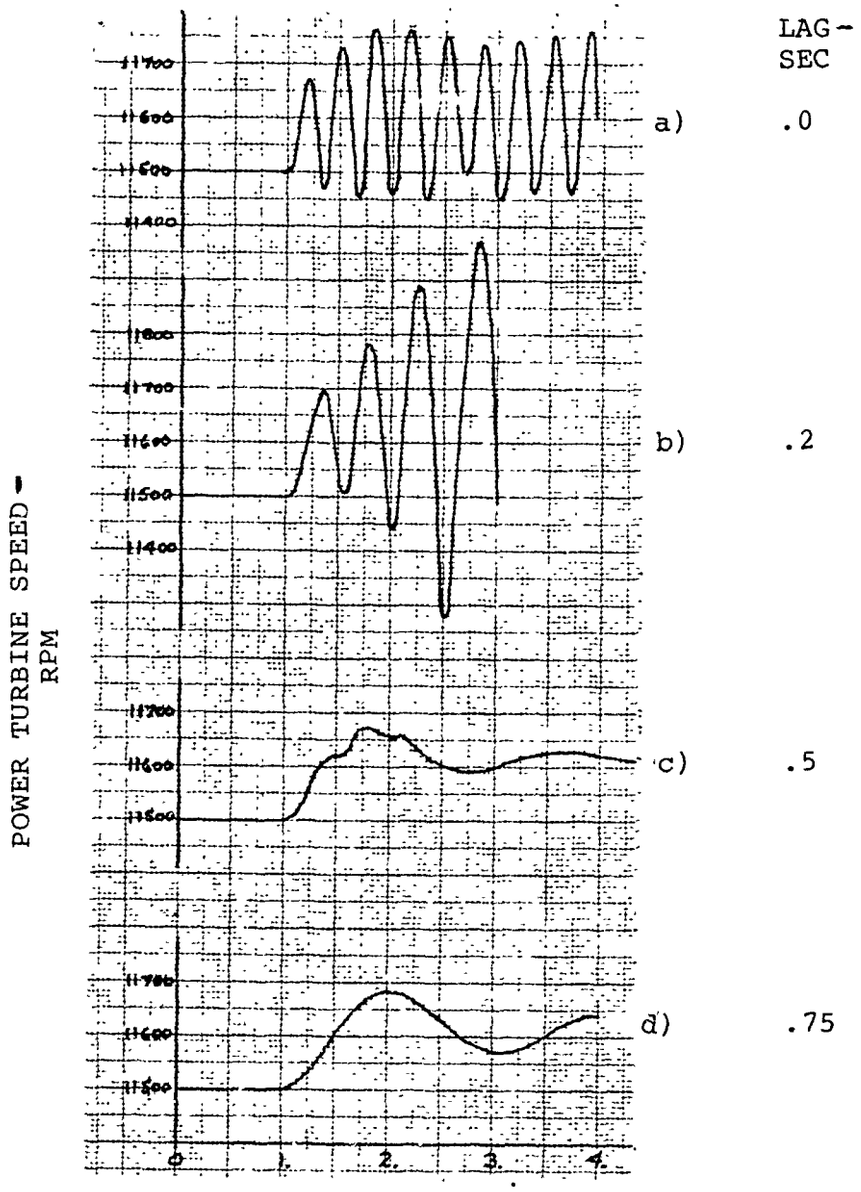

+1% POWER TURBINE SPFED REQUEST STEP

Figure 52. Effect of Control Lag.

system stability with a .5-sec power turbine governor lag is shown on Figure 53 with a three-engine low power case on curve (a); a three-engine cold day, high power case on curve (b); and a two-engine high power case on curve (c). At low power, Figure 53 (a) exhibits a low frequency well-damped oscillation which rapidly decays after two cycles. The increased system gain at high power with three engines operating, Figure 53 (b), picks up the power train resonant frequency which settles out in about 2.0 sec but has a fairly oscillatory characteristic. With two engines operating at high power, the reduced loop gain caused by using two engines has improved stability and results in a very satisfactory system as illustrated on Figure 53(c).

The effect of the lag damper characteristic has been shown to be important through analysis using a linearized program with two engines operating at maximum power. A decrease in the damping rate degrades the stability to the point where, if the dampers are one-half as stiff as normal, limit cycling could occur with three engines at high power. However, this reduced damping level was considered unlikely within DSTR operation.

By July 1974, a simplified engine/control and rotor/drive train simulation with a detailed nonlinear representation of the lag damper had been developed for dynamic analysis of the HLH drive system. This digital computer program was generated (1) to evaluate the lag damper effect on torsional stability, (2) to optimize the engine-control stabilizing compensation for good response characteristics, and (3) to provide verification of the large-scale model being completed at Detroit Diesel Allison.

Revisions to the dynamic simulation had a major impact on estimated overall system stability. Incorporation of a detailed lag damper math model and continued correlation effort leading to several changes to the original program were mainly responsible for the variation in results from those previously presented.

For this analysis, use was made of a computer simulation developed to include linear modeling of the engines, engine controls, and rotor system in conjunction with an existing nonlinear program for the lag dampers. A block diagram of the simulation is given on Figure 54. Figures 55 and 56 define the lag damper representation.

The open loop operation of the dampers and rotor is demonstrated on Figures 57 and 58 which show the response of the system to step inputs in driving torque of 100 and 300 ft-lbs

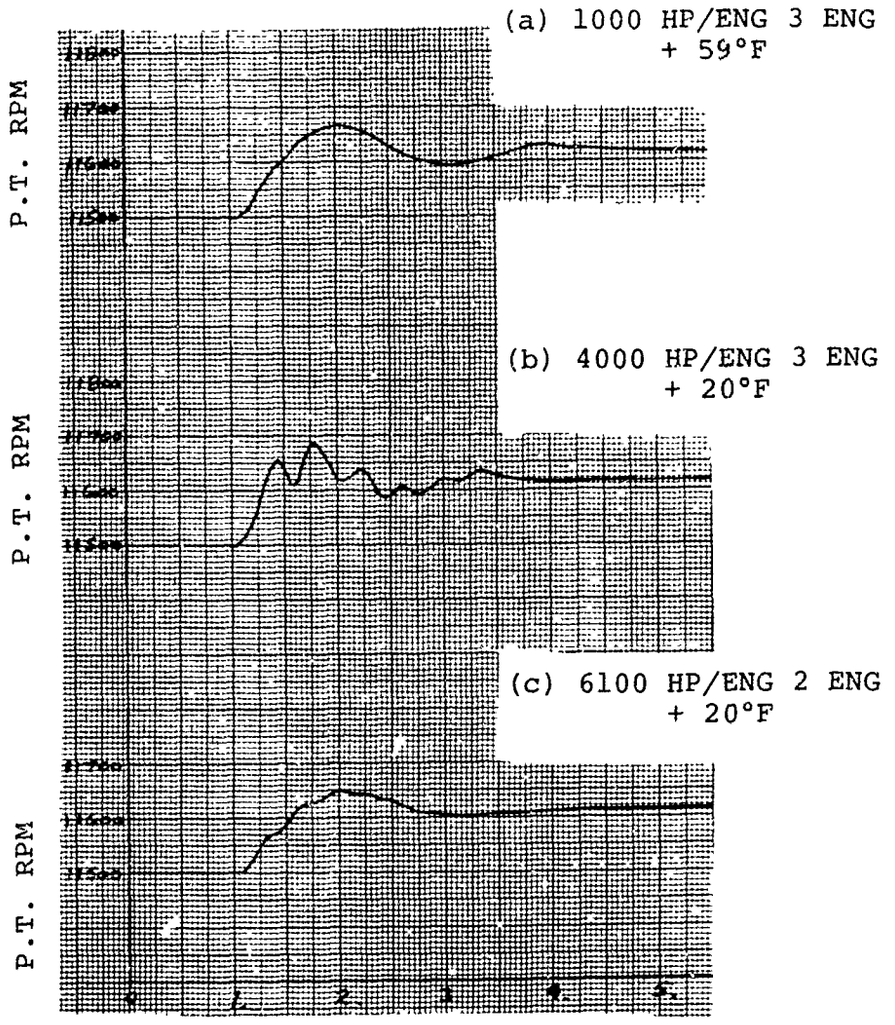

POWER TURBINE SPEED REQUEST STEP INCREASE

Figure 53. Power Variation Effect.

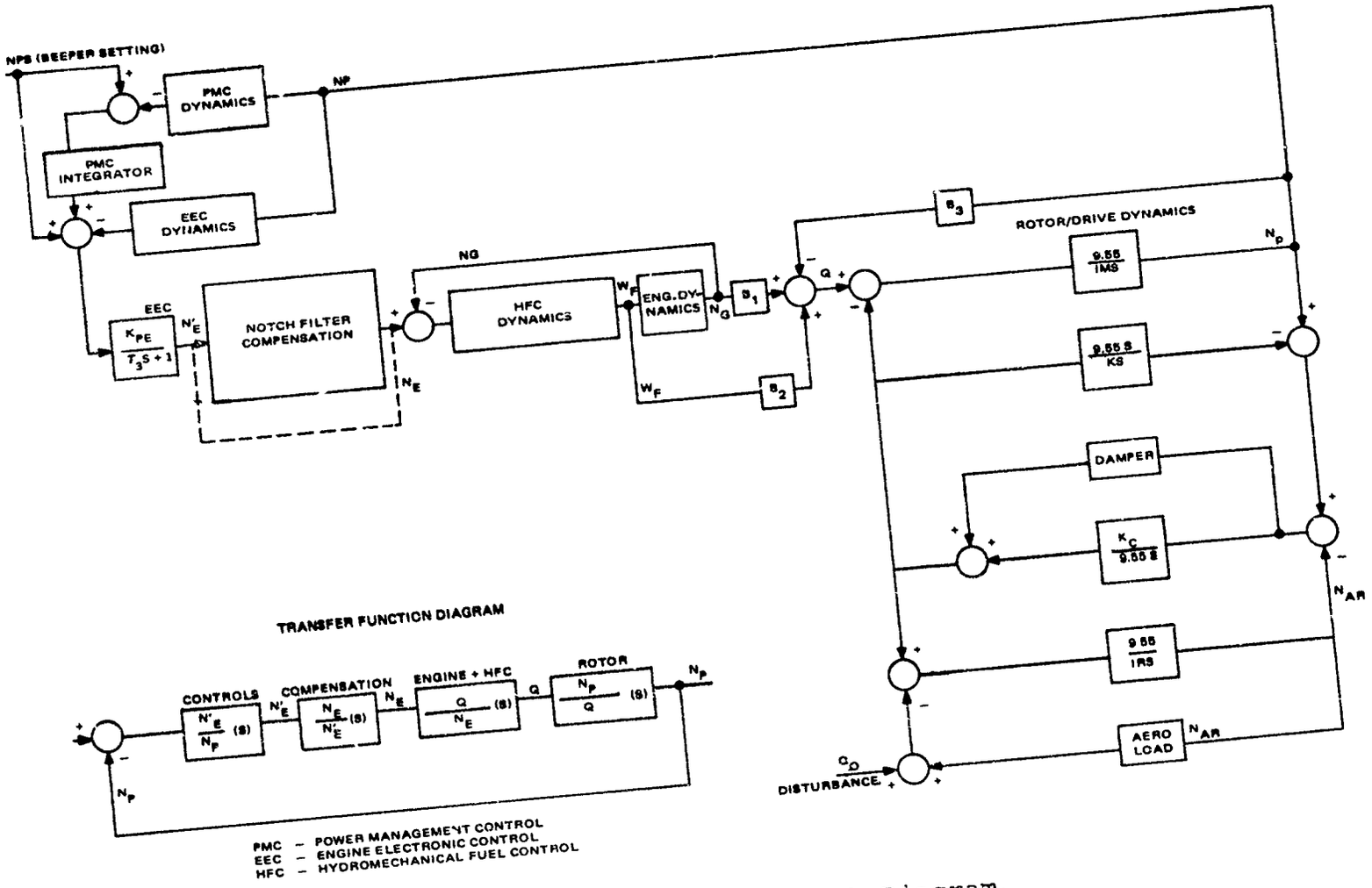

Figure 54. Linear Simulation Block Diagram.

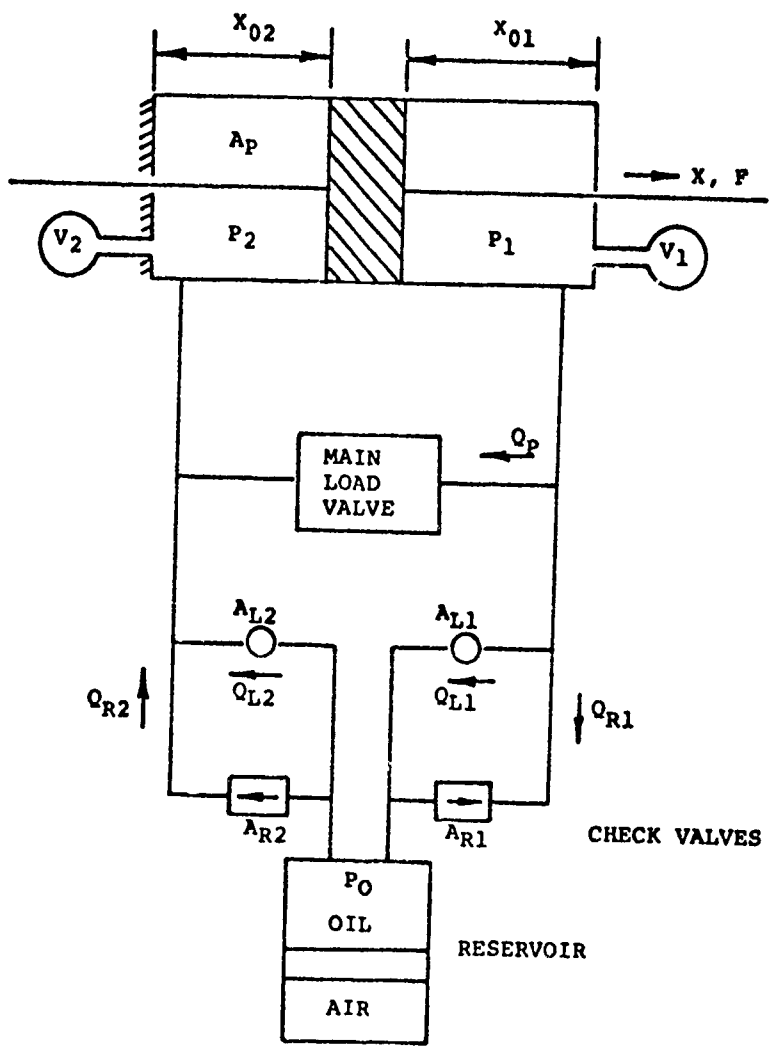

Figure 55. Lag Damper System.

LAG DAMPER EQUATIONS

Force

$$F = (P_1 - P_2) A_p \qquad \text{(Damper Force)}$$

Flow

$$Q_p = f\,(P_1 - P_2) \qquad \text{(Main Load Valve)}$$

$$Q_{L1} = K\,A_{L1}\,(P_1 - P_o)^{1/2} \qquad \text{(Bleed Orifice)}$$

$$Q_{L2} = K\,A_{L2}\,(P_o - P_2)^{1/2} \qquad \text{(Bleed Orifice)}$$

$$Q_{R1} = K\,A_{R1}\,(P_o - P_1 - P_c)^{1/2} \quad [\text{if } (P_o - P) > P_c] \quad [\text{if } (P_o - P_1) \leq P_c] \qquad \text{(Check Valve)}$$

$$Q_{R2} = K\,A_{R2}\,(P_o - P_2 - P_c)^{1/2} \quad [\text{if } (P_o - P_2) > P_c] \quad [\text{if } (P_o - P_2) \leq P_c] \qquad \text{(Check Valve)}$$

Continuity

$$\dot{P}_1 = B(A_p\dot{X} - Q_p - Q_{L1} - Q_{R1}) / [A_p(X_{01} - X) + V_1] \qquad \text{(Damping Chamber)}$$

$$\dot{P}_2 = B(-A_p\dot{X} + Q_p + Q_{L2} + Q_{R2}) / [A_p(X_{02} + X) + V_2] \qquad \text{(Damping Chamber)}$$

LAG DAMPER CONSTANTS

A_p	= in.^{2}	(Damper Piston Area)
A_{L1}	= A_{L2} in.^{2}	(Bleed Area)
A_{R1}	= A_{R2} in.^{2}	(Check Valve Open Area)
X_{01}	= X_{02} in.^{2}	(Chamber Length)
V_1	= V_2 in.^{3}	(Effective Volume)
P_o	= psig	(Reservoir Pressure)
P_c	= psid	(Check Valve Crack Pressure)
B	= psi	(Bulle Modulus)
K	= in.^{2}/sec$\sqrt{\text{lb}}$	(Flow Coefficient, + 80°F)
K		(Flow Coefficient, - 65°F)

Figure 56. Lag Damper Equations and Constants.

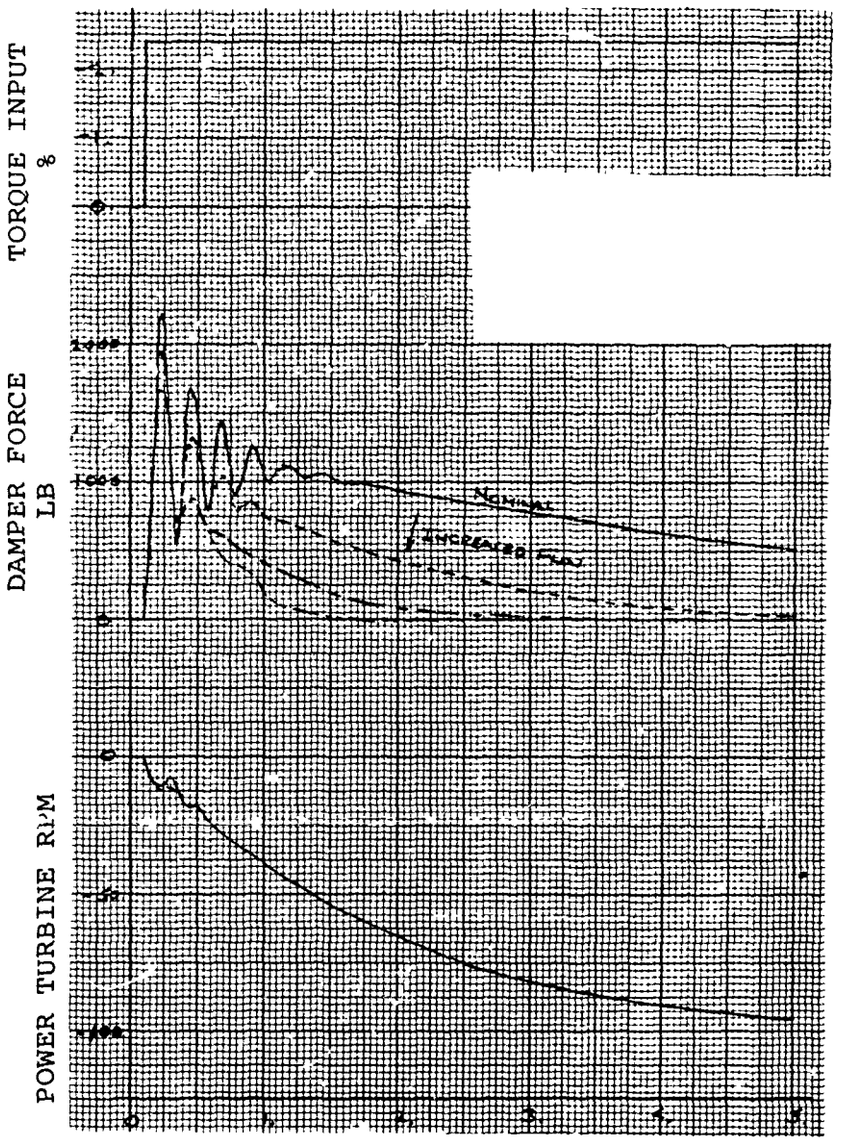

9000 HP, 3 ENGINES, 11,500 RPM

Figure 57. Lag Damper Response-100 Ft-Lb Torque Input.

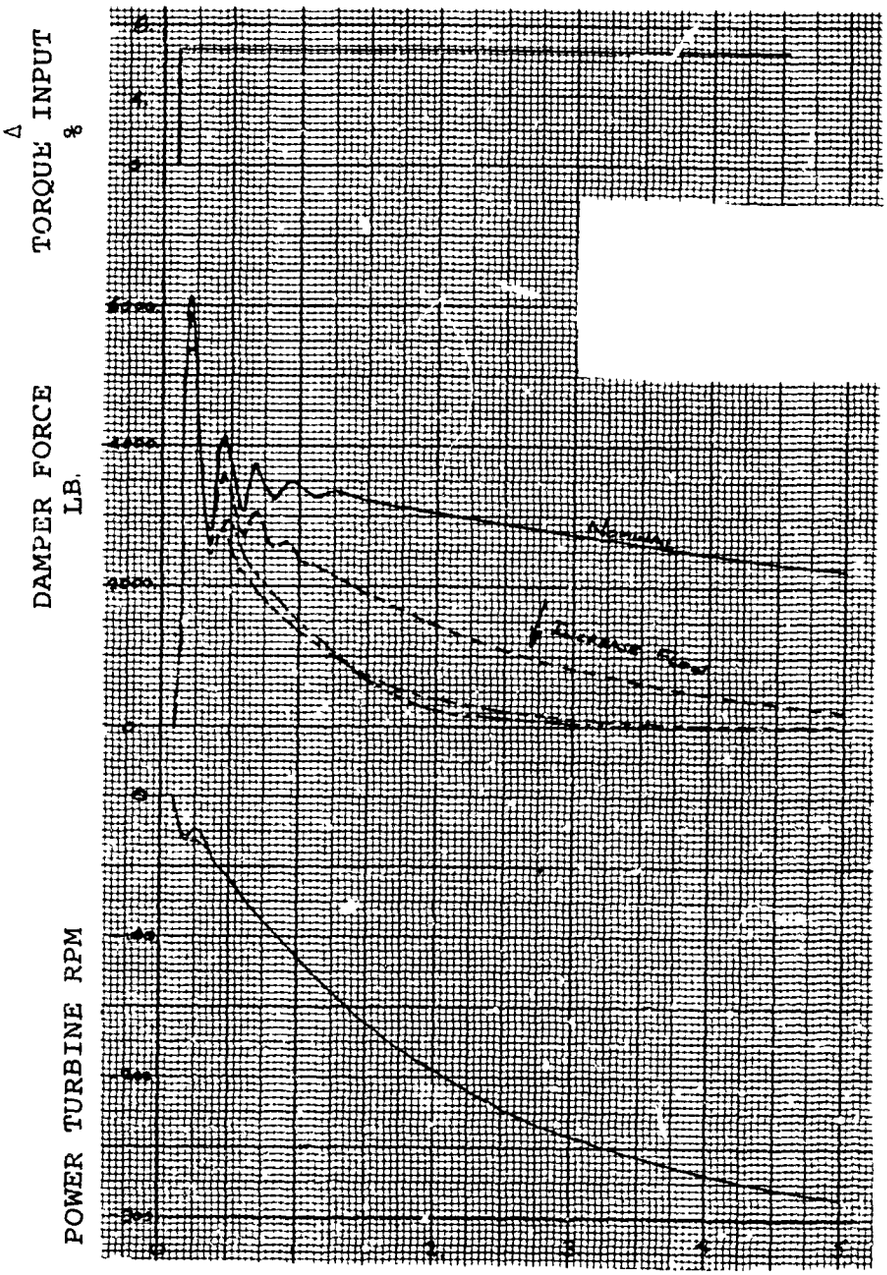

9000 HP, 3 ENGINES, 11,500 PT RPM

Figure 58. Lag Damper Response - 300 Ft-Lb Torque Input.

respectively. For the nominal or current design, this input results in a relatively undamped power turbine-rotor system with a considerable tendency to oscillate and a very long damper recovery time. A significant residual damper force remains after 5.0 sec. By revising the main load valve characteristics to allow flow at low differential pressures, as described on Figure 59 , a more damped transient returning quickly to null is exhibited.

The lag damper, while providing very little damping during low magnitude transients, effectively acts as a spring with a rate determined primarily by the fluid compressibility. This characteristic is caused by the load value overlap which results in a deadzone or zero flow until a damper pressure difference of 300 psi is exceeded. The fluid is thereby trapped in the damping chambers.

The effect of the damper on overall power turbine speed loop stability at high power is demonstrated on Figure 60 for a standard day and Figure 61 for a cold day. Small 1.0% step changes in rotor load torque were applied to the system. For the nominal damper, a continuous oscillation or limit cycle at a frequency of 5-6 Hz is observed at both conditions. The model exhibits a greater tendency toward instability at low temperatures with a significantly greater limit cycle magnitude. It has been assumed for this analysis that damper flow varies inversely with viscosity; therefore, the effect of oil temperature may be included as a viscosity variation. This assumption is valid since the Reynold's numbers within the damper are relatively low and the flow is laminar.

An increase in the damping flow at low force levels improves the stability and completely damps the limit cycling on both standard and cold days. Since the oscillation is basically caused by the spring rate and low damping effectiveness of the lag dampers, it is apparent that the dampers should be altered. The proposed modification consisted of a constant equivalent main load valve area of .00167 in^2 between 300 and 600 psi and a reduction in area below 300 psi as given on Figure 59.

As a result of these analyses, the engine controls were modified to include a nominal lag of .5 sec to provide acceptable transient behavior. The blade lag dampers were modified to provide additional leakage across the piston at low force levels to provide damping to eliminate oscillations.

(a) ——— NORMAL

(b) —·— .000613 IN^2 VALVE AREA AT 300 PSI

(c) – – – .001871 IN^2 VALVE AREA AT 300 PSI

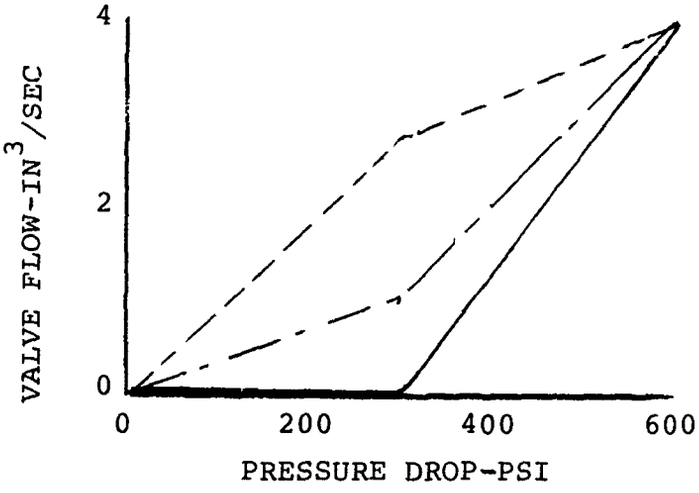

Figure 59. Lag Damper Valve Characteristics.

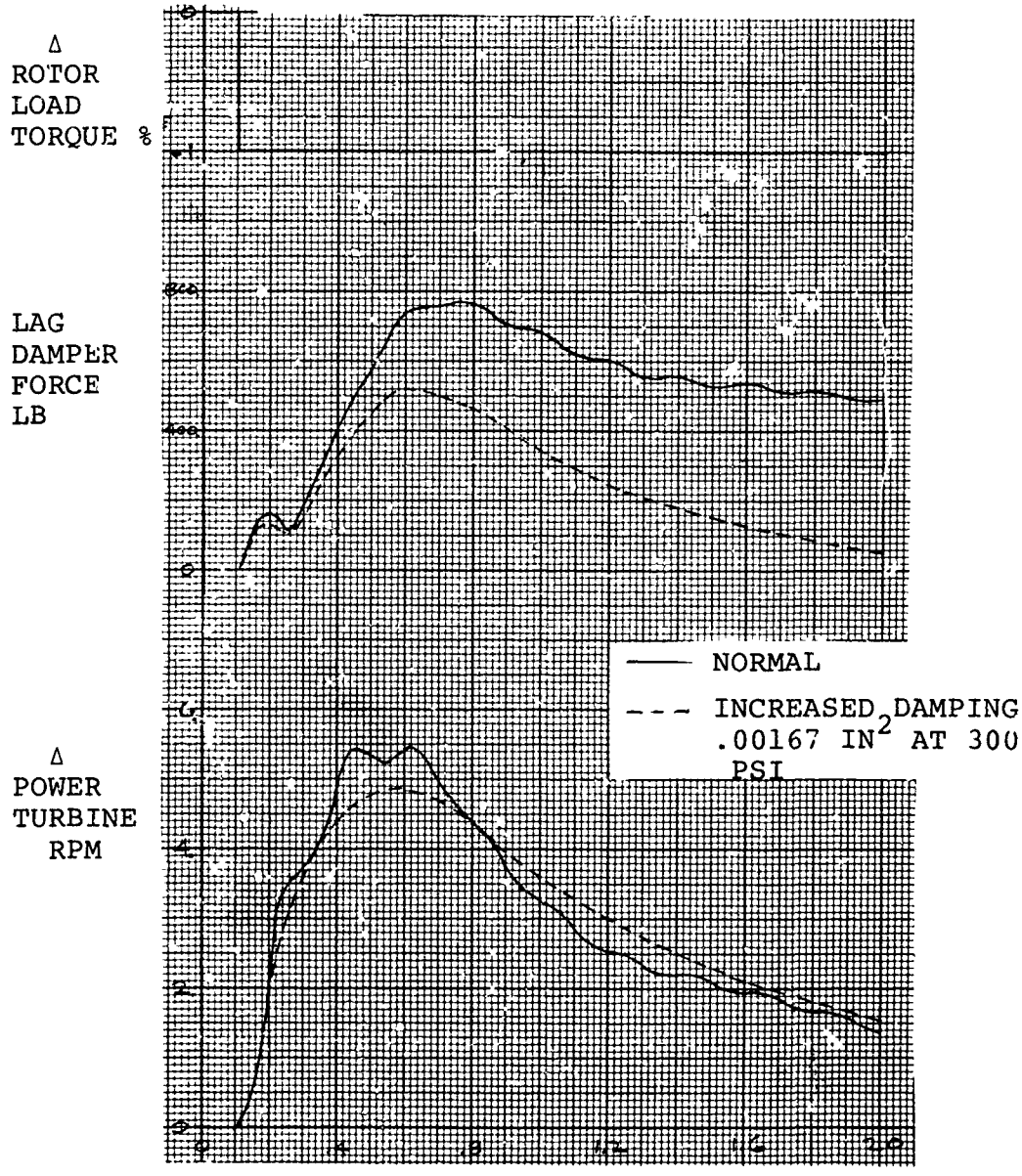

18,000 HP, 3 ENGINE, 11,500 RPM N_p, STD DAY

Figure 60. Standard Day Lag Damper Effect - Response to Load Change.

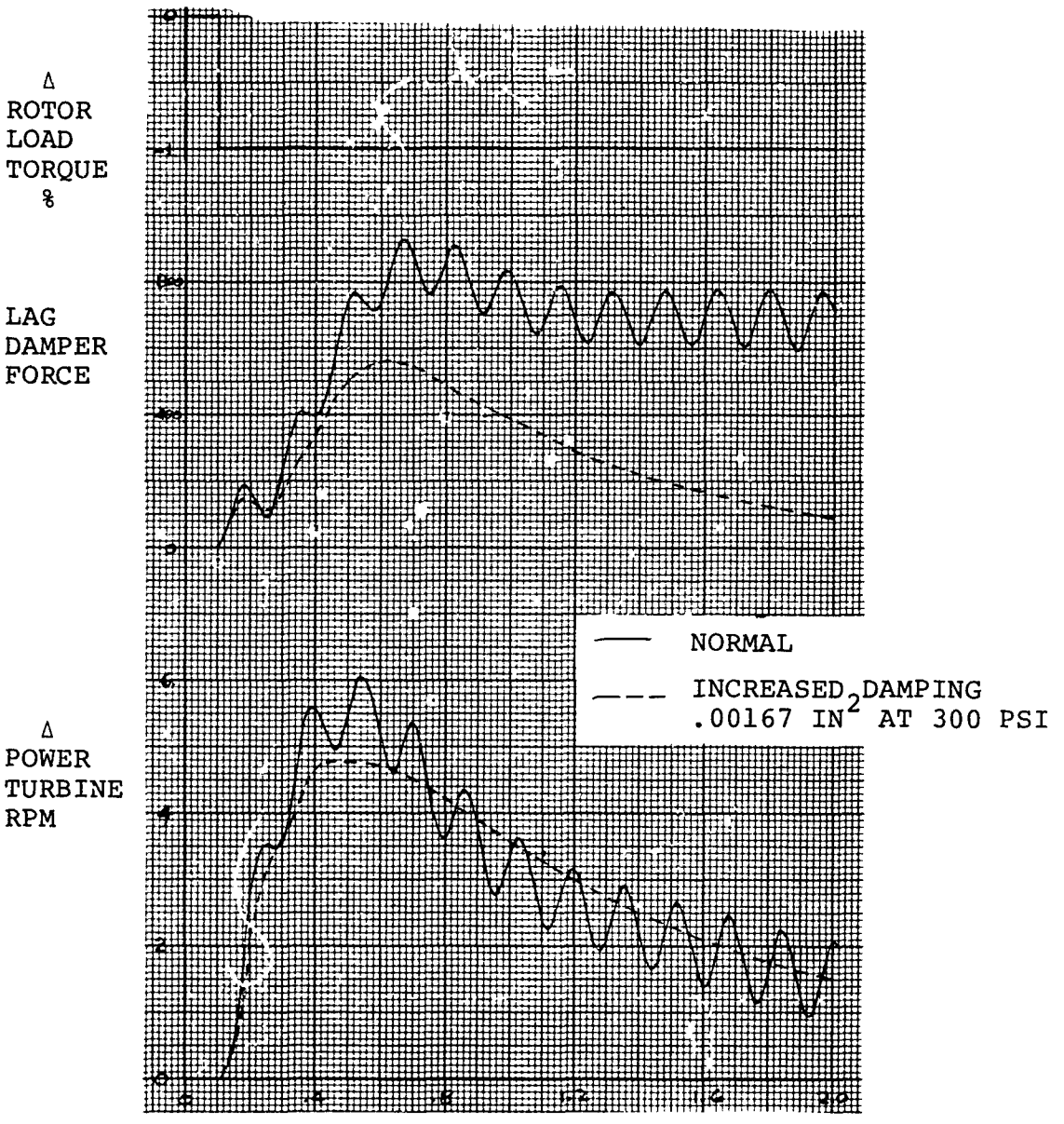

18,000 NP, 3 ENGINE, 11,500 RPM COLD DAY

Figure 61. Cold Day Lag Damper Effect-Response to Load Effect.

In May 1974, the DSTR was operated with the rotor and three engines running for the first time. In December 1974, the initial governing and load stand tests were completed.

DSTR operations demonstrated that the power turbine speed control system had a tendency toward low amplitude oscillations which were somewhat more pronounced when operating in the isochronous governing mode. The magnitude of these fluctuations was very low, not exceeding ± 100 ft-lb (2.7% of intermediate rated torque) at a frequency between 0.3 and 0.6 Hz. Although these oscillations were not considered serious, they did present an annoyance in accurately setting steady state points. A program was undertaken to improve the system in this area.

The most convenient method of effecting a change to closed loop stability was located in the isochronous governing section of the power management control. Since testing had shown that stability on proportional governing only was good and, in addition, that stability during engine development testing was improved by lowering the isochronous gain, revision to this function was analyzed.

The configuration considered during this analysis was three engines at 2400 hp each with nominal lag compensation and original parameter values.

Results of the analysis to determine a value for the integral gain, which will provide better stability while maintaining good response characteristics, are given on Figure 62. The underdamped nature of the original system and the possible improvememt are demonstrated. Selection of isochronous governing "off" significantly increases the effective damping ratio and causes rapid settle-out at a frequency of about 0.6 Hz closely agreeing with test data. Reduction in isochronous gain by a factor of three yields a system which exhibits transient response with a considerably higher damping characteristic. This is the value of gain change incorporated in the DSTR system for June 1975 testing.

This revision was partially effective in steadying the rotor speed during endurance running. However, the results shown on Figure 63 indicate the need for reviewing and optimizing the isochronous gain selected for the prototype to reduce the relatively large excursions caused by the dynamic mismatch between the proportional and isochronous governors. Although the steady-state stability was improved by the decrease in isochronous gain, response during large master beeper increase/decrease transients deteriorated.

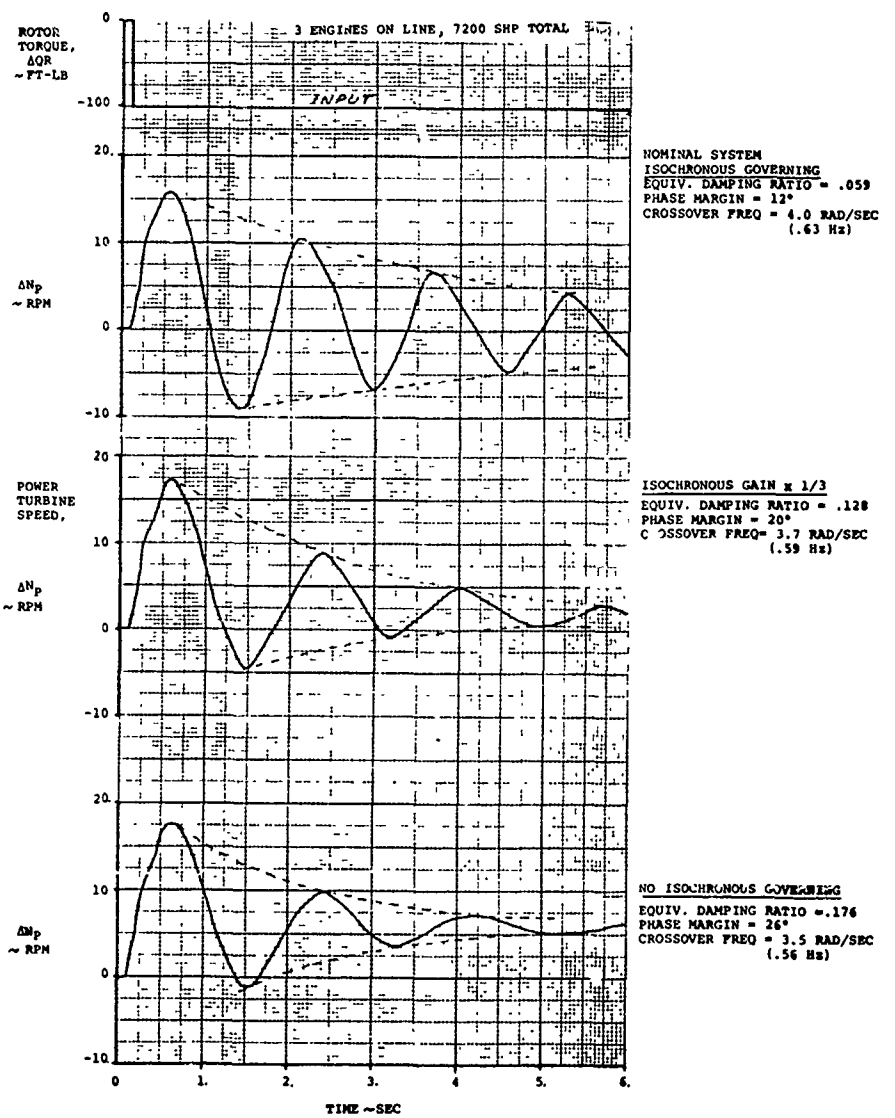

Figure 62. Simulation Transient, Effect of Isochronous Governing.

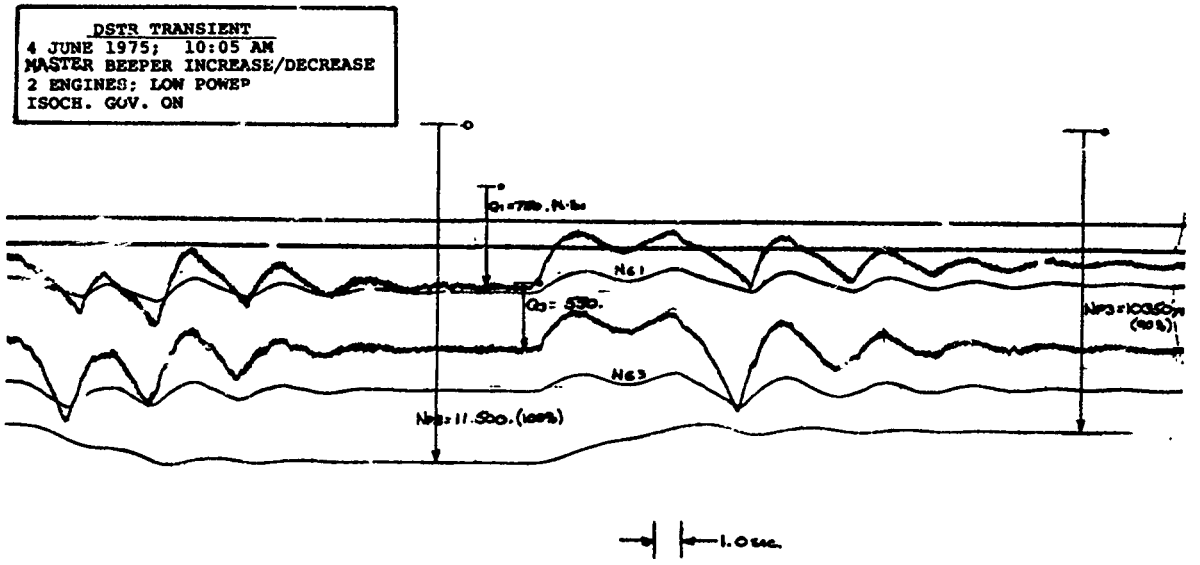

Figure 63. Master Beeper Transient Baseline Isochronous Governing.

The effect of the gain mismatch becomes apparent when the system with no isochronous governor (Figure 64) is compared to the reduced gain system (Figure 63). With isochronous governing disabled, a significantly faster and more stable transient is exhibited. The need for optimizing the isochronous-proportional gain ratio considering both stability and transient effects is clearly shown.

Special engine transient testing was performed to determine system dynamic characteristics regarding torsional stability, to develop stabilizing compensation requirements, and to demonstrate the effectiveness of compensation. During the testing, dynamic data was obtained to permit a comparative evaluation of closed-loop system stability with various types of engine electronic control compensation circuitry. Substantiation of simulation analysis, through correlation of natural frequencies and relative stability levels using the test data, was completed. Subsequent analytical extrapolation to the prototype system was then undertaken.

The DSTR engine control system included a relatively long lag or time constant in the power turbine speed proportional governing loop to provide stable operation as previously discussed. The lag value of T_3 = 0.5 sec (see Figure 62) adequately reduces the gain in the area of rotor/drive train resonance (3-4 Hz) so that oscillations in this frequency range are eliminated. However, because of the additional phase shift associated with this lag at lower frequencies, there is a tendency toward slow response and fluctuations at about 0.3 Hz as shown on Figure 64.

In order to improve system response and stability characteristics, compensation in the form of a second order lead over a second order lag transfer function, or notch filter, was selected, as shown on Figure 54 . The concept of using a notch filter to counteract the drive system torsional resonance has been demonstrated analytically, but had not previously been run as hardware in a dynamic helicopter environment. The DSTR was able to provide an excellent proving ground for this technique.

The program for investigation of stabilizing network requirements was twofold: First, reduce the long time constant included in the DSTR engine electronic control to the point where oscillations are experienced in order to determine system frequencies and second, incorporate various notch filter configurations in the control to verify their capacity to stabilize over an adequate frequency band. All engine electronic control variant testing was accomplished with two engines on-line,

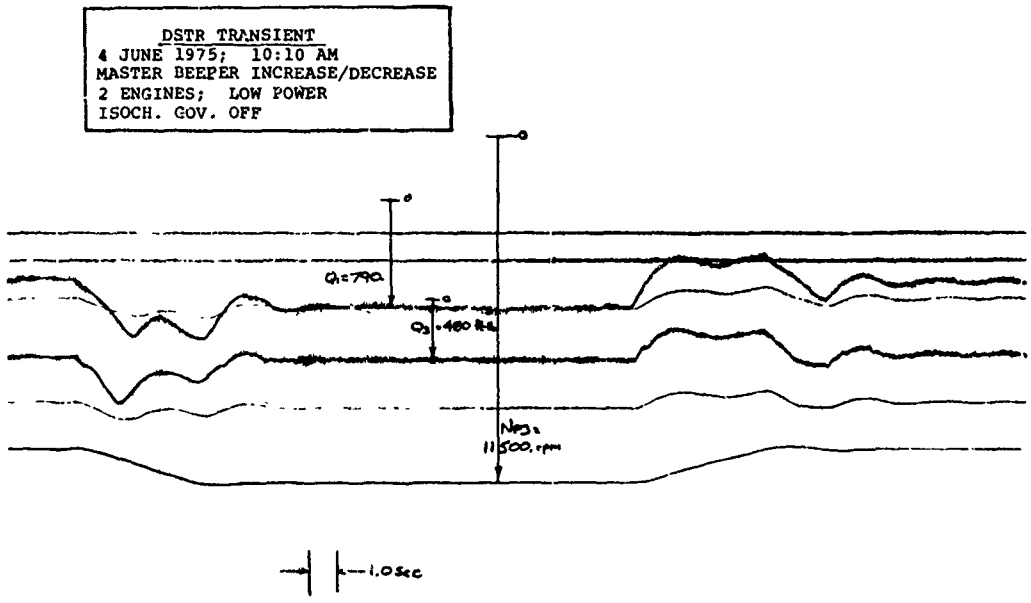

Figure 64. Master Beeper Transient-Isochronous Governing Off.

since only two spare controls were available for revision. Also, isochronous governing was selected "off", as described in the previous section.

A master beeper increase/decrease transient, with the T_3=0.5 sec lag compensation baseline DSTR system at high power, is presented on Figure 65. The relatively slow oscillatory nature of the transient at about 0.4 Hz is apparent.

The lag compensation in the engine electronic controls was changed from 0.5 sec to 0.15 sec to increase the loop gain in the vicinity of rotor/drive natural frequency and reduce stability. This resulted in a tendency to oscillate at about 3 Hz during a master beeper transient as depicted on Figure 66. Triggering the system with a sudden control input by switching isochronous governing off, a limit cycle instability of $\pm$ 175 ft-lb torque and $\pm$ 100 rpm power turbine speed at the system frequency of 3.1 Hz is encountered as shown on Figure 67. This continuous cycling is indicative of a system with neutral torsional stability or zero gain margin. The sustained oscillations are eliminated by reducing engine power, and thereby lowering speed loop gain.

The previously described simulation model was used to demonstrate the effect of stabilizing compensation through the use of open loop frequency responses using classical methods. Figure 43 shows the Bode plots for a system with no compensation, first order lag compensation, and second order notch-filter compensation.

The uncompensated configuration exhibits a high gain peak at the principal rotor drive natural frequency, resulting in a negative gain margin of -6.0 dB, and consequent instability at phase crossover, 3.7 Hz. Reduction in gain is one possible stabilizing technique; however, the magnitude of the necessary reduction would result in an unacceptably slow, inaccurate system.

First order lag compensation of 0.5 sec can adequately reduce the gain near rotor drive resonance to a peak of -16 dB as shown in Figure 68. But the additional phase shift at gain crossover associated with this lag, reducing the phase margin to 30 degrees, causes a tendency toward slow response and underdamped low frequency fluctuations (0.47 Hz).

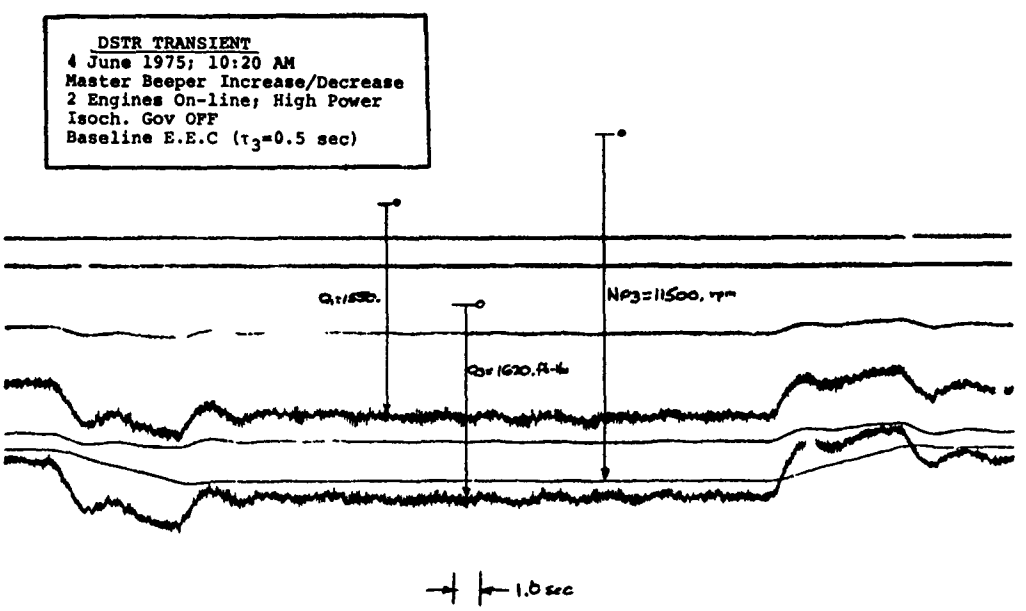

Figure 65. Master Beeper Transient, Baseline (T_3 = .5 Sec).

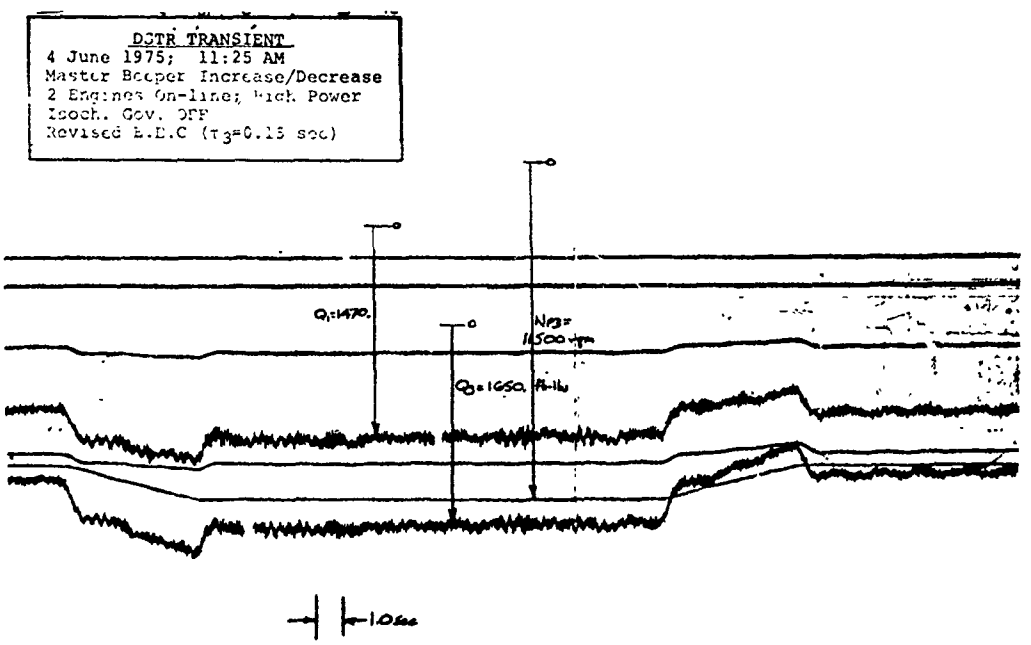

Figure 66. Master Beeper Transient, Reduced Lag (T_3 = .15 Sec) Compensation.

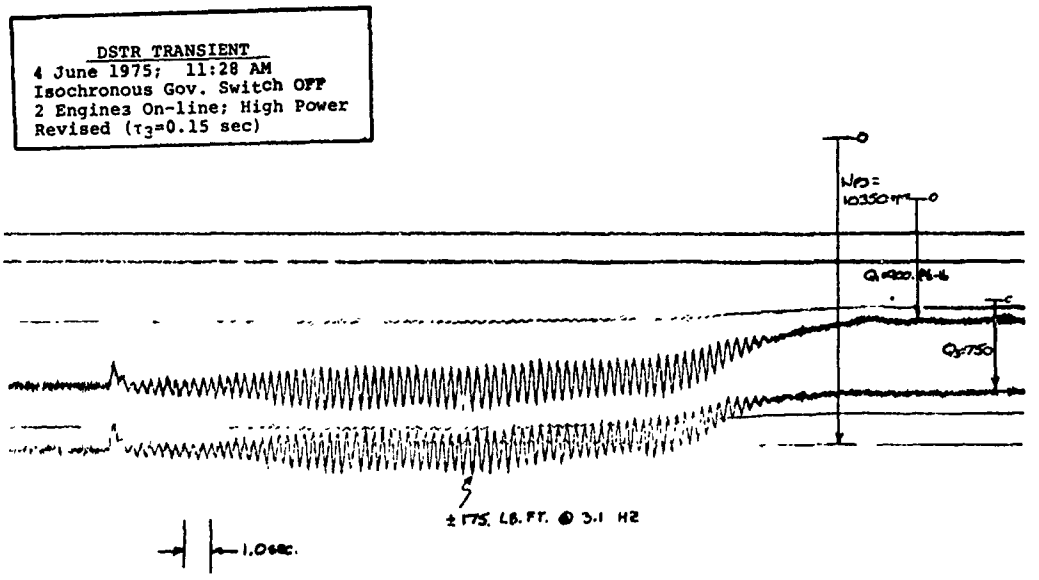

Figure 67. Isochronous Governing Switch Off Transient, Reduced Lag (T_3 = .15 sec) Compensation.

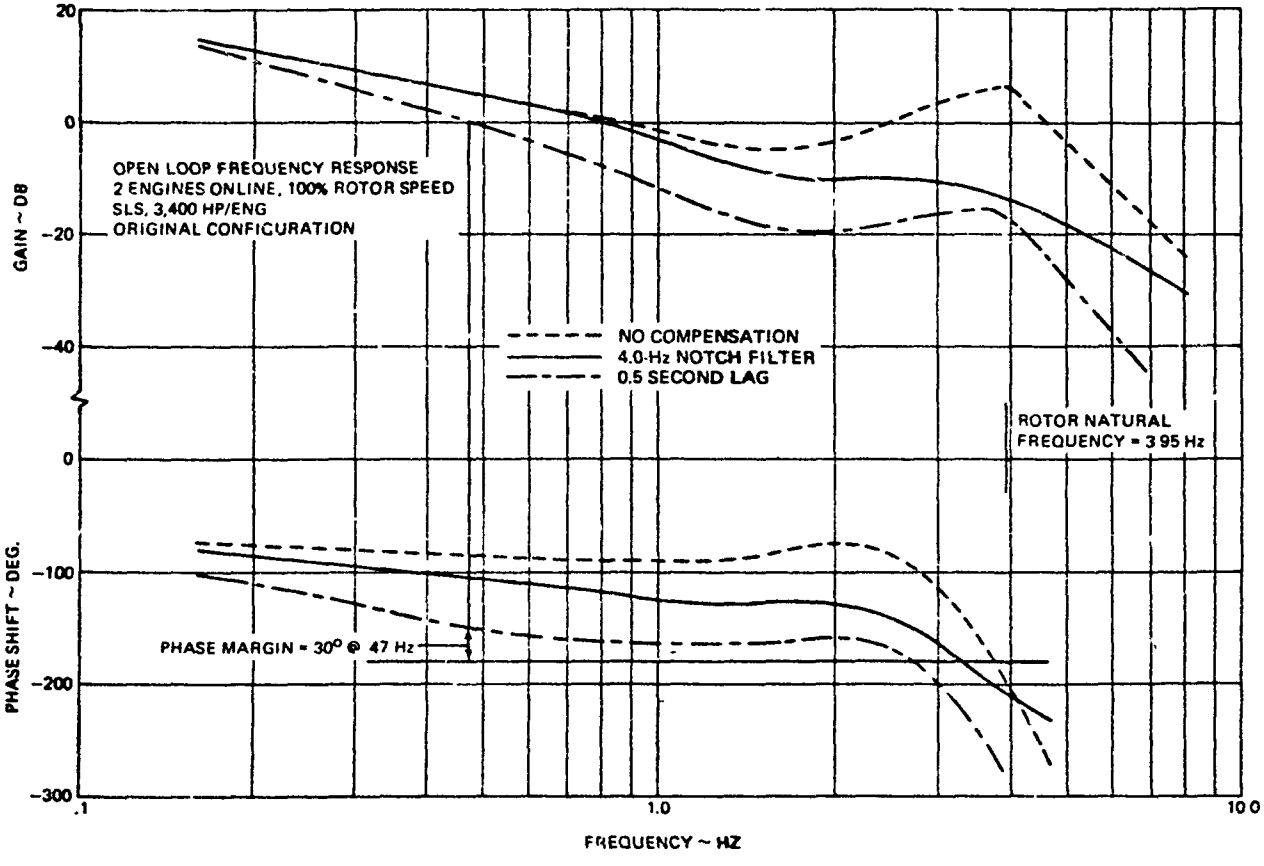

Figure 68. Effect of Compensation on Open Loop Frequency Response.

To improve system dynamic characteristics, control system notch-filter compensation in the form of an underdamped second order lead over a second order lag transfer was analyzed. This means of compensation counteracts the drive system torsional resonance without introducing excessive phase shift at the gain crossover frequency. Figure 69 illustrates the typical frequency response of a 3.0-Hz notch filter with a reduction of 20 dB at the tuned frequency. The value of this type of compensation is apparent by noting the significant improvement in system torsional stability margin for a 4.0 Hz filter as shown on Figure 68. The torsional open loop gain margin is increased to +12 dB while maintaining a 62-degree phase margin at gain crossover. Based on these results, a test program was undertaken to test several stabilizing compensation networks.

Modifications were made to two engine electronic controls to include notch filter-type compensation set at ω = 3.0 Hz to approximately correspond to the system frequency determined previously. The lead quadratic term has a damping ratio (ρ_1 on Figure 54) of 0.15 and a lag damping ratio (ρ_n) of 1.5. Figure 70 demonstrates the response of this system to a master beeper input at high power. Stability is very good with no discernible system frequency and fast, well-damped transient behavior. The tendency to overshoot and wander is significantly less than the baseline configuration, clearly describing the potential value of the selected compensation. These results are also typical of transients at low power and those initiated by step control inputs.

In order to determine the effect of system frequency variation which may be introduced by parameters such as number of engines on-line, power level and lag damper variables, the natural frequency of the notch filter was altered. A low frequency value of 2.2 Hz with lead damping ratio of .107 and lag damping of 1.07 was considered with results depicted on Figure 71. These damping values were determined by parts available during the testing. The master beeper increase caused a very lightly damped transient oscillation at about 4.4 Hz and required 10 sec to settle out. For the DSTR rotor/drive, this compensation is somewhat below the acceptable range since the system is close to exhibiting sustained oscillations.

Figure 72 shows a master beeper transition with the notch compensation tuned at a frequency of 4.0 Hz. Stability is good and compares favorably with the 3.0-Hz configuration. There is, however, a slight tendency to oscillate at about 3.0 Hz, indicating that this compensation is approaching the upper allowable limit.

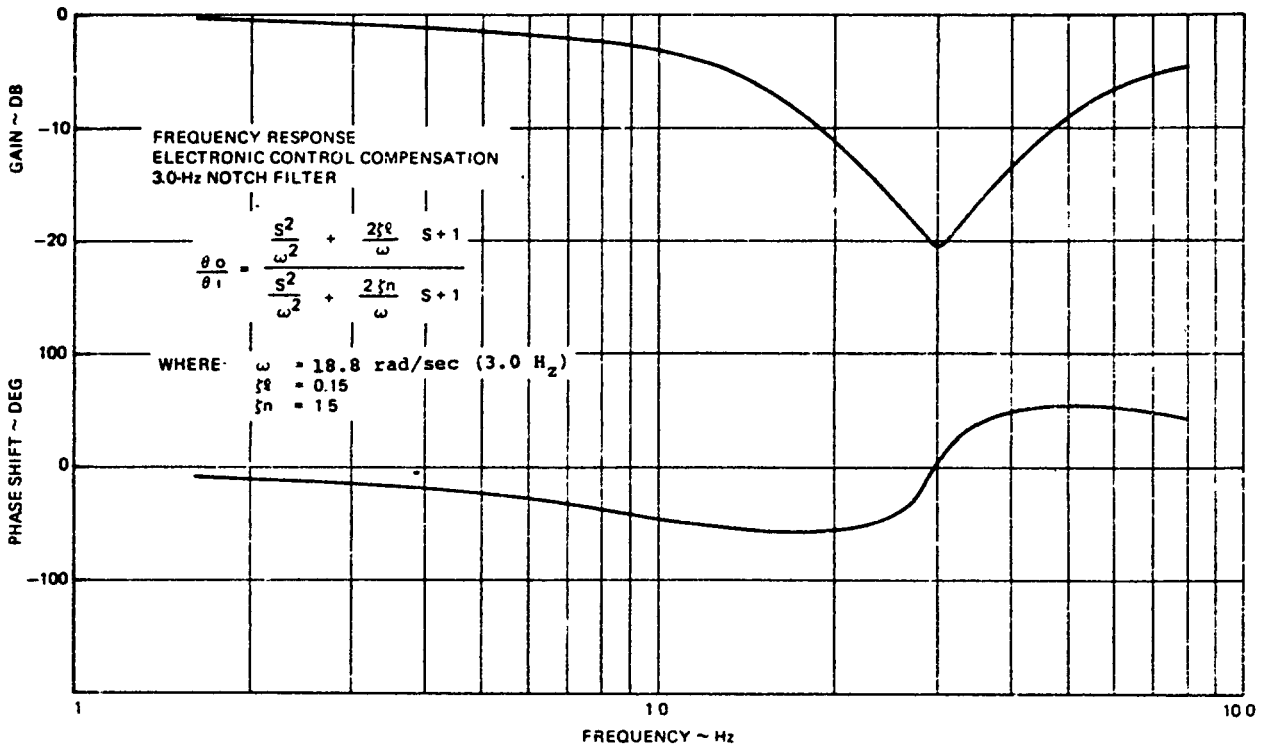

Figure 69. Notch Filter Compensation Frequency Response.

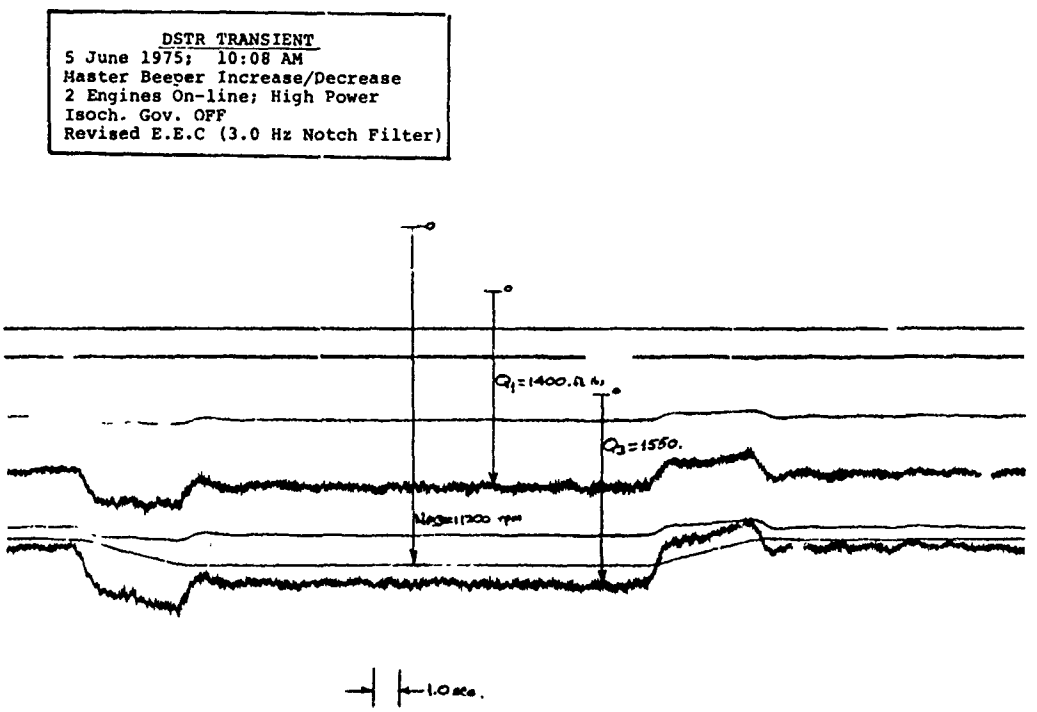

Figure 70. Master Beeper Transient, 3.0 Hz Notch Filter Compensation.

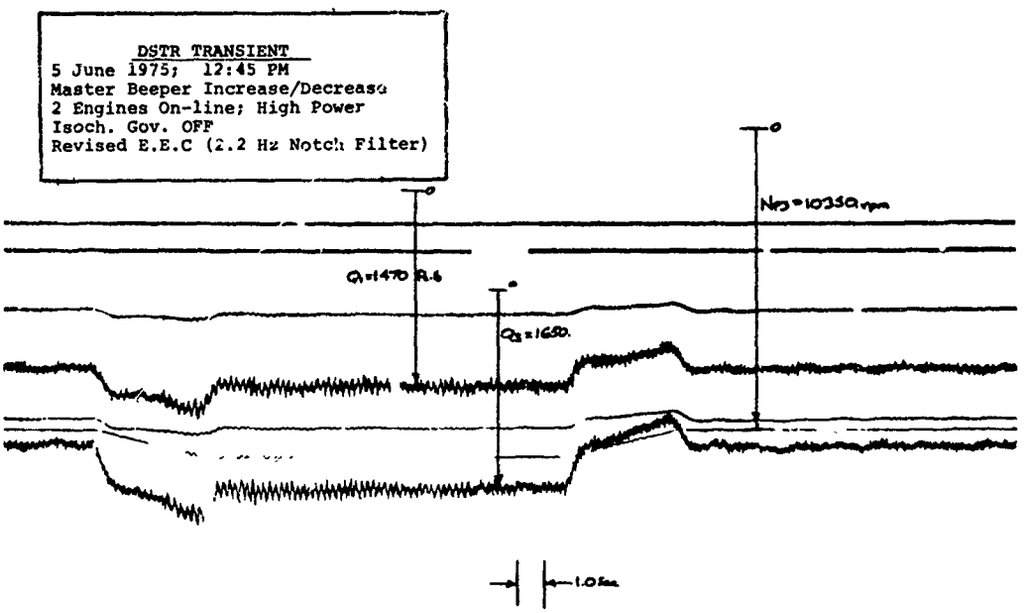

Figure 71. Master Beeper Transient, 2.2 Hz Notch Filter Compensation.

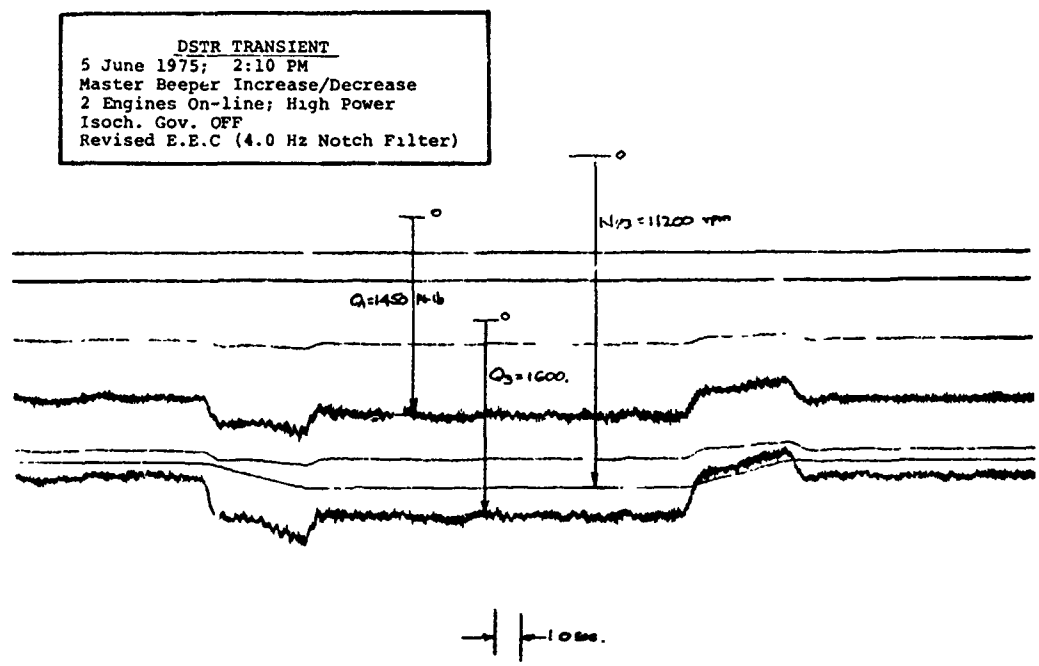

Figure 72. Master Beeper Transient, 4.0 Hz Notch Filter Compensation.

Description of the Solution

In summary, the solution was to modify the blade damper (Figure 59) and incorporate the 3-Hz notch filter.

Limitation of the Solution

Since the DSTR had different dynamic characteristics (single rotor) than the HLH flight vehicle (two rotors), the detail value for the DSTR would not be optimum for the HLH. However, the simulation had been proven and the stabilizing techniques which are applicable to the flight vehicle demonstrated.

PROBLEM - HLH/DSTR TORQUE OSCILLATION

Description of the Problem

During the DSTR test program, a 17 to 20 Hz alternating torque oscillation was observed. On August 30, 1974, a sprag clutch malfunctioned, allowing an engine to overspeed.

Investigation Leading to a Solution

Prior engine development testing had indicated low level torque fluctuations in conjunction with fluctuations in fuel manifold pressure at low power. This testing showed a 14-18 Hz fuel manifold pressure fluctuation with a maximum amplitude of 12 psi peak-to-peak and a pump discharge pressure variation of 45 psi peak-to-peak. The corresponding torque variation was 40 lb-ft peak-to-peak. At gas generator speeds above 13,000 rpm (3500 hp at sea level standard conditions), all fluctuations disappeared. The fuel pressure fluctuation emanating from the fuel control was thought to be caused by a fuel pump/control instability associated with an interaction between the bypass valve, ΔP pilot valve (maintains constant pressure drop across metering valve), pump, and line volume characteristics. Figure 73 is a schematic of this section of the fuel system. This system had a resonant frequency varying from 14 to 18 Hz between ground idle and 13,000 rpm gas generator speed. As a result of these engine test stand observations, a test was conducted to determine the effect of a 15-cubic-inch accumulator in the pump discharge line. The accumulator had the effect of reducing test stand torque fluctuations to a negligible level. However, since the magnitude of these fluctuations (basic configuration) was only 60% of that allowed by the engine specification, the delivered engines were configured without an accumulator.

As a result of the DSTR torque oscillation in September 1974, additional propulsion system torsional analyses were conducted. Results of the analysis for the basic configuration and a number of variations are summarized in Table 2. The basic analytical model is shown in Figure 74.

Since the frequency of interest lies between the first and second blade flexible lag modes, both flexible modes have been included in the rotor effective inertia.

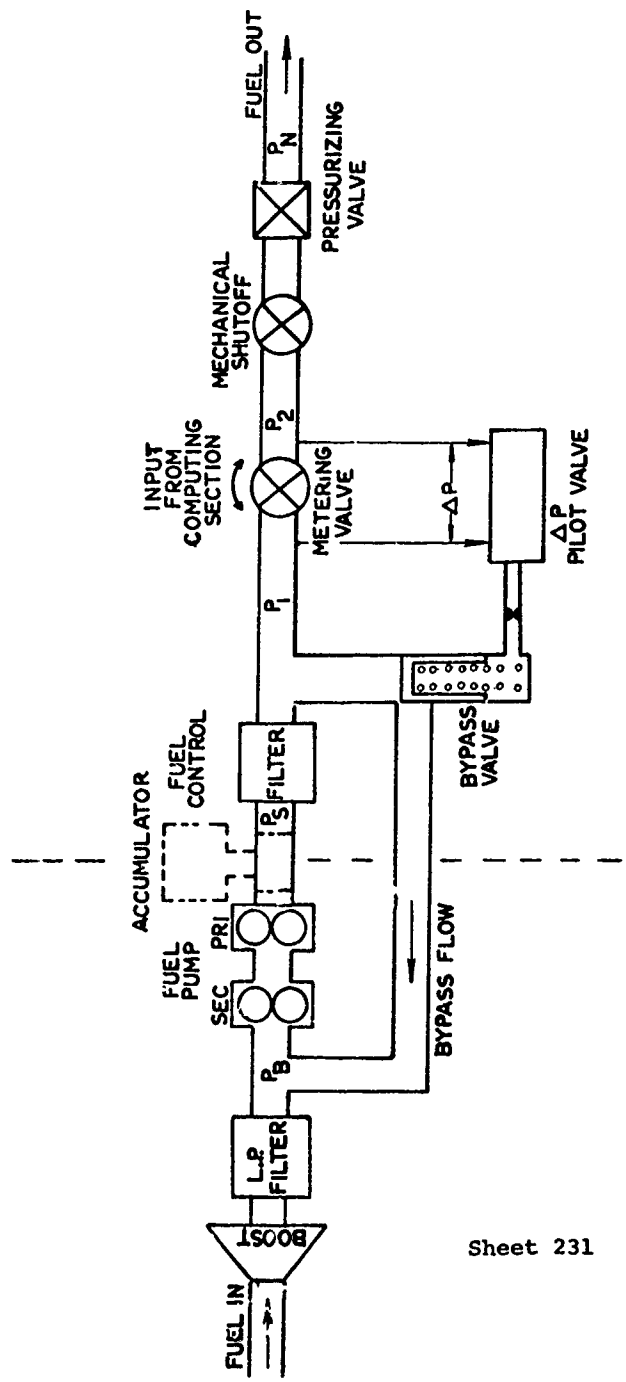

Figure 73. DSTR Engine Fuel System.

TABLE 2. SUMMARY OF DRIVE SYSTEM TORSIONAL NATURAL FREQUENCIES

CONFIGURATION	BASIC	BASIC	BASIC	NO 2ND FLEX. BLADE MODE	K_{TURB} x1/2	K_{ROTOR} x 2	TWO BLADES
NO. ENGINES	THREE	TWO	ONE	THREE	THREE	THREE	THREE
	.54	.59	.67	.54	.54	.54	.44
FREQUENCIES	4.69	4.69	4.70	4.69	4.68	4.74	4.75
PER REV	9.12	9.11	9.01	9.65	8.44	10.32	10.74
	12.96	12.33	11.09	—	10.85	12.99	13.1
	14.85	14.13	13.81	14.4	13.83	16.77	16.71
	1.40	1.56	1.75	1.4	1.40	1.4	1.11
FREQUENCIES	12.19	12.19	12.22	12.19	12.16	12.35	12.35
Hz	23.71	23.68	23.43	25.08	21.93	26.83	27.92
	33.71	32.05	28.84	—	28.2	33.77	34.06
	38.61	36.73	35.90	37.43	35.97	43.61	43.45

TURBINE UNCOUPLED FREQUENCY:

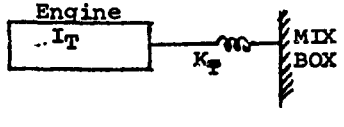

F_n = 21.9 Hz = 8.4/Rev. @ 156 N_R

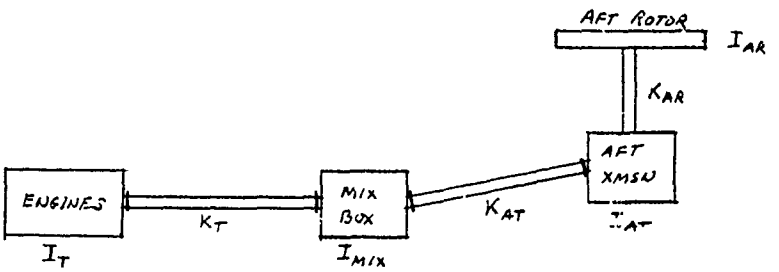

EQUIVALENT INERTIAS AND SPRING RATES AT TURBINE SPEED

INERTIA		SPRING RATES	
I_T = 3.4	IN-LB-SEC^2	(2) K_T = 197000.	IN-LB/RAD
I_{MIX} = 15.	"	K_{AT} = 346000.	"
(1) I_{AT} = 10.4	"	K_{AR} = 56000.	"

(1) PER ENGINE.

(2) SERIES SUM OF TURBINE, TORQUE SENSOR, CLUTCH AND DRIVE SHAFT SPRING RATES

ROTOR EFFECTIVE INERTIA

$$I_{AR} = 156.55 - 154.12 \frac{W_n^2}{W_n^2 - 20.852} - .3825 \frac{W_n^2}{W_n^2 - 6148.}$$

Blades: $\left\{ \begin{array}{l} \omega_\zeta = .27\,\Omega \\ \omega_{\zeta_1} = 4.8\,\Omega \\ \omega_{\zeta_2} = 12.0\,\Omega \end{array} \right\}$ @ 156 N_R $\quad - .2131 \frac{W_n^2}{W_n^2 - 38428.}$

WHERE: W_n = SYSTEM NATURAL FREQUENCY

Figure 74. DSTR Torsional Model.

Typical residual torque plots and torsional mode shapes are presented in Figures 75 and 76. The only mode close to the frequency of interest is the mode at approximately 9/rev. Frequency of the mode is only slightly influenced by the number of engines, while removal of the second blade mode from the analysis produces a mildly significant increase. A significant reduction in modal frequency (.68/rev) is obtained with a 50% reduction in the effective turbine spring rate, and an increase of 1.2/rev is indicated for a 100% increase in rotor shaft stiffness. The importance of rotor inertia is shown by the final configuration (a two-bladed rotor) which indicates an increase of 1.62/rev in the modal frequency.

The uncoupled turbine frequency is 21.9 Hz (8.4/rev), wnich is significant since an engine-to-engine mode is possible at this frequency. Data showing the sensitivity of the natural frequencies to turbine and rotor shaft stiffnesses is shown on Figure 77.

During DSTR checkout on 28 and 30 August 1974, there were two incidents that highlighted the existence of high levels of alternating torque in the drive system. The first incident was a delayed engagement on the No. 3 engine, where the clutch engaged with a 1000 rpm split between the engine input speed and the drive system. This caused a severe torque spike and was subsequently shown to be due to clutch wear. The second incident was a complete disengagement of the No. 3 clutch and consequently an automatic overspeed shutdown on the No. 3 engine; the engine overspeed protection system prevented any secondary damage. These events are shown on Figures 78 and 79.

Inspection of all three clutches showed extensive clutch sprag wear, while review of oscillograph records showed large amplitude alternating torque. Figure 80 illustrates the characteristics of the torque oscillation with one and then two engines driving. With one engine (No. 2) driving the rotor at approximately 130 rpm, the No. 2 engine torque was 1315 lb-ft steady with a $\pm$ 125 lb-ft alternating content at approximately 20 Hz. As the second engine (No. 3) was brought on line, the rotor speed increased to 140 rpm with the No. 2 engine torque at 1250 lb-ft steady $\pm$ 360 lb-ft alternating; the frequency remained at approximately 20 Hz with a 90° phase shift between engines. Because of the low level of positive torque experienced during each cycle, it is likely that the intermittent engaging of the No. 3 clutch resulted in its failure.

It was concluded that a resonance in the drive system was excited by the engine torque output which, in turn, was forced by the fuel control oscillation. Since elements of the dynamic system were tuned closed to a single frequency, each

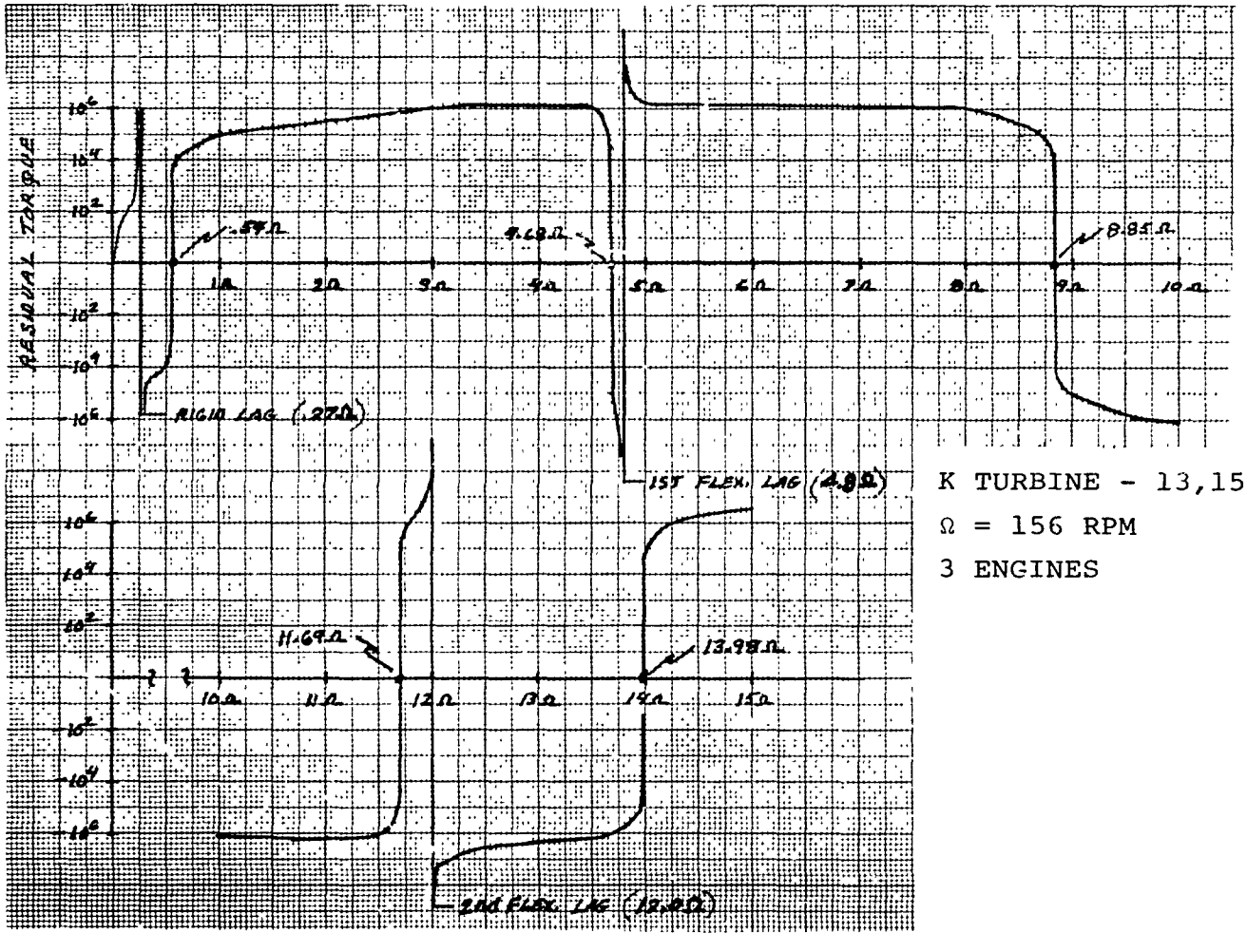

K TURBINE - 13,155 $\frac{\text{IN LB}}{\text{RAD}}$

Ω = 156 RPM

3 ENGINES

DSTR FREQUENCY ANALYSIS

Figure 75. Residual Torque vs Frequency

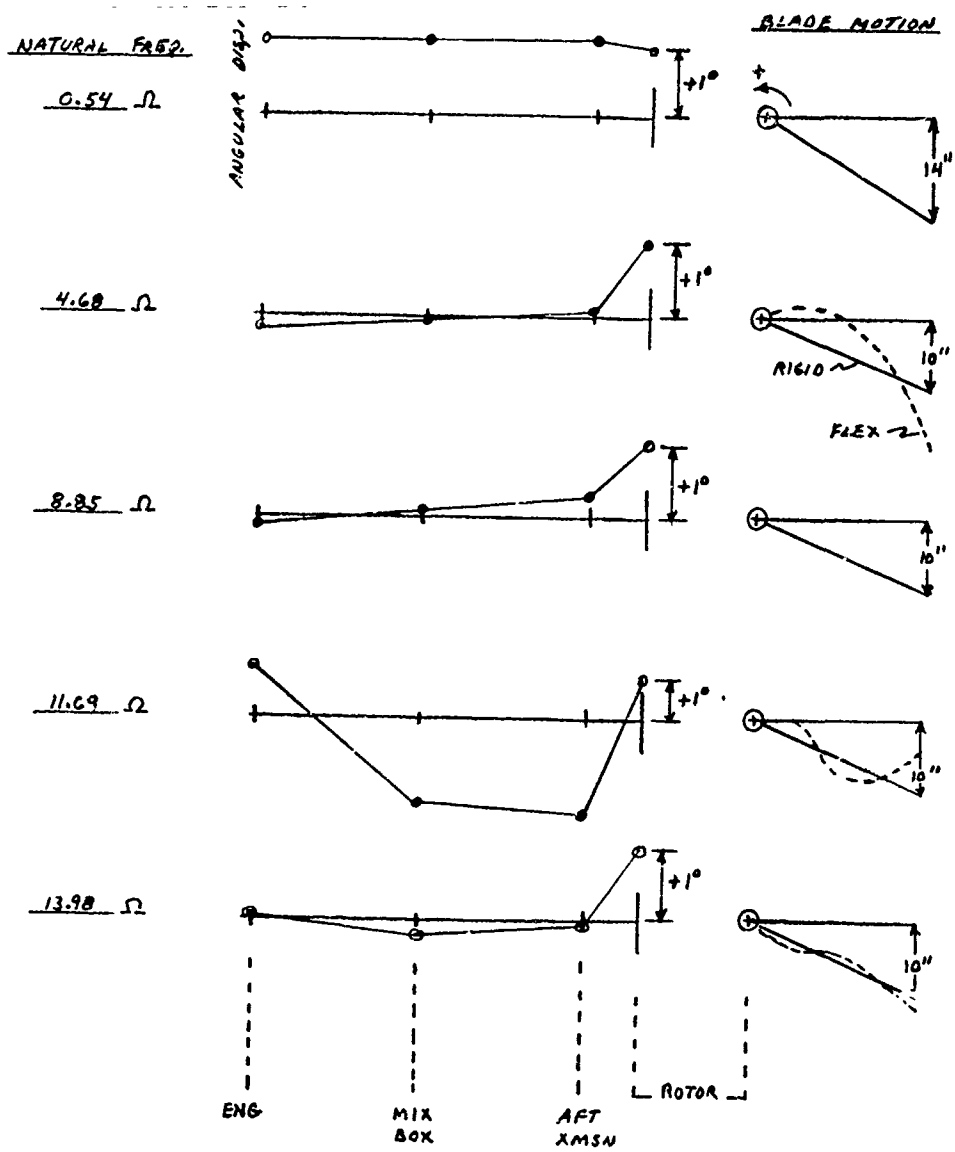

3 ENGINES

K TURBINE = 13,1550 IN-LB RAD

Ω = 156 RPM

Figure 76 DSTR Torsional Analysis - Mode Shapes.

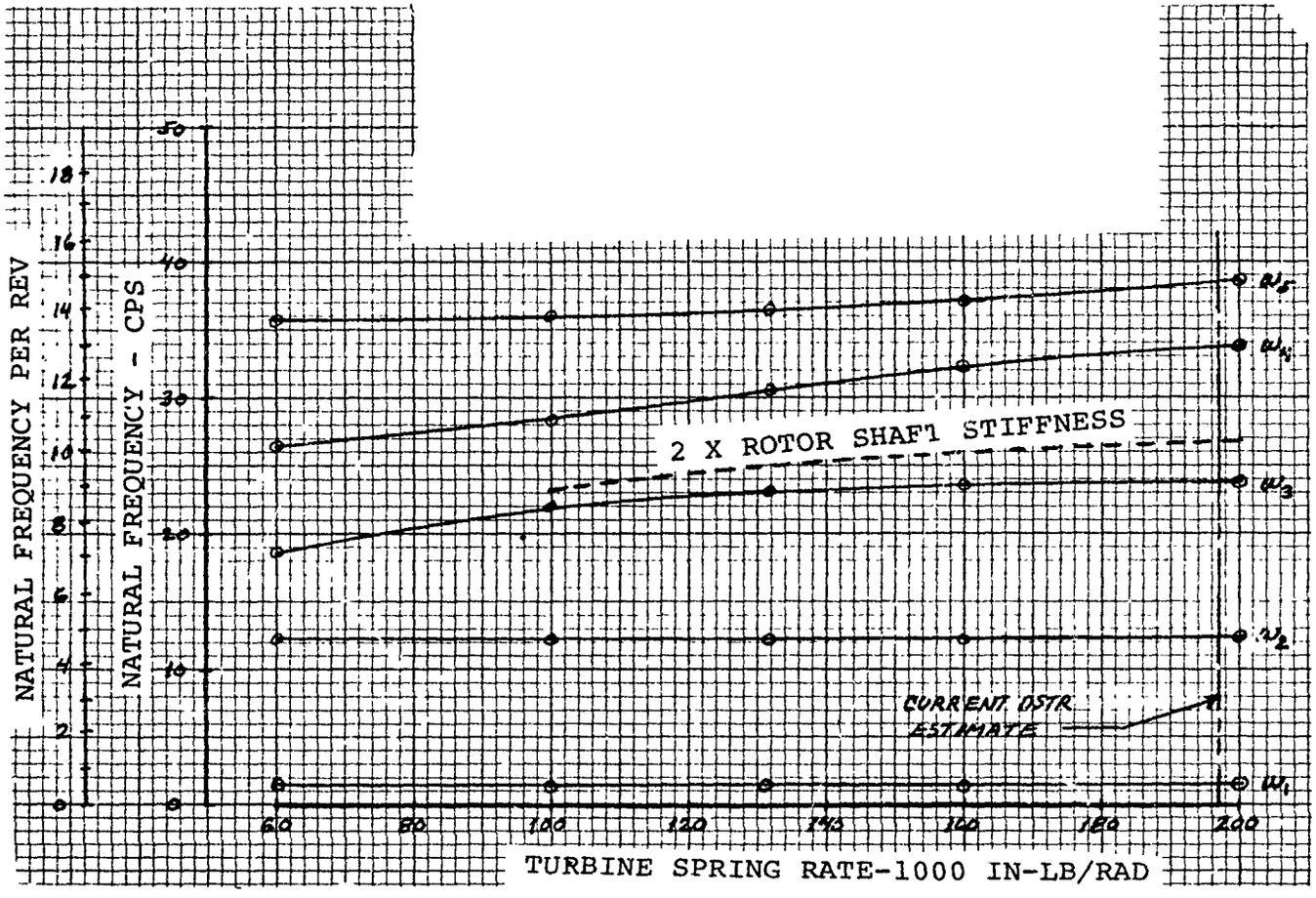

Figure 77. Natural Frequency vs Turbine Spring Rate.

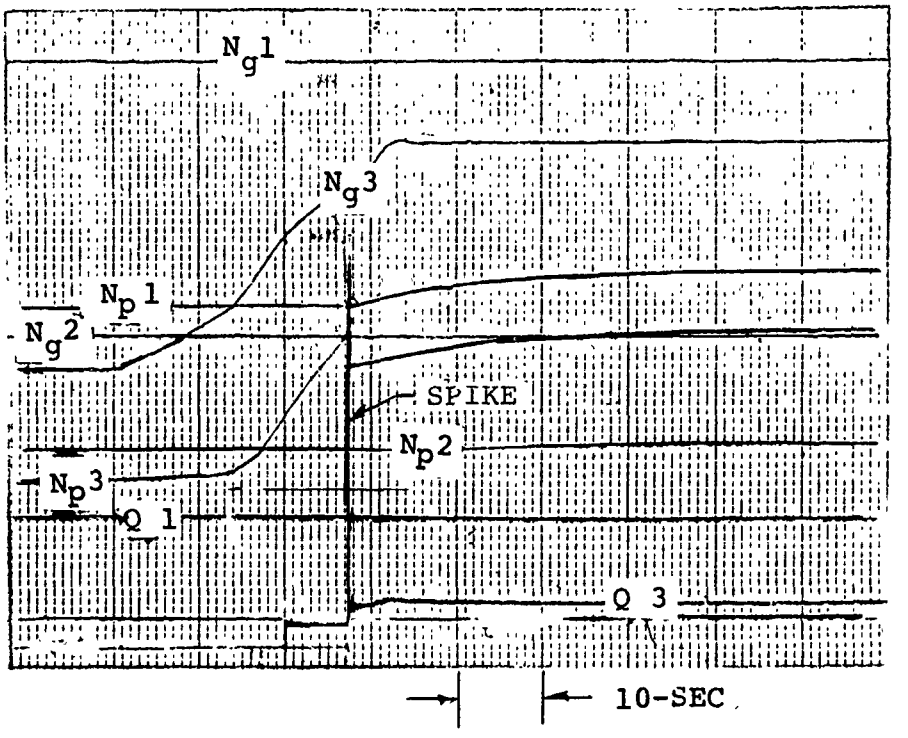

Figure 78. DSTR Engine Engagement and Torque Spike.

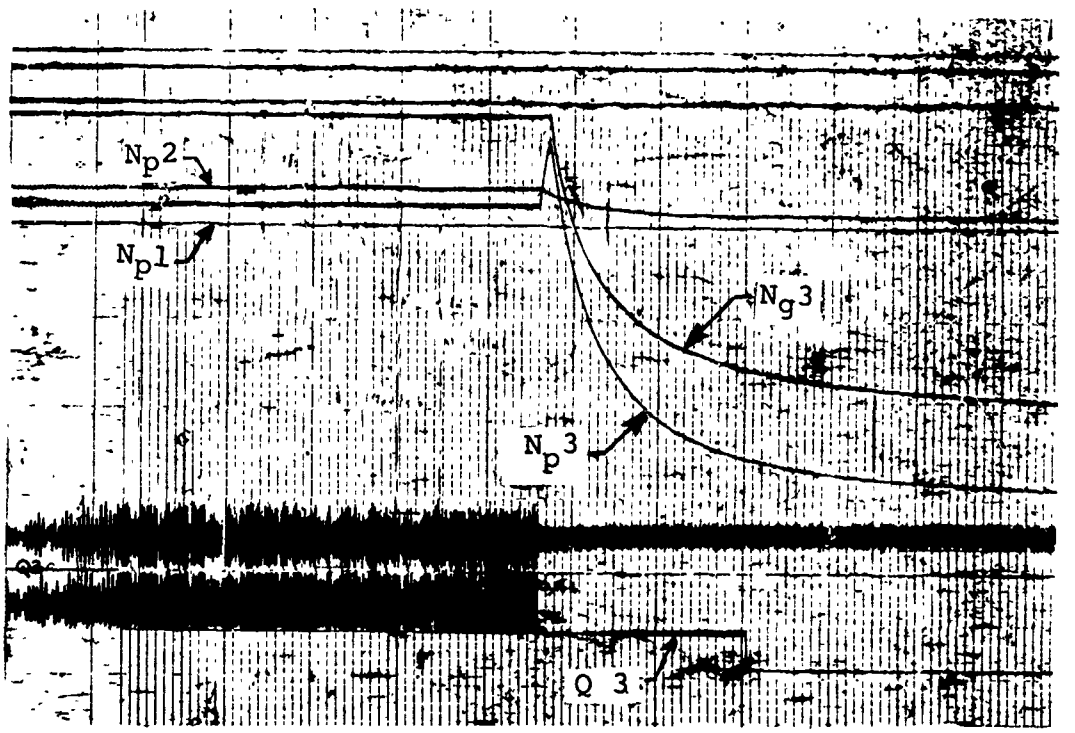

Figure 79. DSTR Clutch Disengagement and Overspeed.

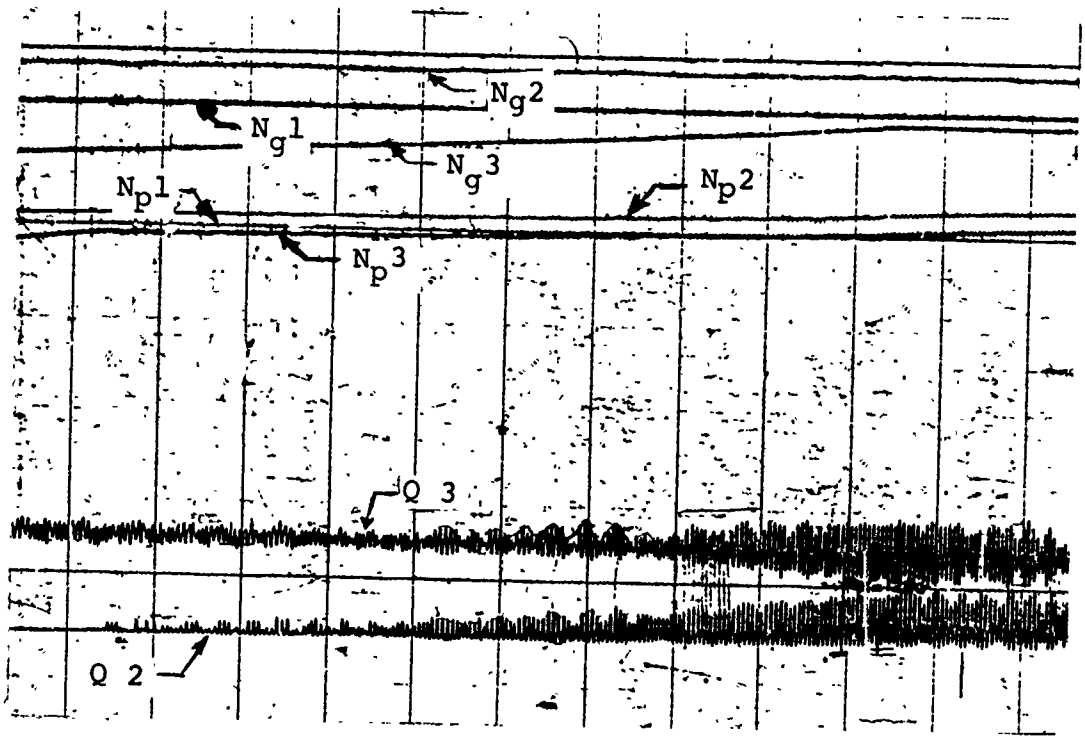

Figure 80. DSTR Torque Oscillation with One and Two Engines.

component tended to oscillate at an amplitude greater than it would as a separate unit due to the magnification effect at resonance and various direct and indirect feedbacks.

A DSTR test program was conducted to obtain comprehensive data required for a detailed system evaluation of the alternating torque characteristics. This test included recording of drive system and engine parameters at various power levels and speeds and included recording of torque and fuel manifold pressure. Testing was initiated on 10 September with No. 1 engine driving and No. 2 and No. 3 engines at ground idle (not engaged). Engine output torque variation was ± 170 lb-ft at a power level of 2030 hp (1087 lb-ft torque) and a frequency of 19.5 Hz. Observed fuel manifold pressure was 204 psi with a ± 21 psi content at 195 Hz clearly demonstrating the link between the torque oscillation and the engine fuel system. Gas generator speed did not vary because of its relatively slow response at the high frequency; torque variation was attributed to combustor temperature and pressure varying with fuel flow and subsequent conversion to power/torque at the power turbine (i.e., at constant pressure ratio, power output is directly proportional to turbine inlet temperature). Figure 81 is an oscillograph recording of this condition. This test also showed that the oscillation frequency was non-rotor-order and did not vary with main rotor speed.

Further DSTR testing on 11 September was directed toward evaluating the effectiveness of an accumulator in the fuel pump discharge to damp the torque oscillations to a level acceptable for continued DSTR operations. The 15-cubic-inch flow-through accumulator tested during engine development was installed on No. 1 engine. The results (Figure 82) showed that the 17-20 Hz oscillation was effectively eliminated, though fuel manifold pressure did show a ± 12 psi high frequency content (approximately 230 Hz) corresponding to 1/rev of the gas generator. Maximum torque variation was ± 15 lb-ft and was random at a power outuput of 3370 hp (1753 lb-ft torque).

As a result, accumulators were installed in each engine position with satisfactory results. It was found that it was necessary to maintain the charge pressure on the accumulator at close to the recommended 275 psi; otherwise, the torque oscillation would reappear.

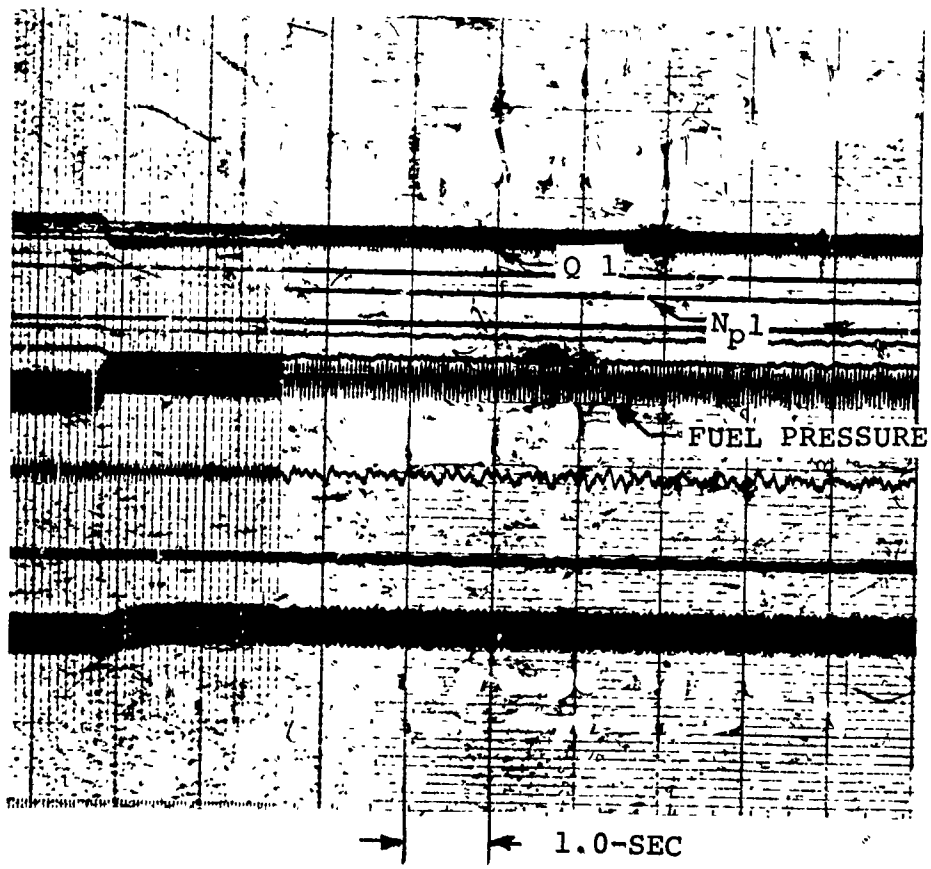

Figure 81. DSTR Torque Oscillation - Without Accumulator.

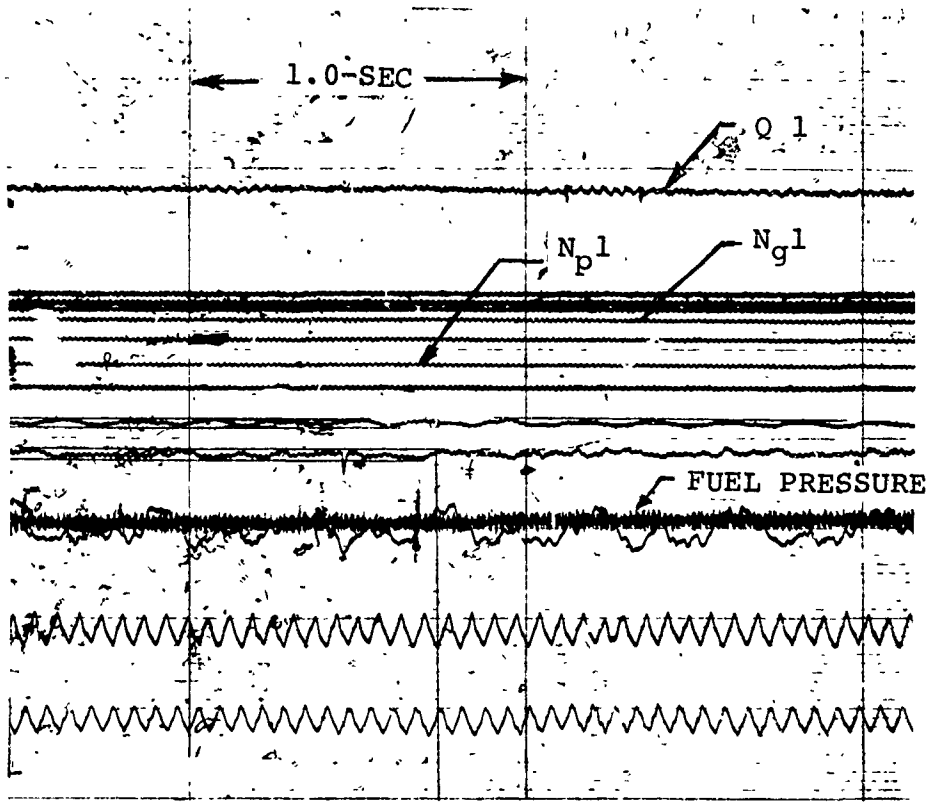

Figure 82. DSTR Torque Oscillation Investigation with 15-Cubic-Inch Accumulator.

The 17-20 Hz alternating torque experienced on the DSTR was a direct result of the dynamic interaction between the engine and the drive system. The fluctuation associated with the fuel control pressure regulating system provided the forcing function into the drive system at, or very close to, the uncoupled power turbine/drive shaft natural frequency.

Installation of an accumulator in the fuel pump discharge line effectively damped output torque oscillation. While the accumulators provided a satisfactory solution for DSTR operations, there was concern relative to the flight vehicle and the flight engine. The engine drive shaft in the aircraft could be expected to have a natural frequency similar to that on the DSTR and therefore, would respond if the flight engine exhibited the same forcing characteristics as the DSTR engine.

An investigation by the fuel control manufacturer (Woodward) showed that a DSTR engine hydromechanical control mounted on a test stand (without either an engine fuel pump or simulated downstream plumbing) would exhibit a 20-Hz instability after a step input into the CDP (compressor discharge pressure input to control) system. However, no bypass system instability was indicated. Based on this result, a DSTR control was modified to incorporate a reduced size dashpot orifice in the CDP pilot valve. This control was run on No. 3 engine on 26 March 1975 with the accumulator removed from the pump discharge line. The modified control exhibited a torque oscillation nearly identical to that observed earlier with a standard configuration control. Therefore, the control was removed and returned to Woodward for restoration to the basic configuration.

Further flow bench testing showed that a DSTR engine control with an engine fuel pump and downstream fuel system plumbing would exhibit a 15-20 Hz instability at idle conditions. Instrumentation showed that the governor (gas generator speed) servo position was steady and that the instability was in the bypass loop only. The substitution of a 75 lb/in ΔP pilot valve reference spring in place of the baseline 50 lb/in spring had no significant effect. Some reduction in the amplitude of the instability was noted when a 0.025-inch-diameter P4 orifice (bypass valve control pressure) was installed in place of the 0.037-inch-diameter orifice. A ΔP pilot valve sleeve with narrow porting (two 0.050-inch-wide slots versus four 0.25-inch-diameter holes) had no significant effect.

The substantiation of a flight engine control into the system (with DSTR engine pump and fuel system plumbing) showed little difference between DSTR and flight engine controls. It was noted that the flight development engines had not shown any tendency toward torque oscillation on the engine test stand. Measurements showed that control inlet flow and pressure were approximately 50 degrees out of phase at the instability frequency and suggested the possibility of an adverse effect of upstream plumbing.

The significance of upstream plumbing to system stability was demonstrated by testing both a flight engine control and a DSTR control with a flight engine configured fuel system on the bench. In the flight engine configuration, the fuel control is mounted directly onto the fuel pump, decreasing the volume associated with the pressure regulating system and increasing the hydraulic natural frequency beyond the response capability of the bypass valve, thereby eliminating the resonance. No 20-Hz oscillations were observed during tests of this configuration.

Figure 83 shows that a DSTR control plus DSTR pump exhibits 15 Hz oscillation, while Figure 84 shows that a DSTR control with a flight engine pump and plumbing is stable.

A flight engine control pump and plumbing give stable operation (Figures 85 and 86). In Figure 86, enrichment solenoid inputs provided a 45% fuel flow forcing function while at idle. Figures 87 and 88, both with flight engine control, pump, and plumbing, show stable operation at high power setting with trim motor inputs providing $\pm$ 11% fuel flow forcing function, and at idle setting with trim motor inputs providing $\pm$ 30% fuel flow, forcing function.

It was concluded that in the flight engine configuration with reduced volume in the plumbing, the hydraulic natural frequency was sufficiently high to avoid resonance with the bypass valve.

Description of the Solution

For the DSTR, an accumulator provided the solution for the non-flight controls. For the flight vehicle, the flight engine pump and flight plumbing were demonstrated by bench test to be stable.

Limitation of the Solution

None.

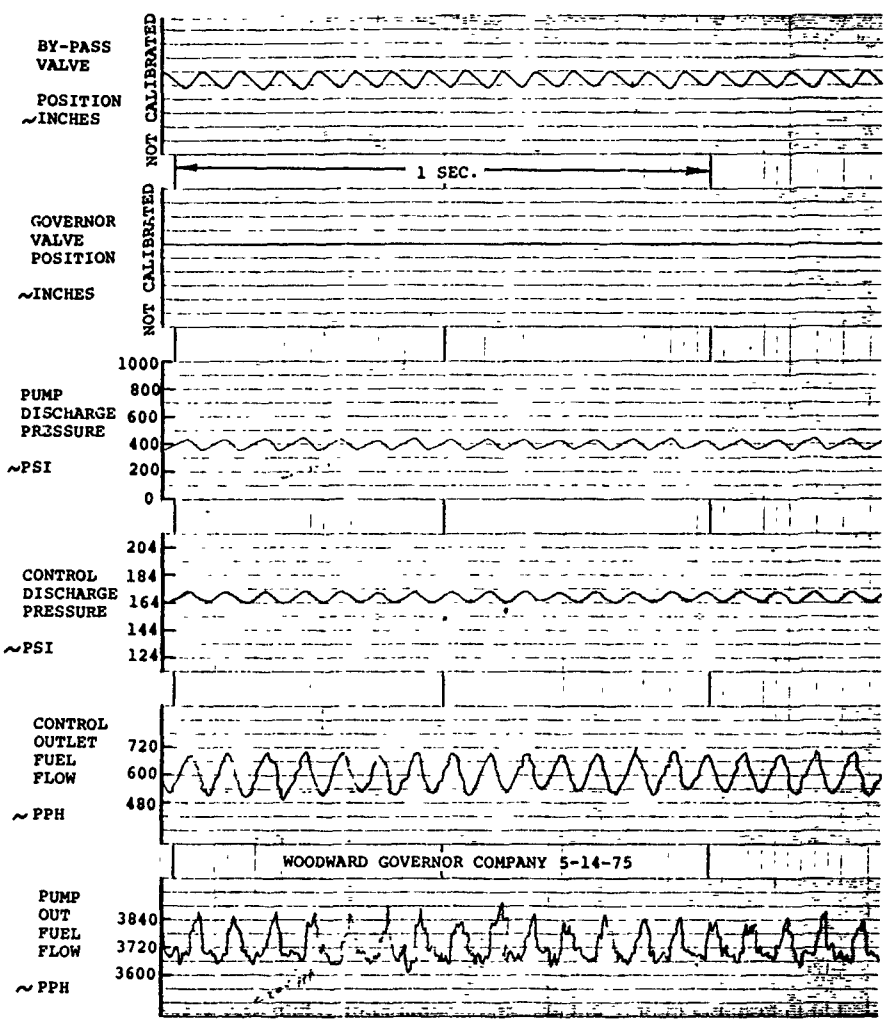

Figure 83. 15-Hz Oscillation DSTR Control with DSTR Pump.

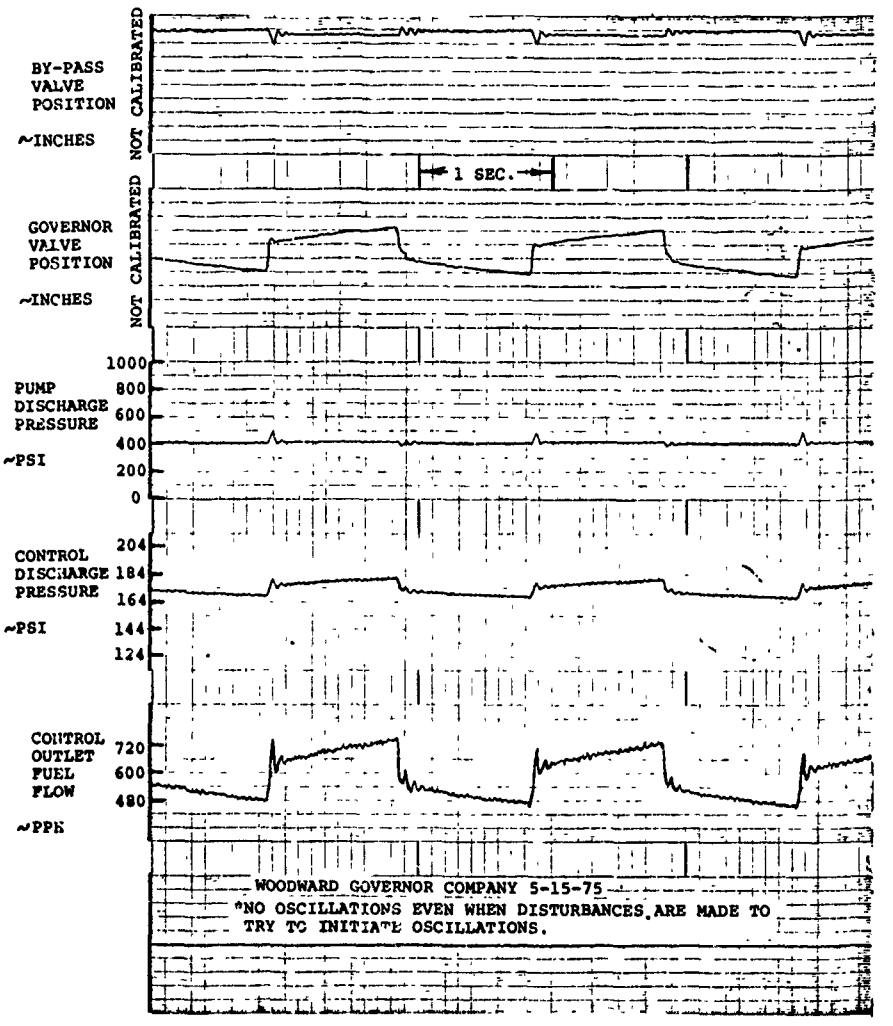

Figure 84. DSTR Control with Flight Engine Pump and Plumbing.

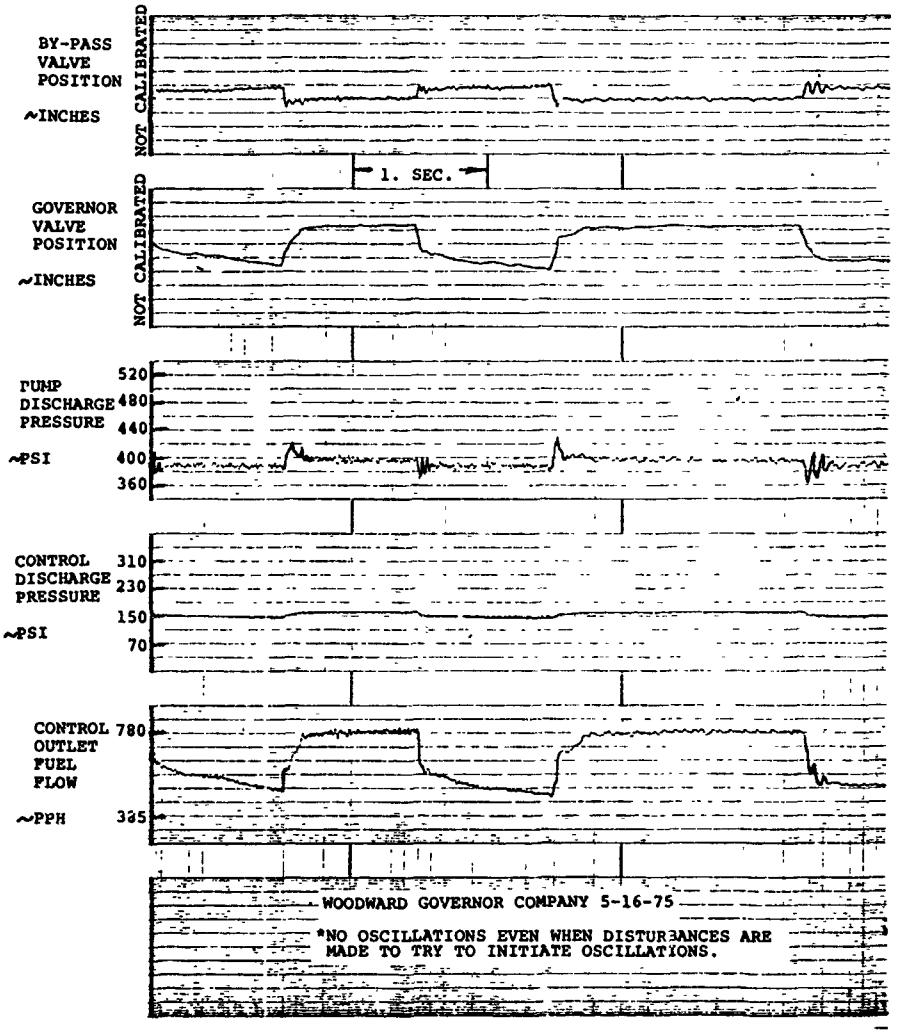

TRIM TORQUEMETER STEPPED

Figure 85. Flight Engine Control and Flight Engine Pump and Plumbing.

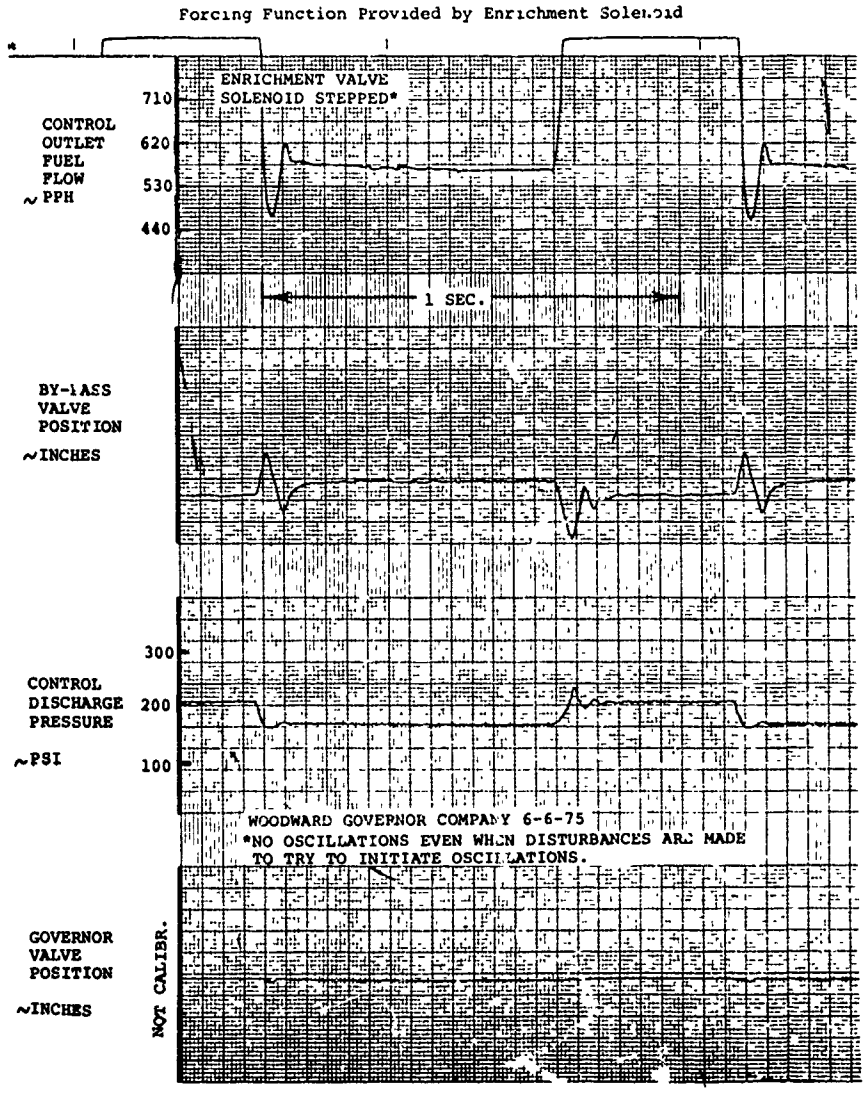

ALTERNATING INPUT AT IDLE

Figure 86. Flight Engine Control with Flight Engine Pump and Plumbing.

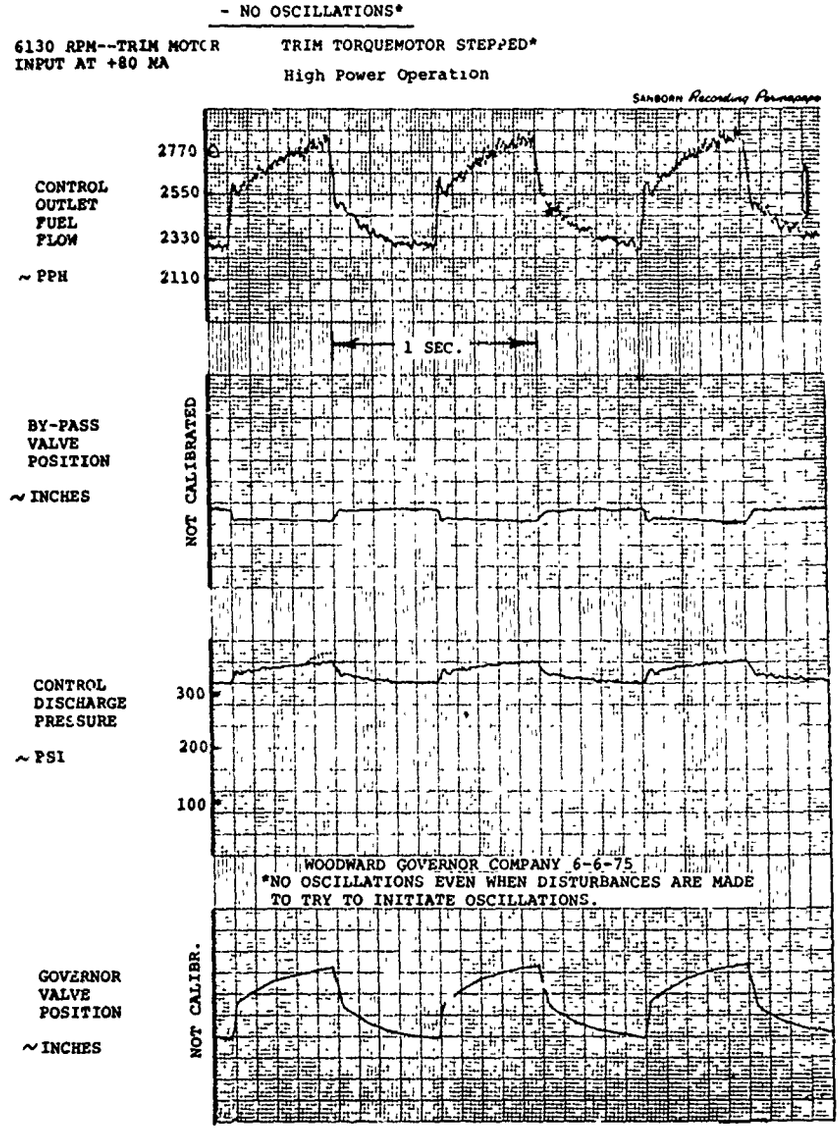

Figure 87. Alternating Input at High Power Flight Engine Control, Pump and Plumbing.

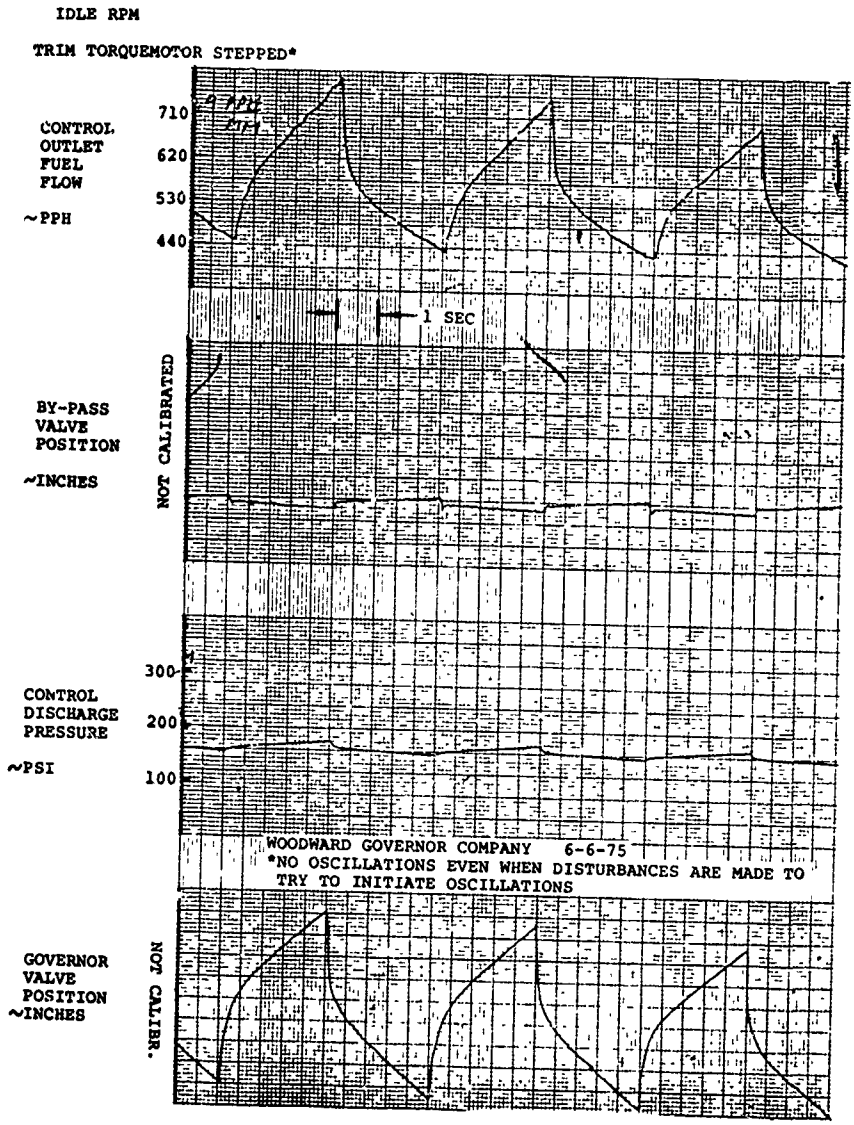

Figure 88. Alternating Input at Idle Flight Engine Control, Pump and Plumbing.

PROBLEM - YUH-61A ENGINE MOUNTING

The mounting of an engine in a helicopter requires a relatively rigid system to prevent excessive shaft misalignment and at the same time, limit the velocities and accelerations of the engine in response to rotor and shaft excited frequencies. The mount study began in 1972.

The following description covers the engine vibration treatment on the YUH-61A. The treatment of a high frequency (240 Hz) vibration is covered under a separate section entitled "non-synchronous whirl". It is not included here, since the engine mounting system was not involved in its cause or solution.

Description of the Problem

The engine manufacturer established upper limits of vibration for the engine; these were specified on the T700-GE-700 installation drawing as follows:

"Vibration Pickup Locations and Limits:

Vibration pickups are to be oriented within 5° of the vertical, lateral, or radial lines. The pickup mount locations are to be as follows:

Location 1	Sta. 200.00	Main Frame
	VHI Lateral	V1 or V3
	VVI Vertical	V2 or V4 (Alt. Sta. 195.31)
	VA1 Axial	V1 or V3
Location 2	Sta. 217.85	Midframe
	VH2 Lateral	V6
	VV2 Vertical	V5
Location 3	Sta. 231.82	Exhaust Frame
	VR31 Radial	V9
	VR32 Radial	V
Location 4	Sta. 203.50	Accessory Gearbox
	VV4 Vertical	C.0

HIGH FREQUENCY LIMITS FOR ENGINE AFTER INSTALLATION AT LOCATIONS 1 AND 3 FOR VERTICAL, LATERAL AND RADIAL.

Maximum total vibratory velocity (in/sec) single amplitude peak at frequencies above 50 Hz generated by engine rotors and airframe components	Maximum total transient vibratory velocity (in/sec) single amplitude peak of less than 5 sec duration.
2.5	3.5

LOW FREQUENCY LIMITS FOR ENGINE AFTER INSTALLATION (SEE NOTE 53)

Location	Maximum total vibratory velocity (in/sec) single amplitude peak at frequencies below 50 Hz generated by airframe rotors or components.	Maximum total transient vibratory velocity (in/sec) single amplitude peak of less than 5 sec duration.
1		
2		
3		
4		
5		

Airframe induced engine response in the range of 25-50 Hz shall not exceed 50% of overall levels permitted in the 4-50 Hz band.

NORMAL VIBRATION LIMITS (See Note 53A)

VERTICAL, LATERAL AND RADIAL	5.0 in/sec	7.0 in/sec
AXIAL	2.5 in/sec	5.0 in/sec

EXTENDED VIBRATION LIMITS (See Note 53B)

VERTICAL, LATERAL	7.0 in/sec	12.0 in/sec
AND RADIAL AXIAL	5.0 in/sec	7.0 in/sec

NOTE 52 INTERPRETATION OF HIGH FREQUENCY VIBRATION LIMITS

A) Maximum total vibratory velocity (in/sec) single amplitude peak is the overall velocity of various components above 50 Hz.

B) An averaging type velocity meter CEC 1-167 or the equivalent is to be used for real time measurement of the maximum total vibratory velocity.

C) The maximum total vibratory velocity recorded during a vibration survey is to be determined by measuring the maximum single peak velocity of the complex wave on an oscillograph trace.

D) To indicate high frequency vibration levels, the vibration signal is to be passed through a 70 Hz high-pass filter during uninstalled testing and through a 90 Hz high-pass filter during installed testing. The filter roll-off is to be 18 dB per octave.

NOTE 53 INTERPRETATION OF LOW FREQUENCY VIBRATION LIMITS

A) Normal vibration level shall apply during the following flight conditions:

1) Takeoff, hovering, and landing.

2) Level flight up to the maximum speed attainable with intermediate rated power.

3) Pullups, climbs, pushovers, descents, and turns with accelerations between 0g and 1.75g or up to 45° of bank angle.

B) Extended vibration limits shall apply to flight maneuvers not specifically defined in note 53A and which can occur for no more than 5% of the total engine operating time.

C) Steady state vibration is the cyclic vibration persisting for more than 5 seconds and normally occurring during a sustained flight condition.

D) Transient vibration is the occasional excursion in vibration level persisting for no more than 5 seconds and usually occurring during some aircraft flight maneuver.

E) Maximum total single amplitude peak is either the arithmetic sum of the velocity components read on a spectral analyzer or the maximum velocity of the complex wave as recorded on an oscillograph."

The problem was to select an engine mounting system which provided the lowest vibration environment for the engine which entailed avoidance of any resonance of the engine on its mounts in any mode at the exciting frequencies of the rotor(s), shafting, etc. The levels must be below the levels specified above.

The chronological order of events for the selection and evaluation of the engine mounts is:

Sept. 1972 to Dec. 1973	Detail analysis and design of engine mounts; mounts selected.
January 1974	GE abusive vibration test successfully completed with the engine mounts.
May 1974	Final design of the engine mounts completed.
June 1974	YUH-61A Static Test Article (STA). Hung shake test defined coupled engine/airframe natural frequencies.
January to April 1975	Flight test results on YUH-61A aircraft 001 and 002.
April 1975	Shake test of ground test vehicle (GTV) at Grumman Aerospace Corporation, Calverton Test Facility, to define engine natural frequencies with rotor and adopt an engine mount configuration for better engine mode placement.
April 1975	Initial flight results of "improved" engine mount on A/C 002.
October 1975	Flight results of final vibration configuration on A/C 002.

The installed engine vibration levels for the GE T700 engine are broken into two frequency domains: low frequency below 3000 rpm (50 Hz) and high frequency above 3000 rpm. While these specs are expressed in velocity, most of the data reported herein is in acceleration g's. Therefore, the following table is provided:

STEADY STATE

N_R = 286 rpm

DIRECTION	GE SPEC VELOCITIES (IN/SEC)(1)	UTTAS MAIN ROTOR FREQUENCIES	EQUIVALENT OF GE SPEC ACCELERATIONS - g (2)
Vertical or Lateral	5.0	1/rev	.39
		4/rev	1.55
		8/rev	3.10
Longi-tudinal	1.2	1/rev	.093
		4/rev	.37
		8/rev	.74

Notes: Transient specification levels are somewhat higher.

(1) Total of low frequency velocities
(2) Assumes all vibration at the one frequency

The YUH-61A engines are mounted to the aircraft at four locations as shown in Figure 89. The mounts were provided with the spring rates as shown to detune the coupled engine/airframe natural frequencies from the important potential rotor forcing frequencies of the YUH-61A. These frequencies for the YUH-61A are 4/rev of the main rotor at 19.1 Hz, 8/rev at 38.2 Hz, and 1/rev at 4.77 Hz with N_R at 286 rpm.

The analytical results for the initial flight configuration are shown in Figure 90. These frequencies were well placed, relative to the potential forcing frequencies, with assurance of dynamic amplification of less than 2.0. This fact, coupled with the low airframe vibration levels required for the cabin of the YUH-61A, assured low engine vibration levels in flight on the YUH-61A. Mounts were therefore procured with the following spring rates:

Mount	Spring Rate*	Residual
Fwd Bottom	45,000 lb/in	2000 lb/in
Fwd Side	45,000 lb/in	2000 lb/in
Aft Bottom	23,000 lb/in	0
Aft Side	11,000 lb/in	0

*This is the rate for the main load path axially; the "residual" refers to the radial load path.

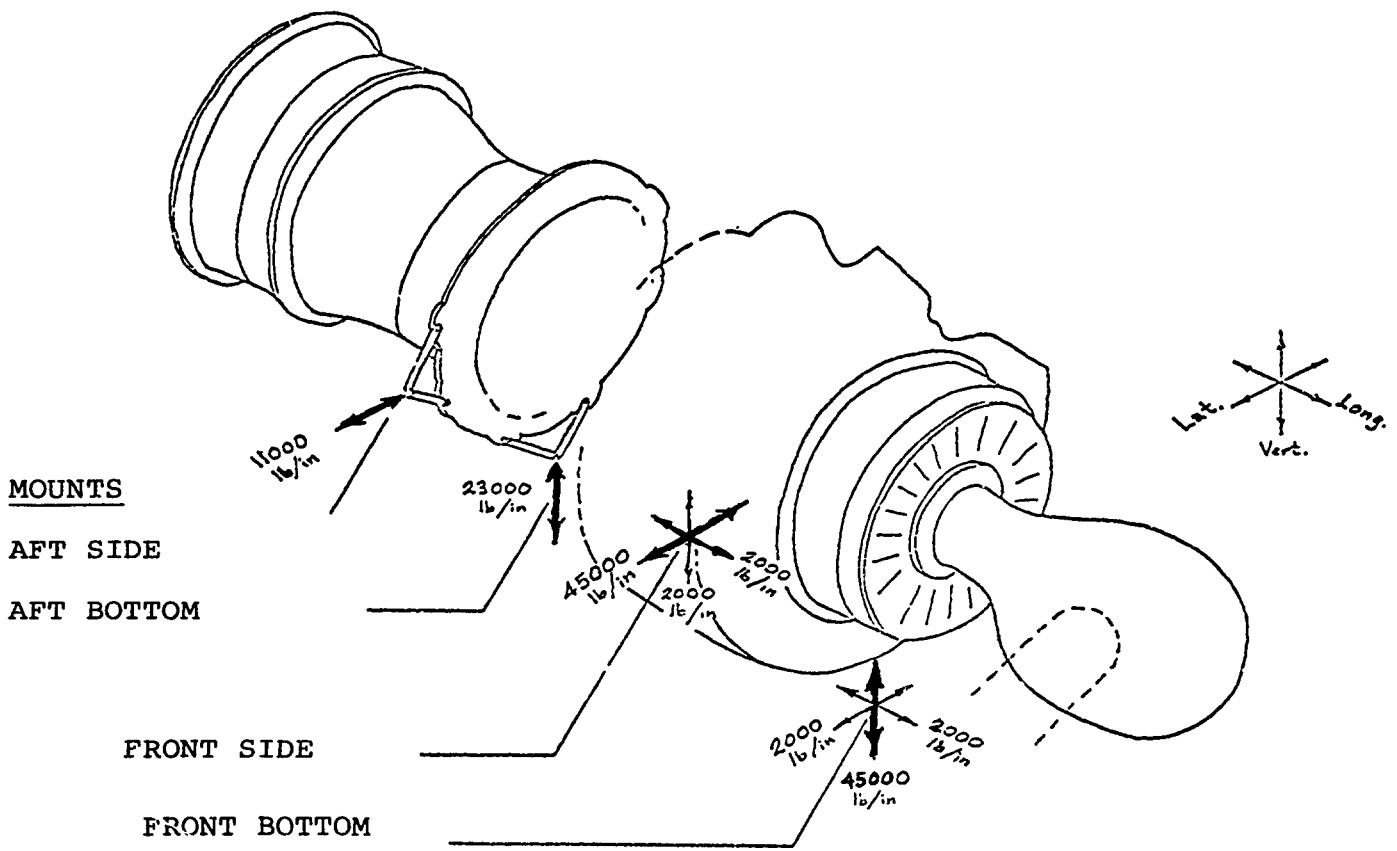

Figure 89. YUH-61A/T700-GE-700 Engine Mount Configuration.

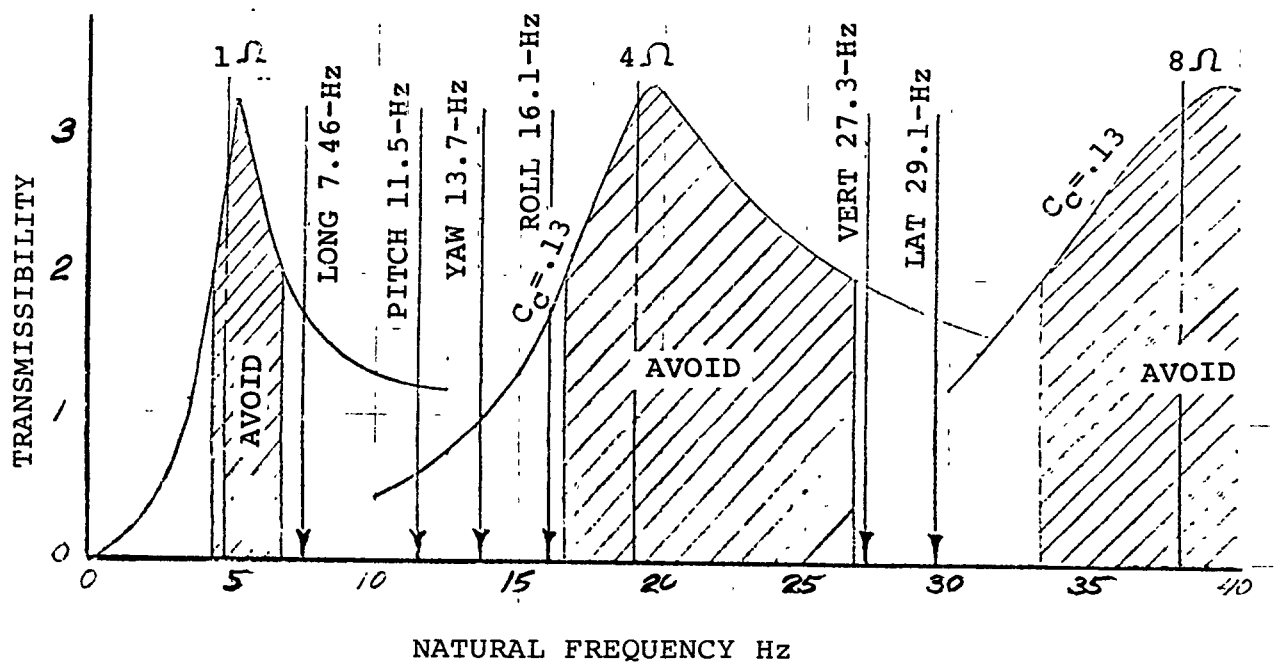

Figure 90. Engine Mount Analysis.

A powered vibration survey was then conducted. For this vibration test, the engine was supported by YUH-61A mounts on a shake table. The shake table was mounted on four air bags. Vibratory excitation of the shake table was provided by means of three vertical electrohydraulic actuators, one beneath the aft mount plane in the center of the table, the other two at the forward end of the shake table, on each side of the table. This shaker configuration was designed because of concern over possible rolling of table during operation of the shakers due to the center of gravity being to the right of table center (aft looking forward); the Boeing Vertol mount supporting structure and rotary actuator (see below) were mounted on the right side of the table. The shake table was quite stable, however, and only the aft vertical shaker was used throughout the test. Power is supplied to the YUH-61A main rotor transmission through a cross shaft connected to the right angle nose gearbox which is mounted on the T700 engine output drive pad flange. For this vibration test, it was the intent to simulate the nose gearbox weight, center of gravity, and cross shaft torque. The simulation was accomplished by mounting a "nose gearbox mounting adapter" to the engine output drive pad to which was mounted a water brake. The water brake was used as the power absorber. The "nose gearbox mounting adapter" incorporated a pad to which a simulated cross shaft was mounted, at the correct orientation. The other end of the simulated cross shaft was mounted to a torque producing rotary actuator. The rotary actuator was mounted to the shake table. Flexible couplings, identical to the YUH-61A cross shaft flexible couplings, were mounted on each end of the simulated cross shaft. These couplings permit relative motion between the powerplant and the aircraft main rotor transmission. Thus, engine power turbine torque was counteracted by the water brake and YUH-61A nose gearbox cross shaft steady state torque was applied by the rotary actuator, resulting in the proper loading on the engine output drive pad and the remainder of the engine. The only deficiency in the simulation was that since the engine used did not produce engine specification power (900 hp vs required 1536 hp), the engine power turbine torque was not as large as will be experienced in actual service. The predominant loading on the engine output drive pad is the pitch moment component of the nose gearbox torque, however, and the deficiency does not significantly affect the results of this test.

The test consisted of starting the engine to idle and accelerating the engine to power. This provided the engine signature with Boeing Vertol hardware in a simulated YUH-61A installation. The electrohydraulic shakers were then turned on and shaker sweeps were conducted wherein the frequency of the

shaker was varied from 5 up to 76 Hz. This was done to obtain a more realistic assessment of the powerplant resonances and responses than the static shake test because of the higher input level possible with the electrohydraulic shakers.

The isolator mount stiffness decreases with increased dynamic input, and as a result, the powerplant resonances decrease in frequency. Therefore, the powerplant resonances obtained in the static shake test are not realistic. The powerplant pitching resonance occurred at 10-15 Hz and the powerplant vertical translation at 23-20 Hz.

The next step in determining where the engine/fuselage natural frequencies were in the YUH-61A was the shake test performed on the STA with "dummy" engines but actual mount flight hardware, completed well ahead (June 1974) of first flight. The results of this testing are shown in Figure 91 and are compared to the original analysis.

MODE	ANALYSIS	STA SHAKE TEST
Longitudinal	7.46	11.7
Pitch	11.5	14.5
Yaw	13.7	15.5
Roll	16.1	18.5 4/rev
Vertical	27.2	23.9 19.67 Hz at
Lateral	29.6	29.6 295 rpm

This comparison indicates several significant differences between the original analytical modes and the shake test derived modes. These differences are essentially caused by the actual "residual" spring rates of the engine mounts, which control the longitudinal and roll modes, and the initial estimate of engine mount backup stiffness used for the analysis. The engine modes, however, relative to the prime forcing frequency (4/rev), were still well placed.

After initial flight testing was underway, a shake test was performed on the GTV to determine if the engine response at 4/rev could be reduced. This test consisted of running the GTV at various power levels and shaking the engine with an external shaker through a frequency range of 8 to 35 Hz to define the installed engine natural frequencies with the rotor tuning. These results indicated that the engine roll mode was closer to 4/rev than desired. Several configurations of engine mount stiffness were shake tested on the GTV to define a better mount configuration. The choice of mount stiffnesses to test was guided by a 6-degree-of-freedom analysis of the engine/airframe installation.

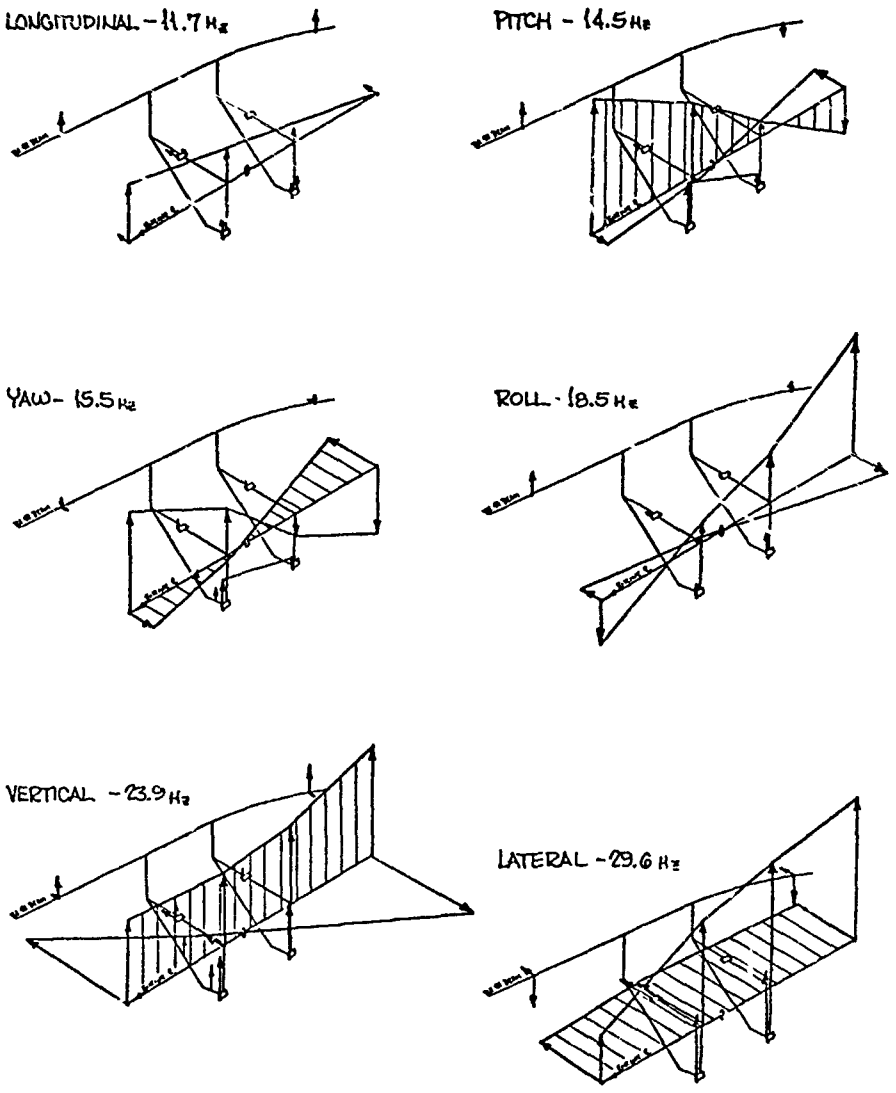

MIN GROSS WEIGHT
100 LB FORCE
50% ROTOR MASS

Figure 91. ENGINE SHAKE TEST MODE SHAPES.

Description of the Solution

The combination of mounts tested for both engines is shown in Table 3. The initial configuration mount springs and the test derived mount arrangement are compared in Table 4 and Figure 92. Frequency sweeps of one engine for the front frame vertical pickup are shown for the baseline and final configuration in Figure 93. These results indicated a mode right at 4/rev for the baseline configuration. A significant improvement in the response at 4/rev is shown with the test derived mount arrangement. In fact, a reduction of about 75% was attained by going to the "current" engine mount stiffness shown in Figure 92.

The flight development program of the final engine mount configuration was completed.

In general, the predominant forcing frequency in the YUH-61A airframe from the main rotor is 4/rev. Therefore, the engine mount design is configured to provide low transmissibility for that excitation. Figure 94 shows a spectral analysis of the No. 1 engine transmission (or nose box) during a typical 150-knot level flight condition. This figure indicates that the primary engine response is at main rotor 4/rev and is at a level of .7g. The sum of 1/rev, 2/rev, 3/rev, 4/rev, 5/rev, 8/rev and 12/rev converted to velocity is 4.1 in/sec assuming all frequencies to be in phase. This compares with a GE limit of 5.0 in/sec.

As previously described, the engine mount configuration was modified as a result of an engine shake test on the GRV. To assess the effect of this on engine vibration, an aircraft was flown with the "new" engine mounts without any aircraft vibration reduction devices (i.e., pendulum rotor absorbers or airframe fixed tune absorbers). This was done to determine if the engine vibration levels were reduced by the percentages (75%) indicated by the GTV testing.

Figure 95 shows a comparison of the engines before and after the engine mount change. While the data is somewhat limited (due to limited instrumentation on the early baseline flight of A/C 002), an improvement in the engine vibration levels is shown.

TABLE 3

GTV ENGINE SHAKE TEST

CONFIGURATIONS EVALUATED

	GR	FWD BOTTOM	FWD SIDE	AFT BOTTOM	AFT SIDE
NO. 1					
Baseline	82	45000 lb/in	45000	23000	11000
	83	Link	45000	23000	11000
	84	Link	45000	7000	11000
	85	7000	45000	7000	11000
	86	Link	45000	Rigid	11000
	87	Link	7000	Rigid	11000
NO. 2					
Baseline	90	45000	45000	23000	11000
	89	Link	7000	Rigid	11000
	88	45000	7000	Rigid	11000

TABLE 4

MOUNTING SPRINGS

		FWD BOTTOM	FWD SIDE	AFT BOTTOM	AFT SIDE
MAIN	BASELINE	45000	45000	23000	11000
LOAD	CURRENT	45000	7000	RIGID	11000
PATH	RESIDUAL	2000	2000	0	0

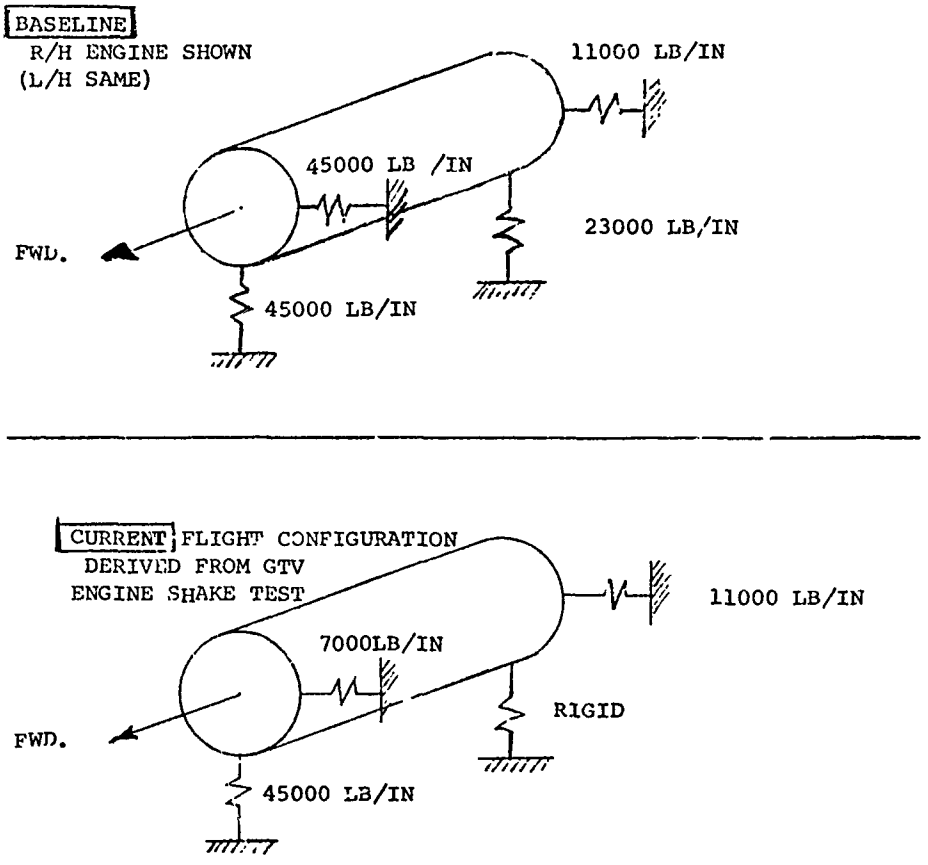

Figure 92. Engine Mount Stiffness.

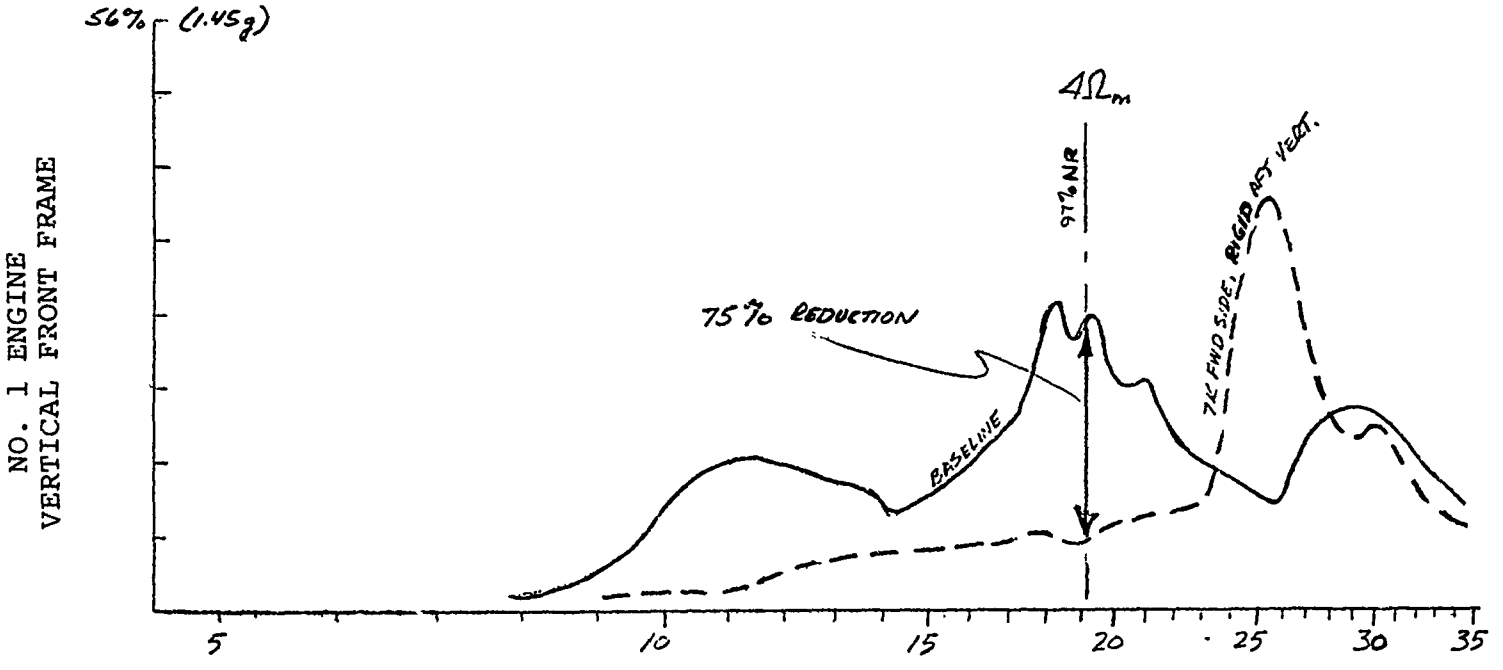

NR = 100% Q_1 = 50% Q_2 = 50%

Figure 93. GTV Engine Shake Test Baseline vs Final.

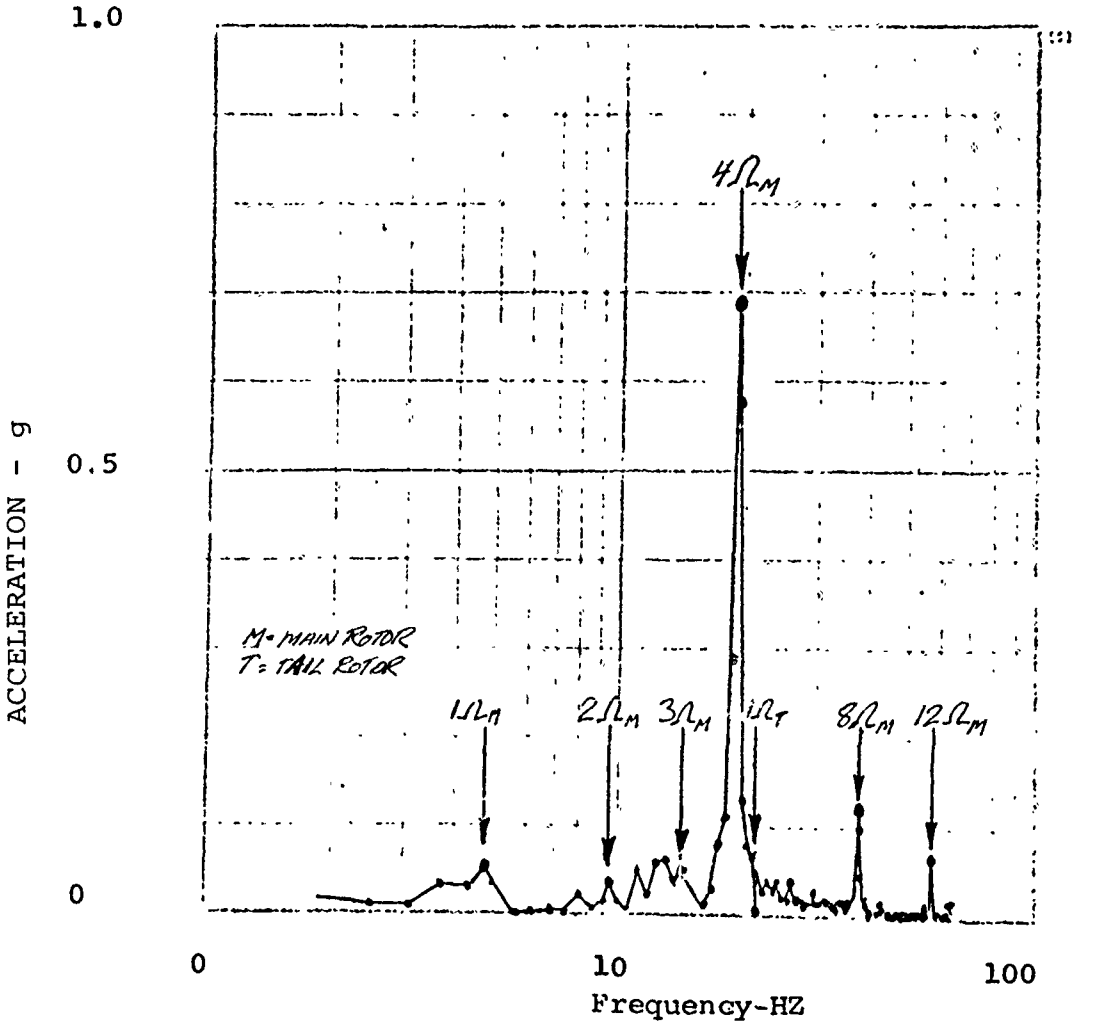

150 KT
286 RPM

Figure 94. Spectral Analysis.

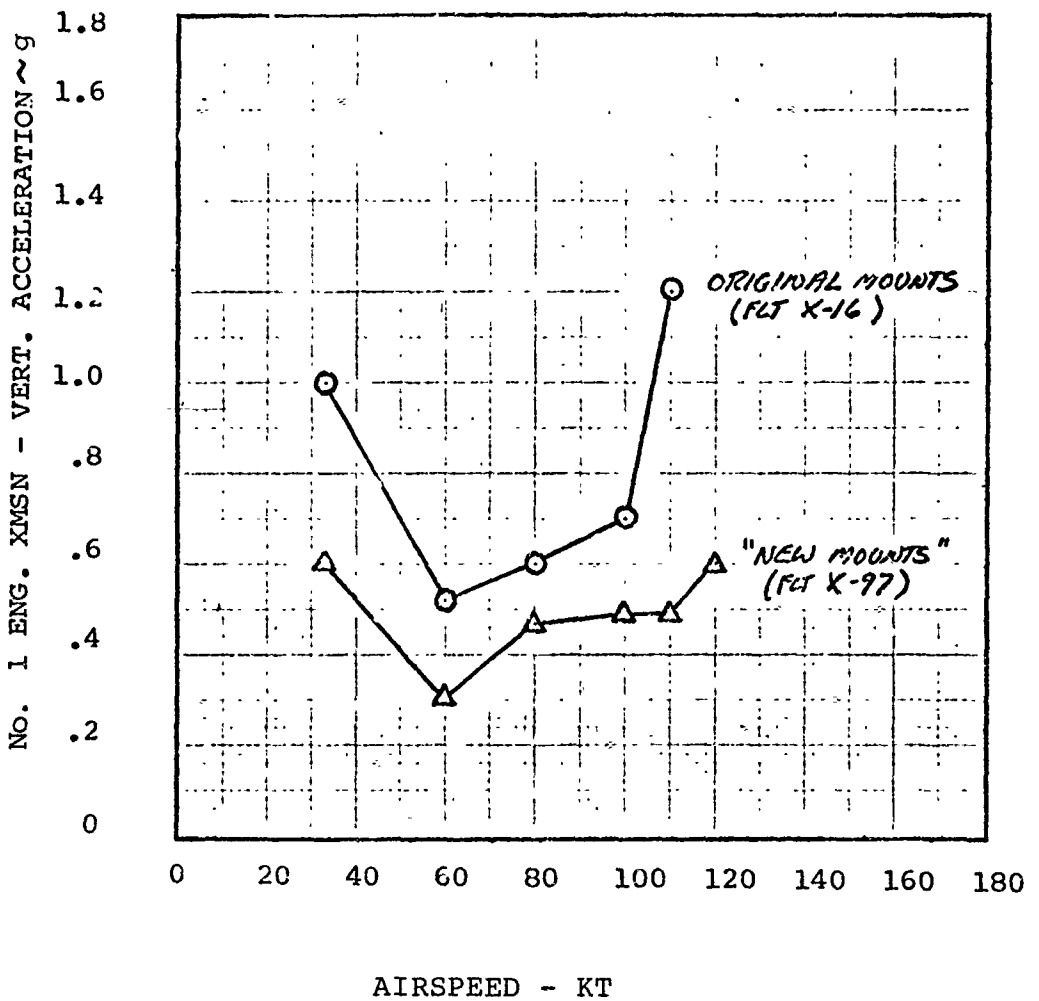

Figure 95. Effect of Mount Change on 4/Rev Vibration,

As indicated, both mount systems had levels below the engine spec of 1.6 g, but the trend of the original mount data at only 110 knots was toward exceeding the spec at higher speed. Also, both of these flights had no 4/rev vibration treatment in the aircraft. However, data shown in the following section, to much higher airspeeds, does have vibration treatment devices installed.

A check was made of airframe vibration levels before and after the engine mount change to determine if the engine mounting adversely affected airframe vibration. It was found not to have any adverse influences.

The aircraft 4/rev vibration configuration was being updated and modified to improve the airframe vibration levels at 4/rev. These levels serve as input to the engines at the mounting locations so that where possible, the instrumentation on each engine was monitored to determine engine vibration levels.

Figures 96 and 97 show 4/rev vibration data for several significant flights of aircraft 002 during this development phase. The locations shown on each engine cover all areas: frame, mid-frame vertical, lateral and roll; auxiliary gearbox on engine; and engine transmission (nose box) accelerometer. Note that the airspeeds flown were increasing, as time progressed, and that all data was not available for all flights due to instrumentation malfunctions. Figures 96 and 97 indicate that when vibration treatment to the airframe is used, as on flights X-110, 124 or 198, the vibration levels on all engine pickups run from 0.4g to 0.8g.

For completeness, Figures 98 and 99 show that while providing low vibrations at 4/rev, the levels at 1/rev and 3/rev were also low.

Limitation of the Solution

There were no limitations associated with the solution described here.

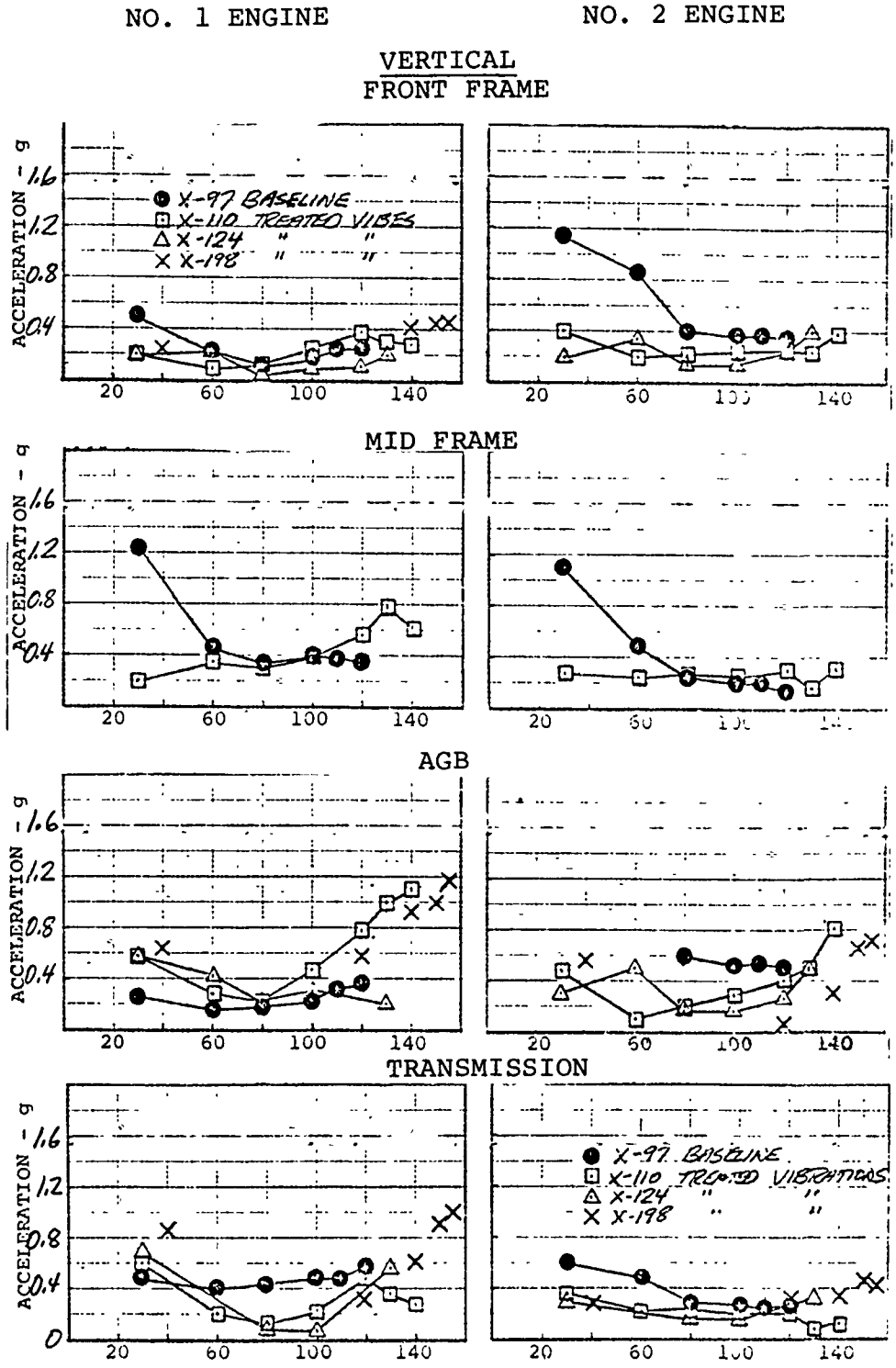

Figure 96. Effect of Vibration Treatment on Engine Vibration (4/rev).

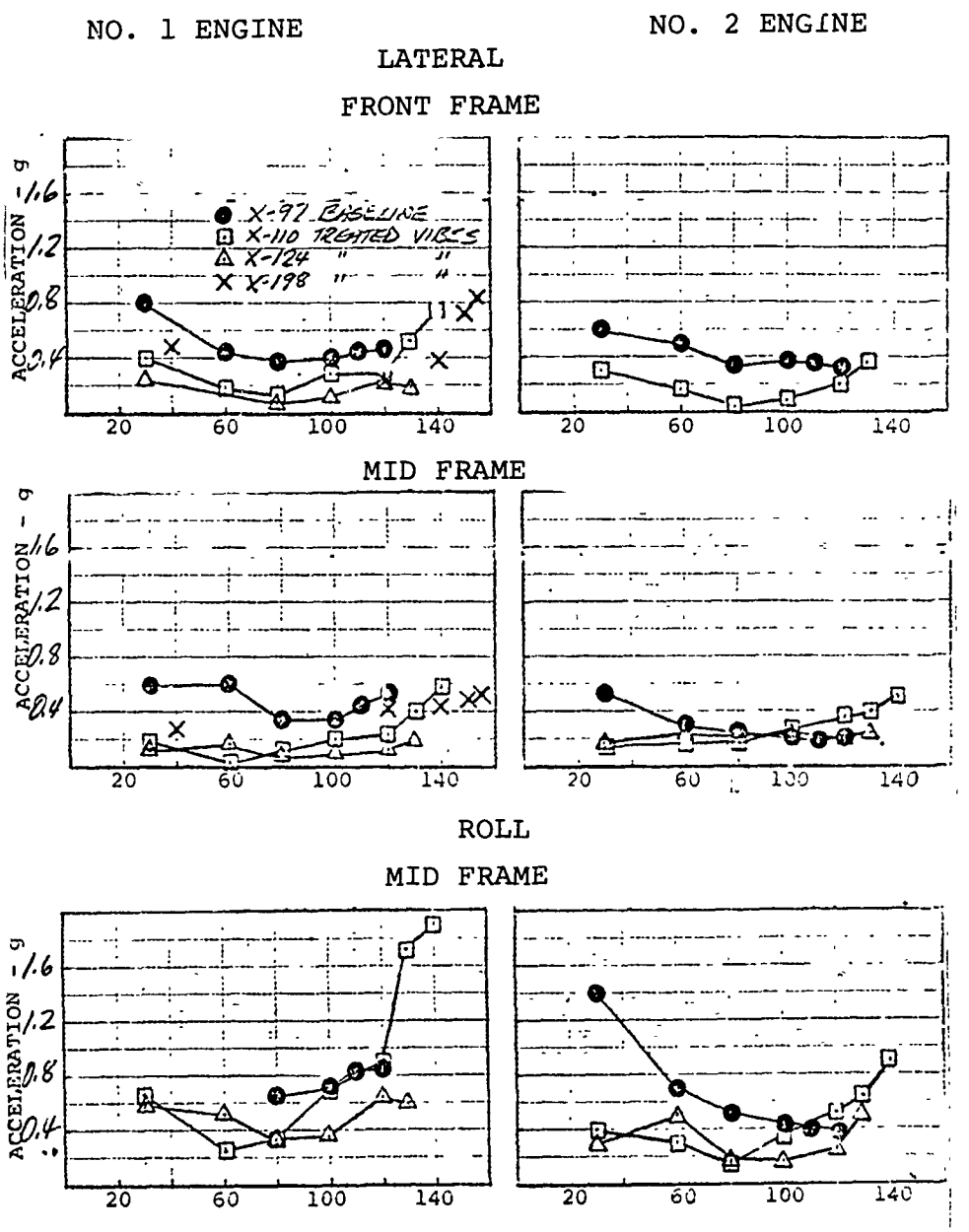

Figure 97. Effect of Vibration Treatment on Engine Vibration (4/rev).

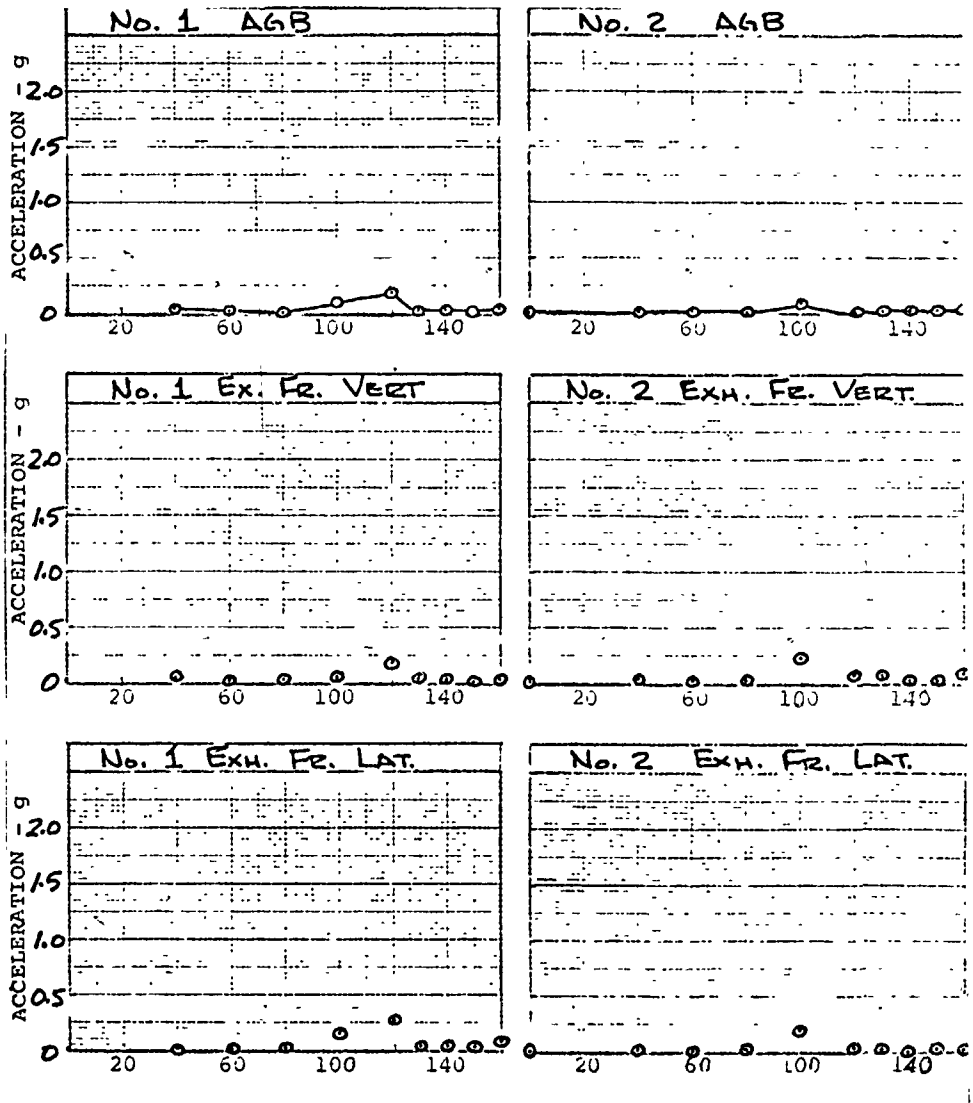

Figure 98. Engine Vibration Survey (1/rev).

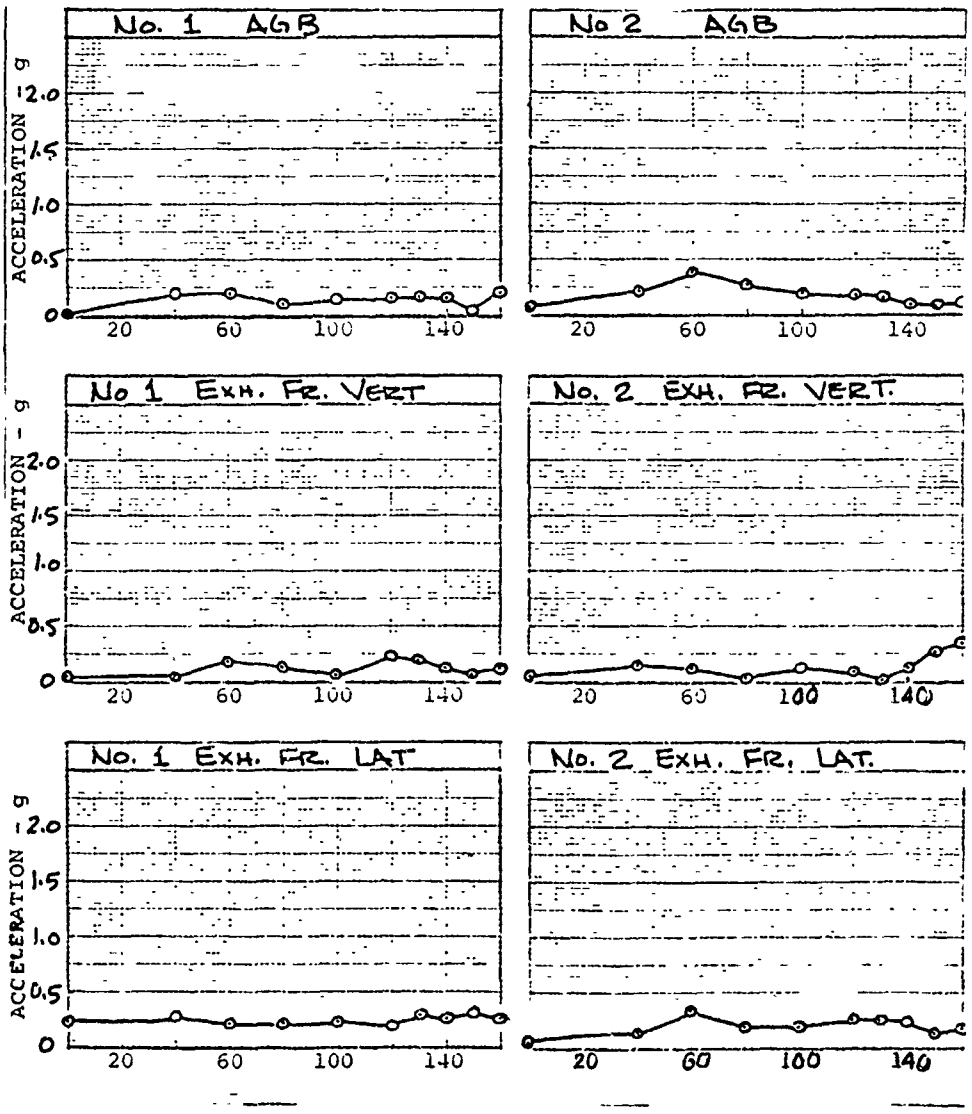

Figure 99. Engine Vibration Survey (8/rev).

PROBLEM - NONSYNCHRONOUS WHIRL

The problem described here is of particular interest since the original manifestation of the problem led to extensive testing and modifications of a component (exhaust duct) because it was believed that it was failing due to the duct resonating. The solution was not fully achieved until the source of the excitation was discovered and corrected.

The powerplant package abusive vibration test described in this report was an all-encompassing test to provide confidence in the suitability of many components; however, in this report comments have been limited to those procedures and data related to this problem.

Description of the Problem

Early in the testing of the ground test vehicle (GTV), exhaust ducts cracked. In addition, the vibration level at the exhaust frame of the engine exceeded the engine manufacturer's limit of 2.5 in/sec at high frequencies (above 50 Hz).

Investigation Leading to a Solution

In February and March 1974, a set of then-current design airframe engine nacelle components were installed on an engine at the engine manufacturer's facility and a vibration test was conducted. The test consisted of a static shake test and a powered abusive vibration test. The static shake test used a small shaker attached to the center of the shake table to which the powerplant package was mounted through the airframe/engine mount isolators. A frequency sweep from 10 to 1000 Hz was conducted at a constant force of 2.1 lb and the resonances of the entire powerplant were determined. The shaker was then attached individually to the airframe hardware (ducts, fairings, etc.), and their responses measured. No exhaust frame or exhaust duct resonances were detected.

For the abusive vibration test, the engine was supported by YUH-61A mounts on a shake table. The shake table was mounted on four air bags. Vibratory excitation of the shake table was provided by means of three vertical electrohydraulic actuators, one beneath the aft mount plane in the center of the table, the other two at the forward end of the shake table, on each side of the table. This shaker configuration was designed because of concern over possible rolling of table during operation of the shakers due to the center of gravity being to the right of table center (aft looking forward); the

Boeing Vertol mount supporting structure and rotary actuator (see below) were mounted on the right side of the table. The shake table was quite stable, however, and only the aft vertical shaker was used throughout the test. The shakers selected were capable of inputting two frequencies plus 2X the fundamental (which would be used to simulate 4/rev N_R + 8/rev N_R for a four-bladed rotor or 1/rev N_R + 2/rev N_R or 2/rev N_R + 4/rev N_R for a two-bladed rotor) or a fundamental frequency plus 4 X the fundamental frequency (which would be used to simulate 1/rev N_R + 4/rev N_R for a four-bladed rotor). The actuators were capable of maintaining a steady load of up to 2500 pounds each while providing a dynamic load sufficient to produce 5 in/sec of dynamic motion from 0-100 Hz. The phase between the components in the complex input wave was variable as well as the phase between shakers.

Power is supplied to the YUH-61A main rotor transmission through a cross shaft connected to the right angle nose gearbox which is mounted on the T700 engine output drive pad flange. For this vibration test it was the intent to simulate the nose gearbox weight, center of gravity, and cross shaft torque. The simulation was accomplished by mounting a nose gearbox mounting adapter to the engine output drive pad to which was mounted a water brake. The water brake was used as the power absorber. The nose gearbox mounting adapter incorporated a pad to which a simulated cross shaft was mounted, at the correct orientation. The other end of the simulated cross shaft was mounted to a torque producing rotary actuator. The rotary actuator was mounted to the shake table. Flexible couplings identical to the YUH-61A cross shaft flexible couplings were mounted on each end of the simulated cross shaft. These couplings permit relative motion between the powerplant and the aircraft main rotor transmission. Thus, engine power turbine torque was counteracted by the water brake and YUH-61A nose gearbox cross shaft torque was applied by the rotary actuator, resulting in the proper loading on the engine output drive pad and the remainder of the engine. The only deficiency in the simulation was that since the engines used did not produce engine specification power (900 hp vs required 1536 hp), the engine power turbine torque was not as large as experienced in actual service. The predominant loading on the engine output drive pad is the pitch moment component of the nose gearbox torque, however, and the deficiency does not significantly affect the results of this test. The predicted fluctuating nose gearbox cross shaft torque was not simulated and there was no deliberate unbalance in the quill shaft between the engine output drive shaft and the water brake.

The vibration survey portion of the abusive test consisted of starting the engine to idle and accelerating the engine to power. This provided the engine signature with Boeing Vertol hardware in a simulated YUH-61A installation. The electro-hydraulic shakers were then turned on and shaker sweeps were conducted wherein the frequency of the shaker was varied from 5 up to 76 Hz. This was done to obtain a more realistic assessment of the powerplant resonances and responses than the static shake test because of the higher input level possible with the electrohydraulic shakers. The shakers were then increased in input until engine vibration/stress limits were reached at each of the fundamental aircraft main rotor excitation frequencies (1/rev N_R - 4.9 Hz, 4/rev N_R - 19.7 Hz, 8/rev N_R - 39.4 Hz). No exhaust frame or exhaust duct resonances were detected.

During the abusive vibration endurance testing, the shaker inputs used were: at 4/rev N_R (19.7 Hz) .25g + 0.20g = 0.32g or 1.0 in/sec and at 8/rev N_R (39.4 Hz) 0.20g + 0.10g = 0.22g or 0.4 in/sec. The test was run for a total of 50 hours. All but the last hour of the abusive test was conducted at 20,000 rpm N_p speed, the last hour being run at 21,000 rpm N_p speed.

As part of the post-test inspection, the exhaust duct was examined. A crack was found. This was felt to be a result of the wall statics which were applied between the vibration test and the cooling test. Specifically, the horizontal seam separated from the aft end of the duct forward to the most aft wall static. From the wall static, a crack was evident running forward and upward from this boss.

In November 1974, during the first 50 hours of testing the ground test vehicle (GTV), the exhaust ducts on each engine cracked. From January 1975 through 1975, both Boeing Vertol's and the engine manufacturer's exhaust ducts were vibrated at the engine manufacturer's facility by mounting the exhaust duct under study on an engine exhaust frame which was mounted to a shake table and vibrated at 4gs. In February the following was reported:

2 nodal diameter (4 node) resonance at 158 Hz
3 nodal diameter (6 node) resonance at 239 Hz

A cold engine shake test showed the exhaust duct resonance at 168 Hz. Correcting for temperature effects on modulus, the frequency would be lower. In operating an engine in a test cell with an unstiffened Boeing Vertol exhaust duct, a marked response was observed at the second N_p critical during starting and showed an increase in overall level above N_p = 20,000 rpm when making N_p sweep at IRP.

There were components at 122 and 225 Hz not present elsewhere, and the increase in overall vibration was in response to the appearance of these nonsynchronous frequencies. A back-to-back test was run using the same engine(s) in a test cell and on the GTV. The data is given in Table 5.

TABLE 5

COMPARISON OF GTV AND TEST CELL DATA

	GE TEST CELL 7/9/74		GTV WEEK OF 11/10/74			RETEST IN GE TEST CELL 12/74				
						BV TAILPIPE			GE TAILPIPE	
	O/A	NSV	O/A	NSV - HZ 140	240	O/A	NSV - HZ 120-130	225	O/A	NSV
XT ENGINE 113										
IRP	0.6	NONE	1.7 2.5	1.2 -	1.5 2.2	1.1 1.2	.9 1.0	- .3	0.5	NONE
2ND NP CRITICAL	0.3 @ 12.9K RPM		1.7 @ 13.5K RPM			2.0 @ 13.8K RPM			0.3 @ 12.5K RPM	
XT ENGINE 101	4/25/74		2/75			2/75				
IRP	1.0	NONE	UNKNOWN			2.5 2.5	2.0 -	2.0	0.6	NONE
2ND NP CRITICAL	0.4 @ 15.0K RPM		UNKNOWN			2.4 @ 14.0K RPM			0.5 @ 13.0K RPM	

NOTES:

ALL VIBRATION DATA IN INCHES/SECOND.

O/A MEANS OVERALL ABOVE 50 HZ AS READ ON A METER.

NSV MEANS NON-SYNCHRONOUS VIBRATION.

ENGINE 113 DATA ON GTV WEEK OF 11/10/74 IS NOT CLEAR AS TO WHETHER STIFFENED OR UNSTIFFENED BV TAILPIPE WAS INSTALLED.

ENGINE 113 DATA IN LYNN 12/74 WAS WITH UNSTIFFENED BV TAILPIPE INSTALLED.

ENGINE 101 DATA IN LYNN 2/75 WAS WITH STIFFENED BV TAILPIPE INSTALLED.

TAILPIPE WEIGHTS: BV 3.2# - GE 16.5#

A variety of ducts were tested on the shake table over a period of time. The data is given in Table 6.

TABLE 6

COMPARISON OF VIBRATION CHARACTERISTICS OF EIGHT DUCT CONFIGURATIONS

EXHAUST DUCT CONFIGURATION	NODAL DIAMETER RESONANCE				ACCELERATION (G)		
	2 Hz	3 Hz	4 Hz	5 Hz	140-160 Hz	240-260 Hz	320-360 Hz
STANDARD TITANIUM	160/	207/240	280/315	382/406	3.5	14.5	8.5
" + 1 Stiffener	187/250	375/395	549/		2	13	5.5
" + 2 Stiffeners	194/248	409/429			1.5	11.5	5.5
" " + .9 Hot			-	-	1.5	7	6
CLAMP ON DUCT OUTLET	170/229	250	304		2	9	6.5
STEEL	165/220	313	388		2.2	7.5	16.5
STEEL WITH SHOT	NO DATA				2.5	7.0	7.5
GE STEEL DUCT	100	155	232	345	3.0	18.5	22

A variety of configurations of exhaust ducts, both titanium and steel (and no tailpipe), were evaluated on the GTV for their effect on the 240-Hz nonsynchronous whirl vibration. These data (Figure 100) show that solutions to the problem of exceeding the engine vibration limits were achieved by the addition of weight/stiffeners to either the steel or titanium exhaust ducts.

The durability of the duct had been improved much earlier when a stiffening band was added to the exhaust end of the tailpipes.

Although the problem was "solved" the cause of the excitation had not been identified; the source was believed to be the engine power turbine's shaft second critical, shown in the engine manufacturer's engine installation manual (dated May 1972) to be 12200/12300 rpm (203/205 Hz). This was calculated by the system vibration and static analysis (VAST) computer program. Later tests of the engine under load showed this mode to occur at 14,400 rpm (240 Hz).

The connection between the engine shaft and the helicopter transmission was through a short (6.69 inches long) "quill" shaft with male splines on both ends of the shaft. These splines mate with corresponding female splines in the ends of the engine shaft and the transmission input pinion (Figure 101).

The quill shaft splines used were side fit splines with a rout clearance of .005 in and .0082 in/side in the engine spline and .025-0331 in/side in the transmission. This arrangement was used because of good experience with a similar quill shaft arrangement used to couple an engine to a transmission in another helicopter although the GE installation drawing recommended OD piloting.

However, because of known problems with nonsynchronous whirl excited by shaft spline misalignment or eccentricity, an investigation was initiated to determine whether the quill shaft was involved.

Figure 101 shows the splined quill drive shaft which connects the engine transmission spiral bevel pinion to the output shaft of the engine. The drive splines are case hardened and ground.

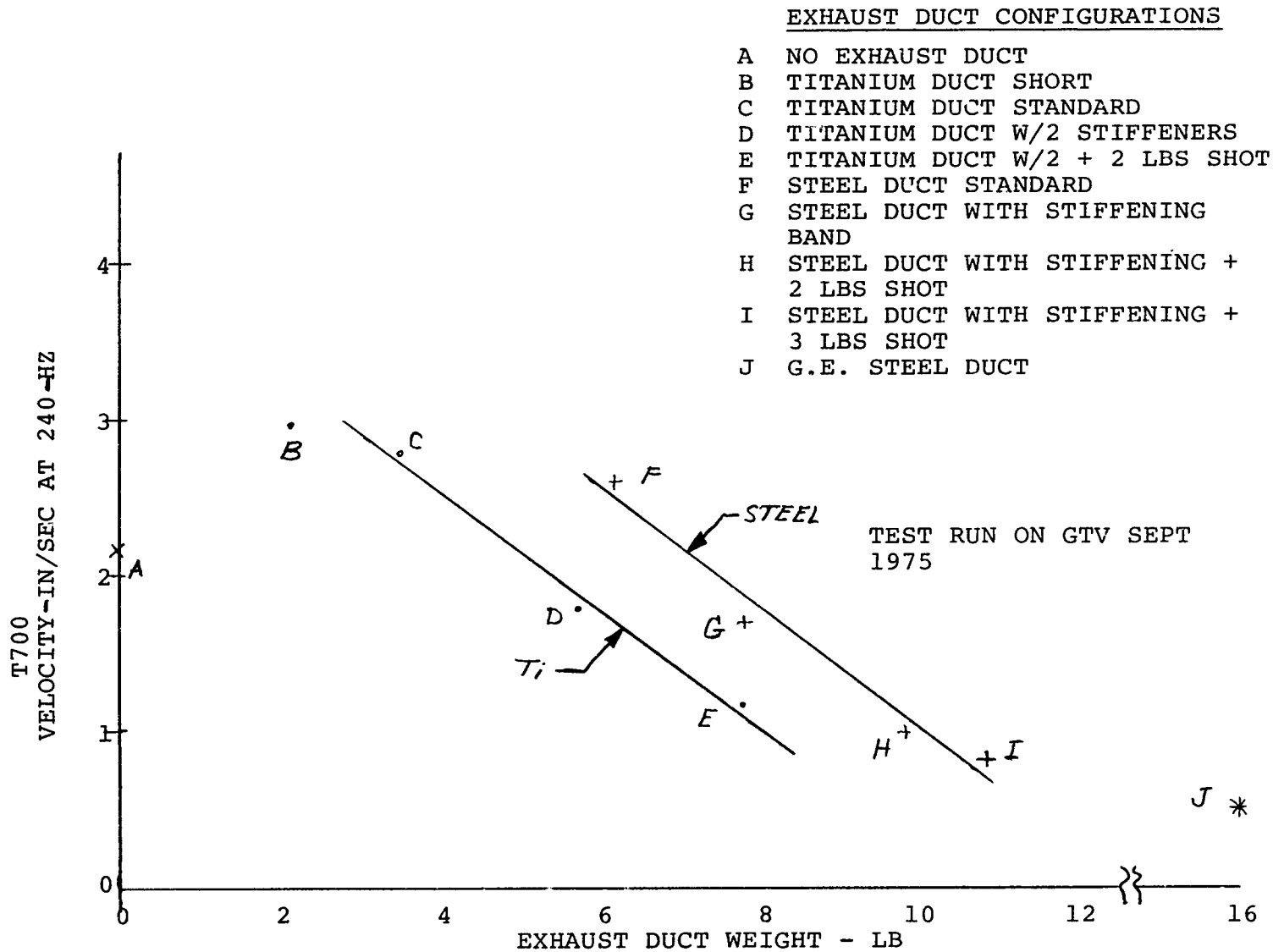

Figure 100. Effect of Exhaust Duct Configuration/Weight on 240-Hz Response.

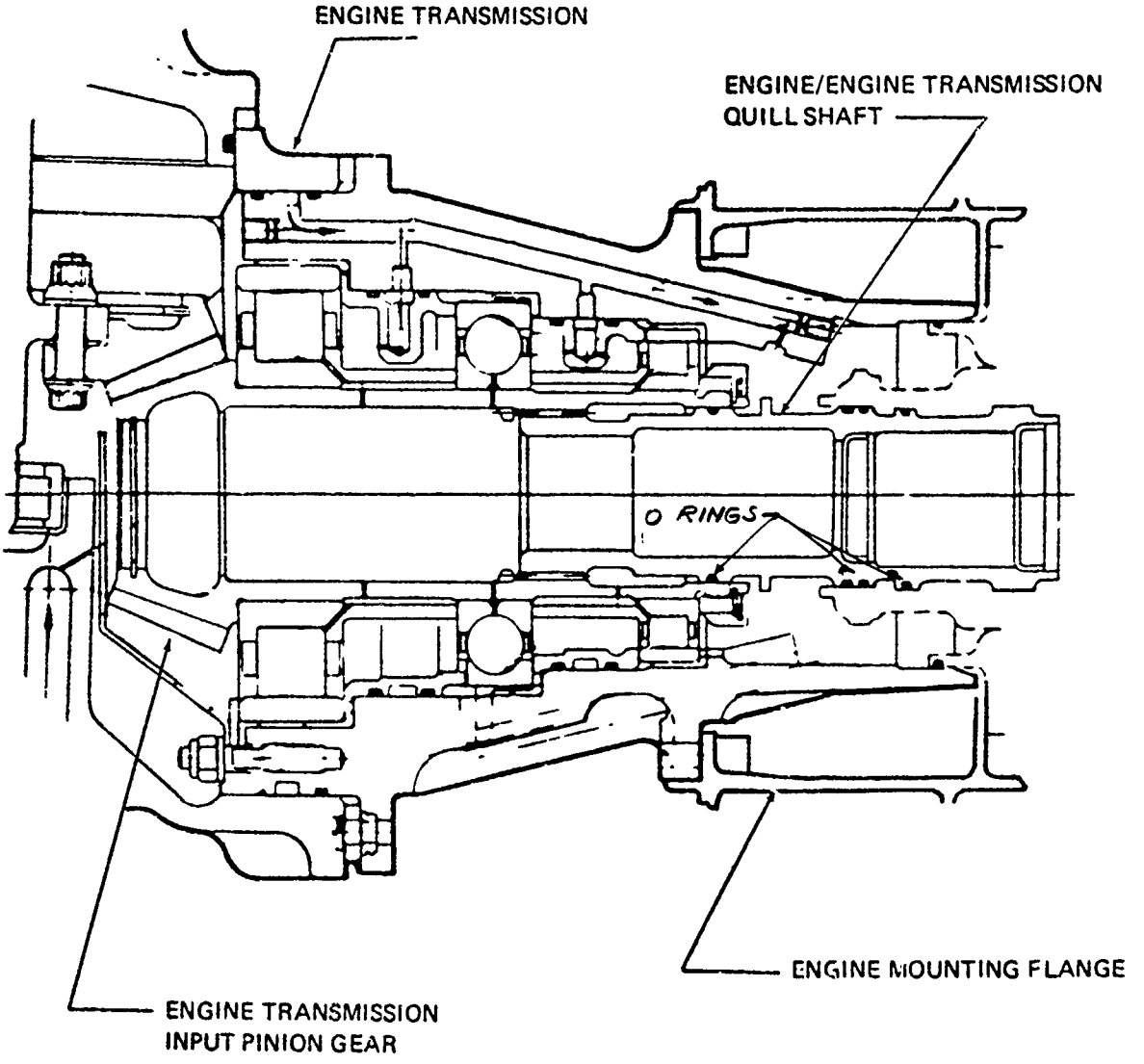

Figure 101. Quill Shaft Location.

The T700 engines provide an oil flow to lubricate the engine end of the quill shaft spline and a dual O-ring seal to isolate the engine and transmission lubrication system.

Split rings with minimum clearances were fitted to an existing quill shaft in two of the O-ring grooves. This provided a pilot within the engine and transmission shafts to reduce possible eccentricities between the quill shaft and the engine. Transmission shaft testing with this arrangement clearly indicated that the quill shaft was involved.

The next experiment was to coat the splines of existing quill shafts with nylon to permit a custom fit of the quill shaft splines to the mating splines. Measurements were made on the flight aircraft (six engines) fitted with these tightly fitted quill shafts in combination with the steel exhaust ducts with stiffeners. During 17 flights, no 240 Hz was observed. (The engines had vibration pickups at the exhaust frame. The data reduction was done on a Ubiquitous spectral analyzer.)

This pinpointed the source of the vibration and a method of suppression. The nylon coating is not a satisfactory production solution, since it does wear. However, it permitted the completion of the aircraft test program without incurring the lengthy delay that would have been required if new quill shafts with close outer diametral fits were required for piloting. The transmission splined component would also have to be replaced since this internal spline has a full radius which is unsuitable for use as a pilot.

Limitation Associated with the Solution

The nylon coated splines did not have adequate life for a production solution. A step toward a production configuration quill shaft which provided improved centering of the quill shaft was tested. The quill shaft splines at the engine end were increased in diameter at their mid length; and at the transmission end, the diametral clearance of the lands at the O-ring was decreased.

Insufficient time was obtained on these pieces to determine if they would demonstrate whirl-free excitation for the minimum of 3000 hours required for a production solution.

No analytical work was done. Williams and Trent* show analytically that for a particular configuration, spline friction as well as unbalance could excite a nonsynchronous whirl condition.

* Williams, R., Jr., and Trent, R., "The Effects of Nonlinear Asymmetric Supports on Turbine-Engine Rotor Stability", 1970 SAE Transactions, Vol. 79, Sec. 2, Paper No. 700320.

PROBLEM - ENGINE STALL

Description of the Problem

During the YUH-61A flight test program and the subsequent Government Competitive Test (GCT), there were a number of engine stalls. These usually occurred during a flare to come to hover.

Investigation Leading to a Solution

The first stall occurred on 20 September 1975 and by 16 November 1975, nine stalls occurred. General Electric has summarized the available data as follows.

"Stall No. 1 - Narrative - 9/20/75 - A/C 001 - #1 Engine 208

During flight X-217, while decelling from 40 knots in preparation for landing, at approximately 30 knots, "bang" was heard. After quick look to see that aircraft was okay, pilots looked at instruments and saw nothing wrong. (T4.5s were around 760°, torque 75%). Quick landing was made, all appeared to be normal, aircraft was shut down. Wind was a 10 knot head wind.

Stall No. 2 - Narrative - 10/30/75 - A/C 001 - #2 Engine 230

Aircraft was being "yanked" into a 10-foot hover with a very rapid collective input. The maneuver was accomplished and aircraft stabilized approximately 1/2 minute at 90% dual engine torque when bang was heard. Aircraft was nose into a 20 knot wind.

Stall No. 3- Narrative - 11/7/75 - A/C 002 - #2 Engine 217 (X-280)

The No. 2 engine experienced a ripple stall during flight (X-280) on Friday, 11/7/75. The stall occurred at a low power setting, the No. 2 was at ground idle to reset from lockout operation. As the No. 2 ECL was advanced and Ng was just above G.I. speed, the ripple (3 pops) were heard. Wind was 8 knots.

Stall No. 4 - Narrative - 11/8/75 - A/C 002 - #2 Engine 217 (X-281)

The aircraft stabilized at the following condition: 5 ft. hover (Tethered) matched torques at 95%. The a/c had been stabilized at this condition for 3 minutes when the stall occurred, OAT = 19°C, P_{10} = 29.92". Wind was a 10 knot head wind.

Stall No. 5 - Narrative - 11/12-75 - Stall event on engine 206 in A/C 002 (X-289)

The aircraft was in level flight at 30 knots in ground effect. OAT was 16°C and barometer was 30.00. The wind was nose on from 40° to right of nose at 8 knots.

The No. 2 engine was in lockout at 30% torque. The No. 1 engine was in fly and at 70% torque.

As the pilot began a deceleration and flare to hover, he advanced the No. 2 engine slightly. Immediately after movement of the ECL, a loud bang occurred which the pilot says came from the No. 1 engine. He estimates airspeed at the time to be between 10 and 30 knots.

Stall No. 6 - Narrative - 11/12/75 - Stall event on engine 217 in A/C 002 (X-289)

The aircraft was in level flight at 5000 feet and 80 knots. The No. 1 engine was at GI and the No. 2 engine was in fly at 70-75% torque. The pilot began to retard the ECL on the No. 2 engine in preparation for a failed engine demonstration of autorotation entry. As soon as he began moving the ECL back, he heard 6-7 "pops" from the No. 2 engine. He reports that when he ceased moving the ECL, the "pops" terminated. Both this event and Stall No. 5 occurred on the same flight.

Stall No. 7 - Narrative - 11/14/75 - Stall event on engine 206 in A/C 002 (X-291)

The aircraft was decelling from 40 knots for hover and landing. The No. 1 engine at 30% torque, throttle retarded, and the No. 2 engine at 70% torque. The ECL on the No. 1 engine was being advanced when a bang occurred at 35% torque. The aircraft was in ground effect approximately 10 feet. Wind was 12 knots.

Stall No. 8 - Narrative - 11/14/75 - Stall event on engine 206 in A/C 002 (X-291)

The aircraft was in a flare hover at 10 feet. The aircraft was simulating a single engine landing with the No. 2 engine at 30% torque and the No. 1 engine at 90% torque when the stall occurred, a total of 6 loud bangs were heard with 6 to 7 more stalls continued until aircraft landed and the No. 1 engine shut down, indicating an unrecoverable stall event. Pilot reported the aircraft pitched and rolled and felt the situation critical. Engine 207206 was removed and returned to Lynn for investigation. This stall occurred on the same flight as stall #7, X-291. The No. 2 engine inlet was instrumented during this flight - no events occurred on the No. 2 engine. Wind was 12 knots.

Stall No. 9 - Narrative - A/C 002 - #2 Engine 217 (X-293)

This event occurred following a day-long attempt to obtain a stall on this engine by repeating aircraft decelerations from 40 knots to hover. These attempts included various power settings, wind directions, yaw angle, pitch angles and altitudes. The stall was achieved during a decel from 40 knots at 10-15 knots airspeed and 5-7 feet AGL. The No. 1 engine was at 30% Q and the No. 2 engine was at 90% Q. Wind was 16-20 knots coming from 45° to the left rear. Aircraft altitude was approximately 7° nose up and 10° nose left. The engine had temperature and pressure instrumentation in the inlet at stations 2, 2.5 and 3.0."

Investigation Leading to a Solution

GE took immediate steps to increase the stall margin and Boeing undertook flight test and wind tunnel testing to establisn the influence of flight conditions and the airframe configuration.

Flight testing using smoke in the exhaust to display the injection visually clearly showed that a horseshore vortex created by interaction of the ground and the rotor captured the engine exhaust and circulated the exhaust to the inlet.

The temperature rises causing the stall have been shown to be most critical during in-ground-effect deceleration of the aircraft. The flight test vehicle was instrumented and tested with high response (time constant = 0.15 sec) thermocouples and in a separate test with high response pressure transducers and lower response thermocouples. About 110 representative

decelerations from 40 or 50 knots to hover were performed utilizing helicopter heights from about 3 to 10 feet, with wind velocities from 0 to 28 knots. The engine power (singe engine) typically varied from around 20% to near 100% through the maneuver. These tests indicated that the instantaneous pressure distortion defined as $\frac{P_T Max - P_T Min}{P_T Average}$ did not exeed 5-7% and, although probably contributory, was not a major factor in inducing surge, since the engine should be capable of 10% without stall. However, the temperature transients determined with the high response thermocouples were as high as 60°C and were determined to be the major factor. The rate of rise was as high as 120°/sec.

Figures 102 and 103 present the maximum inlet temperature rises for the No. 1 and No. 2 engines as a function of wind and flight direction. Analysis of the data indicated that engine power setting had very little effect on maximum temperature reached in the inlet, but helicopter height above the ground had a fairly large effect, with greater heights showing lesser temperatures. Wind direction had a fairly strong overall effect on a given engine inlet temperature rise. Note that the critical wind direction for a given engine is with the wind from the side opposite the engine but is fairly insensitive for that engine over a 90° sector. A summary of the statistical distribution of the recorded temperature rises above ambient is shown in Figure 104. A typical inlet temperature transient which induced a surge is shown in Figure 105.

The actual occurrence of a surge due to reingestion on any particular in-ground-effect deceleration depends on whether a maximum temperature ingestion occurs and on whether it occurs when the engine is operating at a condition where the stall margin is small.

The axial compressor stalled first (as recorded by the high response transducer at the axial compressor discharge plane).

Stalls were recoverable and manifested themselves to observers as two bangs about 1/2 second apart with flame from the engine exhaust. Typical T700 stall frequency is 5 to 6 pops/sec on throttle stalls and 10/sec on decel stalls.

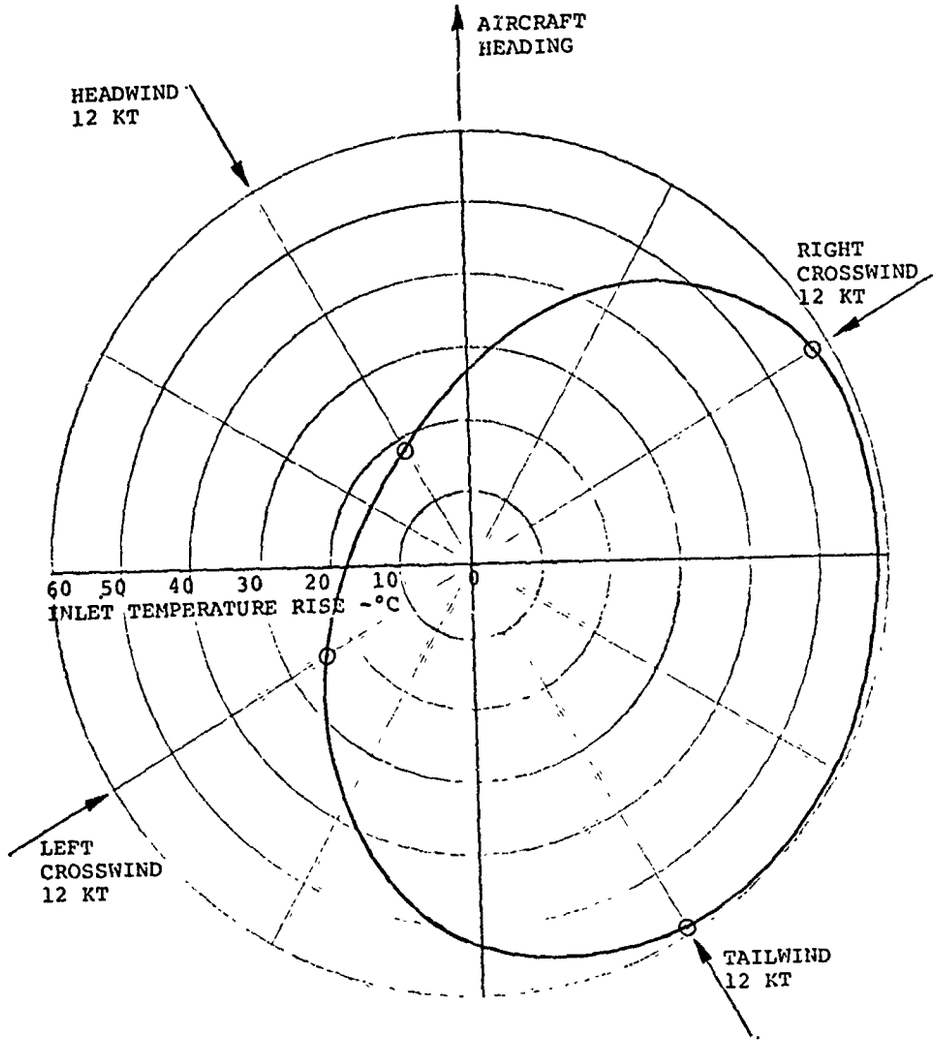

Figure 102. No. 1 Engine Maximum Inlet Temperature Rise Encountered During IGE Decelerations.

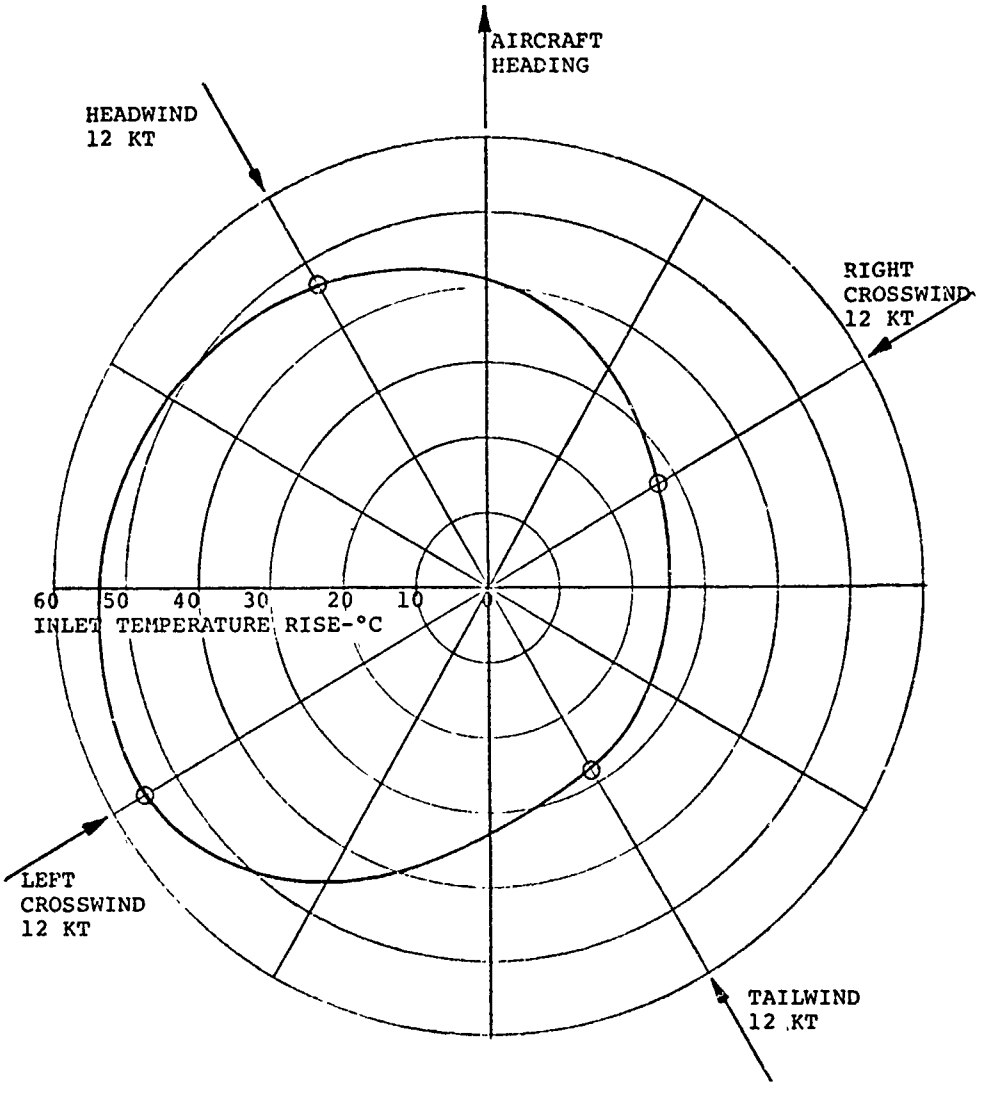

Figure 103. No. 2 Engine Maximum Inlet Temperature Rise Encountered During IGE Decelerations.

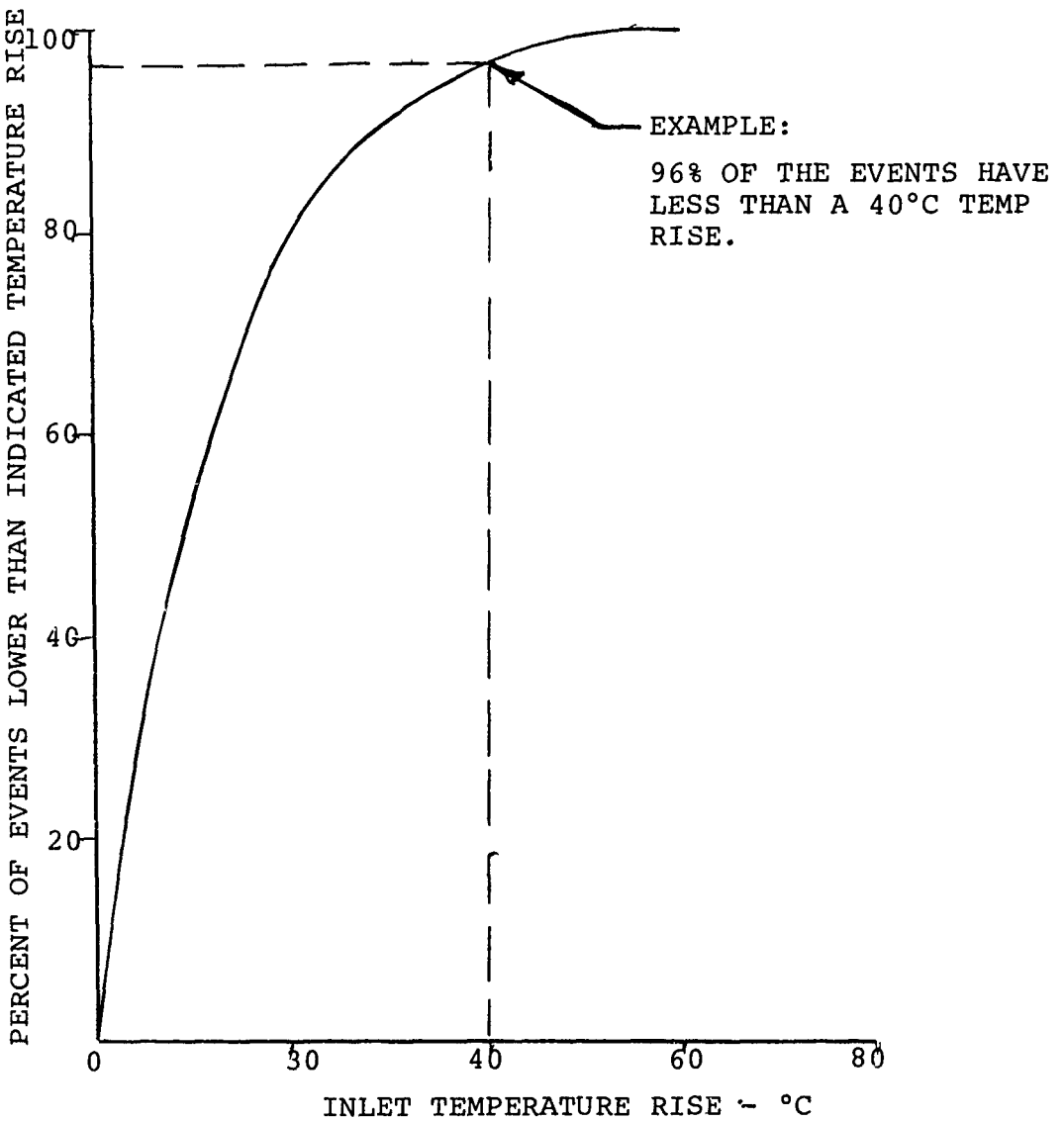

Figure 104. Summary of Inlet Temperature Rises Encountered in Number 1/Number 2 Engines.

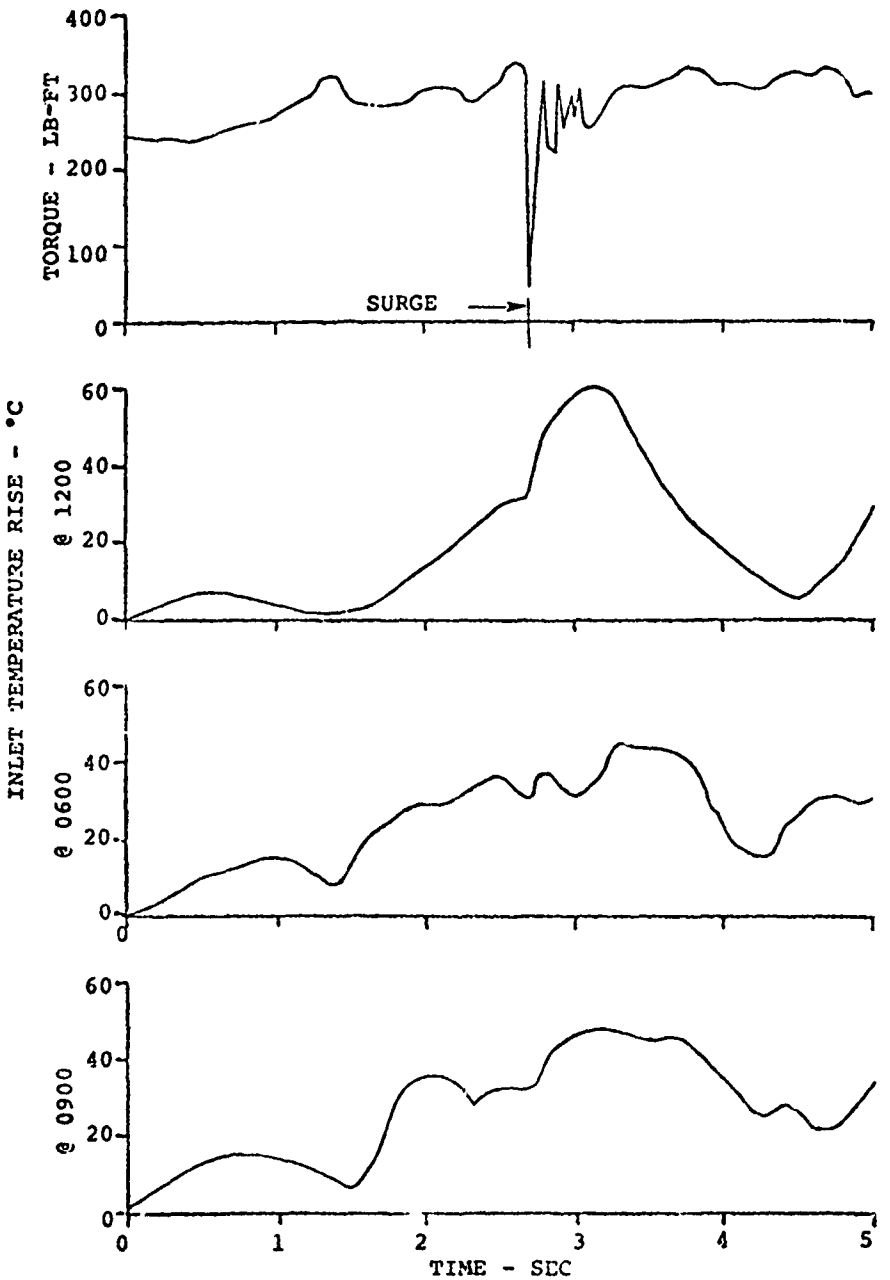

Figure 105. Engine Torque and Inlet Temperature Time History during Stall Event.

The stall is caused by the entrainment of hot gases resulting in a rapid decrease in engine corrected speed ($N_g\sqrt{\theta}$) even though engine mechanical speed is constant or increasing.

The increase in inlet temperature (and decrease in corrected speed) occurs more rapidly than the inlet temperature sensor (T_2) can detect the change and adjust the axial guide vanes (VG) to match the flow conditions. The T_2-sensor time constant was approximately 25 seconds. Consequently, the T_2-sensor cannot respond fast enough to the increase in inlet temperature, which occurs over an interval of 2 seconds or less. The resulting mismatch is greater than can be accepted as angle of attack on the blading and results in flow breakdown or "surge". The path followed by a compressor operating point on the compressor performance map, corresponding to a constant variable geometry excursion, is shown in Figure 106.

In order to provide immediate relief, General Electric introduced a T_2 sensor bias which offset the variable stators by +20°F. Since transient compensation is complicated, this simple and quick across-the-board method was selected to provide the stators with a "head start" on the transient inlet temperature use. Flight testing, however, produced additional stall events and so a 30°F T_2 sensor steady-state bias was introduced along with an increase in the stage 1 turbine nozzle diaphragm area. The turbine area increase reduced the compressor operating line and provided still more stall margin. Flight testing of this configuration produced stalls at very much reduced frequencies compared to the previous configurations. While these changes reduced horsepower margin, and required a higher gas generator speed of the engine to produce a given horsepower, guarantee horsepower levels were unaffected.

For production, the engine manufacturer has decreased the axial compressor operating line while introducing centrifugal compressor configuration changes to maintain overall compressor pressure ratio. The result of this program has been a marked increase in stall margin and a small efficiency increase. The production engine configuration has not been tested in the YUH-61A aircraft, but factory testing shows this improvement and also shows that the production configuration exceeds the requirement for deceleration stall margin which was added to the engine PIDS in collaboration with Boeing to handle the reingestion problem.

Figure 107 shows the throttle stall margin for the YT, MQT and production engines.

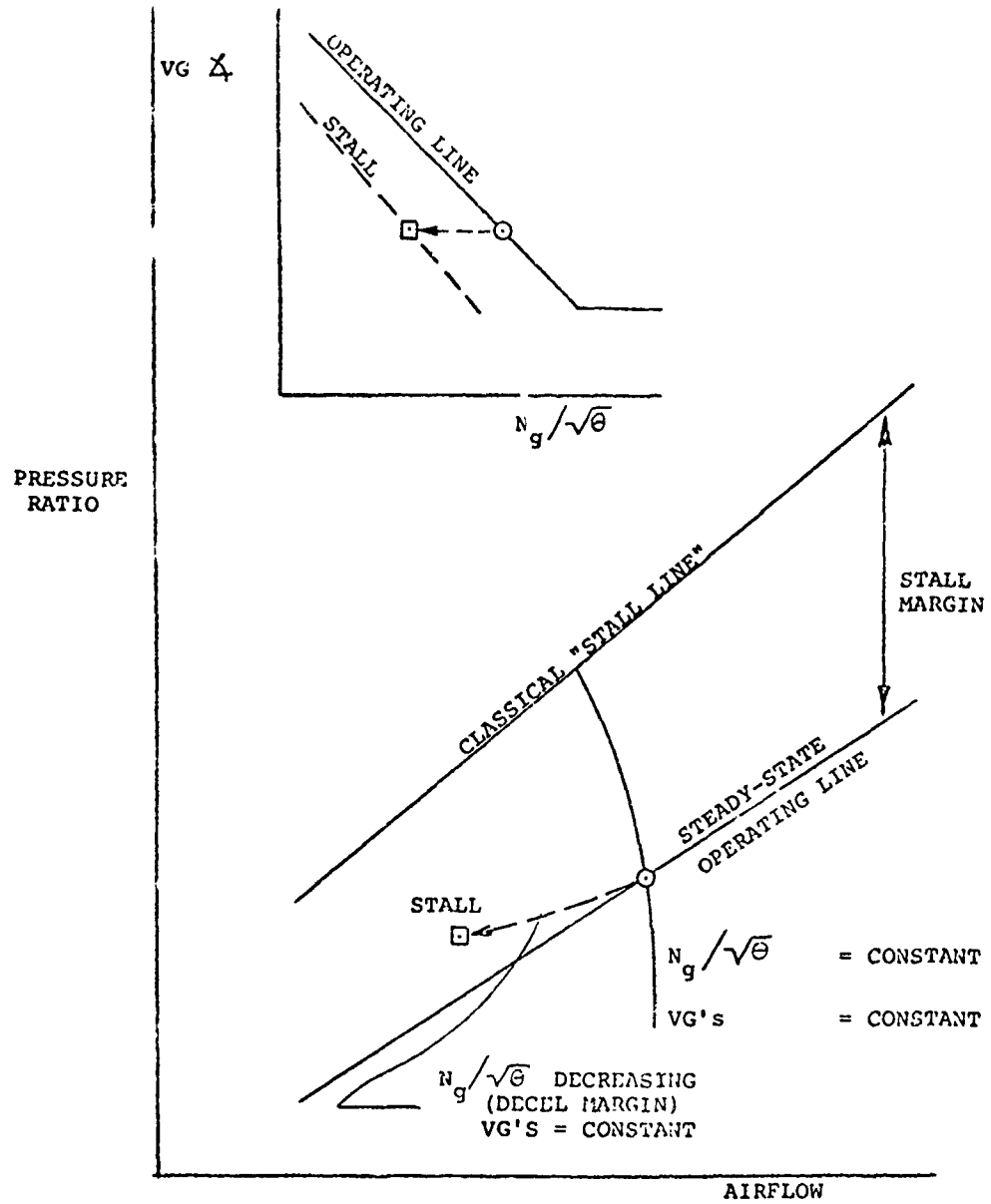

Figure 106. Compressor Stall Line and Paths,

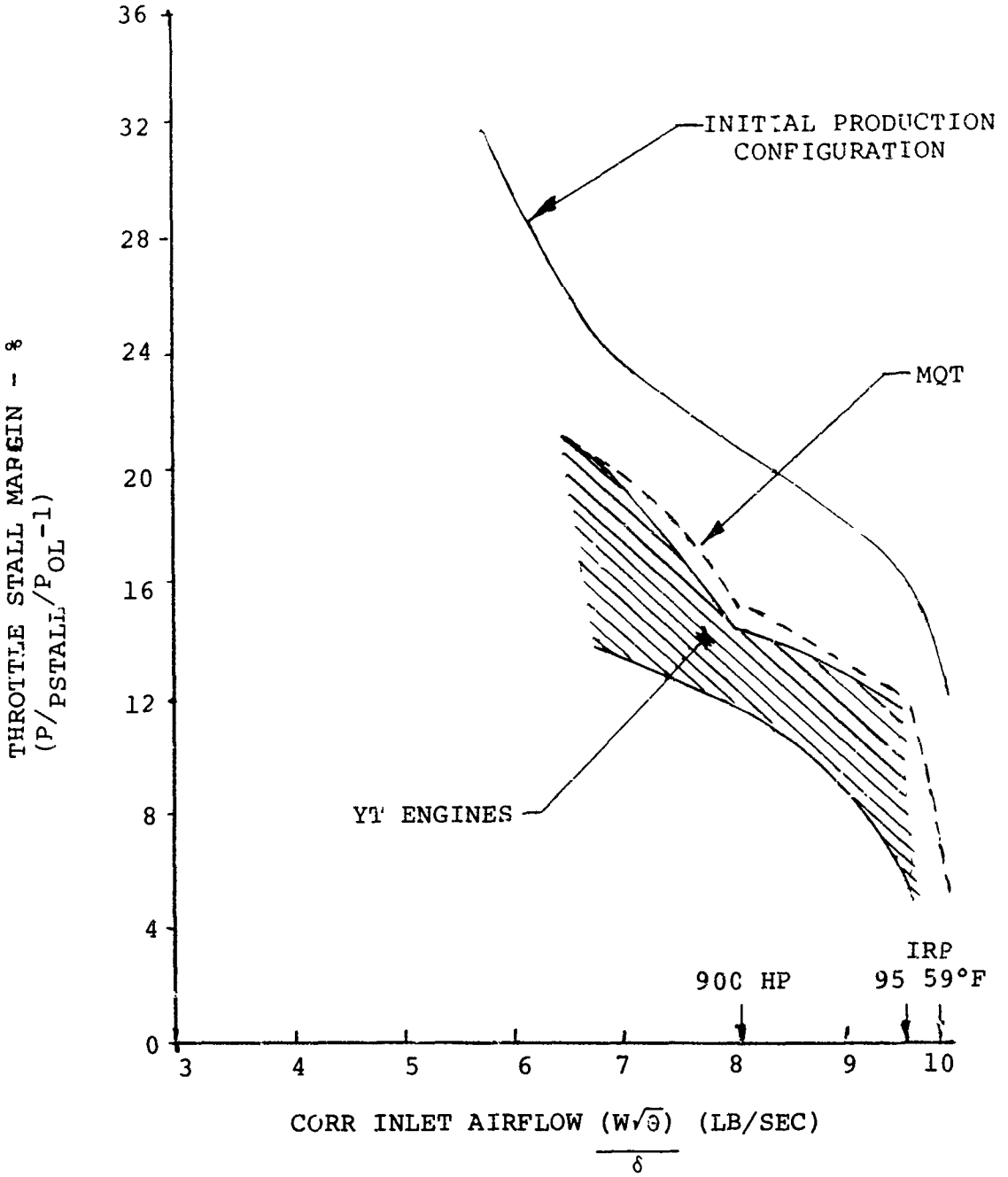

Figure 107. Test Cell Engine Stall Results.

In August 1976, testing of the 1/4.9 scale wind tunnel model began. This testing explored the effects of fuselage angle of attack, forward speed, yaw angle, distance above the ground, exhaust velocity, and exhaust duct angle on the amount of ingestion.

For expediency, the reingestion was simulated by injecting a fixed flow rate of helium as a tracer in the exhaust ducts of the model. Measurements of the concentration of the helium in the inlet duct were then taken and used to quantify the ingestion. No attempt was made to correlate the helium concentration to full-scale aircraft delta inlet temperatures.

These data obtained from the wind tunnel test are shown in Figures 108, 109 and 110. Flight tests generally confirm that the airspeed at which heavy ingestion occurs is from 20 to 35 knots as shown by the wind tunnel data in Figure 110. Flight test did not confirm that doubling the exhaust velocity would give a 6 to 1 reduction in ingestion as indicated in Figure 109.

Limitations Associated with the Solution

Engines with the rematched compressor were not flight tested to demonstrate that no stall would occur in the most adverse condition.

An analytical method or wind tunnel test method to quantitatively predict inlet ingestion is lacking.

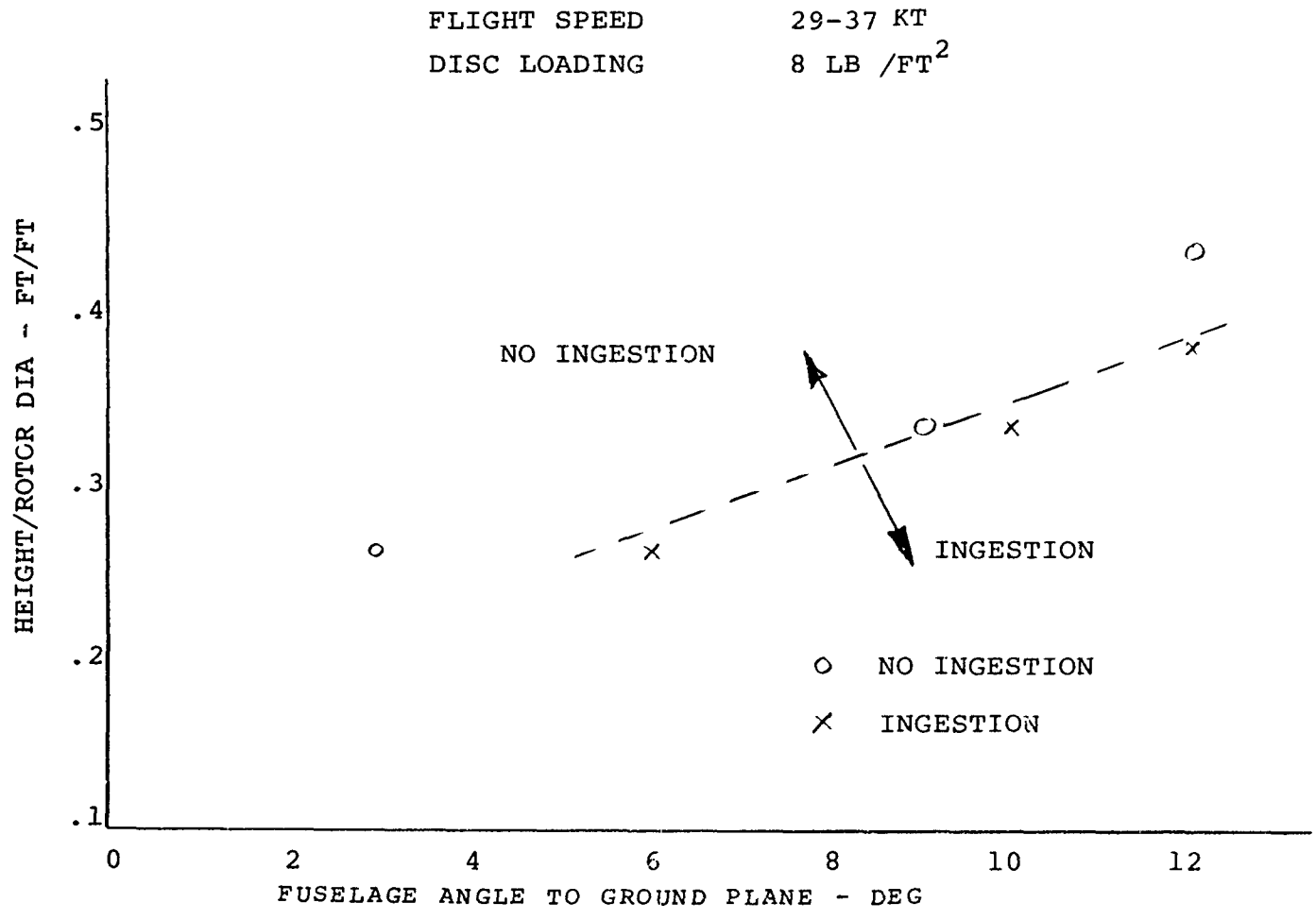

Figure 108. Effects of Fuselage Angle and Rotor Height on Ingestion.

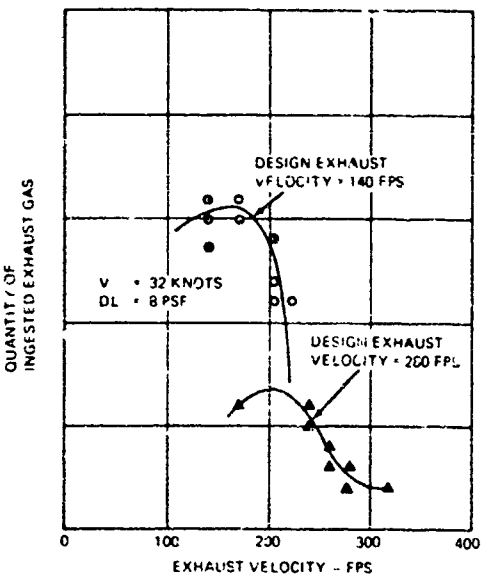

Figure 109. Effect of Engine Exhaust Velocity on Ingestion.

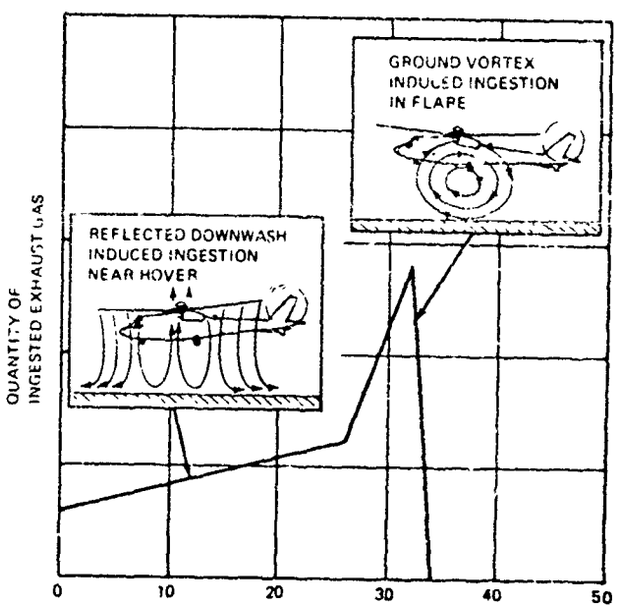

Figure 110. Effect of Airspeed on Ingestion.

PROBLEM - ENGINE CONTROL/AIRFRAME DYNAMIC INTERFACE

In the area of engine controls, there were no problems with stability with the T700 engines in the YUH-61A helicopter. Figure 111 shows representative phase margins and gain. However, obtaining the desired response required modification of the airframe to the engine control and within the engine control.

The T700 engines used in the YUH-61A aircraft were developed following a technology demonstrator program. The engine was contracted for in the first quarter of 1972; the first "XT" engine was delivered in the first quarter of 1974 with first running in the YUH-61A ground test vehicle in August 1974 and first flight in November 1974.

Problems discussed in this section were uncovered in flight testing.

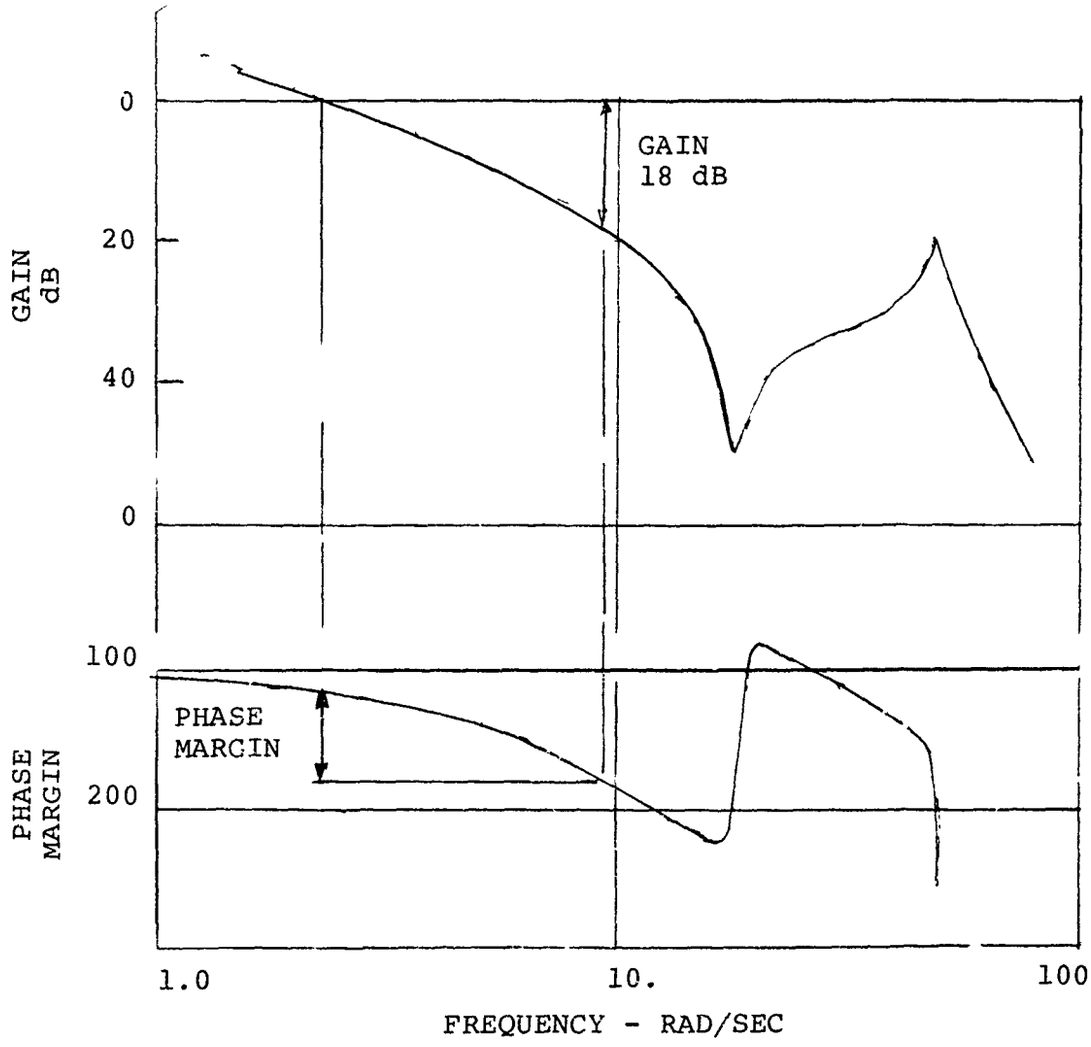

Figure 111. Gain and Lag vs Frequency.

PROBLEM - SLOW RETURN FROM OVERSPEED

Description of the Problem

Rotor overspeed lasting for several seconds following a large reduction in collective pitch was observed during flights in 1975.

Investigation Leading to a Solution

From analysis of the operating conditions, it was concluded by the engine manufacterer that the power turbine speed governor became saturated while operating at the high power. This was because it was on the T4.5 limit during hot days or gas generator speed topping on cold days. This saturation prevented the power turbine governor from reducing engine power as rapidly as the load demand (collective pitch) was reduced.

The engine manufacturer improved this condition by modifying the ECU to relocate the T4.5 limit selector upstream of the proportional plus integral speed limiting function, thus eliminating this saturation problem.

A reduction of the authority of the power turbine governor integrator lessened the effect of governor saturation while on the gas generator speed topping limit.

Limitations Associated with the Solution

The changes noted reduced the overspeed from 5% with slow return to 2% with rapid return. The engine manufacturer anticipated increasing the overall speed governing loop gain which should further reduce the overshoot.

PROBLEM - ROTOR SPEED EXCURSION IN MANEUVERS NOT REQUIRING COLLECTIVE PITCH CHANGES

Investigation Leading to a Solution

Load anticipation by use of a collective pitch input to the fuel control will of course not function when the rotor load is changed without a collective pitch input. Therefore the speed excursions are a function of the power turbine governing gain and effective time constants.

An analysis was made in 1976 to show the effect of increased gain. The results are shown in Figure 112 for a 1.5g cyclic pullup. It can be seen that by a threefold increase in gain, the speed error is reduced to less than one half.

Limitations to the Solution

No limitations are anticipated.

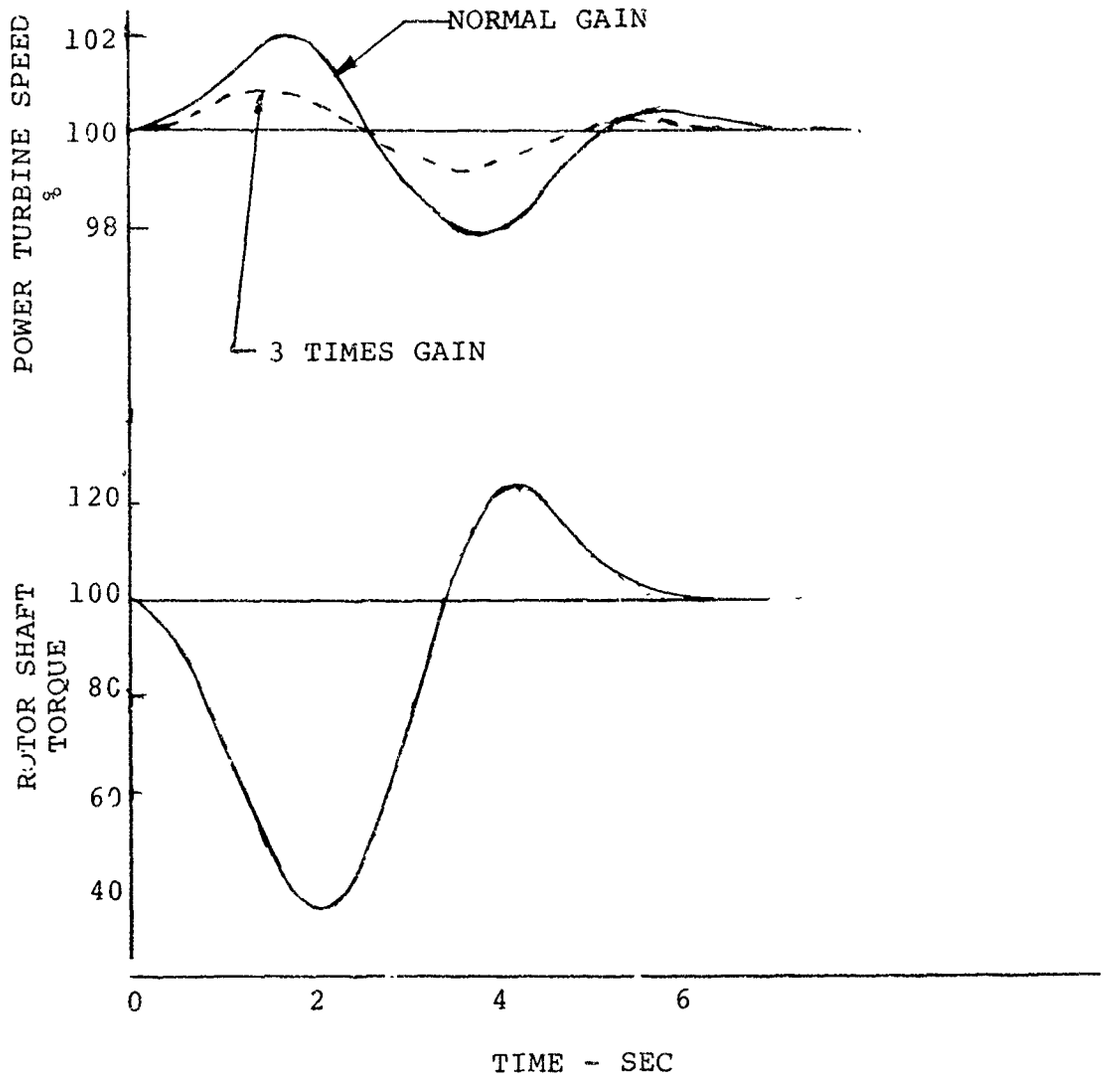

SIMULATION MANEUVER FIXED COLLECTIVE PITCH

Figure 112. Effect of Control Gain.

PROBLEM - LACK OF PRECISE HOVER HEIGHT CONTROL

Description of the Problem

When the pilot of the helicopter made small correction in collective pitch to accurately position and hold the helicopter at the desired distance above the ground, there was a lag between his collective pitch input and the new stabilized thrust. This resulted in a tendency for the pilot to overcorrect. This was found in flight tests in 1976.

Investigation Leading to a Solution

A load demand system had been provided by connecting the collective pitch control to the LDS (load demand spindle) of the HMU (hydromechanical unit) of the engine fuel control as shown in Figure 113.

This provides an anticipatory signal of torque demand whenever collective pitch control movements are the source of changes in the rotor torque. Without this input, the fuel control must wait for the rpm change to provide an error signal in the ECU (electrical control unit) and then, through the torque motor, reset fuel.

The engine governing system senses power turbine speed which is compared to the set reference turbine speed. The difference between the actual and desired speed forms the error signal which is processed in the ECU. The resulting ECU command is made up of a gain proportional to speed error and the integral of the error. The integral gain makes the system isochronous.

If the collective pitch to load demand spindle was exactly the correct relationship, the governing system would have no corrections to make and rapid rpm control would be provided.

In investigating this problem (lack of precise hover control), examination of flight data showed that on most instances the peak of engine torque lagged the collective pitch input by 1 to 1.5 seconds and appeared to be responding primarily to rotor rpm variations from the selected rpm. However, on a run with a large collective pitch change, the engine torque follows collective almost immediately without this lag.

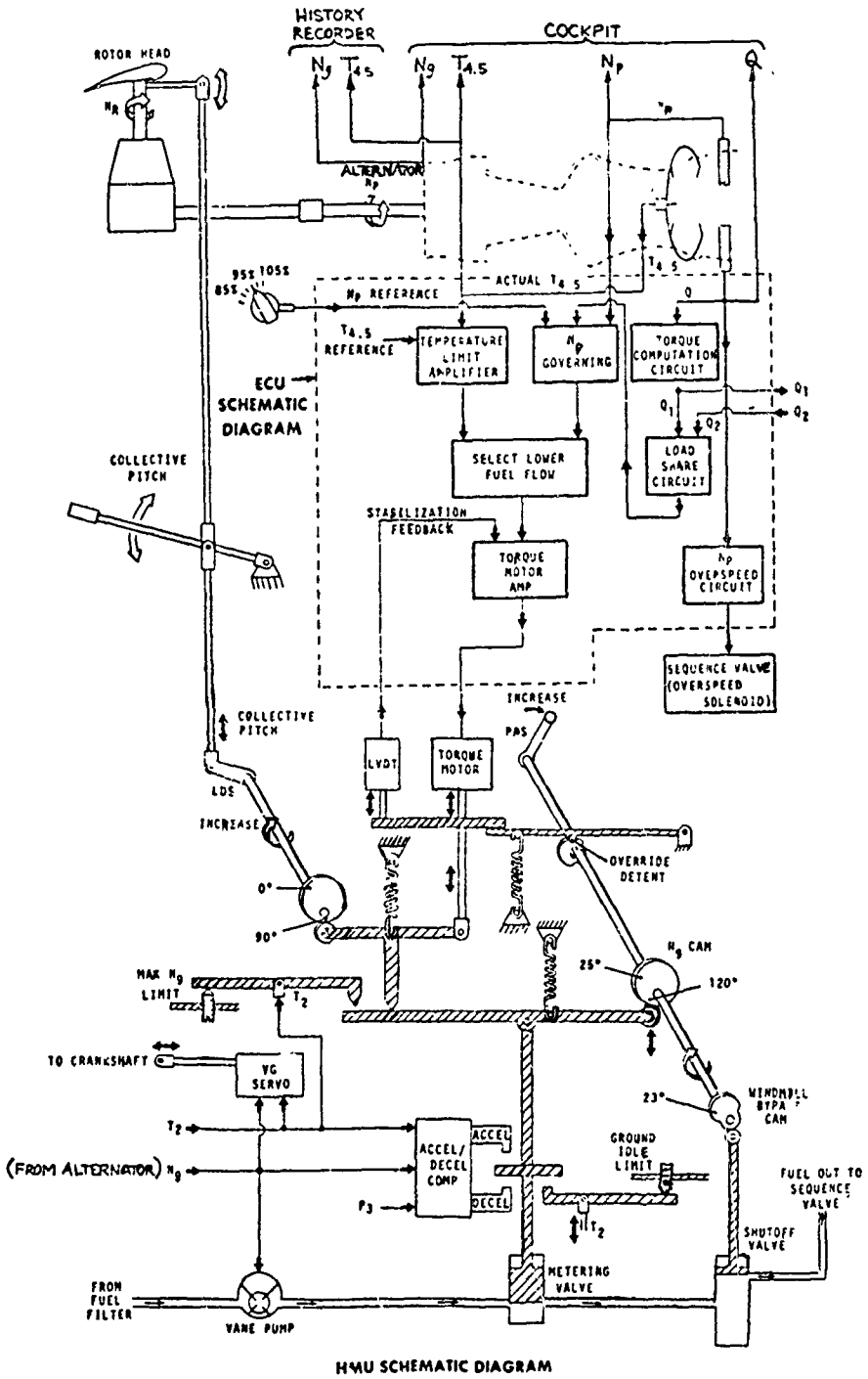

Figure 113. Fuel Control Schematic.

The variations in engine torque and collective pitch become more rapid as the pilot hovers closer to the ground. This may be expected, as the pilot tries to maintain altitude more accurately the closer he is to the ground. In doing so, he uses smaller and more frequent inputs to increase his accuracy.

It appeared from the records that the engines were not responding immediately to small collective pitch motions. Therefore an investigation was made into the mechanical characteristics of the collective pitch to LDS linkage. A test on an aircraft revealed that the linkage to one engine had a deadband of approximately 1.1° of collective pitch (220 hp) and the deadband to the other engine was 1.5° or equivalent to approximately 300 hp.

The design of the LDS linkage used controlex cable which had several bends to make it fit through available spaces between the collective pitch control attachment and the engine LDS.

These bends caused backlash which produced deadbands. This means that for the small collective pitch changes required to accurately control altitude, the LDS may not have moved. Torque adjustment then was dependent on the governing system in the ECU to provide the adjustment which results in a lag.

Description of the Solution

The flight program was completed before corrective action was implemented. However, planned corrective action was to change the mechanical advantage so that a given amount of backlash would represent a smaller amount of collective pitch and reroute the control to reduce the bends and subsequent backlash.

In addition, the engine manufacturer planned to increase the ECU governing gain, thereby decreasing the time to correct a speed error.

PROBLEM - FUEL CONTROL DYNAMICS

Description of the Problem

In the testing of the T700-GE-700 engine in the YUH-61A, a series of problems were uncovered and improvements were made as fixes to the prototype engine controls or were planned for production controls. Two of these have been discussed (pages 185 and 186). A summary of the problems and the changes planned for production fuel controls were contained in GE "Change in Design" dated 18 December 1977. Sections dealing with dynamic interface problems are reproduced on the pages following.

DESCRIPTION TAKEN FROM GE CHANGE IN DESIGN DATED 12/18/77

"Flight testing of YT700 and Maturity engines with various Electrical Control Units (ECUs) showed a need to further improve the engine/AVM rotor system dynamics primarily in the area of engine transient response and stability.

This CID proposes introduction of an improved ECU to improve engine transient response and stability.

The following changes are primarily aimed at improving power turbine (rotor) speed governing and operation on $T_{4.5}$ limiting. The differences can be grouped into three major changes as follows:

a. Simplify Isochronous Governing

The G07 ECU has two separate integrators for isochronous governing; one in the N_p governor circuit and one in the $T_{4.5}$ limiter circuits. The selector circuit determines which circuit should be in control and switches to the output from the appropriate integrator. When not in control, an integrator generates larger and larger error signals until it saturates at some extreme value. Thus, when the selector first switches to an integrator that has not been in control for a while, it allows a very large, irrelevant error signal into the HMU. The large, irrelevant error signal takes time to be corrected. This results in large N_p or $T_{4.5}$ transients and slow engine cut back when $T_{4.5}$ exceeds the limiter value.

One of the integrators was eliminated by relocating the selection function of the integration circuit. Since the one remaining integrator is always functioning in the circuit, it only saturates when a large correction is really necessary.

In addition to smooth conversion from one control mode to another, compromising the design to reduce the transfer transients that result from switching between N_p governing and $T_{4.5}$ limiting is no longer necessary. The $T_{4.5}$ limiter circuit can now be optimized for stability.

Further improvements in response are possible by allowing for two upper saturation levels of the integrator, one defined for single engine operation and the other defined for dual engine operations. Figure 114 shows the separate upper isochronous governing limits (integrator saturation levels). The reduced (relative to G07) twin engine limit together with the single integrator minimizes transient overshoot on load chop, from maximum power.

The increased (relative to G07) single engine limit allows for isochronous governing at flat pitch (LDS = 0).

During single engine operation, with the new limit, isochronous governing can be maintained over the full power range.

b. Tailor Control Gain to Load Inertia

Helicopter engines operate at the extremes of rotor system inertia. During autorotation, the equivalent load inertia is very small (0.062 slug-ft^2). With the rotor system engaged (as in powered flight), the load inertia increases by a factor of 10 to 20, and the increase appears as a step change to the engine when the overrunning clutch engages or disengages.

The G07 ECU compromised the N_p governor so that a single set of dynamics satisfied both extremes of load inertia. In the production ECU, two levels of control gain are available. Each one is selected for one of the extremes of load inertia. The control switches to the appropriate governor dynamics depending on engine output torque. Low engine output torque (less than 20 ft-lbs) implies the helicopter is in autorotation and needs a low gain; higher values of torque imply engaged rotor and the need for high gain.

The low gain switch is also used to further enhance engine response during a burst out of autorotation. During autorotation the power turbine stays near referenced N_p (usually 100%) and the main rotor is allowed to accelerate to a higher speed (around 105%). As collective is pulled, the main rotor slows down due to the increased load. The collective pull also signals the engine to accelerate in anticipation of the impending load. However, the N_p governor wants to cut back on fuel flow to hold N_p at the reference speed. By reducing the gain of the governor in autorotation, the N_p governor does not reduce fuel flow and the engine is allowed to continue accelerating to pick up the rotor load much faster and with less droop in N_p. As the rotor torque exceeds 20 ft-lbs., the control switches to the high gain for engaged rotor operation.

c. Control Dynamic Changes

By reshaping the dynamic characteristics, it is possible to improve the response of the system to slow changes in load demand (less than .4 cps) such as wind gusts, while increasing phase margin in the same frequency range to improve stability. In the high frequency range (>2 cps), the good attenuation of rotor system disturbances remains the same.

d. Table 7

Lists the characteristics which have been improved along with the degree of improvement expected. This measure of improvement is based on the usual set of transients to allow GC7 to proposed ECU comparisons. Other transients may result in different responses, but the delta improvement will be comparable. Also shown is the change which has been the major contributor to the improvement.

Limitations

No limitations are anticipated.

TABLE 7

ECU COMPARISON

	CHARACTERISTIC	G07	PROPOSED	PRIMARY IMPROVEMENT SOURCE
1.	Slow $T_{4.5}$ Cutback	Fast burst 100° sec	70° sec	a
	Slow governor response on $T_{4.5}$ transient overshoots resulting in longer-than-desired temperature excursions over 840°C.	Slow burst 190° sec	14° sec	
2.	$T_{4.5}$ Stability Margin			
	Insufficient stability margin for all hardware combinations HMU, ECU, $T_{4.5}$ harness and engine.	Marginal	Stable	a
3.	N_p overshoot on chop from limiting power - $T_{4.5}$ limiting or topping.	4.0	1.5%	a&c
	N_p governor becomes saturated producing N_p transient overshoot.			
4.	Transient N_p droop on recovery from autorotation.	8%	6-8%	b
5.	N_p overshoot following autorotation recovery.	4.5%	3%	b&c
	As N_p recovers from transient droop, it overshoots the desired speed.			
6.	Gust & cyclic load changes	$<\pm$ 1%	$\pm$ 0.5%	c
	Load change unrelated to collective change causes N_p excursions.			

TABLE 7
ECU COMPARISON - continued

	CHARACTERISTIC	G07	PROPOSED	PRIMARY IMPROVEMENT SOURCE
7.	Autorotation Stability Margin Insufficient stability margin in autorotation results in limit cycle oscillation of N_p.	Marginal	Stable	b
8.	Load Share Stability Margin Analysis indicates additional load sharing margin is desirable.	Marginal	Stable	c
9.	N_p governor stability margin-MQT engine test indicated adequate but less than desirable stability margin.	Stable	26° more phase margin	c
10.	N_p Overshoot Following Jump Take-off Following an N_p speed error, the system is too slow in returning to the desired speed.	5%	25%	c
11.	Steady State N_p Speed Errors Integrator authority limits too narrow to allow isochronous governing at corners of flight envelope. Autorotation max forward velocity - single engine operation or flat pitch on ground.	0 to 2%	0%	a

A FORECAST OF POTENTIAL FUTURE DYNAMIC INTERFACING PROBLEMS AND RECOMMENDATIONS FOR INVESTIGATION/ANALYTICAL TESTING EFFORT TO ACHIEVE AN IMPROVED UNDERSTANDING OF THE PROBLEMS AND POTENTIAL SOLUTIONS

PROBLEM - ENGINE RESPONSE

Reason Problem Will Occur in the Future

MIL-E-8593A, para. 3.2.1.5.6.1, dated October 1975 states that the requirement on a standard day (with no customer power extraction bleed or engine anti-icing air bleed) for time to accelerate from no load to 95% intermediate power shall not exceed 5 seconds at sea level to 9843 feet, and 10 seconds at altitudes above 9843 feet with a power lever movement in .5 second or less. Times shall not exceed 125% of these times with power extraction, bleed, anti-icing, distortion.

The specifying of a time interval does not provide a true identification of the power transient capability of an engine. An engine which at low powers can generate only relatively small accelerating torques can meet the time interval by generating very large accelerating torques at modes or high power. These characteristics would be beneficial for maneuvers which require high power levels; but when required to go from low power to high power, the grossly diverse accelerating torques invite a large underspeed followed by an overtorque.

Large rotor speed droop associated with a maneuver is undesirable and can even be unsafe. It will result in flight path degradation, since during a maneuver the pilot must give his attention to providing multiple corrections to collective pitch and or cyclic pitch to limit both the underspeed and the overtorque which usually occur when the engine control corrects for the underspeed. This action distracts the pilot's attention from other essential tasks.

The reasons for limiting torque are:

1. To keep stress levels of the transmission system within the limits required for long life.

2. To maintain the directional control power of a single-rotor helicopter, which is degraded when the main rotor is overtorqued and is below normal rpm.

Electrical generating systems have a minimum rpm at which they will drop off the line. A time delay is usually provided which will permit further underspeed for a short period without dropping off. However, frequent large underspeeds increase the exposure to a malfunction of these devices.

Helicopter vibration is limited by tuning the helicopter structure, absorbers, and isolation mounts to be optimum at the normal rotor speed. Excursions from that speed result in increased vibration.

Recommended Program

It is recommended that a study be made to quantify the effect of engine response on helicopter rotor speed droop during maneuvers using collective pitch changes and those where collective is held constant.

The collective pitch anticipatory signal and the use of other signals which anticipate torque changes (such as pitch rate x airspeed) and rotor rpm differences from engine rpm (for autorotational recovery) would be evaluated. This would show the effect of optimum airframe generated signals in providing minimum rpm excursions during changing flight conditions.

The engine control would be examined to show what can be accomplished by use of high gain (proportional to signal error) plus rate of change of error processed to match the engine characteristics. Shaping or filters would improve stability to permit the high gains.

The analysis would establish the relationship between acceleration schedule, engine control characteristics, and helicopter maneuver requirements.

The advanced analytical tools available today use compressor and turbine maps, heat transfer data (for thermal lag), duct and nozzle characteristics, bleed and cooling flow effects, and inertias to accurately simulate transient conditions.

To verify this, the accuracy of the Boeing analytical program (General System Analysis) will be demonstrated using flight test records from a CH-47 program currently in progress. Engines with three different response times are being flown and for each of the two engines, the following are continuously recorded: N_1 speed, N_2 speed, engine PTIT, engine torque, engine flow, engine fuel press, engine fuel temp, compressor discharge press, N_2 lever position, rotor speed and thrust lever positions.

The study would provide a fundamental base for establishing response characteristics and the effectiveness of control system features over a range of helicopter/engine parameters. It would establish the range of helicopter parameters that could be handled by a specific engine control configuration. The study would also provide the data for an updating of the engine power transients specification.

PROBLEM - ENGINE DRIVE SHAFT EXCITATION

Reason Problem Will Occur in the Future

Engine output drive shafts that operate at supercritical speeds are commonly used.

These shafts, since they pass through a critical speed and the damping may be small, are easily excited by alternating 1/rev forces or moments which originate in the coupling from the transmission to the engine. If a splined quill shaft is used the spline friction and eccentricity of the shaft can generate moments and forces. Flexible discs or laminated rings of couplings can produce excitations. The shaft vibrations can persist at operating speeds when the spread between shaft frequency and operating speed and or the damping are small.

Recommended Program

It is recommended that an analysis be developed to calculate the forces and moments developed by typical couplings and their effect on representative supercritical engine drive shafts.

The results will provide a method of evaluating drive shafts and couplings during the design phase to determine if sustained vibrations or whirl will occur and require the redesign of the coupling or shaft system. Bench testing would be conducted to verify the analysis.

PROBLEM - ACCEPTABLE TORSIONAL OSCILLATION LIMITS CANNOT BE DEFINED

Reason Problem will Occur in the Future

MIL-E-8593A, para. 3.2.1.5.5, allows power fluctuations up to ±1% of maximum continuous horsepower.

Whether this oscillation will be satisfactory when the engine is installed in a helicopter depends on the response of the total engine/airframe drive system to the particular frequency and the nature of the forcing function and the characteristics of components in the drive system.

For multiengine helicopters, the engines are usually geared to the main rotors symmetrically with the output to the rotor(s) connected at the middle or combining gear. Therefore, a vibratory mode exists with a node at the connection to the rotors and the engines oscillating phased 180° with respect to each other. Since the helicopter rotor(s) do not oscillate, no damping is provided by the rotor(s). Therefore nominally small engine torque fluctuations of the proper frequency can cause large oscillations.

One component whose performance is sensitive to torsional torque fluctuations is the overrunning clutch, since it can creep, slip, or jam depending on the level of torque oscillations.

No satisfactory analytical program exists to describe the operation of an overrunning clutch under steady plus alternating torques.

Recommended Program

A dynamic analysis should be developed to describe the operation of overrunning clutches while transmitting unsteady torques. This analysis should be supported by bench testing to verify the accuracy of the analysis.

This program would then provide the tool for establishing acceptable torque fluctuation limits for overrunning clutches.

PROBLEM - ENGINE STALL

Reason Problem Will Occur in the Future

No criteria exist for the stall margin that should be provided in the engine. A margin has been provided to cover engine manufacturing variations, and degradation in service plus some allowance for distortion due to installation in an aircraft and for engine transients.

Helicopters during close to the ground decelerations can entrain the engine exhaust in the rotor vortex which carries the hot gases forward to the engine inlet. This results in a large rapid inlet temperature rise transient which can produce stall in some engine/helicopter configurations.

There can be a steady state inlet pressure distortion caused by shafting, transmissions or other items which intrude on the inlet flow path. This distortion is included in the normal inlet analysis and test. However, there is a dynamic pressure distortion caused by unsteady rotor flow, particularly tip vortices; this has not been analyzed and tested either separately or in conjunction with the steady state pressure distortion. No method exists for estimating these transients.

Recommended Program

The U.S. Army has initiated a program to measure inlet temperatures and pressures on the CH-47 during maneuvers which produce the maximum effect. Rapid response thermocouples and pressure transducers will be used since this is a dynamic condition being investigated. This work should be extended to other helicopters. In addition, wind tunnel tests should be conducted to develop a technique that will simulate flight test results so that the helicopter configuration may then be varied to determine what parameters influence the ingestion transient and how it can be reduced.

From these programs, margin requirements and required engine demonstration tests can be established with a minimum penalty to the engine or the aircraft. In addition, a guide could be provided to minimize ingestion on new designs of helicopters.

PROBLEM - HIGH TRANSMISSIBILITY OF ENGINE MOUNTING SYSTEM

Reason Problem Will Occur in the Future

Engine mounts (isolators) cannot permit sufficient engine motion to obtain reductions in transmission of airframe vibrations to the engine.

This motion limitation is imposed by the state of the art of high speed shaft couplings.

Recommended Program

AMCP 706-202 (Engineering Design Handbook Part 2) para 403.2.1 reviews the current choices of couplings with their limitations. A service-free redundant or fail-safe lightweight coupling which can provide the freedom for a "soft" mounted engine is not available. Both the engine mount arrangement and the shaft to engine geometry affect the amount of angular and axial motion required to achieve a specific low level of rotor-induced vibration at the engine. However, a coupling which permits greater motion than current couplings without significant penalties in size, cost, weight, and safety would permit improved engine mounting systems. A search for coupling concepts with potential should be undertaken and the more promising designs selected for detailed analysis and testing.

RECOMMENDATIONS FOR ENGINE/AIRFRAME/DRIVE TRAIN SPECIFICATIONS GOVERNING DYNAMIC INTERACTION

MIL-E-8593 should be modified as follows:

1. It should include a requirement that all power turbine torsional frequencies experienced during testing be included (tabulated) in the engine specification even when they are less than the acceptable value. Analyses would then be made to determine whether the installed engine would exhibit excessive oscillations.

2. It should include vibration (engine shake) test with a range of flight weight airframe components (inlet, exhaust, plumbing, etc.) mounted on the engine to search for resonances. This same test should include a search for vibration-induced abnormalities in the operation of the engine fuel control. Frequencies of resonances/ abnormalities should be tabulated in the engine specification.

3. It should specify the minimum stall margins from idle to max power.

4. Para. 3.2.1.5.6 should be updated to specify acceleration characteristics which will limit rotor speed droop to acceptable values and provide satisfactory rotor starts.

The airframe Prime Item Development Specification (PIDS) should require an engine/airframe interface document which would include:

1. Analysis to demonstrate engine/airframe drive system stability. This would also determine whether there is amplification of any engine oscillation experienced in engine testing. This must include examination of engine-to-engine modes for multiengined helicopters.

2. An engine/rotor response analysis to show rotor speed droop/torque excursions during maneuvers.

3. The unbalanced moments and forces at the drive system/ engine connection and the response to these unbalances.

These analyses should be reviewed at design reviews specified in the AQS required by AMCP706-203.

SUMMARY OF PROBLEMS LISTED CHRONOLOGICALLY

YEAR	AIRCRAFT OR SYSTEM	PROBLEM
1967	CH-46	Engine vibration caused by high speed drive shaft unbalance.
1969	CH-47	Torque oscillation.
1970	CH-47	Inlet housing cracking.
1972-1975	YUH-61A	Engine mount selection.
1974	YUH-61A	Nonsynchronous whirl caused by quill shaft eccentricity.
1974	HLH/DSTR	Torsional stability.
1974	HLH/DSTR	Oscillating torque excited by fuel pressure fluctuation.
1974-1975	YUH-61A	Engine stall caused by exhaust ingestion.
1975	CH-46	Rotor overtorque on rotor start.
1975	YUH-61A	Slow return from overspeed.
1976	YUH-61A	Rotor speed excursions in maneuvers not requiring collective pitch changes.
1976	YUH-61A	Lack of precision height control.

BIBLIOGRAPHY

1. "Factors Affecting Fuel Control Stability of a Turbine Engine/Helicopter Rotor Drive System" by C. Fredrickson, K. Rumford, and C. Stephenson, presented at the 27th Annual Forum of American Helicopter Society, May 1971.

2. "Engine Control Stabilizing Compensation-Testing and Optimization" by J. R. Alwang and C.A. Skarvan, Journal of the American Helicopter Society, Vol. 22, No. 3, July 1977.

3. "Engine Airframe Integration, Current Practices and Future Requirements for Army Aircraft" by J. Acurio, V. Edwards, and N. Kailos, presented at the Project Squid Workshop, U.S. Naval Academy 11, 12 May 1977.

4. "The Effects of Nonlinear Asymmetric Supports on Turbine-Engine Rotor Stability" by R. Williams, Jr. and R. Trent, 1970 SAE Transactions, Volume 79, Section 2, Paper No. 700320.